

Flow Meter Guideline

TR-109634

Final Report, March 1999

Effective December 6, 2006, this report has been made publicly available in accordance with Section 734.3(b)(3) and published in accordance with Section 734.7 of the U.S. Export Administration Regulations. As a result of this publication, this report is subject to only copyright protection and does not require any license agreement from EPRI. This notice supersedes the export control restrictions and any proprietary licensed material notices embedded in the document prior to publication.

EPRI Project Manager
T. Eckert

DISCLAIMER OF WARRANTIES AND LIMITATION OF LIABILITIES

THIS PACKAGE WAS PREPARED BY THE ORGANIZATION(S) NAMED BELOW AS AN ACCOUNT OF WORK SPONSORED OR COSPONSORED BY THE ELECTRIC POWER RESEARCH INSTITUTE, INC. (EPRI). NEITHER EPRI, ANY MEMBER OF EPRI, ANY COSPONSOR, THE ORGANIZATION(S) NAMED BELOW, NOR ANY PERSON ACTING ON BEHALF OF ANY OF THEM:

(A) MAKES ANY WARRANTY OR REPRESENTATION WHATSOEVER, EXPRESS OR IMPLIED, (I) WITH RESPECT TO THE USE OF ANY INFORMATION, APPARATUS, METHOD, PROCESS, OR SIMILAR ITEM DISCLOSED IN THIS PACKAGE, INCLUDING MERCHANTABILITY AND FITNESS FOR A PARTICULAR PURPOSE, OR (II) THAT SUCH USE DOES NOT INFRINGE ON OR INTERFERE WITH PRIVATELY OWNED RIGHTS, INCLUDING ANY PARTY'S INTELLECTUAL PROPERTY, OR (III) THAT THIS PACKAGE IS SUITABLE TO ANY PARTICULAR USER'S CIRCUMSTANCE; OR

(B) ASSUMES RESPONSIBILITY FOR ANY DAMAGES OR OTHER LIABILITY WHATSOEVER (INCLUDING ANY CONSEQUENTIAL DAMAGES, EVEN IF EPRI OR ANY EPRI REPRESENTATIVE HAS BEEN ADVISED OF THE POSSIBILITY OF SUCH DAMAGES) RESULTING FROM YOUR SELECTION OR USE OF THIS PACKAGE OR ANY INFORMATION, APPARATUS, METHOD, PROCESS, OR SIMILAR ITEM DISCLOSED IN THIS PACKAGE.

ORGANIZATION(S) THAT PREPARED THIS PACKAGE

Power Generation Technologies

ORDERING INFORMATION

Requests for copies of this package should be directed to the EPRI Distribution Center, 207 Coggins Drive, P.O. Box 23205, Pleasant Hill, CA 94523, (925) 934-4212.

Electric Power Research Institute and EPRI are registered service marks of the Electric Power Research Institute, Inc. EPRI. POWERING PROGRESS is a service mark of the Electric Power Research Institute, Inc.

Copyright © 1999 EPRI, Inc. All rights reserved.

CITATION

This report was prepared by

Power Generation Technologies
200 Tech Center Drive
Knoxville, TN 37912

Principal Investigators

Dr. Jack Missimer, Power Generation Technologies
Keith Gronewold, Power Generation Technologies

This report describes research sponsored by EPRI. The report is a corporate document that should be cited in the literature in the following manner:

Flow Meter Guideline, EPRI, Palo Alto, CA: 1999. Report TR-109634.

REPORT SUMMARY

This document provides help to utility personnel in effectively specifying and implementing the most appropriate flow measurement methodology for a given application. A high level of emphasis is placed on the uncertainty associated with each flow meter covered. The measurement of feedwater flow and similar applications requiring extrapolation of existing test data have specifically been excluded from this guideline.

Background

The issuance of U.S. Nuclear Regulatory Commission (NRC) Generic Letter 89-13, on July 18, 1989, and the conduct of Service Water System Operational and Performance Inspections (SWSOPs) by the NRC, has placed an increased emphasis on the need for flow verification testing to ensure proper flow to all service water system components. As a result (of the SWSOPs), the NRC uncovered weaknesses in the implementation of flow verification programs for:

- Inservice testing (IST) of pumps
- Heat exchanger thermal performance test programs
- Service water flow balancing programs

A predominant weakness is that many plants have instruments that for one reason or the other do not meet specified requirements for accuracy, full-scale range, or both.

Objectives

To provide the engineer who is tasked with providing a flow measurement system specification that will meet the needs of a given application with direction and guidance for the estimate of uncertainty associated with a given flow measurement system.

Approach

The EPRI Plant Support Engineering Program established the Flow Meter Guideline Task Group, which met four times in 1998. The Task Group identified the various types of flow meters encountered within a power plant, reviewed the available literature and uncertainty issues for each, and compiled the best practices to develop this document.

Key Points

- A brief discussion of fluid mechanics, as it applies to incompressible fluid flow in closed conduits, is provided.
- The flow measurement principles of the following fluid meter types are described; differential pressure producers, multiport averaging pitots, pitot traverse, ultrasonic flow meters, dye dilution methods, magnetic flow meters, turbine flow meters, vortex meters, coriolis meters, and variable area flow meters.
- An generic introduction to accuracy, error, and uncertainty is provided.
- Literature that addresses the uncertainty of flow measurement for the selected methods and technologies has been reviewed and presented in a reference document review.
- The generic uncertainty methodology is applied to each of the fluid meter types covered in this guideline. Examples are provided.
- Industry case studies regarding various types of flow meters, and current research regarding upstream flow disturbances are provided in appendices.
- Industry consensus was achieved.

Keywords

Flow meters
Fluid mechanics
Uncertainty analysis
Ultrasonic equipment
Instrumentation
Water flow

ACKNOWLEDGMENTS

The following individuals were ongoing members of Plant Support Engineering's Flow Meter Guideline Task Group. As such, they have made significant contributions to the development of this guide by attending the majority of the task group meetings, reviewing/commenting on various drafts, and writing portions of the document.

George R. Wilhelmsen, Utility Chairman	Commonwealth Edison Co.
Armando Lopez	Advanced Measurement & Analysis Group, Inc.
James B. Nystrom	Alden Research Laboratory, Inc.
Tim Tully	American Electric Power Co., Inc.
William Allen	Baltimore Gas & Electric Co.
Thomas C. Rosetti	Baltimore Gas & Electric Co.
Peter Espina	Controlotron Corp.
David Spitzer	Copperhill and Pointer, Inc.
Joseph P. Logatto	GPU Nuclear, Inc.
Steven Ifft	McCrometer, Inc.
George Mattingly	National Inst. Standards & Technology
Stephen Friedenthal	Proto-Power Corp.
Richard W. Miller	R.W. Miller & Associates
Russell Cobb	Southern California Edison Co.
Steven L. Wisner	Virginia Power
Wayne C. Micheletti	Wayne C. Micheletti, Inc.

CONTENTS

1 INTRODUCTION	1-1
1.1 Background.....	1-1
1.2 Scope	1-3
1.3 Purpose	1-5
1.4 References	1-5
2 FLOW MEASUREMENT PRINCIPLES	2-1
2.1 Principles of Fluid Mechanics.....	2-1
2.1.1 Continuity of Flow Equation	2-1
2.1.2 Bernoulli's Equation of Energy	2-2
2.1.3 Reynolds Number	2-4
2.2 Differential Pressure Producers	2-8
2.2.1 Principle of Measurement.....	2-9
2.3 Multiport Averaging Pitots	2-10
2.3.1 Principle of Measurement.....	2-10
2.4 Pitot Tube Traverse	2-12
2.4.1 Principle of Measurement.....	2-12
2.5 Ultrasonic Flow Meters.....	2-13
2.5.1 Principle of Measurement.....	2-13
2.5.1.1 Transit-Time Ultrasonic Flow Meters	2-14
2.5.1.2 Cross-Correlation Ultrasonic Flow Meters	2-15
2.6 Dye Dilution Methods.....	2-17
2.6.1 Principle of Measurement.....	2-17
2.7 Magnetic Flow Meters.....	2-18
2.7.1 Principle of Measurement.....	2-18
2.8 Turbine Flow Meters	2-20

2.8.1 Principle of Measurement.....	2-20
2.9 Vortex Meters	2-21
2.9.1 Principle of Measurement.....	2-21
2.10 Coriolis Meters	2-22
2.10.1 Principle of Measurement.....	2-22
2.11 Variable Area Meters	2-25
2.11.1 Principle of Measurement.....	2-25
2.12 Flow Meter Performance vs. Cost.....	2-27
2.13 References	2-29
3 UNCERTAINTY	3-1
3.1 Introduction To Accuracy, Error, and Uncertainty	3-1
3.2 Pre-Test Uncertainty Analysis.....	3-1
3.2.1 Test Error	3-2
3.2.1.1 Precision Errors.....	3-2
3.2.1.2 Bias Errors	3-3
3.2.1.3 Classification of Errors	3-4
3.2.1.4 Combined Error Model	3-6
3.2.2 Test Uncertainty	3-6
3.2.3 Identify Elemental Sources of Precision and Bias Uncertainty	3-8
3.2.3.1 Precision Uncertainty	3-8
3.2.3.2 Bias Uncertainty	3-8
3.2.3.2.1 Analytical Bias Uncertainty	3-8
3.2.3.2.2 Measurement Bias Uncertainty	3-9
3.2.4 Evaluate Elemental Sources of Precision Uncertainty	3-10
3.2.4.1 Post-Test Evaluation	3-10
3.2.4.2 Pre-Test Evaluation.....	3-14
3.2.5 Evaluation of Sources of Bias Uncertainty	3-16
3.2.5.1 Analytical Bias Uncertainty	3-18
3.2.5.2 Measurement Bias Uncertainty	3-18
3.2.5.2.1 Instrument Bias Uncertainty	3-18
3.2.5.2.2 Measurement Methodology Bias Uncertainty	3-19
3.2.5.2.3 Spatial Bias Uncertainty	3-20
3.2.6 Conduct Sensitivity Analysis	3-24

3.2.6.1 Analytical Determination of Sensitivity Coefficients	3-25
3.2.6.2 Numerical Determination of Sensitivity Coefficients	3-28
3.2.7 Combine Sources of Uncertainty.....	3-29
3.2.7.1 Precision Uncertainty	3-30
3.2.7.2 Bias Uncertainty	3-31
3.2.7.2.1 Independent Elemental Bias Uncertainties.....	3-31
3.2.7.2.2 Dependent (Correlated) Elemental Bias Uncertainties	3-32
3.2.7.3 Overall Uncertainty of Result.....	3-34
3.3 Manufacturing Considerations	3-35
3.4 Installation Considerations.....	3-35
3.5 Calibration Considerations.....	3-36
3.6 Flow Meter Integrity Considerations.....	3-37
3.7 Spatial Considerations.....	3-37
3.8 Non-Homogeneous Flow Considerations	3-37
3.9 References	3-38
4 REFERENCE DOCUMENT REVIEW	4-1
4.1 Introduction.....	4-1
4.2 Differential Pressure Producers	4-2
4.2.1 General Discussion	4-2
4.2.2 Reference 1, ANSI/ASME. MFC-3M-1989. Measurement of Fluid Flow in Pipes Using Orifice, Nozzle, and Venturi.....	4-4
4.2.2.1 Uncertainty Methodology.....	4-4
4.2.2.2 General Discussion	4-4
4.2.3 Reference 2, ISO 5167-1980. Measurement of Fluid Flow by Means of Orifice Plates, Nozzles and Venturi Tubes Inserted in Circular Cross-Section Conduits Running Full.....	4-5
4.2.3.1 Uncertainty Methodology.....	4-5
4.2.3.2 General Discussion	4-5
4.2.4 Reference 3, ASME. Part II of ASME Fluid Meters, Their Theory and Application, Sixth Edition.....	4-6
4.2.4.1 Uncertainty Methodology.....	4-6
4.2.4.2 General Discussion	4-6
4.2.5 Reference 4, R. Miller. Flow Measurement Engineering Handbook, Third Edition	4-7
4.2.5.1 Uncertainty Methodology.....	4-7

4.2.5.2 General Discussion	4-7
4.2.6 Reference 5, ASME. PTC 6 Report - 1985, Guidance for Evaluation of Measurement Uncertainty in Performance Tests of Steam Turbines	4-8
4.2.6.1 Uncertainty Methodology.....	4-8
4.2.6.2 General Discussion	4-8
4.2.7 Reference 31, Southwest Research Institute Report. Baseline and Installation Effects of the V-Cone Meter.....	4-9
4.2.7.1 Uncertainty Methodology.....	4-9
4.2.7.2 General Discussion	4-9
4.3 Multiport Averaging Pitot Tubes.....	4-9
4.3.1 General Discussion	4-9
4.3.2 Reference 4, R. Miller. Flow Measurement Engineering Handbook, Third Edition.....	4-11
4.3.2.1 Uncertainty Methodology.....	4-11
4.3.2.2 General Discussion	4-11
4.3.3 Reference 9, Dieterich Standard Corporation. Annubar [®] Handbook.....	4-11
4.3.3.1 Uncertainty Methodology.....	4-11
4.3.3.2 General Discussion	4-11
4.4 Pitot Traverses.....	4-12
4.4.1 General Discussion	4-12
4.4.2 Reference 13, Cooling Tower Institute Bulletin. STD-146(95). Standard for Water Flow Measurement	4-13
4.4.2.1 Uncertainty Methodology.....	4-13
4.4.2.2 General Discussion	4-14
4.4.3 Reference 20, Power Generation Technologies Technical Paper. Uncertainty Analysis of Cooling Tower Performance, Presented at the CTI Winter Meeting	4-14
4.4.3.1 Uncertainty Methodology.....	4-14
4.4.3.2 General Discussion	4-14
4.4.4 Reference 27, ISO. ISO 3966-1977. Measurement of Fluid Flow in Closed Conduits - Velocity Area Method Using Pitot Static Tubes.....	4-14
4.4.4.1 Uncertainty Methodology.....	4-14
4.4.4.2 General Discussion	4-15
4.5 Ultrasonic Flow Meters.....	4-15
4.5.1 General Discussion	4-15

4.5.2 Reference 10, ANSI/ASME. MFC-5M-1985. Measurement of Liquid Flow in Closed Conduits Using Transit-Time Ultrasonic Flow Meters.....	4-16
4.5.2.1 Uncertainty Methodology.....	4-16
4.5.2.2 General Discussion	4-17
4.5.3 Reference 11, L. Lynnworth. Ultrasonic Measurements for Process Control, Theory Techniques, Applications	4-17
4.5.3.1 Uncertainty Methodology.....	4-17
4.5.3.2 General Discussion	4-17
4.5.4 Reference 26, Rabensteine and Arnsdorff. Flow Determination by Acoustic Transit Times	4-18
4.5.4.1 Uncertainty Methodology.....	4-18
4.5.4.2 General Discussion	4-18
4.5.5 Reference 28, ISO. ISO Technical Report 12765:1997 (E). Measurement of Fluid Flow in Closed Conduits - Method Using Transit Time Ultrasonic Flowmeters	4-19
4.5.5.1 Uncertainty Methodology.....	4-19
4.5.5.2 General Discussion	4-19
4.5.6 Reference 14, Beck and Plaskowski. Cross-Correlation Flow Meters.....	4-20
4.5.6.1 Uncertainty Methodology.....	4-20
4.5.6.2 General Discussion	4-20
4.5.7 Reference 15, Gurevitch et al. Theory and Application of Non-invasive Ultrasonic Cross Correlation Flow Meter. The 9 th International Conference on Flow Measurement	4-21
4.5.7.1 Uncertainty Methodology.....	4-21
4.5.7.2 General Discussion	4-21
4.5.8 Reference 29, CROSSFLOW [®] - Users Guide for Ultrasonic Flow Measurement	4-21
4.5.8.1 Uncertainty Methodology.....	4-21
4.5.8.2 General Discussion	4-21
4.6 Dye Dilution Methods.....	4-21
4.6.1 General Discussion	4-21
4.6.2 Reference 16, W.H. Morgan, et al. Validation of the Use of the Dye Dilution Method for Flow Measurement in Large Open and Closed Channel Flows	4-23
4.6.2.1 Uncertainty Methodology.....	4-23
4.6.2.2 General Discussion	4-24
4.6.3 Reference 17, Nystrom and Hecker. Uncertainty Analysis of Field Turbine Performance Measurements	4-24
4.6.3.1 Uncertainty Methodology.....	4-24

4.6.3.2 General Discussion	4-24
4.6.4 Reference 18, Hennon and McNutt. Pre-Test Uncertainty Analysis for Dye Dilution Flow Measurement.....	4-24
4.6.4.1 Uncertainty Methodology.....	4-24
4.6.4.2 General Discussion	4-24
4.7 Magnetic Flow Meters.....	4-25
4.7.1 General Discussion	4-25
4.7.2 Reference 4, R. Miller. Flow Measurement Engineering Handbook, Third Edition.....	4-26
4.7.2.1 Uncertainty Methodology.....	4-26
4.7.2.2 General Discussion	4-27
4.7.3 Reference 8, D. Spitzer. Flow Measurement.....	4-27
4.7.3.1 Uncertainty Methodology.....	4-27
4.7.3.2 General Discussion	4-29
4.7.4 Reference 22, ANSI/ASME. MFC-16M-1995. Measurement of Fluid Flow in Closed Conduits by Means of Electromagnetic Flowmeters	4-30
4.7.4.1 Uncertainty Methodology.....	4-30
4.7.4.2 General Discussion	4-30
4.8 Turbine Flow Meters	4-30
4.8.1 General Discussion	4-30
4.8.2 Reference 4, R. Miller. Flow Measurement Engineering Handbook.....	4-32
4.8.2.1 Uncertainty Methodology.....	4-32
4.8.2.2 General Discussion	4-32
4.8.3 Reference 8, D. Spitzer. Flow Measurement.....	4-32
4.8.3.1 Uncertainty Methodology.....	4-32
4.8.3.2 General Discussion	4-32
4.8.4 Reference 19, ANSI/ISA-RP31.1-1977. Specification, Installation, and Calibration of Turbine Flowmeters.....	4-33
4.8.4.1 Uncertainty Methodology.....	4-33
4.8.4.2 General Discussion	4-33
4.8.5 Reference 21, EG&G Flow Technology. FT Series Turbine Flowmeter Installation Operation, and Maintenance Manual, TM-86675.....	4-33
4.8.5.1 Uncertainty Methodology.....	4-33
4.8.5.2 General Discussion	4-33
4.9 Vortex Meters	4-34

4.9.1 General Discussion	4-34
4.9.2 Reference 4, R. Miller. Flow Measurement Engineering Handbook.....	4-35
4.9.2.1 Uncertainty Methodology.....	4-35
4.9.2.2 General Discussion	4-36
4.9.3 Reference 7, D. Spitzer. Industrial Flow Measurement	4-37
4.9.3.1 Uncertainty Methodology.....	4-37
4.9.3.2 General Discussion	4-37
4.9.4 Reference 8, D. Spitzer. Flow Measurement.....	4-37
4.9.4.1 Uncertainty Methodology.....	4-37
4.9.4.2 General Discussion	4-38
4.10 Coriolis Meters	4-38
4.10.1 General Discussion	4-38
4.10.2 Reference 4, R. Miller. Flow Measurement Engineering Handbook.....	4-39
4.10.2.1 Uncertainty Methodology.....	4-39
4.10.2.2 General Discussion	4-39
4.10.3 Reference 8, D. Spitzer. Flow Measurement.....	4-40
4.10.3.1 Uncertainty Methodology.....	4-40
4.10.3.2 General Discussion	4-40
4.10.4 Reference 23, ANSI/ASME. MFC-11M-1989. Measurement of Fluid Flow by Means of Coriolis Mass Flowmeters.....	4-41
4.10.4.1 Uncertainty Methodology.....	4-41
4.10.4.2 General Discussion	4-41
4.11 Variable Area Flow Meters.....	4-41
4.11.1 General Discussion	4-41
4.11.2 Reference 3, ASME. ASME Fluid Meters, Their Theory and Application	4-42
4.11.2.1 Uncertainty Methodology.....	4-42
4.11.2.2 General Discussion	4-42
4.11.3 Reference 4, R. Miller. Flow Measurement Engineering Handbook.....	4-43
4.11.3.1 Uncertainty Methodology.....	4-43
4.11.3.2 General Discussion	4-43
4.11.4 Reference 7, D. Spitzer. Industrial Flow Measurement	4-44
4.11.4.1 Uncertainty Methodology.....	4-44
4.11.4.2 General Discussion	4-44
4.12 References	4-45

5 APPLICATION OF METHODOLOGY	5-1
5.1 Overview.....	5-1
5.1.1 Primary Elements.....	5-1
5.1.2 Secondary Elements.....	5-2
5.2 Differential Pressure Producer.....	5-2
5.2.1 Influence Factors.....	5-2
5.2.1.1 Manufacturing Considerations.....	5-3
5.2.1.2 Installation Considerations	5-3
5.2.1.3 Measurement Loop Considerations	5-3
5.2.1.4 Calibration Considerations	5-3
5.2.1.5 Instrument Integrity Consideration	5-4
5.2.1.6 Spatial Consideration	5-4
5.2.2 Example of Uncertainty Methodology.....	5-4
5.2.2.1 Define the Measurement Process	5-5
5.2.2.2 Identification of Elemental Bias Uncertainty Sources	5-6
5.2.2.3 Identification of Elemental Precision Uncertainty Sources	5-7
5.2.2.4 Evaluation of Elemental Bias Uncertainty Sources	5-7
5.2.2.5 Evaluation of Elemental Precision (Random) Uncertainty Sources.....	5-10
5.2.2.6 Overall Uncertainty of Result.....	5-11
5.3 Multiport Averaging Pitot Tube.....	5-12
5.3.1 Influence Factors.....	5-12
5.3.1.1 Manufacturing Considerations.....	5-12
5.3.1.2 Installation Considerations	5-12
5.3.1.3 Measurement Loop Considerations	5-12
5.3.1.4 Calibration Considerations	5-12
5.3.1.5 Instrument Integrity Consideration	5-13
5.3.1.6 Spatial Consideration	5-13
5.3.2 Example of Uncertainty Methodology.....	5-13
5.3.2.1 Definition of Measurement Process.....	5-14
5.3.2.2 Identification of Elemental Bias Uncertainty Sources	5-15
5.3.2.3 Identification of Elemental Precision Uncertainty Sources	5-15
5.3.2.4 Evaluation of Elemental Bias Uncertainty Sources	5-15
5.3.2.5 Evaluation of Elemental Precision Uncertainty Sources.....	5-18
5.3.2.6 Evaluate Sensitivity Coefficients	5-18

5.3.2.7 Evaluate Uncertainty of Result	5-21
5.4 Pitot Tube Traverses.....	5-22
5.4.1 Influence Factors.....	5-22
5.4.1.1 Manufacturing Considerations.....	5-22
5.4.1.2 Installation Considerations	5-22
5.4.1.3 Measurement Loop Considerations	5-22
5.4.1.4 Calibration Considerations	5-22
5.4.1.5 Instrument Integrity Consideration	5-23
5.4.1.6 Spatial Consideration	5-23
5.4.1.7 Nonhomogeneous Flow	5-23
5.4.2 Example of Uncertainty Methodology.....	5-23
5.4.2.1 Definition of Measurement Process.....	5-24
5.4.2.2 Identification of Elemental Bias Uncertainty Sources	5-25
5.4.2.3 Identification of Elemental Precision Uncertainty Sources	5-25
5.4.2.4 Evaluation of Elemental Bias Uncertainty Sources	5-25
5.4.2.5 Evaluation of Elemental Precision Uncertainty Sources.....	5-27
5.4.2.6 Evaluate Sensitivity Coefficients	5-27
5.4.2.7 Evaluate Uncertainty of Result	5-28
5.5 Ultrasonic Flow Meters.....	5-29
5.5.1 Influence Factors.....	5-29
5.5.1.1 Manufacturing Considerations.....	5-29
5.5.1.2 Installation Considerations	5-29
5.5.1.3 Calibration Considerations	5-30
5.5.1.4 Meter Integrity Considerations	5-30
5.5.1.5 Spatial Considerations	5-30
5.5.1.6 Nonhomogeneous Flow Considerations.....	5-31
5.5.2 Example of Uncertainty Methodology.....	5-31
5.5.2.1 Define the Measurement Process	5-33
5.5.2.2 Identification of Elemental Bias Uncertainty Sources	5-34
5.5.2.3 Identification of the Elemental Precision Uncertainty Sources	5-35
5.5.2.4 Evaluation of the Elemental Bias Uncertainty Sources	5-35
5.5.2.4.1 Calibration Bias Uncertainty	5-35
5.5.2.4.2 Pipe Outside Diameter Uncertainty	5-35
5.5.2.4.3 Wall Thickness Uncertainty	5-36

5.5.2.4.4 Transducer Spacing Uncertainty	5-37
5.5.2.4.5 Pipe Sound Speed Uncertainty	5-38
5.5.2.4.6 Fluid Kinematic Viscosity Uncertainty	5-38
5.5.2.4.7 Measurement Loop Uncertainty	5-39
5.5.2.5 Evaluate Sensitivity Coefficients	5-39
5.5.2.6 Evaluate Bias Uncertainty	5-40
5.6 Dye Dilution Methods.....	5-41
5.6.1 Influence Factors.....	5-41
5.6.1.1 Dye Injection Considerations.....	5-41
5.6.1.2 Sample Extraction Considerations	5-41
5.6.1.3 Concentration Analysis Considerations.....	5-42
5.6.1.4 Interference Considerations	5-42
5.6.2 Example of Uncertainty Methodology.....	5-42
5.6.2.1 Definition of Measurement Process.....	5-42
5.6.2.2 Identification of Elemental Bias Uncertainty Sources	5-46
5.6.2.3 Identification of Elemental Precision Uncertainty Sources	5-46
5.6.2.4 Evaluation of Elemental Bias Uncertainty Sources	5-47
5.6.2.4.1 Dye Injection Rate Uncertainty	5-47
5.6.2.4.2 Sample Concentration Bias Uncertainty	5-48
5.6.2.4.3 Density Measurement Uncertainty.....	5-52
5.6.2.5 Evaluation of Elemental Precision Uncertainty Sources.....	5-53
5.6.2.5.1 Injection Rate Precision Uncertainty.....	5-53
5.6.2.5.2 Sample Concentration Precision Uncertainty	5-53
5.6.2.5.3 Calibration Sample Measurement Precision Uncertainty.....	5-53
5.6.2.5.4 Test Data Precision Uncertainty	5-54
5.6.2.5.5 Density Measurement Precision Uncertainty	5-55
5.6.2.6 Evaluate Sensitivity Coefficients	5-55
5.6.2.6.1 Dye Injection Rate Sensitivity Coefficient	5-55
5.6.2.6.2 Sample Dilution Sensitivity Coefficient	5-55
5.6.2.6.3 Corrected Sample Measurement Sensitivity Coefficient.....	5-56
5.6.2.6.4 Dilution Ratio Sensitivity Coefficients	5-57
5.6.2.6.5 Standard Measurement Sensitivity Coefficients	5-57
5.6.2.7 Evaluate Uncertainty of Result	5-57
5.7 Magnetic Flow Meters.....	5-59

5.7.1 Influence Factors.....	5-60
5.7.1.1 Manufacturing/Specification Considerations	5-60
5.7.1.2 Installation Considerations	5-60
5.7.1.3 Measurement Loop Considerations	5-60
5.7.1.4 Calibration Considerations	5-61
5.7.1.5 Instrument Integrity Considerations.....	5-61
5.7.1.6 Spatial Considerations	5-61
5.7.1.7 Nonhomogeneous Flow Considerations.....	5-61
5.7.2 Example of Uncertainty Methodology.....	5-62
5.7.2.1 Define the Measurement Process	5-62
5.7.2.2 Identification of Elemental Bias Uncertainty Sources	5-62
5.7.2.3 Identification of Elemental Precision Error Sources.....	5-63
5.8 Turbine Meters.....	5-64
5.8.1 Influence Factors.....	5-64
5.8.1.1 Manufacturing Considerations.....	5-64
5.8.1.2 Installation Considerations	5-64
5.8.1.3 Measurement Loop Considerations	5-64
5.8.1.4 Calibration Considerations	5-64
5.8.1.5 Instrument Integrity Considerations.....	5-65
5.8.1.6 Spatial Considerations	5-65
5.8.1.7 Non-Homogeneous Flow Considerations.....	5-65
5.8.2 Example of Uncertainty Methodology.....	5-65
5.8.2.1 Define the Measurement Process	5-66
5.8.2.2 Identification of Elemental Bias Uncertainty Sources	5-66
5.8.2.3 Identification of Elemental Precision Uncertainty Sources	5-66
5.8.2.4 Evaluation of Elemental Bias Uncertainty Sources	5-67
5.8.2.4.1 Calibration Accuracy Uncertainty.....	5-67
5.8.2.4.2 Blade Condition Uncertainty	5-67
5.8.2.4.3 Installation Effect Uncertainty	5-68
5.8.2.4.4 Signal Conditioning Uncertainty	5-68
5.8.2.5 Evaluation of Elemental Precision Uncertainty Sources.....	5-68
5.8.2.6 Evaluate Sensitivity Coefficients	5-68
5.8.2.6.1 Sensitivity Coefficient for the K-Factor.....	5-68
5.8.2.6.2 Sensitivity Coefficient for the Frequency	5-69

5.8.2.7 Evaluate Uncertainty of Result	5-69
5.9 Vortex Meters	5-71
5.9.1 Influence Factors.....	5-71
5.9.1.1 Manufacturing/Specification	5-71
5.9.1.2 Installation Considerations	5-71
5.9.1.3 Measurement Loop Considerations	5-72
5.9.1.4 Calibration Considerations	5-72
5.9.1.5 Instrument Integrity Considerations.....	5-72
5.9.1.6 Spatial Considerations	5-72
5.9.2 Application of Methodology	5-72
5.9.2.1 Define the Measurement Process	5-72
5.9.2.2 Identification of Elemental Bias Uncertainty Sources	5-73
5.9.2.3 Identification of Elemental Precision Uncertainty Sources	5-73
5.10 Coriolis Meters	5-74
5.10.1 Influence Factors.....	5-74
5.10.1.1 Manufacturing/Specification Considerations	5-74
5.10.1.2 Installation Considerations	5-74
5.10.1.3 Measurement Loop Considerations	5-75
5.10.1.4 Calibration Considerations	5-75
5.10.1.5 Instrument Integrity Considerations.....	5-75
5.10.1.6 Spatial Considerations	5-75
5.10.1.7 Nonhomogeneous Flow Considerations.....	5-75
5.11 Variable Area Flowmeters.....	5-76
5.11.1 Influence Factors.....	5-76
5.11.1.1 Manufacturing/Specification Considerations	5-76
5.11.1.2 Installation Considerations	5-76
5.11.1.3 Measurement Loop Considerations	5-76
5.11.1.4 Calibration Considerations	5-77
5.11.1.5 Instrument Integrity Considerations.....	5-77
5.11.1.6 Spatial Considerations	5-77
5.11.2 Example of Uncertainty Methodology.....	5-77
5.11.2.1 Define the Measurement Process	5-77
5.11.2.2 Identification of Elemental Bias Uncertainty Sources	5-78
5.11.2.3 Identification of Elemental Precision Uncertainty Sources	5-78

5.12 References	5-78
6 APPENDIX A: NOMENCLATURE.....	6-1
6.1 Statistical Nomenclature	6-1
6.2 Engineering Nomenclature	6-2
7 APPENDIX B: GLOSSARY	7-1
7.1 General Terms	7-1
7.2 Flow Meter Terms	7-3
8 APPENDIX C: WEIGH TANK CALIBRATION OF ULTRASONIC AND PITOT TUBE FLOW METERS IN SIMULATED COOLING WATER PIPING.....	8-1
9 APPENDIX D: CALIBRATION OF A 16” V-CONE SPOOL PIECE	9-1
10 APPENDIX E: CROSS-CORRELATION ULTRASONIC FLOWMETER EVALUATION TESTS	10-1
11 APPENDIX F: ULTRASONIC FLOWMETER SITE SETUP	11-1
12 APPENDIX G: FLOW METER INSTALLATION EFFECTS.....	12-1
Pipeflow Downstream of a Reducer and Its Effects on Flowmeters.....	12-1
Effects of Pipe Elbows and Tube Bundles on Selected Types of Flowmeters	12-20
13 APPENDIX H: USE OF TIMED ACCUMULATION METHODOLOGY TO DETERMINE FLOW TO SAFETY-RELATED COMPONENTS	13-1

LIST OF FIGURES

Figure 2-1 Continuity of Flow	2-2
Figure 2-2 Bernoulli's Energy Relationship	2-4
Figure 2-3 The Three Flow Regimes: a) Laminar, b) Transitional, and c) Turbulent.....	2-5
Figure 2-4 Laminar Profile	2-7
Figure 2-5 Turbulent Profile	2-7
Figure 2-6 Orifice Meter	2-8
Figure 2-7 Venturi Tube.....	2-8
Figure 2-8 Flow Nozzle	2-9
Figure 2-9 V-Cone Meter	2-9
Figure 2-10 Annubar Diamond II Averaging Pitot Tube	2-11
Figure 2-11 Simplex Pitot Tube	2-12
Figure 2-12 Transit Time Ultrasonic Method (Wetted Transducer)	2-14
Figure 2-13 Transit Time Ultrasonic Method (Clamp-On Transducer)	2-15
Figure 2-14 Cross-Correlation Ultra Sonic Method	2-16
Figure 2-15 Principle of Operation for a Magnetic Flowmeter.....	2-19
Figure 2-16 Turbine Meter	2-20
Figure 2-17 VonKarman Vortex Street Formation Downstream of a Bluff Body	2-21
Figure 2-18 Relationship Between Strouhal and Reynolds Numbers	2-22
Figure 2-19 Principle of Operation for a Coriolis Flowmeter.....	2-24
Figure 2-20 Components of a Variable Area Flow Meter.....	2-26
Figure 5-1 Acoustic Path Geometry for "Clamp-On" Ultrasonic Meter	5-32
Figure 8-1 Test Fittings, Spool Pieces, and Instruments	8-7
Figure 8-2 Ultrasonic Flow Meter Performance with K-Factors = 1000.....	8-8
Figure 8-3 Ultrasonic Flow Meter K-Factors Adjusted.....	8-8
Figure 8-4 Pitot Tube Performance.....	8-8
Figure 9-1 V-Cone Meter Installation	9-5
Figure 9-2 Straight Line Piping	9-6
Figure 9-3 Downstream Elbow.....	9-7
Figure 9-4 Downstream Tee with Cross Flow	9-8
Figure 9-5 Precision Index of Mean Head	9-29

Figure 10-1 Cross-Correlation Flow Meter Block Diagram	10-3
Figure 10-2 Piping Configuration Diagram.....	10-7
Figure 12-1 Sketch of the Reducer Piping Configurations and the Coordinate System.....	12-3
Figure 12-2 Mean Velocity Profiles of the Streamwise and Vertical Components Downstream of a Reducer vs. the Horizontal Diameter Positions for Re=100,000	12-6
Figure 12-3 Root Mean Square Turbulent Velocity Profiles of the Streamwise and Vertical Components Downstream of a Reducer for Re=100,000.....	12-8
Figure 12-4 Percentage Change in Discharge Coefficient.....	12-10
Figure 12-5 Profile Indexes Downstream of a Reducer for Re=100 000.....	12-14
Figure 12-6 Relationship between the Cd Change and Profile Peakness Index for $\beta=0.75$	12-15
Figure 12-7 Relationship between the Cd Change and Flow Displacement Index for $\beta=0.75$	12-16
Figure 12-8 (a) Single Elbow Configuration; (b) Double Elbow Out-of-Plane Configuration with Spacing, s.....	12-22
Figure 12-9 Vertical, V, and Streamwise, W, Velocity Profiles.....	12-23
Figure 12-10 Swirl Angle Distributions.	12-25
Figure 12-11 Cross-Stream Profiles of the Root Mean Square Values of the Vertical, V', and Streamwise, W', Turbulent Velocity Components.....	12-26
Figure 12-12 Streamwise Distributions of the Mean Swirl Angles for the Single Elbow Configuration and for the Double Elbows Out-of-Plane Configurations.....	12-28
Figure 12-13 Calibration Results for Orifice-Type Meters Installed in Non-Ideal Conditions Downstream of: (a) A Single Elbow; (b) A Closely Coupled Double Elbows Out-of-Plane Configuration	12-32
Figure 12-14 Calibration Results for a Turbine-Type Meter Installed in Non-Ideal Conditions Downstream of Single and Double Elbows Out-of-Plane Configurations ..	12-33
Figure 12-15 Flow Conditioning Arrangements: (a) Tube Bundle Geometry; and (b) Insulation Relative to Elbow Configurations	12-34
Figure 12-16 Vertical, V, and Streamwise, W, Velocity Profiles Upstream and Downstream of: (a) The Single Elbow and (b) The Double Elbows Out-of-Plane Configuration.....	12-36
Figure 12-17 Cross-Stream Profiles of the Root Mean Square Values of the Vertical, V', and Streamwise, W', Turbulent Velocity Components Upstream and Downstream of: (a) The Single Elbow and (b) The Double Elbows.....	12-37
Figure 12-18 Calibration Results for Orifice-Type Meters Installed Downstream of: (a) A Single Elbow and a Tube Bundle Flow Conditioner, and (b) A Closely Coupled Double Elbows Out-of-Plane Configuration and a Tube Bundle Flow Conditioner.....	12-39
Figure 12-19 Calibration Results for a Turbine-Type Meter Installed Downstream of Single and Double Elbows Out-of-Plane Configurations and Tube Bundle Flow Conditioner.....	12-41
Figure 13-1 Setup Diagram.....	13-3

LIST OF TABLES

Table 1-1 Requirements and Guidance on Instrument Accuracy and Range	1-2
Table 2-1 Typical Flowmeter Performance Characteristics.....	2-27
Table 2-2 Typical Flowmeter Installation and Service Characteristics	2-28
Table 3-1 Two-Tailed Student t Values for 95% Confidence	3-12
Table 4-1 Orifice, Nozzle, Venturi Differential, and V-Cone Pressure Producer Influence Variable Reference Matrix.....	4-3
Table 4-2 Multiport Averaging Pitot Tube Influence Variables Reference Matrix	4-10
Table 4-3 Traversing Pitot Tube Influence Variable Reference Matrix.....	4-13
Table 4-4 Transit-Time Ultrasonic Flow Meter Influence Variable Reference Matrix.....	4-16
Table 4-5 Cross-Correlation Ultrasonic Flow Meter Influence Variables Matrix	4-20
Table 4-6 Flow Measurement by Dye Dilution Influence Variable Matrix	4-23
Table 4-7 Magnetic Flow Meter Influence Variable Reference Matrix.....	4-26
Table 4-8 Turbine Flow Meter Influence Variable Reference Matrix	4-31
Table 4-9 Vortex Flow Meter Influence Variable Reference Matrix.....	4-35
Table 4-10 Coriolis Mass Flow Meters Influence Variable Matrix.....	4-39
Table 4-11 Variable Area Flow Meters Influence Variable Reference Matrix.....	4-42
Table 5-1 Uncertainty Due to Upstream Flow Disturbance	5-7
Table 5-2 Uncertainty Due to Downstream Flow Disturbance.....	5-7
Table 5-3 Differential Pressure Transmitter Error Specifications	5-8
Table 5-4 Differential Pressure Transmitter Operating Conditions.....	5-9
Table 5-5 Differential Pressure Transmitter Error Values.....	5-9
Table 5-6 Results of Flow Measurements from Annubar	5-14
Table 5-7 Differential Pressure Transmitter Error Specifications	5-17
Table 5-8 Differential Pressure Transmitter Operating Conditions.....	5-17
Table 5-9 Differential Pressure Transmitter Error Values.....	5-17
Table 5-10 Pitot Tube Traverse Data.....	5-24
Table 5-11 Sensitivity Coefficients.....	5-40
Table 5-12 Sample Measurement, D_s , Uncertainty	5-58
Table 5-13 Overall Measurement Precision Uncertainty	5-59
Table 9-1 Results from Flow Test	9-2

Table 9-2 Mass Uncertainty	9-26
Table 9-3 Time Uncertainty.....	9-26
Table 9-4 Density Uncertainty Percent at 100F	9-26
Table 9-5 Overall Flow Uncertainty (%)	9-27
Table 9-6 Differential Pressure Uncertainty Uncertainties in % of Reading	9-27
Table 9-7 Discharge Coefficient Uncertainty.....	9-27
Table 9-8 Thermal Expansion Factors x 10 ⁻⁶	9-29
Table 9-9 Density of Water and Mercury	9-30
Table 10-1 Operating Conditions.....	10-2
Table 10-2 Performance with Different Flow Rates EdF – Everest Flow Laboratory, Chatou France September 9-10, 1998.....	10-5
Table 10-3 Reproducibility Tests – Flow Rate Constant EdF – Everest Flow Laboratory, Chatou France – September 10, 1998.....	10-6

1

INTRODUCTION

1.1 Background

The issuance of U.S. Nuclear Regulatory Commission (NRC) Generic Letter 89-13 [1], on July 18, 1989, and the conduct of Service Water System Operational and Performance Inspections [2] (SWSOPIs) by the NRC, has placed an increased emphasis on the need for flow verification testing to ensure proper flow to all service water system components. As a result (of the SWSOPIs), the NRC uncovered weaknesses in the implementation of flow verification programs for:

- Inservice testing (IST) of pumps
- Heat exchanger thermal performance test programs
- Service water flow balancing programs

A predominant weakness is that many plants have instruments that for one reason or the other do not meet specified requirements for accuracy, full-scale range, or both. Instrument accuracy and full-scale range limits are both important to ensure that inservice testing of pumps provides accurate and repeatable measurements that facilitate the detection of pump degradation.

10 CFR Part 50 Section 55a [3] mandates that the industry commit to the use of the American Society of Mechanical Engineers (ASME) Boiler and Pressure Vessel Code [4], (the Code), Section XI, Subsections IWP and IWV for guidance in efforts related to the IST of pumps (and valves). The 1989 edition of Section XI specifies further that the rules for the IST of pumps are stated in the ASME/ANSI *Operations and Maintenance (OM) Standards*, Part 6, "Inservice Testing of Pumps in Light Water Reactor Power Plants"[5]. In 1995, the NRC issued NUREG-1482 *Guidelines for the Inservice Testing at Nuclear Power Plants* [6], which further clarified the criterion for IST of safety-related pumps. Section 5.5, "Pump Flow Rate and Differential Pressure Instruments," specifically includes further guidance on the matter of allowable instrument accuracy and range.

Instrument inaccuracy results in uncertainty in the flow measurements. The resultant data scatter may be sufficient to mask changes in pump capability that are indicative of

Introduction

degradation. Excessive uncertainty can also result in deviations in test data that are not due to pump degradation, which may result in a false indication of pump degradation.

According to the Code, inservice testing of pumps constrains measurements associated with service water pump flow to low levels of uncertainty. While not governed by a specific code, service water heat exchanger thermal performance test programs and system flow balance programs also constrain the uncertainties associated with the measurement of service water flows to comparably low levels. Table 1-1 summarizes the key Code requirements and related guidance for IST instrument accuracy and range.

**Table 1-1
Requirements and Guidance on Instrument Accuracy and Range**

Document	Section	Requirement/Guidance
Section XI	IWP-4110	Accuracy of $\pm 2.0\%$ of full-scale for pressure, flow, and speed instruments.
OM-6	4.6.1.1	Accuracy of $\pm 2.0\%$ for pressure, flow, and speed instruments. Accuracies are in percent of full-scale for analog instruments, percent of reading over the calibrated range for digital instruments, and percent of total loop accuracy for a combination of instruments.
Section XI	IWP-4120	The full-scale range of instruments shall be three times the reference value or less.
OM-6	4.6.1.1	The full-scale range of each analog instrument shall not be greater than three times the reference value. Digital instruments shall be selected so that the reference value does not exceed 70% of the calibrated range.
NUREG-1482	5.5.1	The range of an installed instrument may be greater than three times the reference value if the instrument is more accurate than that required and the combination of range and accuracy yields a reading at least equivalent to the reading achieved from instruments that meet the Code requirements.
NUREG-1482	5.5.2	When using digital flow and pressure instruments, follow the accuracy and range requirements of OM-6 even if the Code of record is Section XI. Relief need not be requested from IWP if the requirements of OM-6 are met.
NUREG-1482	5.5.4	The accuracy of analog instruments applies only to the calibration of the instrument. However, when test results indicate a change, the staff recommends that the Owner consider phenomena that could affect the indication other than pump degradation.

The uncertainties associated with many permanently installed flow meters, however, do not meet the stringent requirements imposed on these applications. Often, these meters are not calibrated to the required accuracy or are not installed in suitable locations. Furthermore, the performance of such meters degrades over time due to

erosion of the flow element, accumulation of debris inside the pipe or on the flow element, or blockage of pressure-sensing ports.

For plants in which permanent flow meters have not been installed in suitable locations for monitoring and trending individual components, it has become common to use temporary test instrumentation or special measurement methodologies. Such special measurement methodologies include retractable Annubars[®], ultrasonic flow meters, and dye dilution flow measurements. These nonpermanent methodologies are often used in less than ideal circumstances, resulting in loss of accuracy. As evidence of their concern, the NRC has issued notices regarding problems in the industry, in particular with ultrasonic flow meter applications. Examples of these notices include:

- NRC Information Notice 95-08: "Inaccurate Data Obtained with Clamp-On Ultrasonic Flow Measurement Instruments" [7]
- NRC Information Notice 96-16: "BWR Operation with Indicated Flow Less Than Natural Circulation" [8]
- NRC Information Notice 97-90: "Use of Non-Conservative Acceptance Criteria in Safety Related Pump Surveillance Tests" [9]

1.2 Scope

The focus of this guideline is to assess the resources and references that are readily available for the flow measurement instruments listed below. In this document, one will find instruments, such as differential pressure producers, that have a wealth of pertinent empirical information regarding their inherent uncertainties and studies that have been conducted in order to quantify the effect of various influence variables, such as upstream flow disturbances, on the overall flow measurement uncertainty.

This guideline will specifically address the following flow measurement systems and techniques to the extent that relevant information exists:

- Differential pressure producers
 - Orifices
 - Flow nozzles
 - Venturi tubes
 - V-cone meters
- Multiport averaging pitot tubes

Introduction

- Pitot tube traverse
- Ultrasonic meters
 - Transit-time
 - Cross-correlation
- Dye dilution methods
- Magnetic meters
- Turbine meters
- Vortex meters
- Coriolis meters
- Variable area meters

Several issues specific to uncertainty are addressed where information exists, including:

- Uncertainties associated with the manufacturing process of the flow element
- Uncertainties associated with the installation of the flow element
- Calibration uncertainties
- Uncertainties associated with the integrity of the flow element that can be addressed by inspection
- Uncertainties associated with the extent to which the reading of the flow element is representative of a spatial average of the velocity
- Uncertainties associated with entrained air flow

Finally, it is important to note that this guideline is not intended to address those flow situations, as are typically found in feedwater and condensate applications, that require extrapolation of existing test data or experience. Examples requiring extrapolation would include determination of flow coefficients for ultrasonic flow meters or the discharge coefficients of throat tap nozzles at Reynolds numbers beyond the capability of existing calibration facilities ($R_d > 7,500,000$)¹. Guidance for these cases may be found in ASME PTC 6 -1996 "Steam Turbines" [10].

¹ Typical operating temperature and stream velocities found in service water systems would not result in Reynolds numbers that would exceed existing calibration capabilities and experience.

1.3 Purpose

It is the intent and purpose of this guideline to provide the engineer who is tasked with providing a flow measurement system specification that will meet the needs of a given application with direction and guidance for the estimate of uncertainty associated with a given flow measurement system.

Due to the plethora of instruments and available resources, the engineer can easily become overwhelmed with the task of selecting a system that will provide the accuracy to meet Section XI requirements and not be capital intensive. Additionally, the flow metering system must provide long-term reliability and accuracy of data needed for ongoing programs required by regulatory mandate, such as IST of safety-related pumps.

The purpose of this guideline, simply stated, is to:

- Provide the engineer with a document that addresses, in a consistent format, the references that provide guidance in estimating the uncertainty of several flow measurement systems, in both a quantitative and qualitative manner
- Provide the engineer with an abstract of the references available for each type of flow metering system defined in the scope
- Answer the engineer's question...."How do I pull these references together to get an objective and comprehensive assessment of the path I need to follow in order to accurately measure flows and estimate the overall uncertainty associated with the flow measurement?"

In an effort to help utility personnel effectively specify and implement the most appropriate measurement methodology for a given application, EPRI has developed this *Flow Meter Guideline*. The guideline brings together presentations drawn from first-hand industrial experience through discussions of key published technical resources to provide a desktop reference for issues involving flow metering in power plants.

1.4 References

1. United States Nuclear Regulatory Commission. Generic Letter 89-13. "Service Water System Problems Affecting Safety-Related Equipment," 1989.
2. United States Nuclear Regulatory Commission. Temporary Instruction 2515/118. "Service Water System Operational Performance Inspection (SWOPI)," 1992.
3. *Code of Federal Regulations*, Title 10, Section 50.55a, 1989.

Introduction

4. The American Society of Mechanical Engineers. *Boiler and Pressure Vessel Code*. Section XI, Subsection IWP. 1989.
5. The American Society of Mechanical Engineers. ASME OM-6. "Inservice Testing of Pumps in Light Water Reactor Power Plants," Part 6. *Standards and Guides for Operation and Maintenance of Nuclear Power Plants*, 1989.
6. United States Nuclear Regulatory Commission. *Guidelines for Inservice Testing at Nuclear Power Plants*. NUREG-1482. 1995.
7. United States Nuclear Regulatory Commission. NRC Information Notice 95-08. "Inaccurate Data Obtained with Clamp-On Ultrasonic Flow Measurement Instruments," 1995.
8. United States Nuclear Regulatory Commission. NRC Information Notice 96-16. "BWR Operation with Indicated Flow Less Than Natural Circulation," 1996.
9. United States Nuclear Regulatory Commission. NRC Information Notice 97-90. "Use of Non-Conservative Acceptance Criteria in Safety Related Pump Surveillance Tests." 1997.
10. The American Society of Mechanical Engineers. ANSI/ASME PTC-6 - 1976 (Reaffirmed 1996). *Steam Turbines*. 1997.

2

FLOW MEASUREMENT PRINCIPLES

A brief discussion of fluid mechanics, as it applies to incompressible fluid flow in closed conduits, is contained in this section, leading into individual discussions of the basic measurement principles associated with each of the flow measurement techniques addressed by this guideline.

2.1 Principles of Fluid Mechanics

The basis for the flow of fluids, as it applies to the majority of flow meters, can be derived using the following basic concepts of energy and physical properties:

- The continuity of flow equation
- Bernoulli's equation of energy
- Density
- Viscosity

For the scope of this guideline, the condition that the fluid is incompressible is assumed.

2.1.1 Continuity of Flow Equation

The continuity of flow equation has as its basis the conservation of matter, since fluids are comprised of matter. Consider at two discrete points along the axis of flow, the average values for the parameters \dot{m} , ρ_1 , v_1 , D_1 , and ρ_2 , v_2 , D_2 as shown in Figure 2-1.

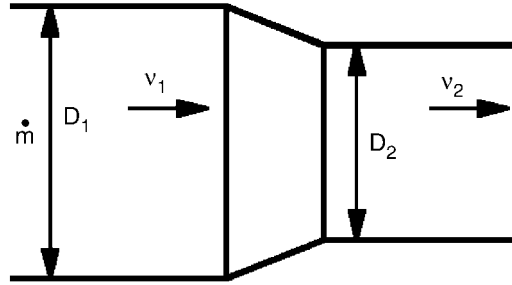


Figure 2-1
Continuity of Flow

The relationship exists such that the mass of the fluid flowing in the pipe at plane 1 is equal to the mass of fluid flowing in the pipe at plane 2 and can be expressed as:

$$\dot{m} = \rho_1 v_1 \frac{\pi D_1^2}{4} = \rho_2 v_2 \frac{\pi D_2^2}{4} \quad (\text{Eq. 2-1})$$

where,

- \dot{m} = mass flow of fluid
- v = average velocity of fluid
- D = diameter at measurement plane
- ρ = mass density of fluid

If, at both planes 1 and 2, the density remains unchanged, then eq. 2-1 reduces to:

$$v_1 A_1 = v_2 A_2 \quad (\text{Eq. 2-2})$$

rearranging eq. 2-2 yields,

$$v_1 = v_2 \frac{A_2}{A_1} \quad (\text{Eq. 2-3})$$

2.1.2 Bernoulli's Equation of Energy

The conservation of energy theory states that the change in total energy, per unit mass, is equal to the work done on it plus the heat added plus any change in gravitational potential and, when compatible units are used, can be expressed as:

$$(E_{k_2} + E_{i_2}) - (E_{k_1} + E_{i_1}) = (\rho_1 v_1 - \rho_2 v_2) + (Z_1 - Z_2) + \dot{Q}_h \quad (\text{Eq. 2-4})$$

where, when using compatible units,

E	=	total energy of fluid
p	=	internal pressure of fluid
v	=	specific volume of fluid
Z	=	elevation of fluid
\dot{Q}_h	=	heat input to fluid

The subscripts “k” and “i” denote kinetic and internal, respectively.

Several assumptions will now be made in order to simplify eq. 2-4 to serve the purposes of this guideline:

- The fluid exhibits fully developed, non-viscous flow across the normal diameter of the flow stream.
- There is no heat added to the fluid between planes 1 and 2.
- There is no change in elevation or temperature of the fluid between planes 1 and 2.
- The pipe is running full.

The energy balance now reduces to:

$$\frac{v_2^2}{2g_c} - \frac{v_1^2}{2g_c} = \frac{p_1}{\rho_1} - \frac{p_2}{\rho_2} \quad (\text{Eq. 2-5})$$

rearranging eq. 2-5 yields,

$$\frac{v_2^2}{2g_c} + \frac{p_2}{\rho_2} = \frac{v_1^2}{2g_c} + \frac{p_1}{\rho_1} \quad (\text{Eq. 2-6})$$

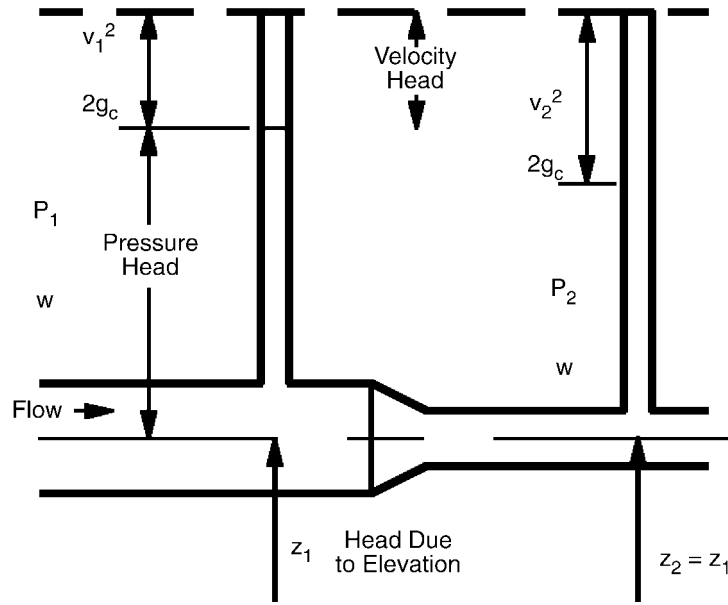


Figure 2-2
Bernoulli's Energy Relationship

Substitution of eq. 2-3 and rearranging provides the following equation:

$$v_2^2 = 2g_c \left(\frac{\Delta p_{1-2}}{\rho} \right) \left[\frac{1}{1 - \left(\frac{A_2}{A_1} \right)^2} \right] \quad (\text{Eq. 2-7})$$

Note that it is the fluid velocity that the majority of the flow elements described in this guideline are measuring. Upon determination of the velocity, the volumetric flow can be easily calculated knowing the normal, cross-sectional area of the measurement plane.

2.1.3 Reynolds Number

In order to investigate the flows of fluids, Osborne Reynolds conducted a group of experiments that included injecting a thin stream of dye into the center of a flowing stream of incompressible fluid. The parameters of fluid velocity and viscosity were varied, and the manner in which the dye behaved in the flow stream was observed. Reynolds observed three strikingly different phenomena of the dye stream traveling in the fluid, which he called:

- Laminar
- Transitional
- Turbulent

He concluded from his observations that in laminar flow the viscous forces of the fluid dominated the inertial forces, and in turbulent flow the inertial forces dominated the viscous forces. Figure 2-3 depicts the three behaviors observed by Reynolds.

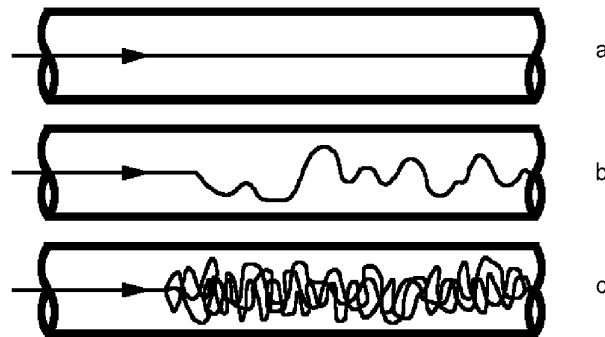


Figure 2-3
The Three Flow Regimes: a) Laminar, b) Transitional, and c) Turbulent

Reynolds postulated that for an incompressible fluid there are three forces acting in equilibrium: inertial (dynamic) forces, viscous (internal friction) forces, and pressure (internal) forces. Further, the only forces that are necessary to consider are inertial and viscous, since the three forces are in equilibrium and can be constrained with only two. Reynolds determined that a significant ratio would be that of the inertial to viscous forces.

The inertial forces are proportional to the mass of the fluid multiplied by the acceleration and can be expressed dimensionally as:

$$\text{inertial} \propto \text{volume} * \text{density} * (\text{velocity} / \text{time}) \quad (\text{Eq. 2-8})$$

or

$$\text{inertial} \propto \frac{L^3 \rho v}{T} = \frac{L^3 \rho v}{L/v} = L^2 \rho v^2 \quad (\text{Eq. 2-9})$$

Flow Measurement Principles

where,

v = fluid velocity (L/T)

L = length (diameter)

ρ = fluid density (M/L³)

T = time

In a similar manner, the viscous forces are proportional to the viscous shear stress (S) times the characteristic length (L) squared. Expressed mathematically:

$$\text{viscous} \propto SL^2 = \mu vL \quad (\text{Eq. 2-10})$$

The result of his experiments and the analysis of his work yielded a dimensionless number, the Reynolds number (Re), that defines in which regime the flow is operating. The Reynolds number is expressed mathematically as:

$$\text{Re} = \frac{\text{inertial}}{\text{viscous}} = \frac{\rho v D}{\mu}$$

where, when compatible units are used,

Re = Reynolds number

ρ = fluid density

D = characteristic dimension of the flow conduit (normal diameter)

μ = absolute fluid viscosity

v = average fluid velocity

Further experiments demonstrated that the two major flow regimes, laminar and turbulent, demonstrate a very characteristic velocity profile, as shown below.

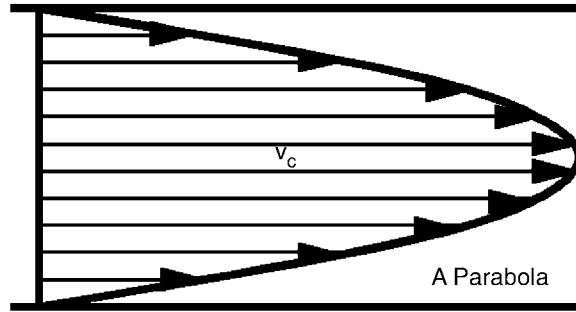


Figure 2-4
Laminar Profile

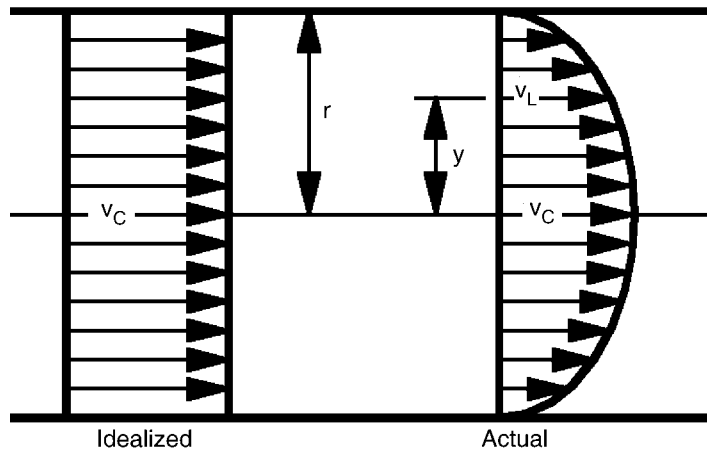


Figure 2-5
Turbulent Profile

The vast majority of service water flow falls into the turbulent regime.

2.2 Differential Pressure Producers

Figures 2-6 through 2-9 illustrate the differential pressure producers discussed in this guideline.

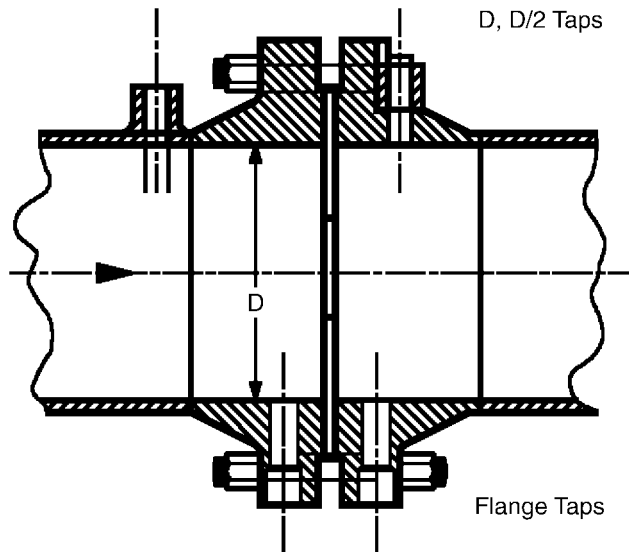


Figure 2-6
Orifice Meter

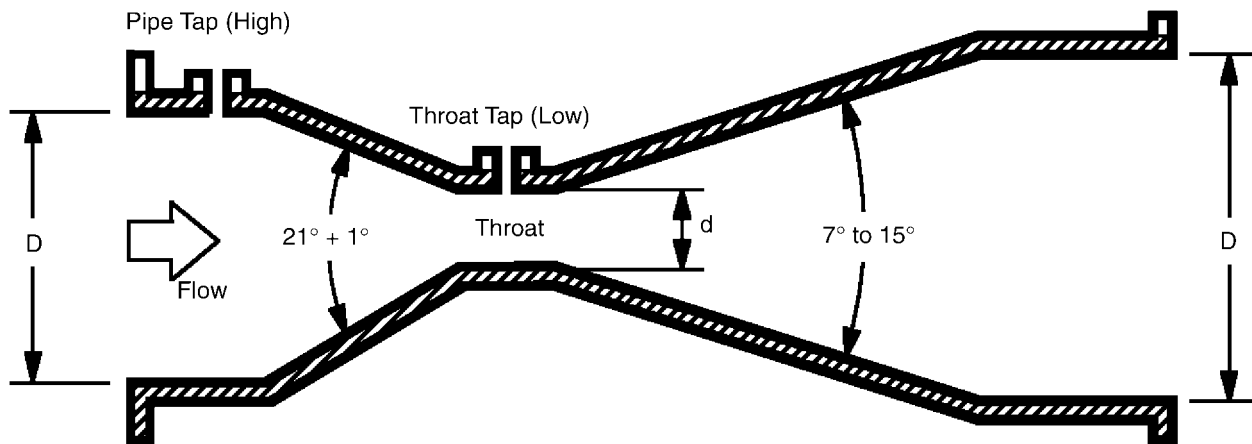


Figure 2-7
Venturi Tube

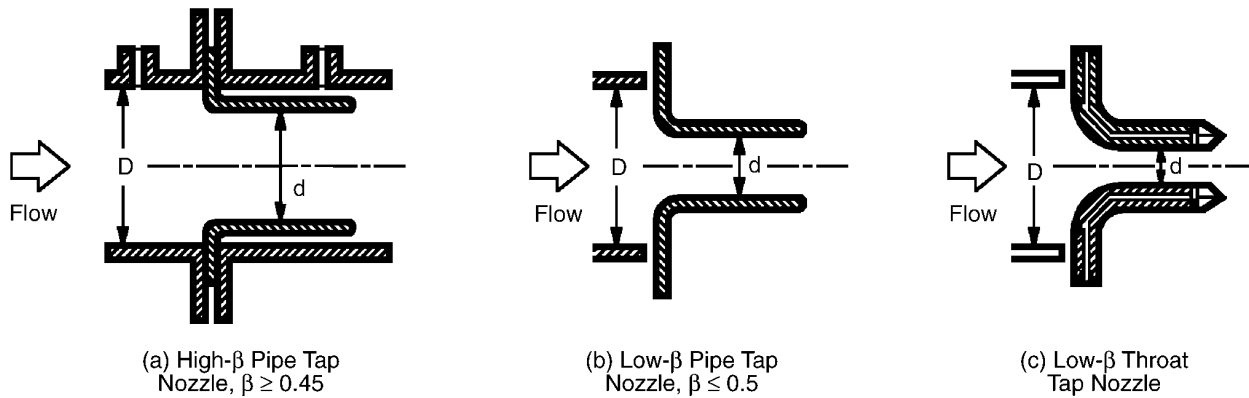


Figure 2-8
Flow Nozzle

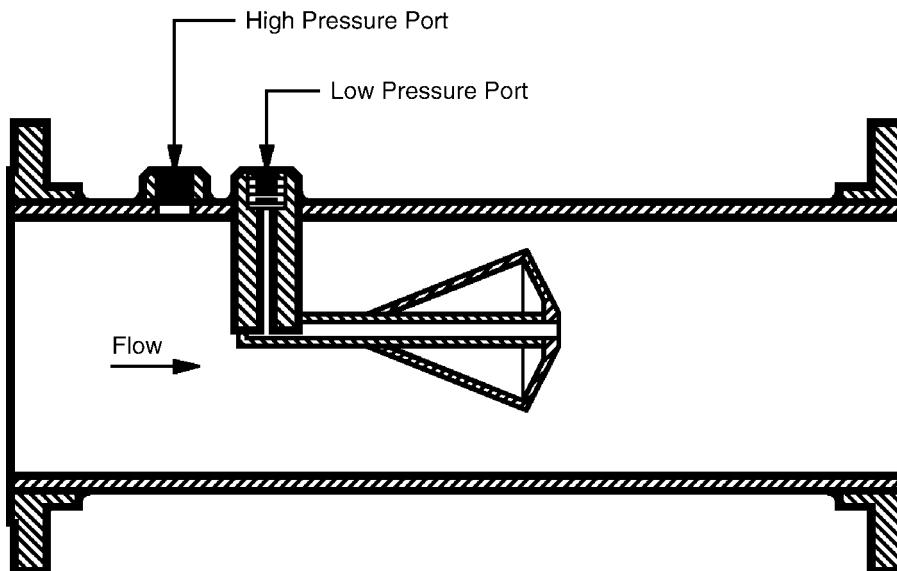


Figure 2-9
V-Cone Meter

2.2.1 Principle of Measurement

The principle of measurement is based on the introduction of a differential pressure producer (orifice, nozzle, or Venturi) into a pipe through which a fluid is running full. The introduction of the differential pressure producer creates a dynamic pressure difference between the upstream and downstream side of the device. The square root of the differential pressure is proportional to the velocity of the fluid. Differential pressure-producing flow meters determine an area average throat velocity from the measured pressure differential in the following manner:

$$q = C_d * K * A * \sqrt{\frac{\Delta p}{\rho}} \quad (\text{Eq. 2-11})$$

where, when using compatible units yields,

q	=	volumetric flow
C_d	=	discharge coefficient
C	=	conversion coefficient
d	=	diameter of throat
B	=	normal, cross-sectional area at measurement plane
Δp	=	pressure differential
ρ	=	density of the flowing fluid

The constant K includes values for the ratio of the cross-sectional area of the pipe to the restriction cross-sectional area¹ and dimensional conversion constants. The accuracy of all differential pressure meters depends on a stable, fully developed velocity profile and an accurate measurement of both the pipe and the restriction diameters. Distortion of the velocity profile, due to upstream disturbances or any change in the pipe or restriction dimensions due to scaling or erosion, negatively impacts the accuracy of the flow measurement.

References 1–6 and 31 provide additional information regarding the principles of flow measurement using differential pressure producers.

2.3 Multiport Averaging Pitots

2.3.1 Principle of Measurement

The principle of measurement is based on a determination of the area averaged velocity of the flow in a pipe through which fluid is running full. The multiport averaging pitot allows the measurement of differential pressure between the high upstream pressure

¹ The ratio of the small diameter to the large diameter (β ratio) differs for the V-cone meter and is expressed as $(1 - (d_{\text{cone}}^2 / D_{\text{pipe}}^2))^{0.5}$.

(also called the impact or stagnation pressure) and the lower downstream pressure (also called the suction pressure since it is lower than the pipe static pressure).

The multiport averaging pitot operates similar to a classical pitot tube, with the following exceptions:

- Instead of a static wall tap, an averaging pitot senses low pressure on the downstream side of the tube, increasing the net differential pressure measured by the flow element.
- The multiport averaging pitot has multiple ports (some types have multiple ports on both the upstream and downstream sides) which are located in such a manner that if weighted equally will be representative of the average flow in the pipe.
- Certain types of multiport averaging pitot tubes have a non-circular shape in order to negate boundary layer separation problems associated with cylindrical-shaped averaging pitot tubes. This design tends to provide a consistent point of separation over a large range of Reynolds numbers.

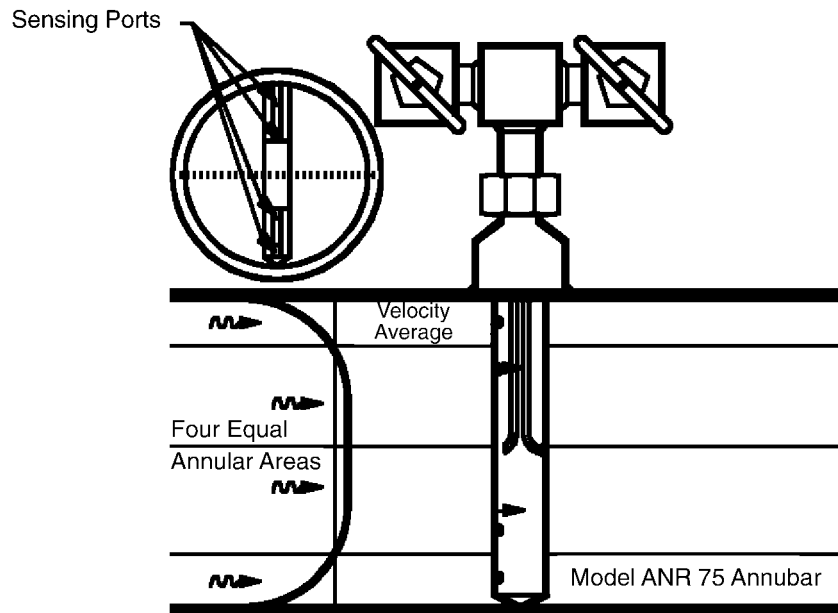


Figure 2-10
Annubar Diamond II Averaging Pitot Tube

The governing flow equation for a multiport averaging pitot tube can be expressed as:

$$q = K * A * \sqrt{\frac{\Delta p}{\rho}} \quad (\text{Eq. 2-12})$$

where, when using compatible units,

- q = volumetric flow
- K = flow coefficient
- A = normal, cross-sectional area of pipe at measurement location
- Δp = pressure differential
- ρ = fluid density

References 4 and 9 provide additional information regarding the principles of flow measurement using multiport averaging pitot systems.

2.4 Pitot Tube Traverse

2.4.1 Principle of Measurement

The principle of measurement for a pitot tube traverse is based on the integration of equal annular area point velocities over the flow area. This method provides, as a result, the average flow through the pipe, given the pipe is full. The pitot tube traverse method is used extensively in the cooling tower industry to accurately determine the flow of water in the riser pipes of both natural and mechanical draft cooling towers. The pitot tube traverse is based on a minimum of two perpendicular traverses of the pipe diameter. This methodology is intended to accurately provide an average fluid velocity profile at the measurement plane. Figure 2-11 illustrates a typical Simplex pitot tube design.

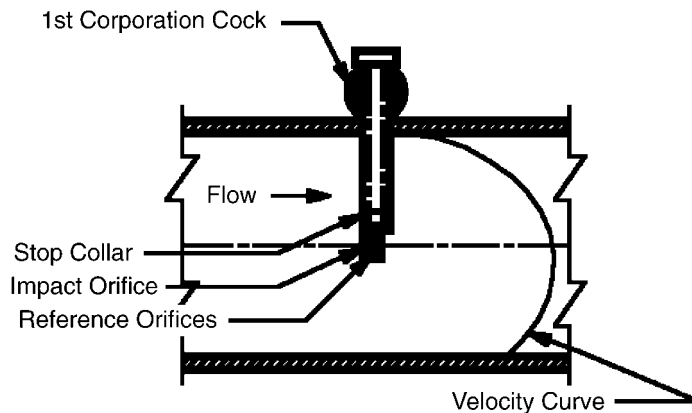


Figure 2-11
Simplex Pitot Tube

Eqs. 2-13 and 2-14 indicate the relationships used to determine the fluid flow from the measured parameters, using an air over water manometer:

$$q = C * A \int (v) dA \quad (\text{Eq. 2-13})$$

Each individual point velocity in the traverse is evaluated from:

$$v = [2g_c \Delta h ((\rho_{mf} - \rho_{ff}) / \rho_{ff})]^{0.5} \quad (\text{Eq. 2-14})$$

where, when using compatible units,

q	=	volumetric flow
C	=	flow coefficient
A	=	normal, cross-sectional area at measurement plane
v	=	equal area point velocity
g _c	=	gravitational constant
Δh	=	manometer deflection
ρ _{mf}	=	metering fluid density
ρ _{ff}	=	flowing fluid density

References 13, 20, and 27 provide additional information regarding the principles of flow measurement using the pitot tube traverse method.

2.5 Ultrasonic Flow Meters

2.5.1 Principle of Measurement

Ultrasonic flow meters operate by transmitting an ultrasonic signal into a flow stream to determine the velocity of the fluid. The velocity is then converted to a volumetric flow measurement using the flow area dimensions and flow profile coefficient. The following types of ultrasonic flow meters are in use for measurement of flow in closed conduits:

Flow Measurement Principles

- Transit time
- Cross-correlation
- Doppler

Although all methods have been demonstrated to provide a viable means of measuring fluid flow, the transit-time and cross-correlation methods have the most applicability for the measurement of service water flow and will be the topics discussed in this guideline.

2.5.1.1 Transit-Time Ultrasonic Flow Meters

The principle of measurement for transit-time ultrasonic flow meters is the measurement of the difference in travel time between an ultrasonic signal transmitted upstream and downstream in a fluid flow. The ultrasonic waves are transmitted across a closed conduit, between an upstream and downstream transducer. The resulting average fluid velocity along the ultrasonic path is determined from the time difference and multiplied by a correction factor to account for the assumed velocity profile. Use of both the upstream and downstream transit times allows determination of both the sound speed and the average axial flow velocity.

Transit-time ultrasonic flowmeter systems may be configured in either a “wetted” transducer arrangement, shown in Figure 2-12, which requires that a spool-piece be inserted into the existing pipe, or a “clamp-on” transducer arrangement, shown in Figure 2-13, which is a nonintrusive method of obtaining a flow. Both methods utilize the same principles to calculate flow.

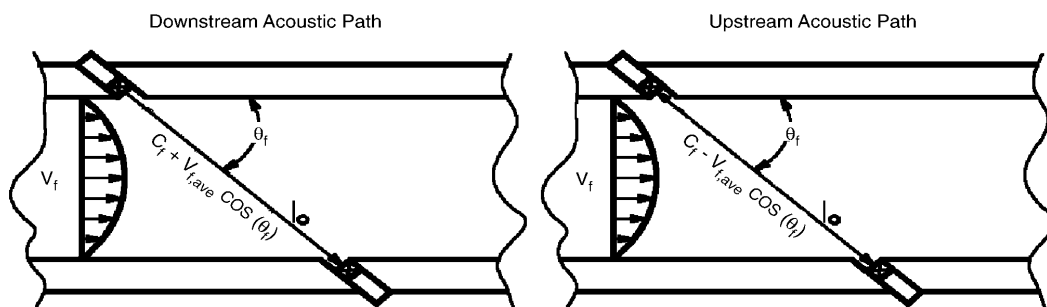


Figure 2-12
Transit-Time Ultrasonic Method (Wetted Transducer)

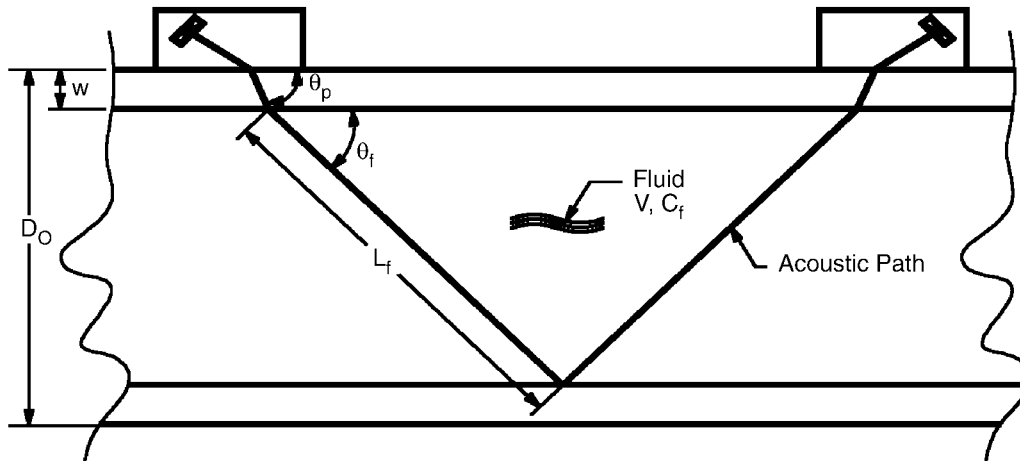


Figure 2-13
Transit-Time Ultrasonic Method (Clamp-On Transducer)

The average flow along the acoustic path for transit-time flow meters can be expressed as:

$$q = K * A * \frac{1}{\cos(\theta_f)} * \left[\left(\frac{1}{t_d} \right) - \left(\frac{1}{t_u} \right) \right] \quad (\text{Eq. 2-15})$$

where, when using compatible components,

- K = flow profile correction factor
- A = normal cross-sectional area at measurement plane
- θ_f = ultrasonic path angle relative to conduit flow axis
- t_d = downstream transit time
- t_u = upstream transit time

2.5.1.2 Cross-Correlation Ultrasonic Flow Meters

The principle of the cross-correlation ultrasonic flow meter system operates by transmitting a beam of ultrasound through the fluid. As a result of discontinuous components or tags, such as gas bubbles, solid particles, etc., the beam is scattered. Furthermore, there are superimposed fluctuations, as in the Doppler effect, caused by turbulent eddies or vortices existing in the flow. The net result is that the received

ultrasound is modulated in both amplitude and phase. This modulation represents a statistically unique “signature.”

A cross-correlation system consists of two sets of transducers, separated by a known distance. Each transducer consists of an ultrasonic transmitter and receiver, which are mounted diametrically on the outside of the pipe as shown in Figure 2-14. As the ultrasonic signal passes through the fluid perpendicular to the direction of flow, turbulent eddies modulate the ultrasound signal. These eddies crossing the upstream and downstream transducers are modulated in the same way but are displaced by the time that it takes for them to pass between the two measurement planes.

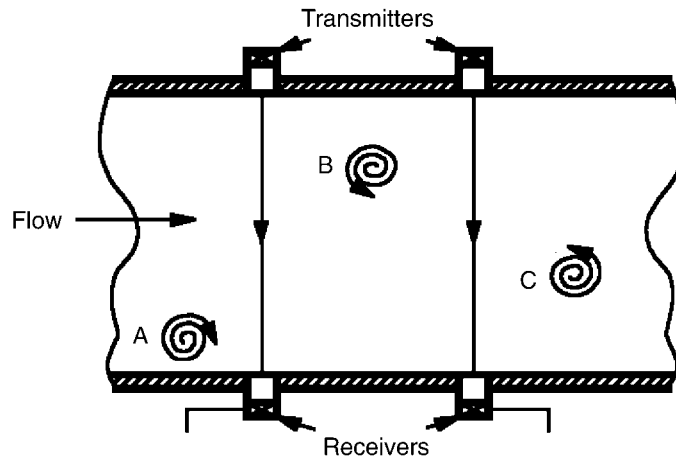


Figure 2-14
Cross-Correlation Ultrasonic Method

In order to evaluate this time delay, a mathematical process called cross-correlation is used. The time delay is calculated from the cross-correlation function:

$$R(\tau) = \int x(t)y(t + \tau)dt \quad (\text{Eq. 2-16})$$

where,

- $R(\tau)$ = cross-correlation function
- $x(t)$ = modulation signals from upstream transducer
- $y(t+\tau)$ = modulation signals from downstream transducer
- t = time
- τ = time delay

The flow in the pipe, q , is then calculated as:

$$q = (\rho * A * L * C_f) / \tau_d \quad (\text{Eq. 2-17})$$

where,

ρ	=	density of fluid
A	=	cross-sectional area of pipe
L	=	distance between transducers
C_f	=	calibration coefficient
τ_d	=	maximum $\{R(\tau)\}$

References 10, 11, 14, 15, 26, 28, and 29 provide additional information regarding the principles of flow measurement using the aforementioned ultrasonic methods.

2.6 Dye Dilution Methods

2.6.1 Principle of Measurement

The overall category for this type of flow measurement is known as tracer dilution; however, for the purposes of this guideline, we will consider the case of the tracer being a fluorescent dye (Rodamine WT, for example, is non-toxic and has been approved by the EPA for water flow measurements). The principle of measurement for the dye dilution method of flow determination is the conservation of mass. The technique consists of injecting a dye solution with an initial concentration (C_{inj}) into the flow stream which is to be measured at a precisely measured rate (\dot{m}_{inj}). At some point downstream, after the dye has fully mixed with the flow, a slipstream is withdrawn from the flow conduit and the resultant concentration of the dye in the sample (C_s) is measured by real time analysis with a fluorometer. The total mass flow rate (\dot{m}_s) can then be calculated from the degree to which the injected dye has been diluted in the flow stream by eq. 2-18:

$$\dot{m}_s = \dot{m}_{inj} * \frac{C_{inj}}{C_s} \quad (\text{Eq. 2-18})$$

where, when compatible units are used,

Flow Measurement Principles

m_s	=	water mass flow
m_{inj}	=	dye injection mass flow
C_s	=	concentration of dye in water
C_{inj}	=	concentration of dye injection

This equation is derived from a mass balance on the injected dye, recognizing that the dye flow rate is very small compared to the water flow rate being measured. Note that the absolute concentrations, C_{inj} and C_s are not required, only their ratio. This concept is important in practical applications of the dye dilution method. In practice, other factors such as temperature and stability of background fluorescence must be taken into account.

There are two discreet methods for this type of flow measurement:

- Slug (batch) injection
- Constant rate injection

Although both methods are considered viable, the constant rate injection is the preferred method when measuring flows encountered in most power stations.

References 16–18 provide additional information regarding the principles of flow measurement using tracer dilution methods.

2.7 Magnetic Flow Meters

2.7.1 Principle of Measurement

The magnetic flow meter is based on Faraday's law of (electro-) magnetic induction. When a conductive fluid passes through an applied magnetic field, a voltage is generated at right angles to the axis of fluid flow and the applied magnetic field. The generated output voltage is a summation of individual voltages generated by differential volumes moving at discreet velocities across the plane of the pipe. In 1961, Shercliff [7] demonstrated that the voltage output signal represents the average velocity for an asymmetric velocity profile. If the magnetic field is constant and the distance between the electrodes is fixed, the induced voltage is directly proportional to the average velocity of the fluid. A depiction of the operational principle is illustrated in Figure 2-15.

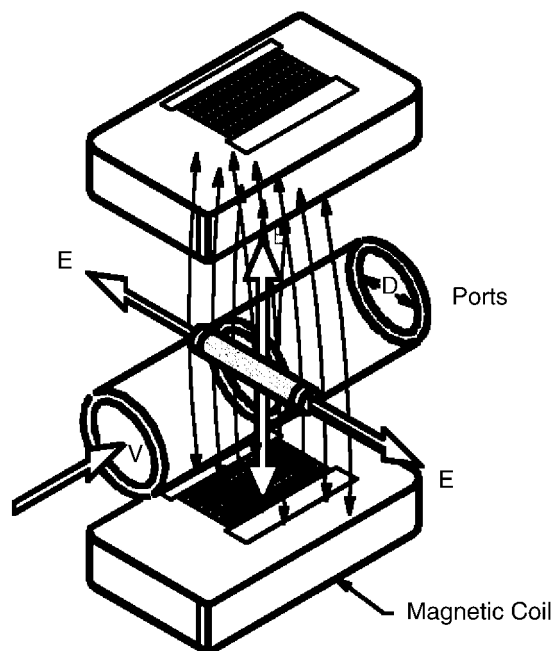


Figure 2-15
Principle of Operation for a Magnetic Flow Meter

Eq. 2-19 expresses the volumetric flow for a circular pipe:

$$q = C * D * \frac{\pi}{4} * \frac{E}{B} \quad (\text{Eq. 2-19})$$

where, when compatible units are employed,

- q = volumetric flow
- C = calibration coefficient
- D = distance between electrodes
- E = signal voltage
- B = magnetic flux density

References 4, 8, and 22 provide additional information regarding the principles of flow measurement using magnetic flowmeters.

2.8 Turbine Flow Meters

2.8.1 Principle of Measurement

The principle of measurement for a turbine flow meter is based on a rotating element, which is positioned in the flow stream such that the rotational speed of the rotor is proportional to the fluid stream velocity and, therefore, the flow through the measurement plane. A turbine flow meter, the primary element, typically outputs a low amplitude frequency signal that is input into a signal conditioner, the secondary element, that converts the meter output to an analog signal proportional to the flow. Each meter has a characteristic K-factor that relates output frequency to a volumetric unit (for example, pulses/gallon or pulses/liter). These types of flow devices are generically categorized as linear flowmeters. A typical turbine flow meter is shown in Figure 2-16:

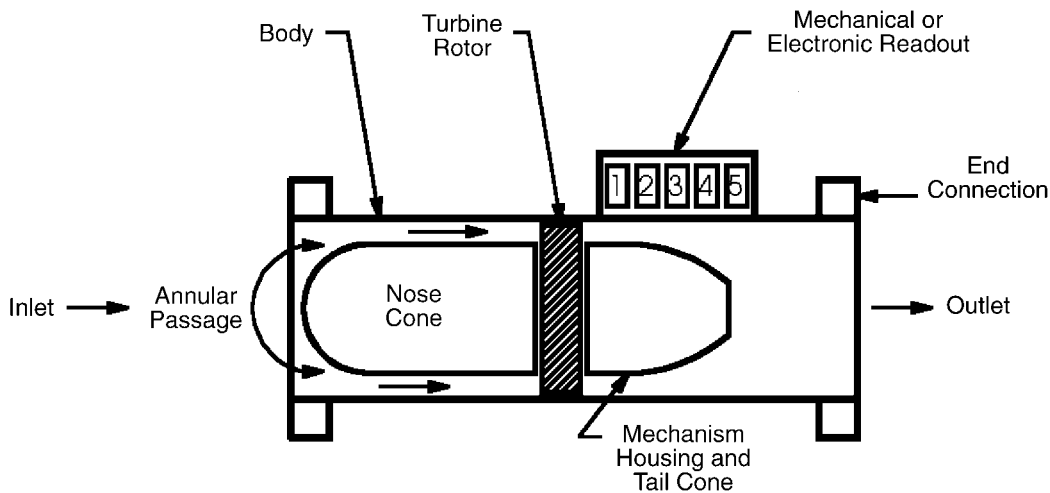


Figure 2-16
Turbine Meter

Eq. 2-20 indicates the relationship developed to determine the volumetric flow through the meter:

$$q = C * \frac{\lambda}{K} \quad (\text{Eq. 2-20})$$

where:

- q = volumetric flow rate
- C = dimensional coefficient

λ = meter output frequency

K = K-factor constant

References 4, 8, 19, and 21 provide additional information regarding the principles of flow measurement using turbine flow meters.

2.9 Vortex Flow Meters

2.9.1 Principle of Measurement

The principle of measurement for a vortex flow meter is based on a phenomenon first explained by VonKarman in 1912 [7]. This phenomenon can be produced when a bluff body is immersed in a steady stream of fluid. As the flow approaches the bluff body, the flow is split into two streams. The instability of the shear layer due to this splitting of the flow causes the fluid to roll up into a well-defined vortex. After formation, the vortex sheds, and a second vortex begins to form on the opposite side of the bluff body. Under steady flow, the time required for the formation of the first vortex and second vortex are the same, with the formation time being proportional to the velocity of the fluid stream. The side-to-side pattern of vortex formation is known as a VonKarman vortex street and is shown in Figure 2-17.

This well-defined shedding and the production of the trailing VonKarman vortex street occurs in the Reynolds number range of $10^2 < Re < 10^7$. The vortex shedding results in velocity and pressure changes downstream of the bluff body element. By placing ultrasonic or pressure transducers downstream of the bluff body or a piezometer imbedded in the bluff body, the vortex shedding frequency can be measured.

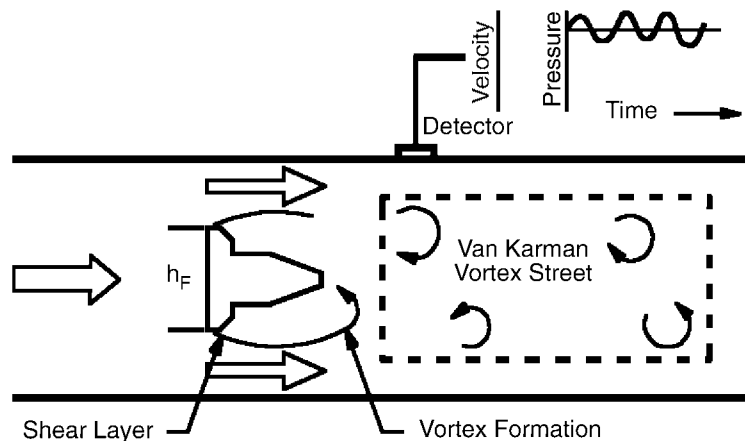


Figure 2-17
VonKarman Vortex Street Formation Downstream of a Bluff Body

Further, this oscillating flow pattern is a function of both the Reynolds and the Strouhal numbers. Depending on the shape of the bluff body, a relatively linear relationship between the Reynolds number and the Strouhal number is depicted in Figure 2-18 below.

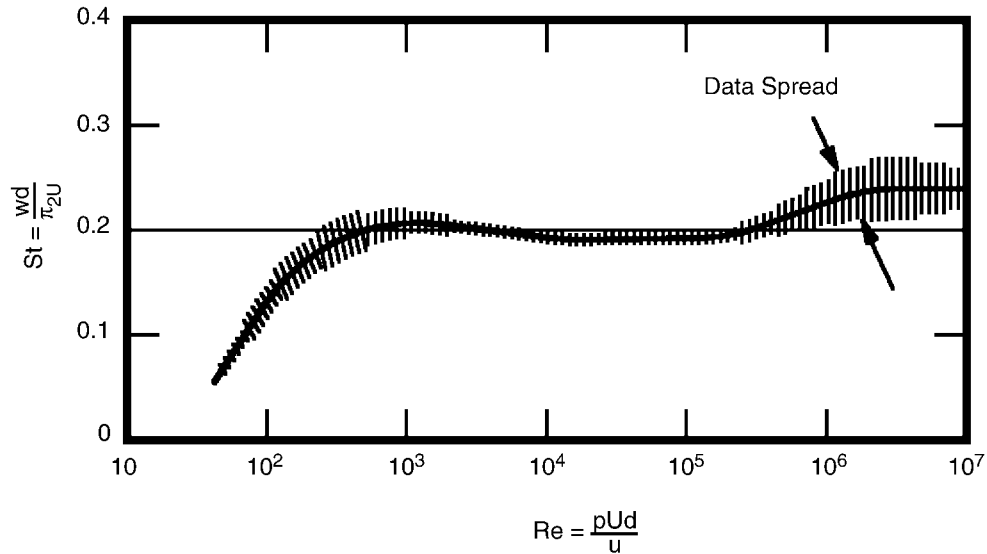


Figure 2-18
Relationship Between Strouhal and Reynolds Numbers

Eq. 2-21 expresses the relationship between the Strouhal number and measurable parameters:

$$q = \frac{\lambda * d}{St} * A \quad (\text{Eq. 2-21})$$

where, when using compatible units,

- q = volumetric flow
- λ = shedding frequency
- d = width of bluff body
- St = Strouhal number
- A = normal, cross-sectional flow area

References 4, 7, and 8 provide additional information regarding the principles of flow measurement using vortex shedding flow meters.

2.10 Coriolis Flow Meters

2.10.1 Principle of Measurement

The principle of measurement for the Coriolis mass flow meter is based on the concept of an element of fluid traveling at constant velocity in a pipe. This element of fluid exhibits zero acceleration since the velocity is constant. If the pipe were rotated at the same time that the element of fluid passes through, then a Coriolis acceleration component would be produced on the fluid. The Coriolis acceleration component produces a force on the pipe that is proportional to the mass flow rate and as such is the measured value in this type of flow meter. The Coriolis force is induced by sinusoidally vibrating the tube in which the fluid is flowing about an axis formed between the inlet and the outlet of the tube, at the natural frequency of the device. On the inlet side of the tube, the flow is away from the axis of rotation; but on the outlet side, the flow is toward the axis of rotation. At any point in time, each half of the tube has a Coriolis acceleration force that is equal, but opposite, in direction.

The governing equation for the measurement of the mass flow of a fluid through the Coriolis flow meter is derived from Newton's Second Law, $F = m \cdot A$. A majority of flow meters using the Coriolis force (torque) principle use a single "U-tube" geometry, which is oscillated and effectively rotated alternately clockwise and counterclockwise. The resultant Coriolis force is then measured by a variety of methods. For example, consider an element of fluid flowing through a tube that is effectively rotating at a constant angular velocity about one end of the assembly. As the segment flows outward from the inlet, the tangential velocity increases, producing an acceleration force that is a result of the Coriolis effect. The direction of the Coriolis force is perpendicular to the flow and the magnitude of the Coriolis force is expressed by:

$$F_c = 2 \cdot m \cdot v_f \cdot \Omega \quad (\text{Eq. 2-22})$$

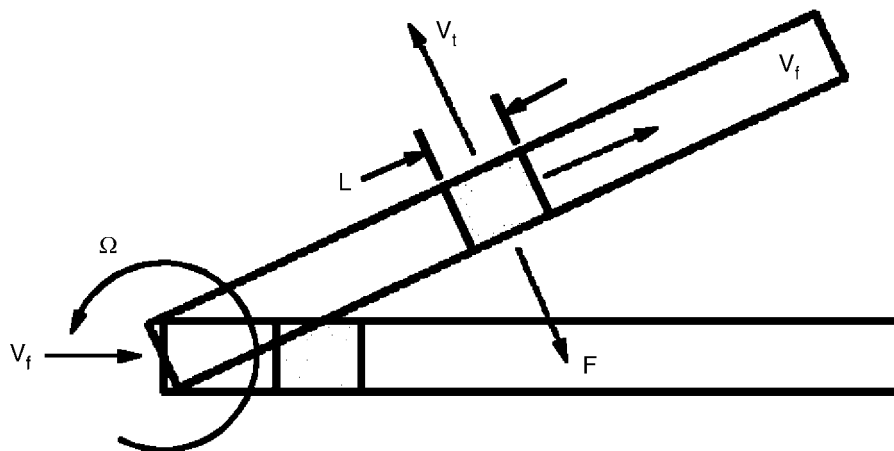


Figure 2-19
Principle of Operation for a Coriolis Flow Meter

where, if compatible units are employed,

- m = mass of fluid element
- v_f = velocity of the fluid
- v_t = tangential velocity of the fluid
- Ω = angular velocity of the tube
- ρ = fluid density
- A = cross-sectional area of flow tube
- L = length of fluid element
- F_c = Coriolis force

The mass flow of a fluid can be expressed as:

$$\dot{m} = \rho * v_f * A \quad (\text{Eq. 2-23})$$

Substitution yields:

$$\dot{m} = \frac{\rho * A * F_c}{2 * \rho * A * L * \Omega} \quad (\text{Eq. 2-24})$$

and, finally:

$$\dot{m} = \frac{F_c}{2 * L * \Omega} \quad (\text{Eq. 2-25})$$

References 4, 8, and 23 provide additional information regarding the principles of flow measurement using Coriolis mass flow meters.

2.11 Variable Area Flow Meters

2.11.1 Principle of Measurement

The principle of measurement for a variable area flow meter is essentially the reverse of a constant area differential producer. Instead of the differential pressure varying with flow through a fixed area, the variable area flow meter utilizes a float that can slide vertically in a tapered cylinder, exposing additional flow area in order to maintain the float in a condition of dynamic balance (for example, the sum of the forces on the float body are zero). Dynamic balance is attained when the weight of the float minus the weight of the fluid that it displaces is equal to the upward force on the float from the velocity pressure of the flowing fluid. The velocity pressure is constant at all flows.

Figure 2-20 depicts the basic components of the variable area flow meter.

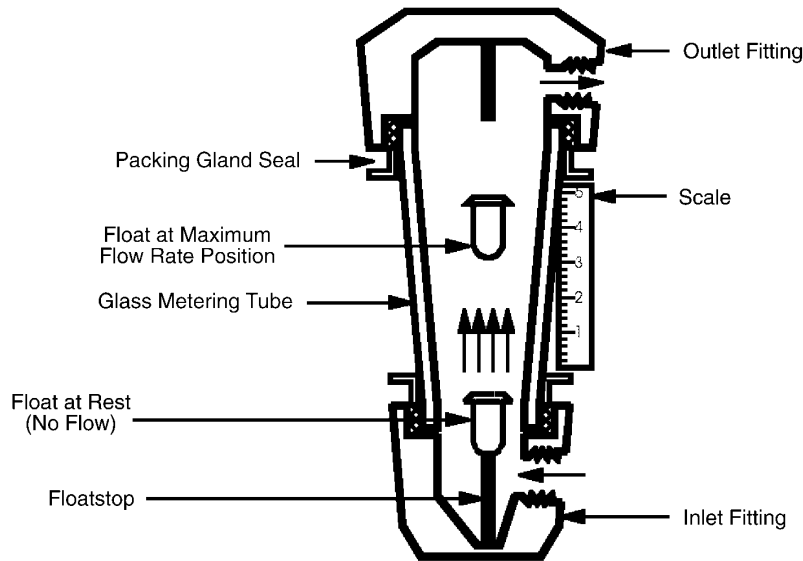


Figure 2-20
Components of a Variable Area Flow Meter

The volumetric flow for this type of meter is expressed below:

$$q = C_d * A \sqrt{\frac{2g_c \rho W_f (\rho_f - \rho)}{\rho_f}} \quad (\text{Eq. 2-26})$$

where, when compatible units are used,

- q = volumetric flow
- C_d = discharge coefficient
- A = normal cross-sectional area
- g_c = gravitational constant
- ρ = density of fluid
- W_f = weight of float
- ρ_f = density of float material

References 3, 4, and 7 provide additional information regarding the principles of flow measurement using variable area flow meters.

2.12 Flow Meter Performance vs. Cost

This section provides the engineer with reference tables that narrow the choices of flow elements for a given application and provide a relative estimate of the cost in an expedient manner.

Table 2-1 provides a comparison between each type of meter based on the performance characteristics.

Table 2-1
Typical Flowmeter Performance Characteristics

Flow Meter	Uncalibrated Accuracy	Rangeability	Cost
Orifice Flow Section	± 0.5 to 2.0%	4:1	\$\$\$
Nozzle Flow Section	± 0.5 to 3.0%	4:1	\$\$\$\$
Venturi Flow Section	± 0.5 to 3.0%	4:1	\$\$\$\$
V-Cone Flow Section	± 0.5 to 1.0%	4:1	\$\$\$
Averaging Pitot Tube	± 1.0%	4:1	\$\$
Ultrasonic (Clamp-On)	± 1.0 to 1.5%	20:1	\$\$\$
Ultrasonic (Wetted)	± 0.5 to 1.0%	30:1	\$\$\$\$
Magnetic	± 0.5%	10:1	\$\$\$\$
Turbine	± 0.5 to 1.0%	10:1 to 30:1	\$\$\$\$\$
Coriolis	± 0.5%	20:1	\$\$\$\$\$+
Vortex	± 0.5 to 1.0%	15:1	\$\$\$\$
Variable Area	± 1.0 to 3.0% of URL	10:1	\$

The cost legend is:

\$	\$0 to \$500	\$\$\$\$	\$5,000 to \$10,000
\$\$	\$500 to \$1,000	\$\$\$\$\$	\$10,000 to \$15,000
\$\$\$	\$1,000 to \$5,000	\$\$\$\$\$+	>\$15,000

Table 2-2 provides guidance on the installation and “inservice” characteristics of the flowmeters.

**Table 2-2
Typical Flowmeter Installation and Service Characteristics**

Flow Meter	Required Upstream Diameters²	Required Downstream Diameters	Fluid Temperature Effect	Permanent Pressure Loss
Orifice Flow Section	10 to 30	5	Yes	Medium
Nozzle Flow Section	5 to 20	5	Yes	Medium
Venturi Flow Section	10 to 30	5	Yes	Low
V-Cone FlowSection	3 to 5	1 to 3	Yes	Medium
Averaging Pitot Tube	10 to 30	5	Yes	Low
Ultrasonic (Clamp-On)	5 to 30	5	Yes	None
Ultrasonic (Wetted)	5 to 30	5	Yes	None
Magnetic	5	3	No	None
Turbine	5 to 10	5	Yes	High
Coriolis	None	None	No	Low
Vortex	10 to 20	5	Yes	Medium
Variable Area	None	None	Yes	Medium

² These values address the range of piping configurations that may be encountered in typical plant installations. If an element is calibrated per ANSI/ASME, MFC-10M, *Methods for Establishing Installation Effects on Flowmeters*, these values would not be pertinent.

2.13 References

1. American National Standards Institute/American Society of Mechanical Engineers. MFC-3M-1989 (Reaffirmed 1995). *Measurement of Fluid Flow in Pipe Using Orifice, Nozzle, and Venturi*. ASME, 1990.
2. International Organization on Standardization. ISO 5167-1980. *Measurement of Fluid Flow by Means of Orifice Plates, Nozzles, and Venturi Tubes Inserted in Circular Cross-Section Conduits Running Full*. ISO, 1981.
3. American Society of Mechanical Engineers. *Part II of ASME Fluid Meters, Their Theory and Application*, Sixth Edition. ASME, 1971.
4. R. Miller. *Flow Measurement Engineering Handbook*, Third Edition. McGraw Hill, 1996.
5. American Society of Mechanical Engineers. *PTC Report - 1985, Guidance for Evaluation of Measurement Uncertainty in Performance Tests of Steam Turbines*. ASME, 1986.
6. American National Standards Institute/American Society of Mechanical Engineers. MFC-2M-1983 (Reaffirmed 1988). *Measurement Uncertainty for Fluid Flow in Closed Conduits*. ASME, 1984.
7. D. Spitzer. *Industrial Flow Measurement*. ISA, 1990.
8. D. Spitzer. *Flow Measurement*. ISA, 1991.
9. Dieterich Standard Corporation. *Annubar Handbook*. Dieterich Standard Corporation, 1993.
10. American National Standards Institute/American Society of Mechanical Engineers. MFC-5M-1985 (Reaffirmed 1994). *Measurement of Liquid Flow in Closed Conduits Using Transit-Time Ultrasonic Flow Meters*. ASME, 1986.
11. L. Lynnworth. *Ultrasonic Measurements for Process Control, Theory, Techniques, Applications*. Academic Press, 1989.
12. *Instrumentation Handbook for Integrated Power Plant Water Management*. EPRI, Palo Alto, CA: 1988. Report CS-5873.
13. Cooling Tower Institute. "Standard for Water Flow Measurement," *CTI Bulletin*, STD-146 (95), 1995.

14. M. S. Beck and A. Plaskowski. *Cross-Correlation Flow Meters*. Adam Hilger, Bristol, England, 1987.
15. Y. Gurevich, A.M. Lopez, R. Flemons, D. Z. Zobin, "Theory and Application of Non-invasive Ultrasonic Cross-Correlation Flowmeter," presented at the 9th International Conference on Flow Measurement, Lund, Sweden (June 1998).
16. W. H. Morgan, *et al*, "Validation of the Use of Dye Dilution Method for Flow Measurement in Large Open and Closed Channel Flows," presented at the NBS Flow Measurement Symposium, Gaithersburg, MD (1977).
17. J. B. Nystrom and G. E. Hecker, "Uncertainty Analysis of Field Turbine Performance Measurements," *Proceedings of an International Conference on Hydropower*, American Society of Civil Engineers, 1985.
18. K. W. Hennon and G. R. McNutt. *Pre-Test Uncertainty Analysis for Dye Dilution Flow Measurement*. Power Generation Technologies Technical Paper. TIN 97-1267.
19. American National Standards Institute/Instrument Society America. RP31.1-1977. *Specification, Installation, and Calibration of Turbine Flowmeters*. ISA, 1977.
20. K. Hennon and D. Wheeler, "*Uncertainty Analysis of Cooling Tower Performance*," Power Generation Technologies Technical Report presented at the Cooling Tower Institute Winter Meeting, 1996.
21. EG&G Flow Technology. *FT Series Turbine Flowmeter Installation, Operation, and Maintenance Manual*. TM-86675, Rev. H-1996.
22. American National Standards Institute/American Society of Mechanical Engineers. MFC-16M-1995. *Measurement of Fluid Flow in Closed Conduits by Means of Electromagnetic Flowmeters*. ASME, 1995.
23. American National Standards Institute/American Society of Mechanical Engineers. MFC-11M-1989 (Reaffirmed 1994). *Measurement of Fluid Flow by Means of Coriolis Mass Flowmeters*. ASME, 1995.
24. Instrument Society of America. 11ISA-RP16.5-1961. *Installation, Operation, and Maintenance Instructions for Glass Tube Variable Area Meters (Rotameters)*. ISA, 1961.
25. American National Standards Institute/American Society of Mechanical Engineers. PTC 6 -1976 (Reaffirmed 1982). *Steam Turbines*. ASME, 1982.
26. J. A. Rabensteine and C. E. Arnsdorf. *Flow Determination by Acoustic Transit Time*. Power Generation Technologies Calculation, 1997.

27. International Organization on Standardization. ISO Standard 3977-1977. *Measurement of Fluid Flow in Closed Conduits - Velocity Method Using Pitot Static Tubes*. ISO, 1997.
28. International Organization on Standardization. ISO Technical Report 12765:1997 (E). *Measurement of Fluid Flow in Closed Conduits - Method Using Transit Time Ultrasonic Flowmeters*. ISO, 1997.
29. Advanced Measurement and Analysis Group, Inc. *CROSSFLOW[®] User Guide for Ultrasonic Flow Measurement*. 1998.
30. International Organization Standardization. ISO-9104:1991. *Measurement of Fluid Flow in Closed Conduits - Methods of Evaluating the Performance of Electromagnetic Flowmeters for Liquids*. ISO, 1991.
31. Southwest Research Institute Report. *Baseline and Installation Effects Tests of the V-Cone Meter*. SRI, 1984.
32. American National Standards Institute/American Society of Mechanical Engineers. MFC-6M-1987. *Measurement of Fluid Flow in Pipes Using Vortex Flow Meters*. ASME, 1987.
33. American National Standards Institute/American Society of Mechanical Engineers. PTC 19.1. *Measurement Uncertainty*. ASME, 1985.
34. American National Standards Institute/American Society of Mechanical Engineers. MFC-10M-1994. *Methods for Establishing Installation Effects on Flowmeters*. ASME, 1994.
35. American National Standards Institute/American Society of Mechanical Engineers. MFC-9M-1988. *Measurement of Liquid Flow in Closed Conduits by Weighing Method*. ASME, 1989.

3

UNCERTAINTY

3.1 Introduction to Accuracy, Error, and Uncertainty

Accuracy is defined as the closeness of agreement between the results of a measurement and the true value of the parameter being measured. The difference between the true value of the parameter and the measured value is the error in the measurement. The uncertainty in a measurement is an estimate of the error.

Given the total population of a parameter, the average measured value, μ , will vary from the true value by an amount equal to the bias error, which is a systematic error that does not vary over the duration of the test. This bias error is estimated by the bias uncertainty. Each individual measurement value will vary from the average, μ , by a random, or precision, error that does vary over the duration of the test. The standard deviation, σ , is a measure of the precision errors. In a normal error distribution, the interval $\mu \pm 2\sigma$ will include approximately 95% of the total scatter of the measurements. The precision uncertainty is an estimate of the interval 2σ [1].

3.2 Pre-Test Uncertainty Analysis

The goal of the pre-test uncertainty analysis is to provide an objective measure of the quality of the test methodology before the test is conducted. As discussed in ANSI/ASME PTC 19.1 [1]:

"It is recommended that an uncertainty analysis always be done before a test . . . This procedure allows corrective action to be taken prior to the test to reduce uncertainties when they are too large or when the difference to be detected in the test is of the same size or smaller than the predicted uncertainty. . ."

The remainder of this section is divided as follows:

- Section 3.2.1 introduces the concept of test error and the types of errors that influence the test result.
- Section 3.2.2 introduces the concept of test uncertainty and outlines the basic approach to the pre-test uncertainty analysis.

Uncertainty

- Sections 3.2.3 through 3.2.7 provide a more detailed discussion of each of the steps of an uncertainty analysis.

3.2.1 Test Error

It is important to realize that all tests are influenced by errors in the analysis and measurements. Since the actual test error cannot be quantified directly, it must be estimated from an evaluation of the many “elemental” error sources that influence the test. These elemental error sources are often classified as either precision (random) or bias (systematic), based on their influence on the test result. The distinction between precision and bias errors is discussed in Sections 3.2.1.1 through 3.2.1.4.

3.2.1.1 Precision Errors

Precision errors are those errors that vary randomly over the duration of the test. Since precision errors vary over the duration of the test, the magnitude of the errors may be observed in the variation or scatter in repeated measurements of a test parameter. Precision errors result from:

- Sources of random variability in each parameter being measured (see the note below)
- Sources of random variability in each component of the measurement system

Note: While random variability in a parameter is in itself not considered error, random variability leads to sampling error, which will be treated in this guideline as a source of precision error. Sampling error is defined as the difference between the average value of a parameter determined from a finite number of discrete measurements and the hypothetical average value of a parameter if the parameter were measured continuously over the duration of the test.

The model for random error is shown in Figure 3-1. Random errors are typically assumed to come from a population of errors that are normally distributed. The population of errors can be described by the mean value of the population, μ , and standard deviation of the population, σ . The mean value of the population is expected to be zero. The area under the curve associated with a range of parameter values equal to $\mu \pm 1\sigma$ is approximately 68% of the total area under the curve. The area under the curve associated with a range of parameter values equal to $\mu \pm 2\sigma$ is approximately 95% of the total area under the curve.

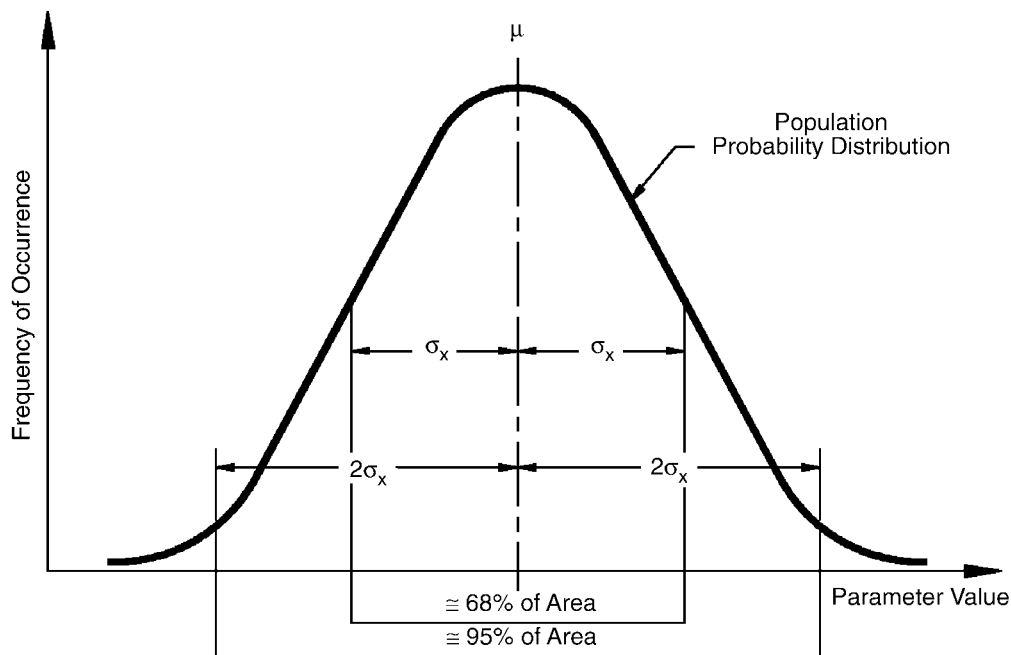


Figure 3-1
Random Error Model

3.2.1.2 Bias Errors

Bias errors are those errors that remain constant throughout the test. Since bias errors do not vary over the duration of the test, it is more difficult to identify and evaluate sources of bias error. Some sources of bias error include:

- Errors associated with the unmeasured inputs and unverified assumptions of the analysis strategy
- Errors associated with the instruments, methods, and spatial averaging techniques specified by the measurement strategy

Bias error, β , is considered a constant offset between the true mean value of a measurement and the true value.

3.2.1.3 Classification of Errors

The difference between precision and bias errors is illustrated in Figure 3-2.

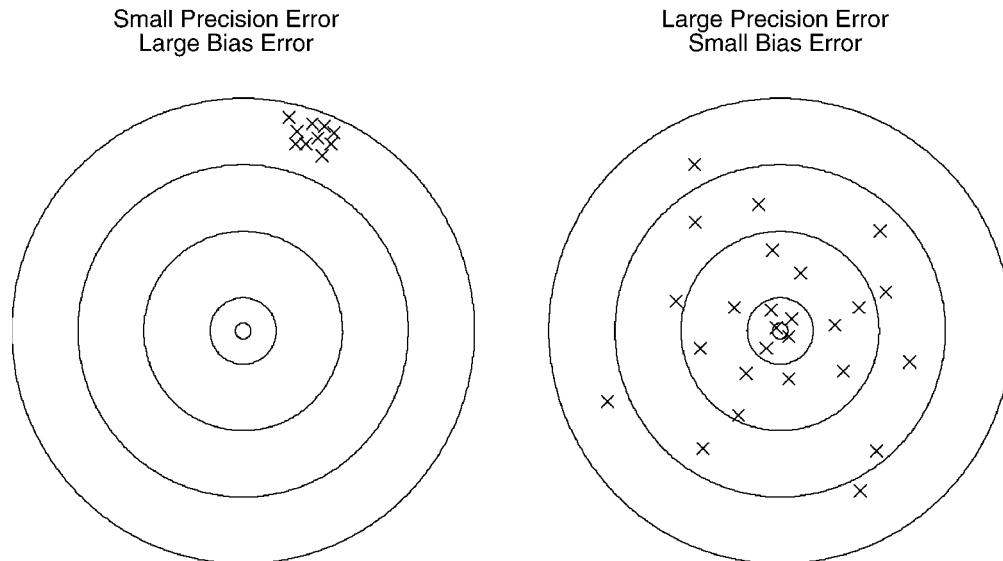


Figure 3-2
Precision and Bias Error

The left side of Figure 3-2 shows repeated measurements (or test results) with small scatter or variation (small precision error). The average of these measurements is not centered about the desired value (large bias error).

The right side of Figure 3-2 shows repeated measurements (or test results) with a large amount of scatter or variation (large precision error). The average of these measurements is centered about the desired value (small bias error).

Proper classification of errors as precision or bias is necessary to ensure that errors are evaluated using the appropriate methods. Classification of an error as precision or bias requires an understanding of how the error is manifested in repeated measurements throughout the duration of the test.

An error may be classified as a precision error if:

- The error is expected to vary randomly for each observation or measurement (the error in each observation is unique or independent of the error in the previous observation).
- The population of errors (and hence the variation in the measurements) is expected to be approximately normal or Gaussian.

- The observed variation is believed to be indicative of the full range of variation for the population of errors.
- The mean value of the population of errors observed over the duration of the test is expected to be zero (therefore, the error will not bias the average value of the measurements).

Conversely, an error may be classified as a bias error if:

- The error is expected to remain relatively constant for each observation or measurement.
- The mean value of the population of errors observed over the duration of the test is expected to be non-zero (therefore, the error will bias the average value of the measurements).

Example - Classification of Errors

For most single-performance tests of relatively short duration, the drift in a measurement system with time should not be classified as a precision error because:

- The drift in the measurement system is relatively slow and is not expected to vary for each observation or measurement.
- Any variation during the test due to drift is not expected to be indicative of the full drift in the measurement system since the time of calibration.
- The mean value of the drift over the duration of the test is not expected to be zero (that is, the magnitude of the drift is expected to be non-zero at the start of the test and is expected to change monotonically throughout the test).

Since the drift cannot be classified as a precision error, it should be classified as a bias error.

3.2.1.4 Combined Error Model

The contribution of both precision and bias errors results in the overall uncertainty of a measurement or test result. The combined error model is illustrated in Figure 3-3.

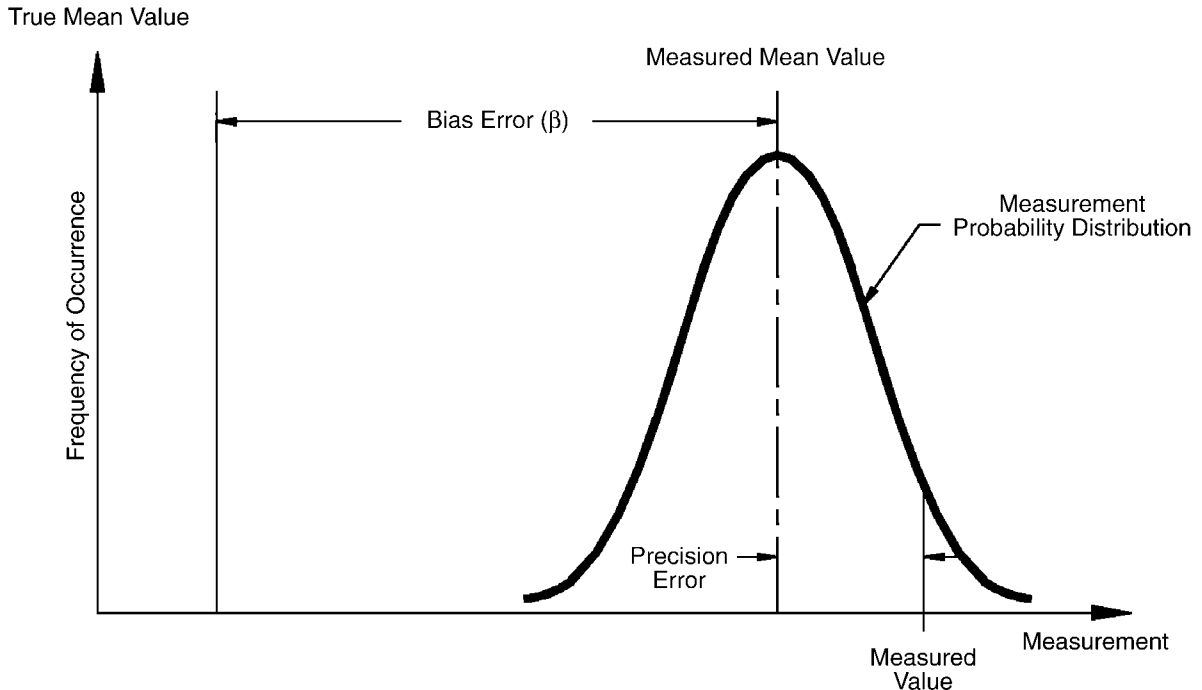


Figure 3-3
Combined Precision and Bias Error Model

3.2.2 Test Uncertainty

As discussed in Section 3.2.1, test error cannot be quantified directly. Instead, test error must be estimated from an evaluation of the many “elemental” error sources that influence the test. The process by which these elemental errors are identified, evaluated, and combined into a meaningful estimate of the limits of the test error is called uncertainty analysis.

The meaningful estimate of the limits of the test error determined by the uncertainty analysis is referred to as test uncertainty. Test uncertainty is always evaluated at a pre-determined level of coverage. The term *coverage* refers to how often the interval of the test uncertainty about the test result may be expected to contain the true value. In the nuclear industry, test uncertainty is often determined with 95% coverage. Per ASME OM-21 [3]:

“A 95% confidence level shall be applied to the calculated result for the purpose of comparing the testing or monitoring results to the acceptance criteria.”

This concept of coverage is illustrated in Figure 3-4.

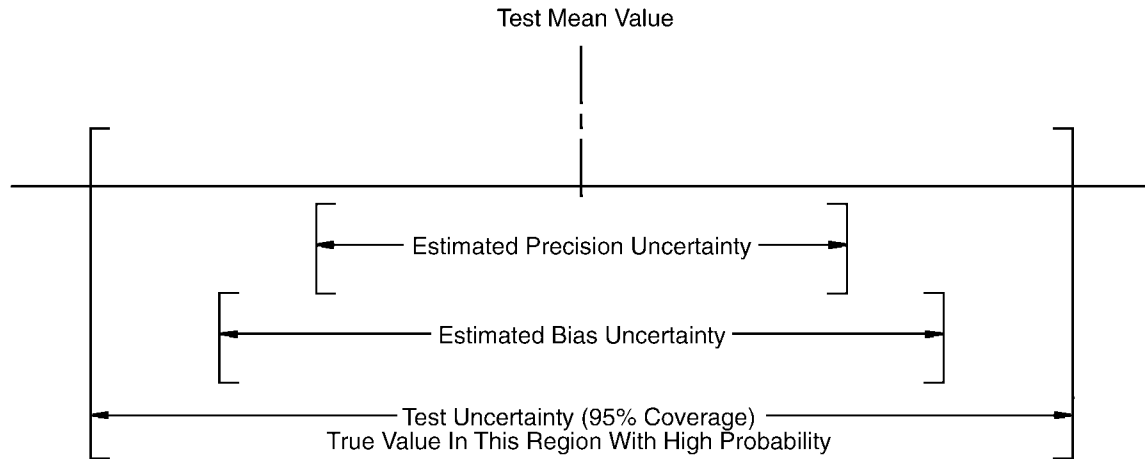


Figure 3-4
Estimated Test Uncertainty and Coverage

The basic approach to evaluating uncertainty involves application of the following steps:

1. Identify all elemental sources of precision and bias uncertainty (discussed in Section 3.2.3).
2. Evaluate all elemental sources of precision and bias uncertainty (discussed in Sections 3.2.4 and 3.2.5).
3. Perform a sensitivity analysis for each elemental source of uncertainty (discussed in Section 3.2.6).
4. Combine all elemental sources of uncertainty to determine the overall uncertainty (discussed in Section 3.2.7).

In the pre-test uncertainty analysis, the aforementioned steps are used to determine estimates of the overall uncertainty of:

- Each measured parameter
- The analysis
- The test result

3.2.3 Identify Elemental Sources of Precision and Bias Uncertainty

Frequently, the focus of the uncertainty analysis is limited to evaluation of the uncertainty associated with the calibration of the instruments used for the test. In typical testing applications, there are many additional sources of uncertainty that are overlooked and can lead to nonrepeatable test data, inconclusive test results, or sometimes erroneous decisions made from inaccurate test data. While ANSI/ASME PTC 19.1 [1] provides guidance on the mechanics of performing an uncertainty analysis, the success of the uncertainty analysis is heavily dependent upon the experience and expertise of the individual performing the analysis. In particular, the analyst should strive to identify and estimate all significant sources of elemental uncertainty. Identification of sources of precision and bias uncertainty are discussed separately in the following sections.

3.2.3.1 Precision Uncertainty

As discussed in Section 3.2.1, many sources of random variability contribute to the overall precision uncertainty associated with each measurement. As discussed in Section 3.2.4, precision uncertainty is evaluated statistically from the observed variation in repeated measurements of each parameter. In general, it is necessary only to identify (and evaluate) an overall precision uncertainty for each measured parameter for the test. It is rarely necessary to identify (and evaluate) the individual sources of variation that combine to cause the overall precision uncertainty for each measured parameter.

3.2.3.2 Bias Uncertainty

Unlike precision uncertainty, bias uncertainty is not evaluated statistically from the observed variation in repeated measurements of each parameter. Therefore, elemental sources of bias uncertainty are more difficult to identify and evaluate. Additionally, the list of elemental sources of bias uncertainty that influence a test result is quite large. To aid in the identification of all of the significant sources of bias uncertainty, it is often helpful to identify categories of bias uncertainty that may influence the test result. Two main categories of bias uncertainty that can be identified are analytical bias uncertainty and measurement bias uncertainty. These categories are discussed below.

3.2.3.2.1 Analytical Bias Uncertainty

Elemental sources of analytical bias uncertainty include all bias errors associated with the unmeasured inputs to the analysis strategy or the unverified assumptions of the analysis strategy. Sources of analytical bias uncertainty can be identified by careful inspection of the terms in the analysis strategy as well as careful review of the specific assumptions of the analysis strategy. An abbreviated listing of sources of analytical bias uncertainty is provided below.

- Any correlation used to predict calculated parameters may be viewed as unmeasured inputs to the analysis strategy. The errors in these correlations are sources of analytical bias uncertainty in the determination of the test result.
- Any published value of physical parameters may be viewed as unmeasured inputs to the analysis strategy. The errors in the estimation of these physical parameters are sources of analytical bias uncertainty in the determination of the test result.
- Any derived relationship used to estimate calculated parameters may be viewed as unmeasured inputs to the analysis strategy. The errors associated with the use of these derived relationships are sources of analytical bias uncertainty in the determination of the test result.
- Any relationship that has assumptions that are approximated. Application of relationships to evaluate calculated parameters is a source of analytical bias uncertainty in the determination of the test result.

3.2.3.2.2 Measurement Bias Uncertainty

There are many sources of elemental bias uncertainty associated with the measurement of each parameter that is a required input to the analysis strategy. These sources of measurement bias uncertainty can be categorized as follows:

- The bias errors associated with each instrument in the measurement system from the sensor through the data acquisition system are often categorized as sources of instrument bias uncertainty. Specific listings of instrument bias uncertainties associated with typical instruments used in testing applications are provided in Section 3.2.2. As a general rule of thumb, three or more sources of instrument uncertainty can be identified for each instrument in a measurement system.
- The bias errors associated with the method used to measure a parameter at a single location (including errors associated with where and how the instrument is installed) are often categorized as sources of measurement methodology bias uncertainty. As a general rule of thumb, at least one source of measurement methodology bias uncertainty can be identified for each measurement associated with the test.
- If the actual value of a parameter varies as a function of spatial position, measurement of the parameter at a finite number of discrete locations may be biased with respect to the average value of the parameter. As a general rule of thumb, spatial bias uncertainty should be identified as a source of uncertainty for each measured parameter associated with the test unless there is sufficient objective evidence that spatial bias uncertainty is negligible or the instrument fully averages the parameter over the defined measurement plane.

Uncertainty

- If the testing methodology is focused on testing under stable (near steady-state) test conditions, measurement of test data under transient conditions will result in additional bias uncertainties due to the time-response characteristics of the measurement systems and installation techniques, which are beyond the scope of this guideline.

3.2.4 Evaluate Elemental Sources of Precision Uncertainty

The techniques used to evaluate precision uncertainty in a pre-test uncertainty analysis are similar to those in a post-test uncertainty analysis with the following exception. In a post-test uncertainty analysis, the precision uncertainty is evaluated directly from the actual test data. In a pre-test uncertainty analysis, the precision uncertainty must be estimated from previous test data or engineering judgment.

In order to simplify the presentation of the evaluation of the precision uncertainty for a pre-test uncertainty analysis, the techniques used for evaluating the precision uncertainty in a post-test uncertainty analysis are presented first.

3.2.4.1 Post-Test Evaluation

Since precision errors are assumed to come from a population of random errors that is normally distributed, it is possible to estimate the magnitude of the overall precision error in a measurement based on a statistical evaluation of a finite sample of measurements. If the test obtains N repeated measurements of a parameter in a time series of measurements (X_1, X_2, \dots, X_N), the standard deviation (or precision index) of the sample of measurements is determined as:

$$S_x = \sqrt{\frac{\sum_{i=1}^N (X_i - \bar{X})^2}{N - 1}} \quad (\text{Eq. 3-1})$$

where,

S_x	=	standard deviation of the data sample
X_i	=	a single measurement in a time series of measurements
\bar{X}	=	time-average value of the measurements
N	=	number of measurements in the time series

Note: All calibration corrections and conversions to engineering units should be applied to each measurement in the time series prior to the determination of the standard deviation so that eq. 3-1 will yield the proper estimate of the standard deviation in terms of the desired engineering units.

The standard deviation of a data sample is a measure of the scatter (or error) of the individual measurements about the mean value \bar{X} of the sample. For testing applications, we are not interested in the scatter (or error) of individual measurements, but in the possible scatter (or error) of the average of the data sample. This is the amount of scatter (or error) we would observe in the average of the data sample if the entire test were repeated multiple times and an average data sample computed for each test. Since it is impractical to replicate a test multiple times, the scatter (or error) of the average of the data sample is estimated as follows:

$$S_{\bar{x}} = \frac{S_x}{\sqrt{N}} \quad (\text{Eq. 3-2})$$

where,

$$S_{\bar{x}} = \text{standard deviation of the sample mean}$$

When combining sources of uncertainty as will be discussed in Section 3.2.7, the standard deviation of the sample mean will be multiplied by an appropriate two-tailed Student's "t" statistic as follows:

$$\frac{2\sigma}{\sqrt{N}} \approx t_{95,v} S_{\bar{x}} \quad (\text{Eq. 3-3})$$

where,

$$t = \text{Student's "t" value for 95\% confidence and } v \text{ degrees of freedom}$$

The product, $t_{95,v} S_{\bar{x}}$, shown in eq. 3-3 is a 95% confidence estimate of the limit of the precision error of the average value of a measurement. Therefore, this product represents the precision uncertainty associated with the average of the measurement. The Student's "t" value used in eq. 3-3 is a correction factor required to determine a 95% confidence estimate from a standard deviation that has finite degrees of freedom (that is, is based on a finite sample size). The degrees of freedom associated with the standard deviation of the sample mean is:

$$v = N - 1 \quad (\text{Eq. 3-4})$$

Uncertainty

Values for a two-tailed Student's "t" at 95% confidence are shown in Table 3-1.

Table 3-1
Two-Tailed Student t Values for 95% Confidence

Degrees of Freedom	t	Degrees of Freedom	t	Degrees of Freedom	t
1	12.706	11	2.201	21	2.080
2	4.303	12	2.179	22	2.074
3	3.182	13	2.160	23	2.069
4	2.776	14	2.145	24	2.064
5	2.571	15	2.131	25	2.060
6	2.447	16	2.120	26	2.056
7	2.365	17	2.110	27	2.052
8	2.306	18	2.101	28	2.048
9	2.262	19	2.093	29	2.045
10	2.228	20	2.086	30 or more	≈2

Note: The above derivation for precision uncertainty assumes that the parameter is measured at a single location. If a parameter is measured at multiple locations, the above equations may be used if the readings at multiple locations at each point in time are first combined using the spatial averaging techniques to yield a single time series of measurements. Alternatively, techniques for pooling precision indexes from multiple locations may be used as described in ANSI/ASME PTC 19.1 [1].

Note: Eqs. 3-2 and 3-3 indicate that the precision uncertainty can be reduced by increasing the number of measurements. In dividing by the square root of the number of measurements in eq. 3-3, it is assumed that each measurement provides an independent observation of the time variation in the parameter at each location. This assumption would not be true, for example, if measurements were taken at 1 second intervals, but the response time of the measurement system was known to be greater than 15 seconds.

Example - Sample Mean Standard Deviation

Three RTDs are used to obtain values of the service water temperature downstream of an orifice meter. Determine the standard deviation of the sample mean in terms of °F.

Time (min)	Location 1 (°C)	Location 2 (°C)	Location 3 (°C)
0	30.15	30.10	30.12
5	30.20	30.11	30.10
10	30.22	30.16	30.15
15	30.18	30.17	30.16

Solution:

Time (min)	Location 1 (°F)	Location 2 (°F)	Location 3 (°F)	Spatial Average
0	86.27	86.18	86.216	86.222
5	86.36	86.198	86.18	86.246
10	86.396	86.288	86.27	86.318
15	86.324	86.306	86.288	86.306

Calculate the average value:

$$\bar{X} = \frac{\sum_{i=1}^N X_i}{N} = \frac{86.222 + 86.246 + 86.318 + 86.306}{4} = 86.273$$

Calculate the sample standard deviation utilizing eq. 3-1:

$$S_x = \sqrt{\frac{\sum_{i=1}^N (X_i - \bar{X})^2}{N-1}} = \sqrt{\frac{(86.222 - 86.273)^2 + (86.246 - 86.273)^2 + (86.318 - 86.273)^2 + (86.306 - 86.273)^2}{4-1}}$$

$$S_x = 0.0463^\circ \text{ F}$$

Calculate the standard deviation of the sample mean utilizing eq. 3-2

$$S_{\bar{x}} = \frac{S_x}{\sqrt{N}} = \frac{0.0463}{\sqrt{4}} = 0.0232^\circ \text{ F}$$

Uncertainty

3.2.4.2 Pre-Test Evaluation

The pre-test evaluation of precision uncertainty mimics the post-test evaluation except that the standard deviation of the sample mean value must be estimated from previous data or engineering judgment. If previous test data are available, a new standard deviation of the sample mean based on a new number of measurements is approximated as follows:

$$S_{\bar{x}}^{\text{new}} = \frac{t_{95, v_{\text{old}}}}{t_{95, v_{\text{new}}}} S_{\bar{x}}^{\text{old}} \sqrt{\frac{N^{\text{old}}}{N^{\text{new}}}} \quad (\text{Eq. 3-5})$$

Note: Use of eq. 3-5 assumes that the random variation associated with the measurements from a previous test is comparable to the variation expected in future tests.

If previous data are not available, the standard deviation of the sample mean is determined by estimating the 95% confidence limit for the expected variation in the value of the parameter. This estimate represents a $\pm 2\sigma$ band that is expected to contain 95% of the population of values from which data will be sampled. Therefore, the standard deviation of the sample mean may be estimated as follows:

$$S_{\bar{x}} = \frac{2\sigma}{t_{95, v} \sqrt{N}} \quad (\text{Eq. 3-6})$$

Example - Estimation of Sample Mean Standard Deviation from Previous Test Data

Estimate the expected standard deviation of the sample mean for the temperature measurement of the cold fluid inlet temperature (using eight data points). Test data from a similar test shows a sample mean standard deviation of 0.0232°F for four data points.

Solution:

Determine the old and new $t_{95,v}$ values from Table 3-1:

$$t_{95,v_{old}} = 3.182 \quad t_{95,v_{new}} = 2.365$$

Calculate the new sample mean standard deviation from eq. 3-5:

$$S_{\bar{x}}^{new} = \frac{t_{95,v_{old}}}{t_{95,v_{new}}} S_{\bar{x}}^{old} \sqrt{\frac{N^{old}}{N^{new}}} = \frac{3.182}{2.365} 0.0232 \sqrt{\frac{4}{8}} = 0.022^\circ \text{F}$$

Example - Estimation of Sample Mean Standard Deviation from $\pm 2\sigma$ Estimation

Estimate the expected standard deviation of the sample mean for the temperature measurement of the cold fluid inlet temperature (using eight data points). Use an estimate of $\pm 0.1^\circ \text{F}$ for the $\pm 2\sigma$ range.

Solution:

Determine the $t_{95,v}$ value from Table 3-1:

$$t_{95,v_{new}} = 2.365$$

Calculate the expected sample mean standard deviation from eq. 3-6:

$$S_{\bar{x}} = \frac{2\sigma}{t_{95,v} \sqrt{N}} = \frac{0.1}{2.365 \sqrt{8}} = 0.015^\circ \text{F}$$

3.2.5 Evaluation of Sources of Bias Uncertainty

Bias uncertainty is the portion of the total measurement uncertainty that is considered reasonably constant for the duration of the test. Therefore, bias uncertainty cannot be evaluated statistically from scatter in the test data. Instead, bias uncertainty must be estimated as the limits of the expected population of bias error at 95% confidence.

If there is no knowledge of the sign or direction of the error, then the uncertainty associated with the error is referred to as a symmetric bias uncertainty. For a symmetric bias uncertainty, the limits of the population of bias errors are expected to be centered about the average value of a parameter. The limits of a symmetric bias uncertainty are expressed as B_x or $\pm B_x$. The \pm symbol is often used to indicate that the error is equally likely to be positive or negative.

Figure 3-5 illustrates a symmetric bias uncertainty. The figure illustrates the results of using an RTD that has been calibrated using symmetrical bias limits of $\pm 0.5^\circ\text{F}$.

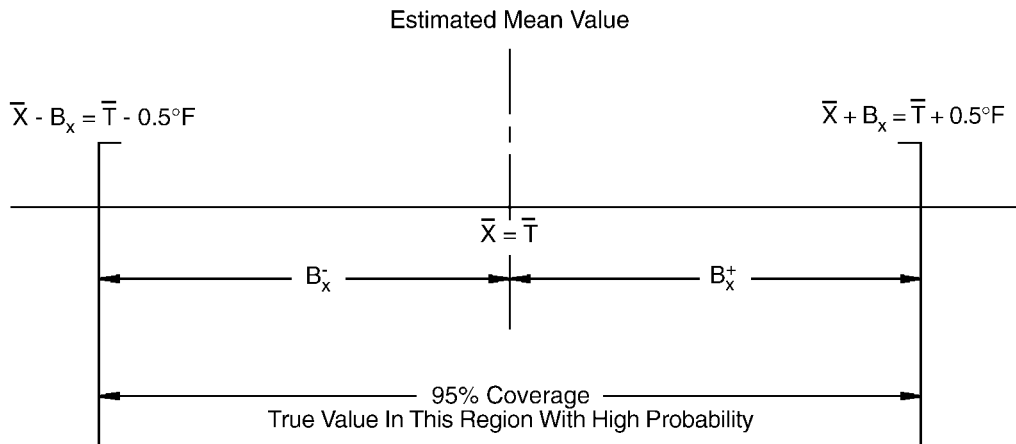


Figure 3-5
RTD Calibrated with Symmetrical Bias Limits

If there is a known tendency for the magnitude of the error to be larger in a particular direction, then the uncertainty associated with the error is referred to as an asymmetric bias uncertainty. For an asymmetric bias uncertainty, the limits of the population of bias errors are not expected to be centered about the average value of a parameter. The limits of an asymmetric bias uncertainty are expressed as B_x^+ and B_x^- where B_x^+ indicates the upper limit of the error band and B_x^- indicates the lower limit of the error band.

Figure 3-6 illustrates an asymmetric bias uncertainty. The figure illustrates the expected results of using an RTD calibrated with an upper bias limit of $+0.7^{\circ}\text{F}$ and a lower bias limit of -0.3°F .

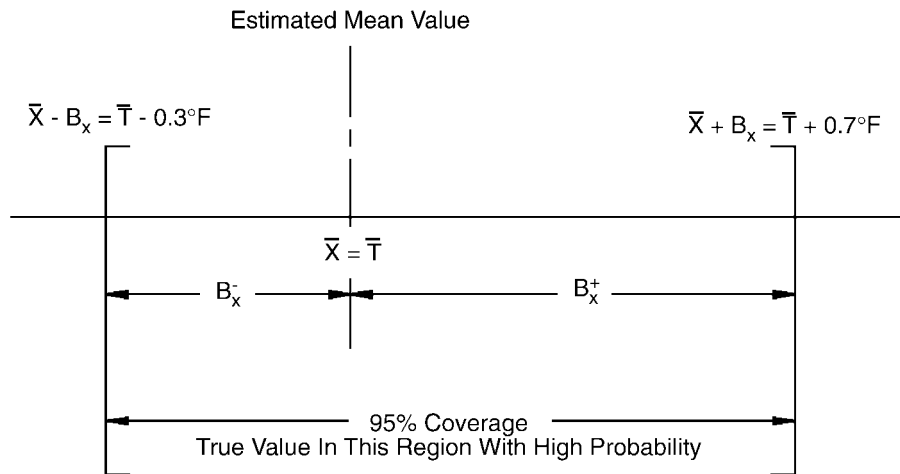


Figure 3-6
RTD Calibrated with Asymmetrical Bias Limits

Note: Rigorous treatment of asymmetric bias uncertainty (in terms of the combination of these uncertainties to determine the overall uncertainty) is considered outside the scope of this guideline. For simplistic treatment of an asymmetric bias uncertainty, the bias uncertainty may be assumed to be symmetric and equal to the larger of the absolute values of either B_x^+ or B_x^- .

The estimate of a bias uncertainty may be based on any of the following:

- Calibrations, special tests, or comparisons of independent analysis or measurement techniques
- Evaluation of the engineering or physical principles causing the error
- Published reports or vendor literature regarding the uncertainty of the analysis or measurement techniques
- Engineering judgment

The above list is presented in order of preference. It is always preferable to use a reliable source of data as opposed to judgment in evaluating significant sources of bias uncertainty. If at all possible, use of engineering judgment alone should be avoided. Use of engineering judgment alone often leads to an underestimation of uncertainties and an uncertainty analysis that is not defensible.

Uncertainty

In evaluating the elemental sources of bias uncertainty for the pre-test uncertainty analysis, it is important to note that the magnitude of an uncertainty may change with test conditions. As discussed previously, the pre-test uncertainty analysis should be considered a worst-case or bounding evaluation of the possible error in the test based on the selected analysis, operational, and measurement strategies for the test. Therefore, elemental sources of bias uncertainty should be evaluated over the full range of acceptable test conditions.

Helpful suggestions for evaluating sources of bias uncertainty are discussed in the following sections.

3.2.5.1 Analytical Bias Uncertainty

Evaluation of sources of analytical bias uncertainty requires a full understanding of the uncertainties of the unmeasured inputs to the analysis strategy and the assumptions of the analysis strategy.

3.2.5.2 Measurement Bias Uncertainty

As discussed in Section 3.2.3, sources of measurement bias uncertainty may be categorized as instrument bias uncertainty, measurement methodology bias uncertainty, and spatial bias uncertainty. Evaluation of the bias uncertainty associated with each of these categories is discussed in the following section.

3.2.5.2.1 Instrument Bias Uncertainty

Evaluation of sources of instrument bias uncertainty typically requires a full understanding of the uncertainties associated with the following:

- The calibration standards, calibration methodologies, and calibration tolerances
- Instrument limitations including linearity, hysteresis, dead band, repeatability, and precision
- Expected instrument drift with time, temperature, humidity, pressure, vibration, and power supply changes
- Sources of parasitic voltages and resistances in the measurement circuits
- Environmental noise including electromagnetic interference, radio frequency interference, and radiation effects

Most instrument bias uncertainties are assessed from:

- The results of calibration and special tests
- Instrument specifications provided by the vendor
- Published literature regarding the uncertainty of the instruments when used in specific applications

Valuable references for evaluation of sources of instrument bias include:

- The ANSI/ASME PTC 19 Series on Instruments and Apparatus
- Nuclear industry standards for the determination of set points for nuclear safety-related instrumentation [4]

Note: The instrument bias uncertainty associated with a measured parameter should be considered independent of the number of sensors or locations used to measure the parameter. This is because the instrument bias uncertainty of the instruments used to measure the parameter is highly correlated (refer to Section 3.2.7). For this reason, the instrument bias uncertainty associated with a parameter that is measured with multiple sensors should not be divided by the square root of the number of sensors.

3.2.5.2.2 Measurement Methodology Bias Uncertainty

Most sources of measurement methodology bias uncertainty are assessed from:

- An evaluation of the engineering or physical principles causing the error
- Published reports regarding the uncertainty of the measurement technique under similar circumstances

This type of uncertainty is specific to the measurement situation and must be addressed on a case-by-case basis. Some examples follow:

- The temperature of a sensor installed in a well or on a pipe surface is not equal to the temperature of the fluid in the pipe due to conduction error. The measurement methodology bias uncertainty associated with the measurement may be estimated by evaluation of the heat transfer between the fluid, the sensor, and the surrounding environment.
- The uncertainty in the measurement of flow in pipes by most common flow elements such as venturis, orifices, annubars, ultrasonic flow meters, etc. will increase when installed in the presence of flow disturbances. The measurement

Uncertainty

methodology bias uncertainty associated with these flow elements may be evaluated from published research regarding the effects of installation of these flow elements under similar flow conditions.

- The uncertainty in the measurement of airflow by a non-directional probe such as a pitot tube or a shrouded anemometer will increase if the direction of flow is not known. The uncertainty may be evaluated by comparison of the actual response of the instrument to the desired (cosine) response over the range of expected flow directions.

3.2.5.2.3 Spatial Bias Uncertainty

In many instances, the quantity measured varies in space, making a single point measurement inadequate. It is often necessary to make measurements of the same parameter at different spatial locations to account for spatial variation. An example of this concept is the pitot tube traverse where velocity measurements are made at several points along the diameters being traversed. This enables an assessment of the spatial variation and a more accurate estimate of the true average velocity of the fluid.

The techniques used to evaluate spatial bias uncertainty in a pre-test uncertainty analysis are similar to those in a post-test uncertainty analysis with the following exception. In a post-test uncertainty analysis, the spatial bias uncertainty is typically evaluated directly from the actual test data. In a pre-test uncertainty analysis, however, the spatial bias uncertainty must be estimated from previous test data or engineering judgment.

In order to simplify the presentation of the evaluation of the spatial bias uncertainty for the pre-test uncertainty analysis, the techniques used for evaluating the spatial bias uncertainty in a post-test uncertainty analysis will be presented first.

Post-Test Evaluation

In a post-test uncertainty analysis, the spatial bias uncertainty, B_{spatial} , is determined from a statistical evaluation of the time-averaged values taken at multiple measurement locations as follows:

$$B_{\text{spatial}} = \frac{t_{95,v} S_{\text{spatial}}}{\sqrt{L}} \quad (\text{Eq. 3-7})$$

and,

$$S_{\text{spatial}} = \sqrt{\frac{\sum_{j=1}^L (x_j - \bar{x})^2}{L - 1}} \quad (\text{Eq. 3-8})$$

where,

- $t_{95,v}$ = Student's "t" value for 95% confidence and v degrees of freedom
 S_{spatial} = standard deviation of the time-averaged values of parameter x at each location
 x_j = time-averaged value of parameter x at location j
 \bar{x} = average value of parameter x at all locations ($\bar{x} = \frac{1}{L} \sum_{j=1}^L x_j$)
 L = number of locations at which parameter x was measured

Note: All calibration corrections and conversions to engineering units should be applied to each measurement prior to application of eq. 3-8 so that eq. 3-7 will yield the proper estimate of the spatial bias uncertainty in terms of the desired engineering units.

Note: The equation above indicates that the spatial bias uncertainty can be reduced by increasing the number of measurement locations. In dividing by the square root of the number of measurement locations, it is assumed that each location provides an independent observation of the spatial variation in the parameter. This assumption would not be true, for example, if a dual-element RTD were installed in a single thermowell.

Uncertainty

Example - Spatial Bias Calculation

Three RTDs are used to obtain values of the cold fluid inlet temperature. Determine the spatial bias of the sample mean in terms of °F.

Time (min)	Location 1 (°C)	Location 2 (°C)	Location 3 (°C)
0	30.15	30.10	30.12
5	30.20	30.11	30.10
10	30.22	30.16	30.15
15	30.18	30.17	30.16

Solution:

Calculate the temperature in °F, the spatial average, and the average values:

Time (min)	Location 1 (°F)	Location 2 (°F)	Location 3 (°F)	Spatial Average
0	86.27	86.18	86.216	86.222
5	86.36	86.198	86.18	86.246
10	86.396	86.288	86.27	86.318
15	86.324	86.306	86.288	86.306
Average:	$x_1 = 86.338$	$x_2 = 86.243$	$x_3 = 86.239$	$\bar{x} = 86.273$

Calculate the spatial bias utilizing eqs. 3-7 and 3-8:

$$S_{\text{spatial}} = \sqrt{\frac{\sum_{j=1}^L (x_j - \bar{x})^2}{L-1}} = \sqrt{\frac{(86.338 - 86.273)^2 + (86.243 - 86.273)^2 + (86.239 - 86.273)^2}{3-1}} = 0.056^\circ \text{F}$$

$$B_{\text{spatial}} = \frac{t_{95, v=3-1} S_{\text{spatial}}}{\sqrt{L}} = \frac{4.303 \cdot 0.056}{\sqrt{3}} = 0.139^\circ \text{F}$$

Pre-Test Evaluation

For the pre-test uncertainty analysis, however, the spatial bias uncertainty must be estimated from previous test data or engineering judgment. If previous test data are available, a new spatial bias uncertainty estimate based on a new number of measurement locations may be estimated as follows:

$$B_{\text{spatial}}^{\text{new}} = B_{\text{spatial}}^{\text{old}} \frac{\sqrt{L}^{\text{old}}}{\sqrt{L}^{\text{new}}} \quad (\text{Eq. 3-9})$$

If previous test data are not available, the spatial bias uncertainty may be determined by estimating a 95% confidence limit for the expected variation in the value of the parameter over the entire measurement space. This estimate represents a $\pm 2\sigma$ band that is expected to contain 95% of the population of values that vary as a function of spatial position. Therefore, the spatial bias uncertainty may be estimated as follows:

$$B_{\text{spatial}} = \frac{(2\sigma)_{\text{spatial}}}{\sqrt{L}} \quad (\text{Eq. 3-10})$$

Note that for a single measurement location, the bias uncertainty is equal to the estimated spatial variation.

Uncertainty

Example - Estimation of Spatial Bias from Previous Test Data

Estimate the expected spatial bias for the temperature measurement of the cold fluid inlet temperature (using five locations). The data from a similar test shows a spatial bias of 0.139 for three locations.

Solution:

Calculate the new spatial bias from eq. 3-9:

$$B_{\text{spatial}}^{\text{new}} = B_{\text{spatial}}^{\text{old}} \frac{\sqrt{L}^{\text{old}}}{\sqrt{L}^{\text{new}}} = 0.139 \frac{\sqrt{3}}{\sqrt{5}} = 0.108^{\circ} \text{ F}$$

Example - Estimation of Spatial Bias from $\pm 2\sigma$ Estimation

Estimate the expected spatial bias for the temperature measurement of the cold fluid inlet temperature (using five locations). Use an estimate of $\pm 0.2^{\circ}\text{F}$ for the $\pm 2\sigma$ range.

Solution:

Calculate the spatial bias using eq. 3-10:

$$B_{\text{spatial}} = \frac{(2\sigma)_{\text{spatial}}}{\sqrt{L}} = \frac{0.2}{\sqrt{5}} = 0.089^{\circ} \text{ F}$$

3.2.6 Conduct Sensitivity Analysis

Prior to combining elemental sources of uncertainty, it is necessary to conduct a sensitivity analysis to express each elemental uncertainty in common terms. For example, if several elemental uncertainties are being combined to determine the overall uncertainty in a measurement, it is necessary to conduct a sensitivity analysis to express each elemental uncertainty in the terms (and units) of the measurement. Likewise, if several elemental uncertainties are being combined to determine the overall uncertainty in the test result, it is necessary to conduct a sensitivity analysis to express each elemental uncertainty in the terms (and units) of the test result. For the remainder of this section, the term *result* will be used to generically refer to either a measurement or test result.

A sensitivity analysis uses a defined functional relationship between the result and the independent parameters required to determine the result to determine sensitivity coefficients relating the result to the independent parameters. A sensitivity coefficient is a linear approximation of the change in the result for a unit change in an

independent parameter. The uncertainty in an independent parameter can be expressed in terms of an uncertainty in the result by multiplying by a sensitivity coefficient.

As described above, the magnitude of a sensitivity coefficient is an indication of how much influence an uncertainty in an independent parameter has on a result. The sign of a sensitivity coefficient is an indication of the sign of the influence of an independent parameter on the result. If the sensitivity coefficient is positive, a positive uncertainty in a parameter will result in a positive uncertainty in the test result. If the sensitivity coefficient is negative, a positive uncertainty in a parameter will result in a negative uncertainty in the test result. As discussed in Section 3.2.7, the sign of a sensitivity coefficient is immaterial when combining independent and symmetrical sources of uncertainty. This is because the sign of the source of uncertainty is not known; therefore, the sign of the product of the sensitivity coefficient and uncertainty is not known. If combining dependent or asymmetrical sources of uncertainty, careful attention must be paid to proper treatment of the sign.

In the pre-test uncertainty analysis, it is important to note that the values of the sensitivity coefficients vary significantly with test conditions. As discussed previously, the pre-test uncertainty analysis should be considered a worst-case or bounding evaluation of the possible error in the test, based on the selected analysis, operational, and measurement strategies for the test. Therefore, sensitivity coefficients should be evaluated over the full range of acceptable test conditions.

Two methods of determining sensitivity coefficients are described in the following sections.

3.2.6.1 Analytical Determination of Sensitivity Coefficients

When a closed form expression for the result as a function of several independent parameters exists, sensitivity coefficients can be determined analytically by taking partial derivatives of the function, relating the dependent and independent parameters as follows:

$$\Theta_i = \frac{\partial r}{\partial P_i} \quad (\text{Eq. 3-11})$$

Uncertainty

where,

Θ_i	=	the absolute sensitivity coefficient relating the i^{th} parameter to the result
r	=	the result
P_i	=	the i^{th} parameter

The sensitivity coefficient determined in eq. 3-11 is referred to as an absolute sensitivity coefficient. The units associated with an absolute sensitivity coefficient are the units of the result parameter divided by the units of the independent parameter. In certain situations, it may be desirable to evaluate uncertainties on a nondimensional basis (for example, when uncertainties are expressed as a percentage of value). For these situations, a relative or nondimensional sensitivity coefficient is determined as follows:

$$\Theta_i' = \frac{\partial r / r}{\partial P_i / P_i} \quad (\text{Eq. 3-12})$$

Example:

An orifice is used to determine water flow through a pipe. The flow uncertainty (U_v) can be determined from a known differential pressure uncertainty ($U_{\Delta p}$) and calibration constant uncertainty (U_c) using the relation:

$$q = C\sqrt{\Delta p}$$

where,

q	=	volumetric flow
C	=	calibration constant of the orifice
Δp	=	differential pressure across the orifice

Calculate the absolute and relative sensitivity coefficients for the flow equation:

$$q = C\sqrt{\Delta p}$$

and develop an expression for the uncertainty in terms of absolute and relative uncertainty of the measurement parameter q .

Determine the absolute and relative sensitivity coefficients:

$$\Theta_c = \frac{\partial V}{\partial C} = \frac{\partial(C\sqrt{\Delta p})}{\partial C} = \sqrt{\Delta p}$$

$$\Theta'_c = \frac{\partial V/V}{\partial C/C} = \frac{\partial(C\sqrt{\Delta p})}{\partial C} \frac{1}{\sqrt{\Delta p}} = 1$$

$$\Theta_{\Delta p} = \frac{\partial V}{\partial(\Delta p)} = \frac{\partial(C\sqrt{\Delta p})}{\partial(\Delta p)} = \frac{C}{2\sqrt{\Delta p}}$$

$$\Theta'_{\Delta p} = \frac{\partial V/V}{\partial(\Delta p)/\Delta p} = \frac{\partial(C\sqrt{\Delta p})}{\partial(\Delta p)} \frac{\sqrt{\Delta p}}{C} = \frac{1}{2}$$

Determine the absolute and relative uncertainty expressions:

$$U_v = \sqrt{\left[(\sqrt{\Delta p})(U_c) \right]^2 + \left[\left(\frac{C}{2\sqrt{\Delta p}} \right) (U_{\Delta p}) \right]^2}$$

$$U'_v = \sqrt{\left[(1)(U_c) \right]^2 + \left[\left(\frac{1}{2} \right) (U'_{\Delta p}) \right]^2}$$

3.2.6.2 Numerical Determination of Sensitivity Coefficients

When a closed form solution for the result is not available or differentiation of the function is difficult, absolute or relative sensitivity coefficients can also be determined numerically as follows:

$$\Theta_i = \frac{\Delta r}{\Delta P_i} \quad (\text{Eq. 3-13})$$

or

$$\Theta_i = \frac{\Delta r / r}{\Delta P_i / P_i} \quad (\text{Eq. 3-14})$$

The basic steps required to numerically determine a sensitivity coefficient for the i^{th} parameter follow:

1. Define the nominal values for the independent variables at which the sensitivity analysis will be conducted ($P_1, P_2, \dots, P_i, \dots, P_j$).
2. Calculate the value of the result using the nominal values for the independent variables, $r = f(P_1, P_2, \dots, P_i, \dots, P_j)$.
3. Change the value of the i^{th} parameter by a small increment and recalculate the result, $r + \Delta r = f(P_1, P_2, \dots, P_i + \Delta P_i, \dots, P_j)$.
4. Compute the absolute or relative sensitivity coefficient as shown in eqs. 3-11 or 3-12.

Note: The selection of an increment, ΔP_i , to determine a sensitivity coefficient numerically requires careful consideration. In theory, the smaller the increment, the better the partial derivative of the function is approximated. In practice, however, the use of small increments may lead to numerical errors due to rounding off or an insufficient number of significant figures.

Example - Numerical Determination of Sensitivity Coefficient

An orifice is used to measure the flow of water to the inlet of a SWHX (flow equation $q = C\sqrt{\Delta p}$; q is the volumetric flow rate; C is 325 gpm/inwc^{1/2}; Δp is the differential pressure in inwc). Numerically determine the differential pressure sensitivity coefficient at a volumetric flow rate of 975 gpm.

Solution:

Determine the associated differential pressure at the flow rate of 975 gpm:

$$\Delta p = (v / C)^2 = (975 / 325)^2 = 9 \text{ inwc}$$

Calculate $\Delta v = v(\Delta p + \Delta(\Delta p)) - v(\Delta p)$ using $\Delta(\Delta p) = 0.1$ inwc:

$$\Delta v = v(\Delta p + \Delta(\Delta p)) - v(\Delta p) = v(9.1) - v(9.0) = 325\sqrt{9.1} - 325\sqrt{9} = 5.402 \text{ gpm}$$

Calculate the sensitivity coefficient utilizing eq. 3-13:

$$\Theta_{\Delta p} = \frac{\Delta r}{\Delta p_{\Delta p}} = \frac{\Delta v}{\Delta(\Delta p)} = \frac{5.402}{0.1} = 54.0 \text{ GPM / inwc}$$

Note: The closed form solution of the sensitivity coefficient (from the previous example) at a differential pressure of 9 inwc is: $\Theta_{\Delta p} = \frac{C}{2\sqrt{\Delta p}} = \frac{325}{2\sqrt{9}} = 54.16 \text{ gpm / inwc}$

3.2.7 Combine Sources of Uncertainty

As described in the previous section, sensitivity coefficients are always required to express elemental uncertainties in common terms (and units) prior to combining. A common mistake is to combine uncertainties without first multiplying them by the appropriate sensitivity coefficient. To avoid this common pitfall, all uncertainty calculations should be checked for dimensional integrity. Additional care should be exercised when performing non-dimensional analysis. For example, a common mistake is to assume that the two uncertainties expressed as percentages may be directly combined (unity sensitivity coefficients are assumed).

As described in ANSI/ASME PTC 19.1 [1], it is recommended that elemental sources of precision and bias be combined separately to determine the overall precision and bias uncertainty of a measurement or test result. For the remainder of this section, the term *result* will be used generically to describe a measurement or test result. Section 3.2.7.1

Uncertainty

addresses the combination of elemental precision uncertainties, Section 3.2.7.2 addresses the combination of elemental bias uncertainties, and Section 3.2.7.3 addresses the final combination of bias and precision to determine the overall uncertainty of the result.

3.2.7.1 Precision Uncertainty

For each source of precision uncertainty identified in Section 3.2.3, a standard deviation (or precision index) of the sample mean should be evaluated as described in Section 3.2.4. These standard deviations are combined to determine the overall standard deviation (or precision index) for the result as follows:

$$S_r = \sqrt{\sum_{i=1}^J (\Theta_i S_{\bar{P}_i})^2} \quad (\text{Eq. 3-15})$$

where,

- S_r = standard deviation of the result
- $S_{\bar{P}_i}$ = standard deviation of the mean value of the i^{th} parameter (this is the same as the $S_{\bar{x}}$'s determined in Section 3.2.4)
- Θ_i = sensitivity coefficient for the i^{th} parameter determined in Section 3.2.6
- J = number of elemental precision uncertainties

The degrees of freedom of the standard deviation of the result is determined as follows:

$$v_r = \frac{S_r^4}{\sum_{i=1}^J \left[\frac{(\Theta_i S_{\bar{P}_i})^4}{v_{\bar{P}_i}} \right]} \quad (\text{Eq. 3-16})$$

where,

- v_r = degrees of freedom associated with the standard deviation of the result
- $v_{\bar{P}_i}$ = degrees of freedom associated with the standard deviation of the mean value of the i^{th} parameter (this is the same as the v 's determined in Section 3.2.4)

Note: When using eq. 3-16, always truncate the result to determine the degrees of freedom as a whole number.

Note: If the degrees of freedom associated with all of the standard deviations in eq. 3-15 are greater than or equal to 30, then the degrees of freedom of the standard deviation of the result is also greater than or equal to 30, and use of eq. 3-16 is not required.

As an alternative, the relative standard deviation (precision index) of the result and associated degrees of freedom may be determined as follows:

$$\frac{S_r}{r} = \sqrt{\sum_{i=1}^J \left(\Theta_i \frac{S_{\bar{P}_i}}{\bar{P}_i} \right)^2} \quad (\text{Eq. 3-17})$$

$$v_r = \frac{\left[\sum_{i=1}^J \left(\Theta_i S_{\bar{P}_i} / \bar{P}_i \right)^2 \right]^2}{\sum_{i=1}^J \left[\frac{\left(\Theta_i S_{\bar{P}_i} / \bar{P}_i \right)^4}{v_{\bar{P}_i}} \right]} \quad (\text{Eq. 3-18})$$

3.2.7.2 Bias Uncertainty

For each source of bias uncertainty identified in Section 3.2.3, a bias uncertainty should be evaluated as described in Section 3.2.5. These bias uncertainties must be combined to determine the overall bias uncertainty of the result. The combination of the bias uncertainties must consider any correlation between the bias uncertainties. The special case where all bias uncertainties are considered independent (uncorrelated) is presented first. This is followed by the more general case, which allows for consideration of correlation between bias uncertainties.

3.2.7.2.1 Independent Elemental Bias Uncertainties

Assuming all sources of elemental bias uncertainty are independent (uncorrelated), the bias uncertainty for the test result is computed as:

$$B_r = \sqrt{\sum_{i=1}^J (\Theta_i B_i)^2} \quad (\text{Eq. 3-19})$$

where,

Uncertainty

- Θ_i = sensitivity coefficient for the i^{th} elemental bias uncertainty determined in Section 3.2.6
- B_i = the i^{th} elemental bias uncertainty determined in Section 3.2.5
- J = the number of elemental bias uncertainty sources identified in Section 3.2.3

As an alternative to eq. 3-19, the relative uncertainty of the result is determined as:

$$\frac{B_r}{r} = \sqrt{\sum_{i=1}^J \left(\Theta_i \frac{B_i}{P_i} \right)^2} \quad (\text{Eq. 3-20})$$

3.2.7.2.2 Dependent (Correlated) Elemental Bias Uncertainties

Use of eq. 3-19 or 3-20 assumes that all elemental sources of bias uncertainty are independent (that is, not correlated). If elemental bias uncertainties are not independent (that is, are correlated), then additional cross product terms must be added to eq. 3-19 or 3-20 to address the correlation between every pair of bias uncertainties for which correlation exists. The general form of the equation for combining correlated bias uncertainties is:

$$B_r = \sqrt{\sum_{i=1}^J (\Theta_i B_i)^2} + \sum (\text{all cross product terms}) \quad (\text{Eq. 3-21})$$

The general form of a cross product term is shown below:

$$(\text{cross product term}) = 2 \Theta_a \Theta_b \rho_{a,b} B_a B_b \quad (\text{Eq. 3-22})$$

where,

- $\Theta_{a,b}$ = sensitivity coefficients for the result with respect to elemental bias uncertainties a and b determined in Section 3.2.6
- $\rho_{a,b}$ = correlation coefficient relating elemental bias uncertainties a and b
- $B_{a,b}$ = elemental bias uncertainties a and b

Note: This is a natural extension of use of the Taylor Series formula for propagation of uncertainties.

Note: Separate cross product terms exist between all pairs of elemental bias sources for which a nonzero correlation exists. The subscripts a and b represent all combinations of elemental bias uncertainties for which a nonzero correlation coefficient exists.

Treatment of correlated bias uncertainties, therefore, greatly complicates the uncertainty analysis.

The correlation coefficient between two elemental bias uncertainties can vary from -1 to +1. The magnitude of the correlation coefficient indicates the degree or extent to which the two elemental bias uncertainties in the cross product term are correlated. A correlation coefficient with a magnitude of -1 or +1 means that the two elemental bias uncertainties are completely correlated. Conversely, a correlation coefficient with a magnitude of 0 means that the two elemental bias uncertainties are completely uncorrelated (independent if normal or Gaussian).

The sign of the correlation coefficient indicates the direction or sign with which the two terms are correlated. A positive correlation coefficient means that a positive error in one term would indicate a positive error in the other term. A negative correlation coefficient means that a positive error in one term would indicate a negative error in the other term.

When treating correlated uncertainties, attention to sign is critical. The effect of a correlation can either increase or decrease the uncertainty of a result.

Obtaining information regarding the correlation between elemental bias uncertainties is difficult. Determination of a credible correlation coefficient would require a reliable source of data. If it is not possible to determine a credible value for the correlation coefficient, a conservative value should be assumed. This is illustrated in the following examples.

1. Provided the same equation (correlation) is used to evaluate a film heat transfer coefficient at both test conditions and limiting conditions, a correlation may exist between the uncertainty in these terms. A correlation in these terms will reduce the uncertainty associated with these terms. The correlation between these terms will approach +1 as the test film coefficient approaches the limiting condition film coefficient. Likewise, the correlation between these terms will decrease as the test film coefficient moves away from the limiting condition film coefficient. A similar argument may be made for test condition and limiting condition surface efficiencies. Note: If a credible value for this correlation coefficient cannot be established, it is more conservative to assume (in this case) that no correlation exists.
2. Depending on how the effective heat transfer surfaces areas are determined, there will likely be a strong, positive correlation in the uncertainties for the hot and cold side heat transfer surface areas. An additional correlation may be determined for the surface area associated with the wall resistance. Note: If a credible value for this correlation coefficient cannot be established, it is more conservative to assume (in this case) that no correlation exists.

Uncertainty

3. Depending upon how the measurement system is calibrated and configured, there may be a correlation between the test measurements. For example, if all temperatures are measured with RTDs that were all calibrated with the DAS as a system at the same time and at the same laboratory, a correlation may exist between the instrument bias uncertainties in these measurements. The correlation between these measurements will increase when measuring the same values and decrease when measuring different values. Note: If a credible value for the correlation coefficient between measurements cannot be established, it is conservative to assume (in this case) that no correlation exists between measurements of different parameters and that a correlation of +1 exists between measurements of the same parameter.

Note: Additional dependencies or correlations may be inadvertently created if uncertainties and sensitivity coefficients are evaluated in terms of dependent parameters as opposed to independent parameters of the analysis.

3.2.7.3 Overall Uncertainty of Result

The precision and bias uncertainties of the result are combined using the following equation:

$$U_r = \sqrt{B_r^2 + (t_{95, v_r} S_r)^2} \quad (\text{Eq. 3-23})$$

where,

- U_r = uncertainty in the result with 95% coverage
- B_r = the bias limit for the result
- S_r = precision index for the result
- t = Student's "t" value for 95% coverage based on v_r degrees of freedom

Note: The degrees of freedom of freedom, v_r , is determined using eq. 3-16. The Student's "t" value is obtained from Table 3-1.

As an alternative to eq. 3-23, the relative uncertainty of the result is determined as:

$$U'_r = \sqrt{B_r'^2 + (t_{95, v_r} S_r')^2} \quad (\text{Eq. 3-24})$$

This document divides uncertainties into the following categories of consideration:

- Manufacturing
- Installation
- Calibration
- Flow meter integrity
- Spatial
- Nonhomogeneous flow

In each area of consideration, there are numerous variables that may influence the overall uncertainty associated with the flow measurement. Such variables are termed influence variables and are discussed in the appropriate area of consideration.

3.3 Manufacturing Considerations

The manufacturing process should be capable of consistently producing flow meters within stated tolerances of all identified influence variables. Only vendors with viable quality assurance programs should be considered when purchasing flow elements.

3.4 Installation Considerations

The conditions under which measurement devices are installed may have a significant effect on the accuracy of the measurement. Installation considerations not only address influence variables in the immediate vicinity of the flow measurement, but also include both upstream and downstream influence variables. For flow measurements, errors may increase to an unacceptable degree if the piping arrangements are such that the pipe does not run full or distorted flow conditions result in the measurement zone. Distortions of the velocity profile can significantly affect the accuracy of the flow measurement. Such distortion can be caused by a projecting gasket, misalignment or burr on a pressure tap, roughness of the pipe wall, poor mating of pipe sections, or elbows and bends in the pipe preceding and following the primary element. While some of these may have a minor effect, others can introduce significant errors.

If concern exists that the calibration coefficient of the flow element is reflecting the true velocity or flow profile for a given installation, ANSI/ASME MFC-10M-1994 [5] should be considered as an option to evaluate the installed calibration coefficient of a flow element.

3.5 Calibration Considerations

The objective of the calibration process is to reduce known bias errors to some "acceptable" level. The determination of the "acceptable" level is normally a trade-off involving the objectives of the test program and the cost of achieving those objectives. The calibration process can be the largest contributor in achieving the test program objectives by exchanging relatively large bias errors associated with an uncalibrated or poorly calibrated primary device for the relatively smaller bias errors associated with a primary device that has been calibrated to a NIST traceable standard in a manner that reflects the installed flow profile. This exchange of bias error is fundamental to all calibration processes and requires that the uncertainty of the calibration standard be substantially less than that of the measurement device. A 4:1 ratio is normally deemed acceptable; however, on some types of state-of-the-art field equipment, a 1:1 ratio is acceptable.

It is important to note that the calibration process should include a reasonable simulation of test conditions. The need for approximating test conditions varies widely with the type of measurement device, and each case must be examined carefully. The calibration process must be done in such a manner that the instrument response may be assumed to be identical to that which would be obtained in its test environment. Any violation of this requirement could provide a false sense of security and may lead to a costly mistake.

Flow meter calibrations may employ a primary standard, secondary standard, or a "dry" calibration. A primary standard provides the best accuracy and may employ the gravimetric or volumetric method. The gravimetric method, described in ASME MFC-9M-1988 [6], diverts flow into a tank mounted on scales for a timed period. The flowmeter output is averaged over the diversion period to characterize the performance. In the volumetric method, the weigh tank is replaced with a volume tank. These primary methods achieve uncertainties of 0.1 to 0.2% and are generally traceable to national standards.

A secondary standard is a flow meter that has been calibrated by a primary method and is used as a transfer standard. Secondary standard calibrations usually achieve uncertainties of 0.5 to 1.0%.

Dry calibrations are either inspections of a meter for dimensions of a throat diameter, upstream diameter, surface roughness, and tap fabrication in the case of a differential pressure producer or bench testing of the electronics of an ultrasonic flow meter. These "dry" calibrations generally verify the electronics of the meter and should not be considered as a substitute for a primary or secondary standard calibration.

Some types of meters, such as magnetic meters with electronic outputs, have adjustment factors that are varied so that the meter output may be brought "into

calibration” relative to a given specification or signal input. Other meter types, such as the differential pressure producers have intrinsic performance characteristics such as discharge coefficients, which are not adjustable and are defined by the calibration process.

3.6 Flow Meter Integrity Considerations

The integrity of a flow meter is a time issue and depends on the time in service, inspection interval, and routine maintenance. Most properly applied and installed flow meters require very little maintenance and can operate for extended periods of time with few problems. A few, however, may require some routine service. Maintenance problems and frequency of routine maintenance vary with the process fluid, type of flow meter, and the nature of upset condition. Some flow meters lose their accuracy as they get dirty from the process fluid. This change can occur slowly and can alter the dynamic response and/or the accuracy of the measurement. Instruments should be periodically inspected and calibrated to controlled standards to maintain their integrity and accuracies. Guidance on recommended periods for inspections, maintenance, and calibrations are normally provided in vendor literature and industry performance standards.

3.7 Spatial Considerations

Spatial considerations focus on the ability of discrete point measurements to approximate a spatial average of the parameter value. As a general rule of thumb, spatial bias uncertainty should be identified as a source of uncertainty for each measured parameter associated with the test unless there is sufficient objective evidence that spatial bias uncertainty is negligible or the instrument fully averages the parameter over the defined measurement plane.

3.8 Nonhomogeneous Flow Considerations

Nonhomogeneous flow considerations focus on the influence of entrained air and entrained debris on the flow measurement. The majority of flow meters evaluated in this guideline are not recommended for applications that may involve nonhomogeneous flow streams.

3.9 References

1. American National Standards Institute/American Society of Mechanical Engineers. PTC 19.1 - 1985. *Instruments and Apparatus. Part 1, Measurement Uncertainty*. ASME, 1986.
2. R. Miller. *Flow Measurement Engineering Handbook*. McGraw Hill, 1996.
3. American Society of Mechanical Engineers. "Inservice Performance Testing of Heat Exchangers in Light-Water Reactor Power Plants, Part 21." *Standards and Guides for Operation and Maintenance of Nuclear Power Plants*. ASME OM-S/G, 1994.
4. Instrument Society of America. RP67.04 - Part 11 - 1994. *Methodologies for the Determination of Setpoints for Nuclear Safety-Related Instrumentation*. ISA, Sept. 1994.
5. American National Standards Institute/American Society of Mechanical Engineers. ANSI/ASME-MFC-10M. *Methods for Establishing Installation Effects on Flowmeters*. ASME, 1994.
6. American National Standards Institute/American Society of Mechanical Engineers, ANSI/ASME-MFC-9M. *Measurement of Liquid Flow in Closed Conduits by Weighing Method*. ASME, 1989.

4

REFERENCE DOCUMENT REVIEW

4.1 Introduction

Substantial industry guidance is available that addresses the various flow measurement techniques. Many of the available references, however, do not address the issue of uncertainty. The intent of this section is to provide a review of literature that addresses the uncertainty of flow measurement for the various selected methods and technologies surveyed in this document.

Many “tried and true” methods that have been used and studied extensively, such as differential producers and turbine meters, have a wealth of references that quantitatively address the subjects of accuracy and uncertainty. However, relatively new methods, such as vortex shedding and Coriolis mass flow meters, have limited literature pertaining to the quantification of the various influence variables that contribute to the uncertainty of the flow measured by these techniques. Additionally, there is little, if any, connectivity among the numerous references with regard to the assessment of the uncertainty of flow measurement.

Presented in this section is a selection of relevant references for each flow measurement technique. Connectivity among the references is provided in the form of a matrix of associated topics and influence variables addressed by each reference. The discussions for each reference in this section form the framework from which specific methodologies are developed in Section 5 for estimating uncertainties for the various measurement techniques.

4.2 Differential Pressure Producers

4.2.1 General Discussion

This section is globally titled “differential pressure producers” because there are many devices used to provide the differential pressure associated with a given rate of flow. Specifically, the four differential producers addressed in this section are:

- The orifice
- The flow nozzle
- The Venturi tube
- The V-cone meter

The accuracy of flow measurements made with these devices depends largely on the coefficients of discharge used in computing the flow. The coefficients of discharge are affected by the design and quality of construction of the primary element. The empirical equations developed for the calculation of the discharge coefficients are the result of thousands of tests conducted in many different facilities and under many different operating conditions. Uncertainties exist in the determination of the coefficient that must be quantified to assess the confidence that can be attributed to the flows calculated from these coefficients.

Additionally, there are other uncertainty contributors associated with differential producers, such as the measurement of diameters, pressures, and temperatures, which must be considered when determining the uncertainty of a flow measurement. The combination of these aforementioned factors in a systematic method is, therefore, an estimate of the overall uncertainty one can expect to achieve for a flow measurement made under a particular set of operating conditions.

Table 4-1 below presents a comparison of the areas of consideration and the associated influence variables addressed by References 1–5 for the traditional differential pressure producers, while Reference 31 pertains solely to the V-cone meter.

Table 4-1
Orifice, Nozzle, Venturi Differential, and V-Cone Pressure Producer Influence Variable
Reference Matrix

Area Of Consideration	Influence Variable	References					
		1	2	3	4	5	31
Manufacturing	Material Thermal Expansion	√	√		√		
	Orifice Thickness	√	√		√		
	Orifice Surface Flatness	√	√		√		
	Pressure Tap Configuration	√	√	√	√		√
	Drain/Vent Holes				√		
	Orifice Shape/Size	√	√	√	√		√
	Installation	Pipe Surface Roughness	√	√	√		
Trueness of Internal Diameter		√	√				
Flow Disturbances		√	√	√	√	√	√
Orientation of Sensing Lines				√	√		
Presence/Location of Flow Straighteners		√	√	√	√	√	√
Initial Flushing of Pipe						√	
Eccentricity		√	√				
Calibration	Calibration versus Uncalibrated			√	√	√	
	Frequency					√	
Flow Meter Integrity	Inspections					√	
Spatial	NA						
Nonhomogeneous Flow	Entrained Air				√		

4.2.2 Reference 1, ANSI/ASME. MFC-3M-1989. Measurement of Fluid Flow in Pipes Using Orifice, Nozzle, and Venturi

4.2.2.1 Uncertainty Methodology

ASME's approach in this document is to prescribe a methodology to achieve a cited accuracy. This reference bounds the expected uncertainty achievable when measuring the flow of fluids with orifices, flow nozzles, and Venturi tubes manufactured and installed to the specified standards.

4.2.2.2 General Discussion

Developed by ASME to be consistent and technically equivalent with ISO 5167 [8], this document appears to be the most detailed and technically complete presentation of the specifications necessary to fabricate a differential producer, resulting in an uncertainty component for the coefficient of discharge or flow of minimal magnitude.

Sections 3 and 4 review in detail the definitions and equations necessary for sizing the primary device and for calculating a subsequent flow rate from the differential pressure obtained from the device. Section 4.1 provides the recommended methods of calibration for the flow section.

Section 6 provides material and installation specifications for the pipe upstream approach and for the downstream section. Table 2 presents the minimum recommended straight lengths of piping for a properly installed orifice or flow nozzle in order to bound the value for installation effect uncertainty to $\pm 0.5\%$ of reading. The reference notes that this value can be diminished to zero if twice the minimum values are present in the installation.

Section 7 through 9 provides manufacturing specifications for orifice, flow nozzle, Venturi tube, and associated pressure tap configuration. With a beta ratio no greater than 0.75, a bounding value of $\pm 0.75\%$ of reading may be used for the uncertainty associated with the coefficient of discharge.

Section 10, "Uncertainties in the Measurement of Flow Rate," references ANSI/ASME MFC-2M-1983 [6] and develops a method for the practical computation of the uncertainty of mass flow.

4.2.3 Reference 2, ISO 5167-1980. Measurement of Fluid Flow by Means of Orifice Plates, Nozzles and Venturi Tubes Inserted in Circular Cross-Section Conduits Running Full

4.2.3.1 Uncertainty Methodology

ISO's approach in this document is to prescribe a methodology to achieve a cited accuracy. This reference is nearly identical to ASME MFC-3M [1] in both content and methodologies.

4.2.3.2 General Discussion

Section 3 deals with the principal method of measurement and computation of diameter ratio, rate of flow, and mass density. Section 4 provides the criteria for selection of the primary device. Section 6 provides recommendations on the general installation for differential producers, specifically addressing:

- The minimum straight lengths expressed as multiples of the pipe diameter D for various fittings located upstream and downstream from the primary device. When the upstream or downstream straight lengths of pipe are shorter than the minimum requirement for "zero additional uncertainty" and equal to or greater than the minimum requirement for incurring " $\pm 0.5\%$ additional uncertainty" as given in Tables 3 and 4, an additional uncertainty of $\pm 0.5\%$ shall be added arithmetically to the uncertainty on the flow coefficient. Uncertainties are stated as a percent of reading.
- Recommendations on the use of flow straighteners.
- Recommendations on the location of primary devices.

Section 7 provides the general manufacturing requirements such as shape, diameter, thickness, angle of the bevel, arrangement of pressure taps, and pipe wall roughness. Uncertainty associated with the use of calculated discharge coefficients is also given for different types of pressure taps. Using the guidance in Section 7, a bounding value of $\pm 0.75\%$ of reading may be used for correctly manufactured differential producers with beta ratios no greater than 0.75.

4.2.4 Reference 3, ASME. Part II of ASME Fluid Meters, Their Theory and Application, Sixth Edition

4.2.4.1 Uncertainty Methodology

ASME's approach in this document is to prescribe a methodology that will achieve a cited accuracy. This reference bounds the expected uncertainty achievable when measuring the flow of fluids with orifices flow nozzles and Venturi tubes manufactured and installed to the specified standards.

4.2.4.2 General Discussion

In addressing the uncertainties of orifice, nozzle, and Venturi differential producers, ASME provides instruction in two areas:

- Recommended values for the uncertainties associated with the coefficients of discharge and flow when the primary elements are manufactured to the prescribed specifications
- Recommended values for the uncertainties associated with the installation and location of the primary elements to the prescribed specifications

Chapter II-II provides recommendations on the general installation of orifices, flow nozzles, and Venturis specifically addressing:

- The recommended minimum lengths of straight pipe upstream and downstream of the differential producer, with or without flow straighteners. If the recommendations are followed, the uncertainty associated with the presence of upstream or downstream flow disturbances will be less than $\pm 0.5\%$ of reading. If it is not possible to provide the recommended minimum lengths, even with the use of straightening vanes, this reference recommends an additional uncertainty of $\pm 0.5\%$ of reading should be applied to the flow measurement.
- Recommendations addressing the pipe surface conditions and pipe diameter immediately upstream and downstream of a primary element
- Installation requirements associated with the mounting of a primary element
- Installation requirements associated with the location and configuration of pressure taps
- Installation requirements associated with the location and configuration of the sensing lines and pressure transmitters

Chapter II-III of this reference provides the general manufacturing requirements and the methodology to calculate coefficients of discharge and flow. Equations are provided for the calculation of the coefficients or they may be looked up in an appropriate table.

Chapter II-IV, in Table II-V-1, provides recommended values for the uncertainty associated with the coefficients of discharge and flow for differential producer primary elements manufactured to the stated specifications.

4.2.5 Reference 4, R. Miller. *Flow Measurement Engineering Handbook, Third Edition*

4.2.5.1 Uncertainty Methodology

The approach used by this reference is to prescribe a methodology to achieve a cited accuracy. Miller bounds the uncertainty for the coefficient of discharge for a β ratio of 0.75 at $\pm 0.75\%$ of reading, while the ASME nozzle is bounded at $\pm 2.0\%$ for β ratios 0.25 to 0.75.

4.2.5.2 General Discussion

Chapter 8 provides material and installation requirements for the condition of the pipe, pressure tap design, mating of pipe sections, and straight length of the pipe preceding and following the primary element.

The accuracy and uncertainty for differential producers are discussed in detail in Chapter 9. Specifically, Table 9.54 summarizes the coefficient of discharge accuracies and associated constraints for various differential producing primary elements. Table 9.56 provides closed form, differentiated equations for the sensitivity coefficients of the major parameters. Table 9.57 provides a summary of the elemental bias uncertainties for various installation effects. Also, there are several examples of uncertainty computations contained in this section.

Chapter 10 provides design information for the coefficients of discharge for differential producers. Recommendations and figures are provided for plate thickness, pressure-tap spacing, discharge coefficients, and permanent pressure loss.

4.2.6 Reference 5, ASME. PTC 6 Report - 1985, Guidance for Evaluation of Measurement Uncertainty in Performance Tests of Steam Turbines

4.2.6.1 Uncertainty Methodology

ASME's approach in this document is to prescribe a methodology to achieve a cited accuracy and to provide a means to estimate the additional uncertainty associated with deviations from the specified recommendations.

4.2.6.2 General Discussion

The primary intent of this reference is to provide a means of estimating the expected measurement uncertainty in the performance of steam turbine tests when deviations exist from the requirements of ASME PTC 6 [25]. The overall flow measurement uncertainty is discussed in terms of the following elemental uncertainties. Sections 4.15 through 4.17 provide tabular and graphical estimates of these elemental uncertainties as functions of appropriate influence variables. The six elemental uncertainties may be discussed in terms of bounding values as follows:

- Base - this elemental uncertainty is a function of the calibration and/or inspection. A bounding value for a calibrated flow section is $\pm 3.0\%$ of reading, while no bounding value exists for an uncalibrated, un-inspected flow section.
- LNS - this elemental uncertainty is a function of the number of equivalent lengths of straight pipe upstream of a primary device when no flow straightener is in use. This component is for Beta ratios no greater than 0.7 and the minimum required equivalent lengths of straight pipe upstream of a primary device prior to a flow disturbance. When no flow straightener is used, a bounding value of $\pm 2.2\%$ of reading may be used.
- LS1 - this elemental uncertainty is a function of the number of equivalent lengths of straight upstream pipe between a primary device and a flow straightener. This component is for Beta ratios no greater than 0.7 and at least two equivalent lengths of upstream pipe between a primary device and a flow straightener. A bounding value of $\pm 3.0\%$ of reading may be used.
- LS2 - this elemental uncertainty is a function of the number of sections in a flow straightener. This component is for Beta ratios no greater than 0.7 and at least 8 straight sections in a flow straightener. A bounding value of $\pm 1.6\%$ of reading may be used.
- DSL - this elemental uncertainty is a function of the number of equivalent lengths of straight downstream pipe from a primary device. The reference states that with at

least 80% of the minimum recommended equivalent lengths of straight downstream pipe from a primary device, a bounding value of $\pm 1.0\%$ of reading may be used.

- Beta - this elemental uncertainty is a function of the beta ratio for uncalibrated primary devices. The reference states that for Beta ratios no greater than 0.75, a bounding value of $\pm 1.0\%$ of reading may be used.

The reference, in Section 4.18, provides an example of the methodology used to estimate the total expected uncertainty of a flow nozzle for the calibrated and uncalibrated cases.

4.2.7 Reference 31, Southwest Research Institute Report. Baseline and Installation Effects of the V-Cone Meter

4.2.7.1 Uncertainty Methodology

The methodology of this reference is to provide baseline and installation calibration data that will facilitate the evaluation of the installation effect uncertainty for various configurations of piping.

4.2.7.2 General Discussion

This is a report that details the uncertainty in the calibration of the V-cone meter.

4.3 Multiport Averaging Pitot Tubes

4.3.1 General Discussion

The multiport averaging pitot tube is a device that spans the pipe and provides an “averaged” stagnation pressure via the use of multiple ports on the upstream side. The averaged stagnation pressure is used in differential with the downstream static pressure to produce an “averaged” velocity pressure in the conduit.

When properly located in a pipe that is running full to minimize any installation effects, the multiport averaging pitot tube can provide flow rates at $\pm 1.0\%$ accuracy and $\pm 0.1\%$ repeatability [9]. If the situation precludes installing this type of device in such a manner as to provide the recommended straight pipe upstream and downstream installation margins, an *in situ* calibration can generally provide a calibrated flow coefficient that will produce a $\pm 1.0\%$ accuracy.

The industry references listed in Section 2.3 discuss various aspects of the preparation and use of multiport averaging pitots for the measurement of flow rate. Table 4-2

Reference Document Review

below presents a comparison of the areas of consideration and the associated influence variables addressed by each of the cited references.

**Table 4-2
Multiport Averaging Pitot Tube Influence Variables Reference Matrix**

		References	
Area Of Consideration	Influence Variable	4	9
Manufacturing	Sizing	√	√
	Probe Blockage	√	√
	Probe Configuration	√	√
Installation	Alignment		√
	Equivalent Pipe Diameters From Upstream & Downstream Flow Disturbances	√	√
	Orientation of Sensing Lines		√
	Presence of Flow Straighteners	√	√
Calibration	Calibrated vs. Uncalibrated	√	√
Flow Meter Integrity	Inspections		√
	Port Blockage		√
Spatial	Integrated Velocity Measurement	√	√
	Spacing & Number of Sensing Ports	√	√
Nonhomogeneous Flow	Entrained Debris/Air		√

4.3.2 Reference 4, R. Miller. Flow Measurement Engineering Handbook, Third Edition

4.3.2.1 Uncertainty Methodology

This reference provides a methodology to attain a stated accuracy. It provides no uncertainty data from which an estimate of overall uncertainty can be made on any deviations due to installation effects. The recommended upstream and downstream straight pipe lengths for various piping configurations are listed in Table 8.2. This reference bounds the overall accuracy of an uncalibrated Annubar[®] (including the differential pressure transmitter) of $\pm 1.25\%$ of the upper range value (URV), and constrains this value to $Re_d > 10,000$.

4.3.2.2 General Discussion

This reference addresses the use of the Annubar in the measurement of liquid and gas flows. Much of the information pertinent to the Annubar is presented under the more general heading of differential producers, and is therefore not specific to Annubar. Topics include installation, sensing lines, and upstream and downstream flow disturbances.

This reference discusses the standard Annubars flow calculations, flow coefficients, and several correction factors. Tables are presented giving values for flow coefficient and Reynolds number correction factors as a function of the pertinent parameters.

4.3.3 Reference 9, Dieterich Standard Corporation. Annubar[®] Handbook

4.3.3.1 Uncertainty Methodology

The approach used by this reference is to prescribe a methodology to achieve a bounding accuracy of $\pm 1.0\%$, as stated by the manufacturer. No uncertainty data is provided by which an estimate can be made of the impact on the overall uncertainty by not meeting the specifications of the methodology.

4.3.3.2 General Discussion

This reference addresses the application of the Annubar multiport averaging pitot tube measuring system for liquid and gas service, although this guideline limits the scope to liquids. The discussion begins with the basics of fluid flow in pipes ultimately deriving the governing flow rate equations from Bernoulli's theorem. The bounding

value for a Diamond II Annubar flow coefficient, as provided by the manufacturer is $\pm 1.0\%$ of reading for Reynolds numbers $4000 < Re_D < 30,000,000$.

Chapter 1 deals with fluid flow theory as it applies to pipe flow. A discussion is provided addressing the physical properties of liquids and gases. Additional information on the physical properties of fluids is contained in Appendix A.

Chapter 2 discusses the standard annubar flow calculations, flow coefficients, and several correction factors that may be required. The correction factors associated with liquids address:

- Reynolds number
- Manometer factor
- Thermal expansion factor
- Gage location factor

Tables are presented giving values for flow coefficients and each of the correction factors as a function of the pertinent parameters.

Chapter 3 provides guidance on the installation and use of Annubars[®] to obtain flows in pipes. Recommended distances from both upstream and downstream flow disturbances is presented. No quantitative information is provided from which bounding uncertainty estimates can be derived for any of the installation effects.

4.4 Pitot Traverses

4.4.1 General Discussion

The pitot tube is a flow measuring device that is temporary by design. Specific pipe wall taps and bushing devices allow the insertion of the pitot tube into a closed conduit stream. A frequently used pitot tube design for the measurement of water flow is the Simplex/Leopold. This type of unreinforced tube provides the necessary rigidity to diametrically traverse pipes up to 48" (1.2 m) in diameter. Larger pipes require radius traverses or reinforced tubes. The pitot tube operates similar to any differential pressure producing device in that one port is directed into the flow stream to sense the total pressure and another port is oriented perpendicular to the flow stream to sense the static pressure; the difference between these two values is the velocity pressure. The pitot tube is traversed across a minimum of two diameters with velocity pressure readings taken at equal area points. The result is an area averaged velocity pressure that can be used to calculate the volumetric flow in the pipe. Table 4-3 below presents a

comparison of the areas of consideration and the associated influence variables addressed by each of the cited references.

Table 4-3
Traversing Pitot Tube Influence Variable Reference Matrix

		References		
Area Of Consideration	Influence Variable	13	20	27
Manufacturing	Sizing			√
	Probe Blockage	√	√	√
	Probe Configuration	√		√
Installation	Alignment	√		√
	Upstream & Downstream Flow Disturbances	√		√
	Orientation of Sensing Lines			√
	Presence of Flow Straighteners	√		√
Calibration	Calibrated vs. Uncalibrated	√	√	√
Flow Meter Integrity	Inspections			√
	Port Blockage	√		√
Spatial	Integrated Velocity Measurement	√	√	√
	Spacing & Number of Traverse Point	√	√	√
Nonhomogeneous Flow	Entrained Debris/Air	√		√

4.4.2 Reference 13, Cooling Tower Institute Bulletin. STD-146(95). Standard for Water Flow Measurement

4.4.2.1 Uncertainty Methodology

The approach employed by this reference is to prescribe a methodology to achieve a cited accuracy. This reference states that the pitot tube is the Cooling Tower Institute (CTI) basic reference standard instrument for the measurement of water flow. Section 2.0 discusses the piping requirements regarding straight upstream and downstream lengths, pipe circularity, pipe internal surface roughness, and straightening vanes. Section 3.0 addresses nonhomogeneous flow streams and the impact on the measured

flow. Appendix II-F specifically deals with the pitot tube and states a cited accuracy, if all installation and calibration requirements are satisfied, of $\pm 1.0\%$ of flow.

4.4.2.2 General Discussion

This reference is useful in providing guiding principles for the measuring water flow. Sections 1.0 and 2.0 discuss the requirements for attaining the cited accuracies. Section 3.0 discusses issues with contaminants or disturbances in the flow. Sections 4.0 and 5.0 address in detail the necessary specifications for pitot tubes (and other flow metering devices). Section 6.0 discusses the considerations for calibrating a pitot tube. Section 7.0 addresses the available secondary devices for signal readout and conditioning.

4.4.3 Reference 20, Power Generation Technologies Technical Paper. Uncertainty Analysis of Cooling Tower Performance, Presented at the CTI Winter Meeting

4.4.3.1 Uncertainty Methodology

This reference describes in detail the factors that influence the uncertainty of a water flow measurement obtained with a traversing pitot tube. The authors provide a comprehensive closed form analysis of both the elemental bias and precision uncertainties that contribute to the overall uncertainty of the flow measurement.

4.4.3.2 General Discussion

This paper does not provide details regarding the manufacture, installation, or other influence variables.

4.4.4 Reference 27, ISO. ISO 3966-1977. Measurement of Fluid Flow in Closed Conduits - Velocity Area Method Using Pitot Static Tubes

4.4.4.1 Uncertainty Methodology

The methods and techniques prescribed in this reference will yield a level of uncertainty of no greater than $\pm 2.0\%$ of flow. Specific methods espoused in Section 12 detail the various classifications of errors and their impact on the flow calculated by an area integration technique. Annex G includes a detailed sample uncertainty calculation.

4.4.4.2 General Discussion

This ISO standard is extremely comprehensive and should be regarded as an excellent source for specification and use of the pitot static tube for the measurement of fluid flow. Sections 1 through 3 address the basic scope, nomenclatures, and principles of flow measurement with a pitot tube. Section 4 deals with the design of pitot tubes and provides detailed specifications for construction and allowable tolerances. Section 5 explores the requirements for the use of pitot tubes. Sections 7 through 11 address methods that are used to calculate the velocity.

4.5 Ultrasonic Flow Meters

4.5.1 General Discussion

The ultrasonic method of non-intrusively measuring the velocity of a fluid in a closed conduit is gaining wide use in the industry today. The three types of ultrasonic flow meters in use for closed pipe flow measurement are:

- Transit time
- Cross-correlation
- Doppler

The application of transit-time ultrasonic flow metering is gaining acceptance in the utility industry. Clamp-on, portable systems facilitate the measurement of flow without the burden and cost of intruding into the existing piping system to install a flow element. The Doppler method has limited application in the measurement of flow for the industry; therefore, the focus of the following abstracts will be on the transit-time method and the cross-correlation method. Table 4-4 summarizes the areas of consideration and influence variables with respect to the selected references for the transit-time method.

**Table 4-4
Transit-Time Ultrasonic Flow Meter Influence Variable Reference Matrix**

Area Of Consideration	Influence Variable	Reference			
		10	11	26	28
Manufacturing	Transducer Type	√	√		√
	Acoustic Path Configurations	√	√	√	√
	Velocity Profile Correction Factor	√	√	√	√
Installation	Flowcells vs. Field Mounted		√	√	√
	Intervening Material	√	√	√	√
	Transducer Configurations	√	√	√	√
	Acoustic Noise	√	√	√	
	Flow Area	√	√	√	√
	Surface Roughness		√		√
	Flow Disturbances	√	√		√
Calibration	Calibration Method	√	√		√
Flow Meter Integrity	Inspections		√		
Spatial	Ultrasonic Path			√	√
	Number of Paths		√		√
Nonhomogeneous Flow	Entrained Air or Gas		√	√	√
	Entrained Debris		√		

4.5.2 Reference 10, ANSI/ASME. MFC-5M-1985. Measurement of Liquid Flow in Closed Conduits Using Transit-Time Ultrasonic Flow Meters

4.5.2.1 Uncertainty Methodology

None are stated in this document, but the classification of error sources and various ways to reduce them are discussed in Section 3.

4.5.2.2 General Discussion

This standard applies to ultrasonic flow meters that base their operation on transit-time measurements. It deals with liquids exhibiting homogeneous acoustic properties and flowing in a completely filled closed conduit. Section 2 provides the operating principles for the transit-time and frequency difference measurements. It also provides information about primary and secondary devices, measurement sections, acoustic paths, data processing, and output display.

Section 3 describes possible error sources for ultrasonic flow meters covered by this standard. Section 4 provides information on performance parameters including accuracy, linearity, repeatability, stability, rangeability, resolution, response time, and power requirements. Proper installation guidelines for error reduction that should be addressed during the project design phase are mentioned in this section. The three principal methods of determining the meter factor (laboratory calibration, field calibration and analytical procedures) are discussed in Section 5.

No quantitative information is provided from which bounding uncertainty estimates can be derived.

4.5.3 Reference 11, L. Lynnworth. *Ultrasonic Measurements for Process Control, Theory Techniques, Applications*

4.5.3.1 Uncertainty Methodology

The approach of this reference is to describe case studies that have demonstrated a specific uncertainty.

4.5.3.2 General Discussion

This reference provides a general discussion of the application of ultrasonic flow meters. Much of the discussion focuses on past work done with ultrasonic flow meters in various applications and the degree of success achieved in each case. The uncertainty methodology presented does not prescribe a methodology to achieve a cited accuracy as much as it attempts to present past works that show a certain level of accuracy is achievable. Typical accuracies are cited ranging from 0.5% to 1.5% for transit-time flow meters.

4.5.4 Reference 26, Rabensteine and Arnsdorff. Flow Determination by Acoustic Transit Times

4.5.4.1 Uncertainty Methodology

This reference provides a methodology to calculate the uncertainties associated with a transit-time method of flow metering using clamp-on transducers. In the case presented, the composite flow instrument bias uncertainty is estimated to be $\pm 1.4\%$ of flow.

4.5.4.2 General Discussion

This reference provides calculations necessary to determine the composite bias uncertainty of an ultrasonic flow measurement. In calculating the composite instrument bias uncertainty, the following sources of instrument bias uncertainty are addressed:

- Accuracy and stability of calibration - The discussion addresses both intrinsic calibrations of the flow meter's electronics and wet calibrations of the flow meter's overall flow measurement ability.
- Correction factor application - The discussion addresses the uncertainty associated with the determination of a flow profile correction factor.
- Determination of pipe dimensions - The discussion addresses the uncertainty associated with determining the pipe outer diameter and the wall thickness.
- Transducer spacing - For portable flow meters, the uncertainty due to the transducer spacing is not included in the calibration uncertainty because the transducers must be remounted at the test site.
- Determination of pipe speed of sound - For portable flow meters, the uncertainty due to the pipe speed of sound is not included in the calibration uncertainty due to the variations in the pipes used for calibration and the test site.
- Determination of fluid kinematic viscosity - The uncertainty due to the fluid kinematic viscosity is a function of the fluid temperature.
- Measurement loop - The uncertainty associated with the measurement loop is discussed in terms of both an intrinsic and wet calibration.

4.5.5 Reference 28, ISO. ISO Technical Report 12765:1997 (E). Measurement of Fluid Flow in Closed Conduits - Method Using Transit Time Ultrasonic Flowmeters

4.5.5.1 Uncertainty Methodology

This reference prescribes a methodology to attain an uncertainty. There are no quantitative values presented. Section 7 is devoted entirely to the assessment of uncertainty in various configurations of transit-time ultrasonic metering. Section 7.2 addresses various influence factors that contribute to the flow measurement uncertainty.

4.5.5.2 General Discussion

This is a comprehensive reference for all aspects of flow measurement with transit time ultrasonic meters. Sections 1 through 5 develop the nomenclature, definitions, conventions, and equations necessary to evaluate the physics involved with the propagation of ultrasonic signals. Section 6 addresses the design, configuration, and operation of transducers. Section 8 highlights the various procedures and techniques involved in the calibration of the transit-time ultrasonic flow metering system.

The following table summarizes the areas of consideration and influence variables with respect to the selected references for the cross-correlation method. Table 4-5 below presents a comparison of the areas of consideration, and the associated influence variables, addressed by each of the cited references.

**Table 4-5
Cross-Correlation Ultrasonic Flow Meter Influence Variables Matrix**

Area Of Consideration	Influence Variable	Reference		
		14	15	29
Manufacturing	Type of Transducer			√
Installation	Intervening Material	√		√
	Transducer Configuration			√
	Transducer Location	√	√	√
	Flow Area	√		√
	Surface Roughness	√		√
	Flow Disturbances	√		√
Calibration	Calibration Method			√
	Velocity Profile		√	√
Nonhomogeneous Flow	Entrained Air/Gas - Multiphase	√		
	Entrained Debris	√		

4.5.6 Reference 14, Beck and Plaskowski. Cross-Correlation Flow Meters

4.5.6.1 Uncertainty Methodology

This reference describes in detail possible sources of uncertainty. The focus of this reference is the technique of cross-correlation analysis of ultrasonic signals for the flow measurement.

4.5.6.2 General Discussion

The reference addresses the basic fundamentals of cross-correlation flow measurement.

4.5.7 Reference 15, Gurevitch et al. Theory and Application of Non-invasive Ultrasonic Cross Correlation Flow Meter. The 9th International Conference on Flow Measurement

4.5.7.1 Uncertainty Methodology

This reference explores the extrapolation of the calibration factor to higher Reynolds numbers and the associated uncertainty.

4.5.7.2 General Discussion

This reference describes the theoretical derivation of the calibration factor for cross-correlation flow meters.

4.5.8 Reference 29, CROSSFLOW[®] - Users Guide for Ultrasonic Flow Measurement

4.5.8.1 Uncertainty Methodology

The reference includes an introductory discussion of uncertainty calculations. An example of a detailed calculation for a cross-correlation ultrasonic flow meter is contained in Section 10.

4.5.8.2 General Discussion

This reference provides a discussion and instruction on the application and use of the CROSSFLOW[®] flow meter. It describes setup procedures, the input of the required parameters, and interpretation of various diagnostic messages.

A brief discussion of the theory is given in the introductory section of this reference. A more detailed discussion on how the specific parameters affect the flow measurement is contained in Section 10.

4.6 Dye Dilution Methods

4.6.1 General Discussion

The dye dilution technique of flow determination can be used to measure flow in service water systems. Dye dilution is a way of overcoming the problems and expense of establishing installation effects due to disturbances on the flow profile without

having to model the piping system in a calibration laboratory. Two methods of dye dilution have been developed:

- Slug injection
- Constant rate injection

The slug injection technique is a time of travel method where a slug of the tracer is injected into the flow stream. The application requirements for slug injection are so onerous that there is little industry experience with this method.

The continuous injection method is commonly used in the industry. The constant rate injection of a fluorescent dye such as Rhodamine WT, with detection by a fluorometer at the downstream sampling station is used almost exclusively in the industry to measure the water flow. This review will focus on the continuous injection method.

With the continuous injection method, the flow rate is determined from the rate of dye injection and the concentration of the dye at the measurement station:

$$q_w = \frac{C_o}{C_w} * q_o \quad (\text{Eq. 4-1})$$

The influence variables associated with the continuous injection method are cross-referenced in Table 4-6 below. This table presents a comparison of the areas of consideration and the associated influence variables addressed by each of the cited references.

Table 4-6
Flow Measurement by Dye Dilution Influence Variable Matrix

Area Of Consideration	Influence Variable	Reference		
		16	17	18
Dye Addition	Dye Injection Rate	√	√	√
	Concentration of Injected Dye	√	√	√
	Injection Method	√	√	√
Dye Sampling	Mixing Characteristics		√	√
	Sample Extraction	√	√	√
Concentration Analysis	Standards Preparation	√	√	√
	Temperature Effects	√	√	√
	Fluorometer Repeatability	√	√	√
Interferences	Sediment	√	√	√
	Salinity		√	√
	Microscopic Air	√		
	Background Fluorescence			√

4.6.2 Reference 16, W.H. Morgan, et al. Validation of the Use of the Dye Dilution Method for Flow Measurement in Large Open and Closed Channel Flows

4.6.2.1 Uncertainty Methodology

The flow rate calculated by the dye dilution method was compared to that calculated by volumetric measurement to establish an overall uncertainty interval of $\pm 3.0\%$ over a total of five runs. This accuracy was achieved despite the interference effect of microscopic air bubbles in the water, which was compounded by the low level of dye at the measurement station. Field measurements were conducted as part of a test program to establish the performance curve for a pump. Field measurements indicated an agreement of $\pm 1.5\%$ with the volumetric flow predicated by the pump performance curve. These results were obtained despite a large and variable amount of sediment in the water.

4.6.2.2 General Discussion

This reference presents the only direct validation of the dye dilution method against a volumetric standard. It also gives a complete discussion of the difficulties encountered in the validation and measurement phases of the work performed. The uncertainty values obtained represent the values obtained by the authors, and it is likely that better accuracy can be obtained by utilizing methods designed to avoid the difficulties that they experienced.

4.6.3 Reference 17, Nystrom and Hecker. Uncertainty Analysis of Field Turbine Performance Measurements

4.6.3.1 Uncertainty Methodology

This reference provided by Alden Research Laboratories, prescribes a methodology to achieve a cited uncertainty of $\pm 1.3\%$. The application reported in this reference provides comparative data from two independent methods; the first is the dye dilution method and the second is the point velocity integration method using Ott-type propeller/current velocity meters.

4.6.3.2 General Discussion

This reference provides good detail on the methods and techniques necessary to conduct a successful and conclusive dye dilution flow measurement. The effort described in this reference utilized a volumetric dilution scenario to prepare the calibration standards.

4.6.4 Reference 18, Hennon and McNutt. Pre-Test Uncertainty Analysis for Dye Dilution Flow Measurement

4.6.4.1 Uncertainty Methodology

The methodology outlined in this reference is for a pre-test uncertainty analysis of the dye dilution method for a service water flow measurement application. The estimated uncertainty on a pre-test basis was found to fall in a range of 1.1 to 1.8% of flow.

4.6.4.2 General Discussion

This reference provides a complete closed form pre-test uncertainty analysis for the application. The effort described by the authors is for a typical service water flow

measurement. In this application, the calibration standards were prepared using a mass dilution scenario.

Commentary: Most of the effects of interferences are mitigated by using the test service water when performing the standards dilutions. Standards and samples should be analyzed immediately. A linear calibration curve should be expected even in the presence of interferences although the slope may be different than that for distilled water.

4.7 Magnetic Flow Meters

4.7.1 General Discussion

The magnetic flow meter has been in commercial use since the 1950s. Applications are specifically indicated in the measurement of corrosive fluids as there are minimal wetted parts. The flow meter falls into an overall category known as linear flow meters. In order to properly assess the uncertainty of the flow measured by a “magmeter,” the entire system, both primary and secondary, must be considered.

Magnetic flowmeters consist of two distinct parts:

- Primary device - An integral portion of the piping system and consists of the flow tube and means for attaching it in the pipeline. Additionally, it includes magnetic field coils and two (or more) signal sensing electrodes, which may be wetted or non-wetted. Finally, it may include grounding conduits as required by the design of the meter.
- Secondary device - The electronic transmitter and its mounting (integral with the primary or remotely). The secondary device generally provides output from the meter and power to the magnetic field coils. The output from the secondary may be an analog signal, a pulsed output, or a digital signal.

**Table 4-7
Magnetic Flow Meter Influence Variable Reference Matrix**

Area Of Consideration	Influence Variable	Reference		
		4	8	22
Manufacturing/Specification	Materials of Construction	√	√	√
	Electrode Design	√	√	
	Analog or Frequency Signal Output	√	√	√
Installation	Orientation	√	√	
	Upstream & Downstream Flow Disturbances	√	√	√
	Electrical Installation		√	
	Local Electrical Interference		√	
	Flow Conditioners		√	
Calibration	System vs. Component	√	√	√
Flow Meter Integrity	Inspections	√	√	√
	Electrode Coatings	√	√	√
Spatial	Conductivity Gradient		√	
	Velocity Profile	√	√	
Nonhomogeneous Flow	Entrained Air	√	√	
	Slurry Flow		√	

4.7.2 Reference 4, R. Miller. Flow Measurement Engineering Handbook, Third Edition

4.7.2.1 Uncertainty Methodology

The author provides a methodology that allows the reader to determine the requirements necessary to attain a stated accuracy and additional information necessary to quantify the increase in uncertainty if the requirements are not met.

Chapter 14, page 14.31, discusses the concept of a “reference accuracy envelope,” wherein all bias error and datapoint precision are included. The bounding value of accuracy is stated as being representative of typical magnetic flow meters in the following three cases, which are illustrated on page 14.32:

- $\pm 1.0\%$ of rate or $\pm 0.2\%$ of upper range value (URV) whichever is greater
- $\pm 1.0\%$ of URV flow rate
- $\pm 0.5\%$ of URV and $\pm 0.5\%$ of rate

Table 14.8 presents the calibration reference conditions, extracted from ISO 6817 - 1992, for the parameters incumbent to the magnetic meter water calibration. Table 14.9 presents the results of Tsuchida’s work in 1982 regarding the minimum upstream lengths of piping required after a disturbance.

Section 15, page 15.23, lists the influence quantities considered in this reference. Specifically, installation effects and the effect of multicomponent flows are quantified by graphical means, while the effects from deposition and miscellaneous bias conditions are qualitatively assessed. The graphs which quantify the effects of upstream disturbances and multi-component flows are found on pages 15.23 to 15.28.

4.7.2.2 General Discussion

Magnetic flow meters fall into the general category of “linear output flowmeters.” “Principles of Operation,” located on pages 14.23 to 14.26, discuss the theory and governing equations for the magnetic flow meter. Further, the author presents the various methods available for producing a magnetic field in the flow meter, with emphasis on the pros and cons of each type.

In the section “Industrial Flowmeters,” the author provides information regarding the design and manufacture of the primary device. The applications of the various liner materials are discussed with a focus on the indication of a specific liner material for a given process application and how sizing can play an important role in the longevity of the meter in a given process application.

4.7.3 Reference 8, D. Spitzer. Flow Measurement

4.7.3.1 Uncertainty Methodology

The author initiates the discussion by stating, “Accuracy over a wide range (typically 10:1) has evolved from 1% of full scale reading to 1% of rate as standard. Higher accuracies are available for special applications.” The author maintains, as have all

references in this section, that the combination of the magnetic meter (primary device) and the signal conditioner (secondary device) is a system. As such, each component is calibrated prior to leaving the manufacturer. The accuracy statement of the magnetic flow meter includes both pieces of equipment. For applications requiring higher accuracy, the meter should be calibrated with the exact secondary device that will be used after installation.

The sections titled “Rangeability” and “Range Limits,” on pages 178 to 181, discusses the impact on the calibrated accuracy of selecting the proper range of “upper limit” to “lower limit” of flow. The focus on the rangeability is the inherent characteristic of a magnetic flow meter, namely, the meter does not accurately measure flow below the 10:1 turndown ratio, but the accuracy deteriorates at a predictable rate. Further, the sections details the difference between “% of flow” and “% of full scale” and the impact on both the accuracy of the flow measurement and the impact on the rangeability of the meter (system).

The section titled “Construction” constrains the ability to fabricate a magnetic flow meter to a flange to flange length that is no less than 1.5 times the diameter without causing a span shift. A meter that has a length of 1.3D can produce an error of 0.2%.

The author, in discussing the magnetic field on pages 190 to 192 , indicates that the pulsed dc system results in less zero shift than the standard ac type and may marginally improve the accuracy of the measurement system. Further, he states that the standard accuracy of the magnetic meter “appears to be moving from 1% of rate to 1/2% of rate on frequency outputs from these units. Optional 1/4% of rate accuracy is possible in some applications over a limited rangeability.”

Pages 192 to 199 address the importance of the electrode system in the primary device and point out that electrode coating is one of the most common problems encountered in the use of magnetic flow meters. The phenomena of electrode coating is inherent to the type of process application.

Coatings that are more conductive than the process (industrial waste, metal slurries) are more serious and more difficult to deal with than a coating that is less conductive than the process. Coatings that are more conductive than the process may cover the internal liner and constitute a short circuit between the electrodes. The result is a reduced flow signal, which can drop to a zero output over an extended period of time if the coating is highly conductive.

Coatings that are less conductive than the process tend to contribute to shifts in the zero and span of the magnetic flow meter. Zero shifts are inherent in ac-type magnetic meters. The deposition of a coating that is somewhat insulating can change the characteristics of the electrode circuit. Coupled with the ac-type system, shifts as large as 20% of the full scale flow may occur.

Span reduction can occur when an insulating type coating builds up and the impedance increases, resulting in a reduction in span, potentially to the point where the signal is completely lost. Additionally, up to an approximate 2% increase in impedance, the electrode becomes more susceptible to electrostatic pickup, resulting in a noisy signal. Several electrode cleaning methods are outlined in this section.

The section on calibration, pages 210 to 212, stresses that in order to optimize the accuracy of the magnetic flow meter, it is imperative that the primary and secondary devices be calibrated as a system. The standard 1% of rate accuracy, as specified by the manufacturer can be obtained by independent calibrations of the primary and secondary devices. However, if the same system has as an option a 0.5% of rate accuracy, it is very likely that they will be calibrated as a system.

The calibration of a magnetic meter must be performed by passing a known volume of liquid through the meter and checking the output against a weigh tank or more frequently a master meter that is accurate to better than 0.15%. All calibration standards must be traceable to the National Institute of Standards and Technology (NIST). Master meter calibrations, when based on the aforementioned criteria, can be used to calibrate meters to 1/2% of rate accuracy.

The section on installation, pages 212 to 213, discusses acceptable orientations and minimum piping straight run requirements necessary to maintain the stated accuracy of the meter.

4.7.3.2 General Discussion

In general, of all the references reviewed, this document provided the most informative and complete analysis of the overall function, application, and potential accuracy of magnetic flow meters. There are sections in this reference that address, to some degree, most aspects of magnetic flow meters.

4.7.4 Reference 22, ANSI/ASME. MFC-16M-1995. Measurement of Fluid Flow in Closed Conduits by Means of Electromagnetic Flowmeters

4.7.4.1 Uncertainty Methodology

This reference does not provide a methodology to achieve a given level of uncertainty, but does address several error sources in the measurement of flow with electromagnetic flow meters.

4.7.4.2 General Discussion

This document briefly addresses the theory of velocity determination with magnetic flow meters. The reference is quite explicit in drawing a distinction between the primary and secondary devices. Several areas of consideration are discussed such as velocity profile, piping effects, electrical interference, and electrode and liner materials.

4.8 Turbine Flow Meters

4.8.1 General Discussion

The references listed in this section address the basics of turbine flowmeter measurements. Reference 21, *FT Series Turbine Flowmeter Installation, Operation, and Maintenance Manual*, is specific to EG&G Flow Technology's meters but also contains information that pertains to turbine flow meters in general. Reference 4, *Flow Measurement Engineering Handbook*, has many empirically developed corrections for various influence variables. Table 4-8 below presents a matrix of the areas of consideration and the associated influence variables addressed by each reference.

Table 4-8
Turbine Flow Meter Influence Variable Reference Matrix

Area Of Consideration	Influence Variable	Reference			
		4	8	19	21
Manufacturing/Specification	Fluid Properties	√	√	√	√
	Flow Range	√	√	√	√
	Process Pressure		√	√	
	Non-recoverable Pressure Drop	√	√	√	
Installation	Configuration	√		√	√
	Upstream and Downstream Piping Configuration	√		√	
	Electrical Installation			√	
	Flow Conditioners	√	√	√	
Calibration	System vs. Component	√		√	√
	Multiple Viscosities	√	√	√	√
	Frequency of Calibration				
Flow Meter Integrity	Inspections	√			
	Bearings	√	√		√
Spatial	Velocity Profile	√	√		
Nonhomogeneous Flow	Entrained Air	√			

4.8.2 Reference 4, R. Miller. Flow Measurement Engineering Handbook

4.8.2.1 Uncertainty Methodology

The approach used by this reference is to prescribe a methodology to achieve a cited accuracy.

4.8.2.2 General Discussion

In the first part of Chapter 14 in this reference, there is a discussion of turbine flow meters and their associated K-factors with information regarding corrections for various parameters. Also, there is a discussion of the basic operating principle of the turbine flow meter. Liquid flow turbine meters and gas flow turbine meters are divided into two separate categories. There is more of a discussion of the liquid-type meters and their associated calibrations than the gas flow meters. In Chapter 15, there are detailed charts showing the impact of design and installation effects on the K-factor for turbine flow meters.

4.8.3 Reference 8, D. Spitzer. Flow Measurement

4.8.3.1 Uncertainty Methodology

This reference describes a methodology to use in the determination of individual uncertainties that can be applied to the overall flow measurement uncertainty of $\pm 0.5\%$ of flow if there is linearity over the range of Reynold's numbers and the calibration is conducted at an appropriate viscosity.

4.8.3.2 General Discussion

In Chapter 17 of this reference, the basics of turbine flow meters are covered: operation constraints, performance, sizing, and maintenance. There are some example problems about flow meter sizing in this chapter as well. There are several other chapters that go into greater detail about fluid flow fundamentals (temperature, pressure, density, viscosity, etc.), measurement terminology, linearization and compensation, and flow meter performance that can be applied to turbine flow meter measurements.

4.8.4 Reference 19, ANSI/ISA-RP31.1-1977. Specification, Installation, and Calibration of Turbine Flowmeters

4.8.4.1 Uncertainty Methodology

This ANSI/ISA document contains little if any information on the uncertainty of turbine flow meters. It does address some elemental uncertainties associated with the systems that are used to calibrate turbine flow meters.

4.8.4.2 General Discussion

This reference provides detailed information on specification, installation, and calibration considerations. It also briefly discusses some optional features such as temperature, pressure, and viscosity that might be necessary to correctly interpret the flow data from the turbine flow meter.

Section 5, which is the largest part of the document, details several methods and considerations for calibration of turbine flow meters. There is a small discussion on the effects of fluid temperature differences from calibration to usage and a correction to the K-factor.

4.8.5 Reference 21, EG&G Flow Technology. FT Series Turbine Flowmeter Installation Operation, and Maintenance Manual, TM-86675

4.8.5.1 Uncertainty Methodology

The EG&G reference contains accuracy specifications of their flow meters but does not cover any of the other uncertainties associated with turbine flow metering. The accuracies stated are in general standard industry accuracy specifications, so they could be applied to other manufacturers' turbine flowmeters.

4.8.5.2 General Discussion

This is an actual manual for EG&G FT series flow meters, but it has a vast amount of information that is useful when applying and considering other manufacturers' flow meters. It contains specific information for the type of fluid media being measured, which influences which type of bearings should be used and how the meter should be calibrated. There is a section on meter sizing, piping requirements, flow conditioning, and filtration that should be considered to achieve accurate flow measurements. The section on calibrations mentions single versus multiple viscosity calibrations for liquid service meters and single versus multiple pressure calibrations for gas service meters.

Specific maintenance information for EG&G turbine flow meters is discussed, but it can be carried over for other models of flow meters.

4.9 Vortex Meters

4.9.1 General Discussion

The vortex flowmeter is also in the category of linear output devices. The velocity of the fluid is directly proportional to the rate at which the alternating vortices are formed, also referred to as the vortex shedding frequency. The vortex meter is indicated in the measurement of flows for clean liquids, gas, and steam, given that the pipe Reynolds number is greater than 10–20,000 and up to 10,000,000. The general bounding value for the accuracy of a vortex flow meter, having a factory water calibration, is $\pm 0.75\%$ of flow (or better) for liquids and $\pm 1.5\%$ for gases and steam. The advantages to the vortex flow meter are no moving parts, easy installation, and a relatively moderate cost.

The calibration of a vortex meter should be conducted as closely as possible to the flow range that it will encounter in service. This allows for the engineer to minimize the uncertainty that would be encountered by the use of an average K factor. The flow measurement for a service water pump, for example, can be made using the primary output (frequency) from the device and interpolating a value for the K factor from the calibration data. In this manner, the uncertainty attributed to the linearity envelope can be greatly reduced.

Table 4-9 below presents the influence variables that are discussed in each reference.

Table 4-9
Vortex Flow Meter Influence Variable Reference Matrix

Area Of Consideration	Influence Variable	References		
		4	7	8
Manufacturing/Specification	Fluid Properties	√	√	√
	Flow Range	√	√	√
	Process Pressure		√	
	Non-recoverable Pressure Drop	√	√	√
Installation	Orientation	√	√	√
	Upstream and Downstream Piping Configuration	√	√	√
	Electrical Installation		√	√
	Maintainability		√	√
	Flow Conditioners	√	√	
Calibration	System vs, Component	√		√
Flow Meter Integrity	Bluff Body Wear	√	√	√
Spatial	Velocity Profile	√		
Nonhomogeneous Flow	Entrained Air	√		

4.9.2 Reference 4, R. Miller. Flow Measurement Engineering Handbook

4.9.2.1 Uncertainty Methodology

The author of this reference provides a methodology to attain a cited accuracy along with adjustment factors for deviations from ideal conditions. He does point out in Section 14, page 14.18, that the vortex shedding flow meter is similar in nature to the turbine meter in that the output from the vortex frequency sensor is a frequency (or pulsed output) that is proportional to the velocity in the conduit. The result of a water calibration is a K factor that relates the number of pulses to a volumetric flow rate as shown in the following equation:

$$K_v = \frac{\lambda_{Hz}}{q_v} \quad (\text{Eq. 4-2})$$

Further, given an envelope of linearity (for example $\pm 0.5\%$) over a flow range, the mean K factor can be calculated by the following equation:

$$\bar{K}_v = \frac{(K_v)_{\max} + (K_v)_{\min}}{2} \quad (\text{Eq. 4-3})$$

Upon calculation of the average K factor, the accuracy of the K factor may be estimated from the following equation:

$$(\text{Acc})_{K, v} = \pm (\text{Acc})_{\text{Lab}} \pm \sqrt{L^2 + 4\sigma_p^2} \quad (\text{Eq. 4-4})$$

where, when compatible units are employed

- q = volumetric flow rate
- λ_{Hz} = vortex frequency (or linearized frequency function)
- K_v = K factor for meter
- Acc_{Lab} = accuracy of K factor determination from calibration lab
- L = average linearity envelope
- $2\sigma_p$ = precision of the two data points defining the linearity envelope

4.9.2.2 General Discussion

This reference provides general information on design and operational considerations. It briefly discusses the ability of this type of meter to measure two-phase flows, such as wet steam, with reasonable accuracy. The limiting element of this measurement is the ability to accurately characterize the resultant density of the mixture.

The author states that currently all vortex meters are individually water calibrated to determine a mean K factor. In an analysis of 167 similarly constructed meters, there was a variance of only $\pm 0.3\%$ in the mean K factors. This is significant such that in the future, meters of the same design may be assigned K factors and not be individually calibrated.

4.9.3 Reference 7, D. Spitzer. Industrial Flow Measurement

4.9.3.1 Uncertainty Methodology

This reference provides a given set of criteria required to attain the stated uncertainty of $\pm 0.5\%$ to 1.0% of flow rate for liquids and ± 1.5 to 2.0% of flow for gas service. These accuracy statements are based upon water-calibrated flow meters operated in their range of linearity.

4.9.3.2 General Discussion

This reference provides a great deal of information regarding the principles of operation, construction, operational constraints, and flow ranges. The author indicates that most manufacturers recommend that a “flow section” be utilized in this application, such that four pipe diameters upstream and two pipe diameters downstream of the meter have a 350 finish, free of mill scale, pits, and bumps, and that the pipe diameter not depart from the average by more than 0.33% . Further, he indicates that this exceeds the ASTM specifications for commercial pipe, so it may be necessary to have a spool piece that is of the same schedule as the flowmeter, fabricated such to meet these specifications.

At lower flows, these types of meters are subject to vibration that may be induced in the pipe from nearby sources. The vibration may cause the sensing systems to measure a vortex that does not exist or nullify a vortex that does exist, leading to errors in the resultant measured flow. The pros and cons of various sensing systems are discussed in this reference.

The information regarding the calibration of the meters states that the meters should be water calibrated such that the effects of thermal expansion on the flow meter body are quantified. The thermal expansion of the flow meter body can affect the K factor by as much as 0.5% per 100°C in a stainless steel flow meter. A typical manufacturer’s correction curve is displayed on page 243.

4.9.4 Reference 8, D. Spitzer. Flow Measurement

4.9.4.1 Uncertainty Methodology

The approach used by this reference is to prescribe a methodology to achieve a cited accuracy with additional information available to estimate the effects on uncertainty of specific nonconformances. This reference offers more detailed information for quantifying the effects of less than ideal conditions, specifically on piping configurations and installation effects, than the previous reference.

4.9.4.2 General Discussion

This reference provides the requisite sections on the operating principles. The section on “when to use the vortex meter” discusses fluid property constraints, with some discussion on the rangeability of these types of meters.

The author discusses the procedures for correctly sizing the flow meter but qualifies his discussion with these two statements:

- “.....In fact, many vendors have a computer program that will take inputs of the process operating conditions and automatically select the best size meter for the application. Often, these programs are offered to users either free or for a nominal charge.”
- “As a general rule, the best size selection often is one pipe size smaller than the pipe into which the meter will be installed. The reason for this is that the vortex shedding flowmeter works best when the flowing velocity is high. Pipe sizes are selected so that the flowing velocity is relatively low.”

Finally, the author addresses the maintenance and calibration of vortex flow meters. The discussion states that due to the fact there are no moving parts and the internal parts are rugged, there is very little maintenance required. If the electronics were to fail and require replacing, the need to wet flow calibrate the meter body is seldom required. In fact, a second wet calibration may be required only if the sensor were to fail and have to be replaced, and in many designs even then it might not be necessary.

4.10 Coriolis Meters

4.10.1 General Discussion

Coriolis mass flow meters are commercially available for the measurement of liquid flows and for high-pressure gases. Specifications from the manufacturers indicate that the mass flow accuracy of these meters vary between ± 0.15 and $\pm 0.4\%$. Table 4-10 provides a summary of key references.

Table 4-10
Coriolis Mass Flow Meters Influence Variable Matrix

Area Of Consideration	Influence Variable	Reference		
		4	8	23
Manufacturing	Tube Material	√		
	Single vs. Double Tube	√		
	Cyclic Stress/Fatigue	√	√	
Installation/Operation	Orientation	√	√	√
	Vibration Damping	√		√
	Piping/Valving Arrangements	√	√	√
	Cavitation	√		√
Calibration	Calibrated vs. Uncalibrated	√		√
	Zero Stability	√		
Flow Meter Integrity	Cyclic Stress Failure		√	
	Material Buildup		√	
Nonhomogeneous Flows	Entrained Gas or Air	√		

4.10.2 Reference 4, R. Miller. Flow Measurement Engineering Handbook

4.10.2.1 Uncertainty Methodology

There is no methodology developed in this reference to provide for a given uncertainty. The Coriolis mass flow meter is essentially insensitive to the effect of upstream piping and fluid properties in the direct measurement of mass flow. This reference provides an example of a typical Coriolis mass flow meter that has been gravimetrically calibrated with water, yielding a flow uncertainty of $\pm 0.25\%$, including zero drift at a rangeability of 20:1.

4.10.2.2 General Discussion

In this reference, Miller reviews the basic measuring concepts of the Coriolis mass flow meter leading into a discussion on meter design considerations. Dual vs. single tube

design is addressed as are cyclic stresses of the tube joints as they relate to material selection and overall meter application.

The reference indicates that the meters are considered to be insensitive to upstream disturbances, but sensitive to orientation and externally driven vibratory influences. The installation should be vertical to preclude the formation of any gas or air pockets, which can lead to large zero errors. Finally, the high pressure loss characteristics of this meter may lead to cavitation or flashing if used in an improper application.

4.10.3 Reference 8, D. Spitzer. Flow Measurement

4.10.3.1 Uncertainty Methodology

An uncertainty methodology is not developed within this document, but the identification of the existing error sources and various ways to reduce them are discussed in Chapter 10. Spitzer cites an accuracy range of the Coriolis mass flow meters as ± 0.15 to $\pm 0.25\%$ of rate, plus a “zero shift” error stated as a percent of the upper range value ($\pm 0.01\%$ of URV).

4.10.3.2 General Discussion

This reference begins with a complete discussion on the theory of the Coriolis measurement technique. The reference addresses the subject of how density is measured in the dynamic process. A discussion on the overall construction and design is focused on the ability of the device to measure a deflection in a semi-rigid vibrating tube system, which may amount to no more than ten-one millionths of an inch. The concept of how the overall design parameters, such as pressure rating, flow range pressure drop, signal amplitude, etc., are interdependent to the accurate measurement of the mass flow in these types of meters.

The section devoted to “Performance/Limitations” discusses the various ranges and sizes available. The typical range of flow turndown ratios is 25:1 with excellent accuracy envelopes. The impact of the “zero shift” component of the accuracy specification and how very low flow can become a significant portion of the metering error is also discussed. Due to the zero shift, metering accuracy degrades as the flow approaches zero. Due to the significant pressure drop characteristics of this meter, the sizing should be a trade-off between pressure drop and the best attainable accuracy.

Additional sections are devoted to the sizing considerations of material vs. process pressures and temperatures, process fluids to be measured, allowable pressure drops, and velocity limits for abrasive slurries.

Regarding maintenance issues, the reference points out that “One of the major benefits of Coriolis mass flow meters is the lower maintenance requirement. The benefit of no moving parts and low maintenance have been, in many cases, a primary reason for justification of the higher capital expense for this technology.” The author further explains that a complete functional check of the transmitter should be performed on a semi-annual basis. In this case, just the electronics are calibrated.

4.10.4 Reference 23, ANSI/ASME. MFC-11M-1989. Measurement of Fluid Flow by Means of Coriolis Mass Flowmeters

4.10.4.1 Uncertainty Methodology

There is no basis to develop a methodology for the estimate of the uncertainty in the measurement of flow through a Coriolis mass flow meter, other than a reference to ASME-MFC-2M [6].

4.10.4.2 General Discussion

This reference provides the basic information on considerations for the specification and use of these meters. It provides a comprehensive discussion of the theory of operation for Coriolis meters. Regarding installation and installation effects, MFC-11M defers to the manufacturers’ recommendations. Several calibration methods are listed as being acceptable for a primary standard calibration.

4.11 Variable Area Flow Meters

4.11.1 General Discussion

The industry references listed in Section 2.8.1 discuss various aspects of the preparation and use of variable area flow meters (rotameters) for the measurement of flow. Table 4-11 below presents a comparison of the areas of consideration and the associated influence variables addressed by each of the cited references. This type of meter will have limited application in the metering of typical service water flows simply due to the maximum measurable flow of <200 gpm (<757 liters per minute or lpm).

**Table 4-11
Variable Area Flow Meters Influence Variable Reference Matrix**

Area Of Consideration	Influence Variable	Reference		
		3	4	7
Manufacturing	Tube Material/Design	√	√	√
	Float Material/Design	√	√	√
	Standard/Armored Construction		√	√
	Method of Indication	√	√	√
Installation/Operation	Orientation	√	√	√
	Piping/Valving Arrangements		√	√
	Flow Straighteners		√	√
Calibration	Calibrated vs. Uncalibrated	√	√	√
	Method	√		√
	Correction Factors	√	√	√
Flow Meter Integrity	Inspections			√
	Time in Service			√
	Material Buildup		√	√
	Entrained Debris		√	√

4.11.2 Reference 3, ASME. ASME Fluid Meters, Their Theory and Application

4.11.2.1 Uncertainty Methodology

An uncertainty methodology is not developed within this document. The classification of error sources and various ways to reduce them are discussed in Chapter I-6.

4.11.2.2 General Discussion

Chapter I-6 of this document discusses theoretical principles and flow rate indication for variable area flow meters. Operational design descriptions are presented for the most common forms of variable area flow meters: tapered tube and float, cylinder and piston, and orifice and plug. General theory of operation and working equations of the

tapered tube and float variable area flow meter are the same or of the same form for each variable area flow meter. Viscosity effects are discussed through the development of a viscosity influence number. Variable area flow meters are normally calibrated for use at specific operating and fluid conditions. If flow conditions change, this document provides development of applicable adjustment or correction factors. For compressible fluids, ASME “Fluid Meters” [3] introduces an expansion factor to correct for density variations across the float. A correction factor is introduced when it becomes necessary to obtain true flow for a variable area flow meter that is not used at its design operating (or calibrated) conditions.

4.11.3 Reference 4, R. Miller. Flow Measurement Engineering Handbook

4.11.3.1 Uncertainty Methodology

An uncertainty methodology is not developed within this reference. The classification of error sources and various ways to reduce them are discussed in Chapter 14. Accuracy ranges for variable area flow meters are listed as ± 0.5 to $\pm 2\%$ of the URV flow.

4.11.3.2 General Discussion

Chapter 14 of this document discusses theoretical principles and flow rate indication for the linearly tapered tube and float variable area flow meter. Design variations of the variable area flow meter include: linearly tapered tube and float, orifice and plug, slotted cylinder and piston, and piston. Cited advantages of variable area flow meters are the nearly constant overall pressure loss, the small size of the meters, and the ability to meter nearly any corrosive fluid. Chapter 6 breaks variable area flow meters into two distinct types: float in a tapered tube and mechanically variable restriction with a means for direct differential pressure measurement across the restriction. Chapter 6 states that the variable area flow meters may be used to measure liquids, gases, and vapors (steam) over a range of flow rates from $0.01 \text{ cm}^3/\text{min}$ to 4,000 gpm (15, 142 lpm). This liquid flow seems impractical because of a contradictory statement that appears in Table 6.1 Flowmeter Selection Table, which indicates that the size limitation on pipe diameter is $< 3.0''$ ($< 7.6 \text{ cm}$). Tapered glass tubes may be used up to 350 psig, 400°F (2413 kPa , 204°C) and tapered metal tubes may be used up to 720 psig, 1000°F (4964 kPa , 538°C).

Chapter 14 provides detailed discussion of the linearly tapered tube and float variable area flow meter. This chapter presents various float designs, specific gravities of some float materials, liquid and gas correction factors for mass, and base-volume flow. Flow readings are obtained visually through magnetic coupling, dial indication, or other methods of standardized output. Direct viewing of a glass tube flow meter is the most

popular for economic reasons. Armored tube flow meters extend application to harsh and high-pressure service. The basic geometry of the tapered tube and float variable area flow meter is described by Bernoulli's general energy equation for a liquid, which is further reduced to a basic liquid equation for variable area flow meters. Correlation equations are provided for liquids and gases, for selected float materials, and for predicted changes of fluid density.

4.11.4 Reference 7, D. Spitzer. Industrial Flow Measurement

4.11.4.1 Uncertainty Methodology

An uncertainty methodology is not developed within this reference. Classification of error sources and various ways to reduce them are discussed in Chapter 20. Accuracy ranges for variable area flow meters are listed as ± 0.5 to $\pm 2.0\%$ of URV.

4.11.4.2 General Discussion

Chapter 20 of this document presents general theoretical principles, construction designs, installation methods, and flow indication for variable area flow meters. The advantages of variable area flow meters are stated as providing economical local readouts and control of gases and nonviscous liquids. Construction of tapered tube and float flow meters is categorized as standard or armored. Discussion of the tapered tube and float flow meter construction includes metering tube design, float design, meter sizing, meter scale range, meter mounting, flow indication, and fluid contact materials. Tapered tube and float flow meter applications include clean fluids with a viscosity of less than approximately 30 cP and most gases. Flow rates range from 0.05 to 200 gpm (0.2 to 757 lpm). A brief discussion of flow meter installation involves hydraulic requirements, pipe orientation, pipe vibration, and cabling. Although tapered tube and float variable area flow meters require no routine maintenance, maintenance concerns such as material buildup, flow meter pluggage, metering tube failure, electronic failure, calibration, and spare parts are reviewed.

4.12 References

1. American National Standards Institute/American Society of Mechanical Engineers. MFC-3M-1989 (Reaffirmed 1995). *Measurement of Fluid Flow in Pipe Using Orifice, Nozzle, and Venturi*. ASME, 1990.
2. International Organization on Standardization. ISO 5167-1980. *Measurement of Fluid Flow by Means of Orifice Plates, Nozzles, and Venturi Tubes Inserted in Circular Cross-Section Conduits Running Full*. ISO, 1981.
3. American Society of Mechanical Engineers. *Part II of ASME Fluid Meters, Their Theory and Application*, Sixth Edition. ASME, 1971.
4. R. Miller. *Flow Measurement Engineering Handbook*, Third Edition. McGraw Hill, 1996.
5. American Society of Mechanical Engineers. *PTC Report - 1985, Guidance for Evaluation of Measurement Uncertainty in Performance Tests of Steam Turbines*. ASME, 1986.
6. American National Standards Institute/American Society of Mechanical Engineers. MFC-2M-1983 (Reaffirmed 1988). *Measurement Uncertainty for Fluid Flow in Closed Conduits*. ASME, 1984.
7. D. Spitzer. *Industrial Flow Measurement*. ISA, 1990.
8. D. Spitzer. *Flow Measurement*. ISA, 1991.
9. Dieterich Standard Corporation. *Annubar Handbook*. Dieterich Standard Corporation, 1993.
10. American National Standards Institute/American Society of Mechanical Engineers. MFC-5M-1985 (Reaffirmed 1994). *Measurement of Liquid Flow in Closed Conduits Using Transit-Time Ultrasonic Flow Meters*. ASME, 1986.
11. L. Lynnworth. *Ultrasonic Measurements for Process Control, Theory, Techniques, Applications*. Academic Press, 1989.
12. *Instrumentation Handbook for Integrated Power Plant Water Management*. EPRI, Palo Alto, CA: 1988. Report CS-5873.
13. Cooling Tower Institute. "Standard for Water Flow Measurement," *CTI Bulletin*, STD-146 (95), 1995.

14. M. S. Beck and A. Plaskowski. *Cross-Correlation Flow Meters*. Adam Hilger, Bristol, England, 1987.
15. Y. Gurevich, A.M. Lopez, R. Flemons, D. Z. Zobin, "Theory and Application of Non-invasive Ultrasonic Cross-Correlation Flowmeter," presented at the 9th International Conference on Flow Measurement, Lund, Sweden (June 1998).
16. W. H. Morgan, *et al*, "Validation of the Use of Dye Dilution Method for Flow Measurement in Large Open and Closed Channel Flows," presented at the NBS Flow Measurement Symposium, Gaithersburg, MD (1977).
17. J. B. Nystrom and G. E. Hecker, "Uncertainty Analysis of Field Turbine Performance Measurements," *Proceedings of an International Conference on Hydropower*, American Society of Civil Engineers, 1985.
18. K. W. Hennon and G. R. McNutt. *Pre-Test Uncertainty Analysis for Dye Dilution Flow Measurement*. Power Generation Technologies Technical Paper. TIN 97-1267.
19. American National Standards Institute/Instrument Society America. RP31.1-1977. *Specification, Installation, and Calibration of Turbine Flowmeters*. ISA, 1977.
20. K. Hennon and D. Wheeler, "*Uncertainty Analysis of Cooling Tower Performance*," Power Generation Technologies Technical Report presented at the Cooling Tower Institute Winter Meeting, 1996.
21. EG&G Flow Technology. *FT Series Turbine Flowmeter Installation, Operation, and Maintenance Manual*. TM-86675, Rev. H-1996.
22. American National Standards Institute/American Society of Mechanical Engineers. MFC-16M-1995. *Measurement of Fluid Flow in Closed Conduits by Means of Electromagnetic Flowmeters*. ASME, 1995.
23. American National Standards Institute/American Society of Mechanical Engineers. MFC-11M-1989 (Reaffirmed 1994). *Measurement of Fluid Flow by Means of Coriolis Mass Flowmeters*. ASME, 1995.
24. Instrument Society of America. 11ISA-RP16.5-1961. *Installation, Operation, and Maintenance Instructions for Glass Tube Variable Area Meters (Rotameters)*. ISA, 1961.
25. American National Standards Institute/American Society of Mechanical Engineers. PTC 6 -1976 (Reaffirmed 1982). *Steam Turbines*. ASME, 1982.
26. J. A. Rabensteine and C. E. Arnsdorf. *Flow Determination by Acoustic Transit Time*. Power Generation Technologies Calculation, 1997.

27. International Organization on Standardization. ISO Standard 3977-1977. *Measurement of Fluid Flow in Closed Conduits - Velocity Method Using Pitot Static Tubes*. ISO, 1997.
28. International Organization on Standardization. ISO Technical Report 12765:1997 (E). *Measurement of Fluid Flow in Closed Conduits - Method Using Transit Time Ultrasonic Flowmeters*. ISO, 1997.
29. Advanced Measurement and Analysis Group, Inc. *CROSSFLOW[®] User Guide for Ultrasonic Flow Measurement*. 1998.
30. International Organization Standardization. ISO-9104:1991. *Measurement of Fluid Flow in Closed Conduits - Methods of Evaluating the Performance of Electromagnetic Flowmeters for Liquids*. ISO, 1991.
31. Southwest Research Institute Report. *Baseline and Installation Effects Tests of the V-Cone Meter*. SRI, 1984.
32. American National Standards Institute/American Society of Mechanical Engineers. MFC-6M-1987. *Measurement of Fluid Flow in Pipes Using Vortex Flow Meters*. ASME, 1987.
33. American National Standards Institute/American Society of Mechanical Engineers. PTC 19.1. *Measurement Uncertainty*. ASME, 1985.
34. American National Standards Institute/American Society of Mechanical Engineers. MFC-10M-1994. *Methods for Establishing Installation Effects on Flowmeters*. ASME, 1994.
35. American National Standards Institute/American Society of Mechanical Engineers. MFC-9M-1988. *Measurement of Liquid Flow in Closed Conduits by Weighing Method*. ASME, 1989.

5

APPLICATION OF METHODOLOGY

5.1 Overview

In order to estimate the uncertainty of a given type of flow measurement system, the generic methodology described in Section 3 of this guideline must be applied to each specific situation. This section will focus on the application of a consistent methodology for each given meter examined in this guideline. The steps outlined below describe an approach that will result in an estimate of the uncertainty for each type of flow element:

- Define the measurement process
- Identify all elemental sources of precision (random) and bias (systematic) errors
- Evaluate all elemental sources of precision (random) and bias (systematic) errors
- Conduct a sensitivity analysis for each identified error
- Combine all the elemental sources of uncertainty to determine the overall uncertainty

The scope of this guideline will be limited to the measurement loop, which is comprised of the primary and secondary elements.

5.1.1 Primary Elements

Primary elements are the flow element and those integral measurements that provide an output parameter that is functionally representative of the velocity or flow through the device. Examples of primary devices are differential pressure-producing flow sections (differential pressure), turbine flow elements (frequency), and Coriolis mass flow elements (displacement or strain).

In many cases, the flow meter calibration is performed on only the primary element. For example, take the case of a 6" (15 cm) thin plate orifice where the entire pipe section (roughly 20 feet (6.1 m) in length) is shipped to a flow laboratory for calibration. The

calibration is conducted using a gravimetric primary standard method, described in ASME-MFC-9M-1988 [35]. The primary standard can achieve an uncertainty of 0.1% to 0.2% which is traceable to NIST.

5.1.2 Secondary Elements

Secondary elements are devices that have as input the signal generated in the primary element and condition that signal to provide a functionally representative, measurable output that can be input to data acquisition or control systems. Examples of secondary elements are differential pressure transmitters (both analog and digital), signal conditioners such as square wave converters, amplifiers, and linearization circuits.

In the selection of the flow measurement system, it is imperative to consider the compatibility of the primary and secondary elements. In the case of the differential pressure-producing orifice flow section described in Section 5.1.1, assume that the design basis flow produces a differential pressure of 100 in. w.g. Further, assume that this primary element, which was assessed an uncertainty of $\pm 0.75\%$ based on the primary standard calibration, was mated with a differential pressure transducer that had an upper range limit (URL) of 500 in. w.g. and a calibrated accuracy of 0.5% of URL. The uncertainty introduced by the improper selection of the secondary element range would introduce an uncertainty into the flow measurement of 2.5% of the measured differential pressure. However, if the transmitter was specified such that the URL was 200 in. w.g., the subsequent error introduced in the measurement of differential pressure would be 1%.

5.2 Differential Pressure Producer

5.2.1 Influence Factors

Many influence factors affect the accurate measurement of primary flow. The following discussion of influence factors is based largely on information provided in ANSI/ASME PTC 6 Report-1985 [5] and ASME MFC-3M-1989 (Reaffirmed 1995) [1]. These references provide a means of specifying the proper orifice tolerances, pipe surface roughness, and constraints on the beta ratio that also provide a methodology for estimating the additional uncertainty introduced by using primary elements that do not meet ANSI/ASME PTC 6-1976 (R1982) [25] requirements but are installed in configurations similar to those typically found in power plants. The remaining references abstracted in Section 4 cover much of the same information addressed by the major references discussed in this section and as such are not mentioned in great detail.

5.2.1.1 Manufacturing Considerations

MFC-3M-1989 (Reaffirmed 1995) [1] provides an excellent reference regarding the manufacturing considerations and specifications that must be adhered to for orifice, nozzle, and Venturi fabrication. Overall, the elements should be fabricated from stainless steel or other suitable material for the fluid to be metered at the expected operating conditions. PTC 6 Report-1985 [5] does not provide any information regarding the materials and manufacturing of differential pressure producing primary elements, but indicates that information relative to construction, calibration, and installation of flow-measuring devices can be found in ASME Interim Supplement 19.5 on Instruments and Apparatus-1972 [36].

5.2.1.2 Installation Considerations

MFC-3M-1989 (Reaffirmed 1995) [1], Section 6, provides extensive guidance regarding installation requirements. Table 4-11 of PTC 6 Report-1985 [5] provides the minimum straight length of pipe required between various flow disturbances located at the inlet and outlet of the primary device. Figure 4-5 used with Table 4-11, Columns 1 through 6, of PTC 6 Report-1985 estimates the flow section uncertainty for the straight length of pipe preceding the primary flow element. Figure 4-6 is applicable to flow sections with or without flow straighteners. In the ASME Interim Supplement 19.5 on Instruments and Apparatus-1976 [36], due consideration is given to the configuration of taps and the location and orientation of sensing lines for various applications.

If the application requires strict accuracy, such that the uncertainty introduced due to the installation location is unacceptable, then ASME-MFC-10M-1994 [34] should be reviewed to provide guidance to further reduce the uncertainty attributed to installation effects.

5.2.1.3 Measurement Loop Considerations

PTC 6 Report 1985 [5] specifies the instruments used for measuring the various fluid pressures and refers to PTC 6-1976 (R1982) [25], Par. 4.64. Typical uncertainties for different types and calibrations of deadweight gages and Bourdon gages are addressed in Tables 4-14 and 4-15, respectively. Transducers and their applications are mentioned in PTC 6-1976 (R1982), Par. 4.83. Additionally, ASME-MFC-8M-1988 [37] provides guidance on the connections for pressure signal transmissions between primary and secondary elements.

5.2.1.4 Calibration Considerations

Section 3 of PTC 6 Report 1985 [5] provides information on calibration of differential pressure-producing primary elements. It notes that flow measuring devices shall be

calibrated with the upstream and downstream pipe sections including flow straightener and recovery cone where applicable.

5.2.1.5 Instrument Integrity Consideration

In PTC 6 Report-1985 [5], Items A through E of Table 4-10 provide information on categories of uncertainty based on whether an inspection was done before or after initial system flushing or installation and for calibrated and uncalibrated flow sections. The assigned values represent the effect of possible damage during initial flushing or from deposits that accumulated during operation for liquid measurement. Items F, G, H, and I of Table 4-10 provide information regarding inspection of uncalibrated flow sections. ASME-MFC-3M-1989 (Reaffirmed 1995) [1] provides guidance on tolerances and dimensions to be used during a physical examination of the flow section.

5.2.1.6 Spatial Consideration

The differential pressure producer inherently integrates the flow velocity over the normal, cross-sectional flow area. Hence, there are no considerations for any spatial bias.

5.2.2 Example of Uncertainty Methodology

Water, at 60°F (15.6°C) and 100 psig (689.5 kPa), was measured using an orifice of 8.5479" (21.7117 cm) bore installed in a nominal 12" ID pipe. The orifice section was not calibrated but was inspected immediately before and after testing. Thirty readings of differential pressure were taken with a differential pressure transmitter calibrated to $\pm 0.2\%$ of the URL. The average value for differential pressure was determined to be 70.25 in w.g. yielding a measured flow rate of 2419.8 gpm (9160 lpm). The standard deviation of the mean was calculated to be 0.6 in w.g. Two elbows in the plane of the pipe are located 16.5 pipe diameters upstream of the primary element and an in plane elbow is located 4.6 pipe diameters downstream of the primary element. The orifice Beta ratio is calculated to be 0.712.

5.2.2.1 Define the Measurement Process

The governing flow equation is:

$$q = C * C_d * \frac{d^2}{\sqrt{1 - \beta^4}} * \sqrt{\frac{\Delta p}{\rho}} \quad (\text{Eq. 5-1})$$

where, when using compatible units,

q	=	volumetric flow
C	=	conversion coefficient
C _d	=	discharge coefficient
d	=	diameter of the orifice bore
D	=	diameter of pipe
β	=	Ratio of orifice bore diameter to pipe diameter (d/D)
Δp	=	measured differential pressure
ρ	=	flowing water density

In this example, several assumptions are made to provide guidance in the calibration of the system in order to minimize the impact on the flow uncertainty:

- The differential pressure transmitter is mounted and calibrated in the field such that the mounting position effect, static pressure span effect and temperature effect are removed.
- The differential pressure transmitter is calibrated a maximum of 14 days prior to the conduct of the test. This will serve to remove any stability and drift errors from the transmitter calibration.
- The pressure transmission legs are verified full and the transmitter is zeroed at line pressure to ensure measurement accuracy and to correct for static pressure zero effects.
- The orifice and pipe taps are inspected on an annual basis.

The equation that is used by the secondary element to provide an output that is proportional to the flow reduces to:

$$q = C^* \sqrt{h_w} \quad (\text{Eq. 5-2})$$

where,

q	=	volumetric flow
C*	=	flow constant (288.7 gpm/in. w.g. ^{0.5})
h _w	=	measured differential pressure head

5.2.2.2 Identification of Elemental Bias Uncertainty Sources

Using the techniques espoused in ASME PTC 6 Report [5], which has empirically assessed uncertainties sources, the elemental bias uncertainties for a thin plate orifice primary flow element are identified as:

- Base Uncertainty of Primary Flow Measurement (U_{Base}) - This parameter reflects the bias uncertainty associated with the type of primary element, the inspected integrity of the element, and the calibration history.
- Minimum Straight Run of Upstream Pipe After Flow Disturbance, No Flow Straightener (U_{LNS}) - This parameter is an index for the bias uncertainty associated with distortions in the velocity profile due to upstream disturbances, such as an out-of-plane elbow.
- Beta Ratio Effect (U_β) - This is an index of the bias uncertainty associated with the ratio of the differential pressure producer bore to the pipe bore.
- Effect of Number of Diameters of Straight Pipe After Flow Straightener (U_{LS1}) - This parameter describes the additional bias uncertainty assigned to straight run pipe diameters after a flow straightener, regardless of the upstream disturbances.
- Effect of Number of Sections in Flow Straightener (U_{LS2}) - This parameter describes the additional bias uncertainty associated with the number of sections in a flow straightener of length 2D.
- Effect of Downstream Pipe Length (U_{RAL}) - This parameter is also provides an index of the bias uncertainty associated with a distortion of the velocity profile due to a downstream disturbance.

- Secondary Element Errors - In typical service water flow applications, the differential pressure is typically measured using a differential pressure transmitter as a secondary element; hence, an uncertainty attributed to the secondary loop measurement is introduced.
- Water Density Determination Error - This parameter is a function of the accuracy of the measured temperature of the water.

5.2.2.3 Identification of Elemental Precision Uncertainty Sources

The precision errors associated with the measurement of the flow are the random errors in the acquisition of the differential pressure data.

5.2.2.4 Evaluation of Elemental Bias Uncertainty Sources

Since the orifice and taps were inspected before and after the testing, the base uncertainty, taken from Reference 5, Table 4-10, is:

$$U_{\text{Base}} = \pm 1.0\% \text{ of flow}$$

The following tables summarize the elemental uncertainty values taken from Reference 5.

**Table 5-1
Uncertainty Due to Upstream Flow Disturbance**

Minimum Upstream Straight Lengths (Diameters)	Existing Upstream Straight Lengths (Diameters)	Ratio	U_{LNS} (%)
21.5	16.5	.767	2.4

**Table 5-2
Uncertainty Due to Downstream Flow Disturbance**

Minimum Downstream Straight Lengths (Diameters)	Existing Downstream Straight Lengths (Diameters)	Ratio	U_{DSL} (%)
4.5	4.6	1.022	0.70

Application of Methodology

The uncertainty due to the Beta ratio is based on the fact that as the Beta ratio increases, the value of the sensitivity coefficient increases; hence, the overall uncertainty in the result will increase. Figure 4-6 from Reference 5 and a Beta ratio of 0.71 yield an uncertainty value of:

$$U_{\beta} = \pm 0.8\% \text{ of measured flow}$$

The composite bias uncertainty of the flow section with 95% confidence is computed as:

$$B_{FS} = \pm \sqrt{(U_{Base})^2 + (U_{LNS})^2 + (U_{DSL})^2 + (U_{\beta})^2 (U_{LS1})^2 + (U_{LS2})^2} \quad (\text{Eq. 5-3})$$

or,

$$B_{FS} = \pm \sqrt{(1.0)^2 + (2.4)^2 + (0.7)^2 + (0.8)^2 + (0)^2 (0)^2} = \pm 2.81\% \quad (\text{Eq. 5-4})$$

Expressed in absolute terms, the measured flow rate representing the estimate for overall bias uncertainty in the primary element of the flow section is ± 68 gpm (257 lpm).

The differential pressure produced by the flow element is measured by a differential pressure transmitter (secondary element). The error specifications and operating conditions for the differential pressure transmitter are contained in Tables 5-3 and 5-4.

Table 5-3
Differential Pressure Transmitter Error Specifications

Error Source	Listed Specification
Calibration Accuracy	$\pm 0.2\%$ of calibrated span
Temperature Effect	None
Static Pressure Zero Effect	None
Static Pressure Span Effect	None
Mounting Position Effects	None
Stability	0.1% of calibrated span

Table 5-4
Differential Pressure Transmitter Operating Conditions

Parameter	Nominal Value
Transmitter URL	150 in w.g.
Calibration Span	0 150 in w.g.
Calibration Interval	15 days
Static Pressure Variation	± 0.0 psi (0 kPa)

Based on these values the transmitter error specifications can now be converted into absolute error values. The error values are presented in Table 5-5.

Table 5-5
Differential Pressure Transmitter Error Values

Elemental Error	Error Value
Calibration Accuracy	± 0.3 in. w.g.
Temperature Effect	0 in w.g.
Static Pressure Zero Effect	0 in w.g.
Static Pressure Span Effect	0 in w.g.
Mounting Position Effect	0 in w.g.
Stability	± 0.015 in w.g.

The error values are now combined in a root-sum-square (RSS) fashion to provide the total error for the transmitter.

$$B_{h_w} = \sqrt{(0.3)^2 + (0)^2 + (0)^2 + (0)^2 + (0)^2 + (0.15)^2} = \pm 0.33" \text{ w.g.} \quad (\text{Eq. 5-5})$$

Unlike the uncertainty values for the primary element, this error has not been propagated into a value that represents an uncertainty estimate of the flow. ASME PTC 19.1- Measurement Uncertainty [33] defines a sensitivity coefficient, Θ , which is used to propagate the uncertainty in a measured parameter, h_w in this case, to the measurement uncertainty in the result, which in this case is flow. In order to derive this sensitivity coefficient, a closed form analytical method is used.

Application of Methodology

The governing equation for the calculation of flow, based on the measured differential pressure is given in Equation 5-2. The equations used in deriving the sensitivity coefficient are provided below:

$$Q_{q,h_w} = \frac{\partial q}{\partial h_w} \quad (\text{Eq. 5-6})$$

Differentiating and substituting known values yields:

$$\Theta_{q,h_w} = \frac{C}{2\sqrt{h_w}} = \frac{288.7}{2\sqrt{70.25}} = 17.22 \left(\frac{\text{gpm}}{\text{w.g.}} \right). \quad (\text{Eq. 5-7})$$

The differential pressure bias error may now be propagated to the uncertainty in flow using the sensitivity coefficient calculated above and the following equation:

$$B_{h_w} = B_{h_w} * \Theta_{q,h_w} \quad (\text{Eq. 5-8})$$

Solving for the uncertainty attributed to the measurement of the differential pressure yields:

$$B_{h_w} = 0.33 \text{ w.g.} * 17.22 \text{ gpm/w.g.} = \pm 5.7 \text{ gpm} \quad (\text{Eq. 5-9})$$

This value is combined in an RSS fashion to provide the composite bias limit for the measured flow.

$$B_q = \sqrt{(68)^2 + (5.7)^2} = \pm 68 \text{ gpm} \quad (\text{Eq. 5-10})$$

Hence, the composite bias (systematic) limit of the differential pressure producing flow section is ± 68 gpm.

5.2.2.5 Evaluation of Elemental Precision (Random) Uncertainty Sources

The precision or random uncertainty arises from taking repeated measurements using the same primary and secondary measurement device. The index for the estimation of the random uncertainty is the standard deviation of the sample (S_x), which was given in the example as 0.06 in. w.g. (1.52 mm w.g.). Hence, the standard deviation of the sample mean or the scatter of the average of the data sample is calculated as:

$$S_x = \frac{S_x}{\sqrt{N}} = \frac{0.06}{\sqrt{30}} = 0.011" \text{ w.g.} \quad (\text{Eq. 5-11})$$

In order to calculate the standard deviation of the result, it is necessary to propagate the standard deviation (eq. 5-12 of the sample mean to the final result using the previously) determined sensitivity coefficient, $\Theta_{g_{hw}}$.

$$S_q = 0.011 * 17.22 = 0.2 \text{ gpm} \quad (\text{Eq. 5-12})$$

5.2.2.6 Overall Uncertainty of Result

The bias and precision uncertainties of the result are combined using the following equation:

$$U_q = \sqrt{B_q^2 + (t_{95,n,q} S_q)^2} \quad (\text{Eq. 5-13})$$

where,

- U_q = uncertainty in the flow with 95% coverage
- B_q = bias or systematic limit for the flow
- S_q = precision or random index for the flow
- t = Student's "t" value for 95% coverage based on v_r degrees of freedom

Since there were 30 data points in the population, the degrees of freedom in the result is N-1 or 29. The Student's "t" value associated with 29 degrees of freedom can be found in Table 3-1 of Section 3 and is 2.045. Hence the overall uncertainty of the flow measurement is:

$$U_q = \sqrt{(68)^2 + (2.045 * 0.2)^2} = \pm 68 \text{ gpm} \quad (\text{Eq. 5-14})$$

5.3 Multiport Averaging Pitot Tube

5.3.1 Influence Factors

5.3.1.1 Manufacturing Considerations

The multiport averaging pitot tube can be designed to function as a permanent installation or as a “hot-tap” device such that the element can be inserted to the flow stream as required for measurements and extracted when not in use. The ability to extract the element facilitates the inspection of the stagnation pressure ports to determine if pluggage or damage has occurred. The most representative information available on the manufacture and design of this type of flow element can be found in the manufacturers’ literature. The design of multiport averaging pitot tubes provides extremely low permanent pressure loss when compared to a device such as the orifice plate.

5.3.1.2 Installation Considerations

The location of these types of primary elements is critical in obtaining an accurate and repeatable flow measurement. Several configurations have been tested in flow laboratories, and the results published in the Dieterich Standard *Annubar[®] Flow Handbook* [9] and Miller’s *Flow Measurement Engineering Handbook* [4]. The referenced publications provide minimum straight piping requirements but do not quantify any additional uncertainty for not meeting these requirements. If the application requires that this type of sensor be in a piping configuration that does not meet the minimum requirements, ASME-MFC-10M [34] should be consulted for options.

5.3.1.3 Measurement Loop Considerations

The measurement loop considerations are essentially the same as the differential pressure producers. Guidance can be found in ASME-MFC-8M-1988 [37] regarding proper installation of sensing lines. Further, Dieterich Standard recommends that if the transmitter is less than 50 feet from the element, 1/4” tubing is sufficient; however, if this is not possible, the diameter should be increased by 1/8” for each additional 50 feet of tubing length.

5.3.1.4 Calibration Considerations

An Annubar can be wet calibrated against a primary standard or dye dilution. ASME-MFC-10M-1994 [34] should be consulted for proper methods for establishing installation effects due to piping and other flow profile disturbances.

5.3.1.5 Instrument Integrity Consideration

The major source of performance degradation is from pluggage of the upstream impact ports. The elements should be periodically inspected for pluggage.

5.3.1.6 Spatial Consideration

Area averaging of the velocity pressure is inherent in the design of the multiport averaging pitot tube if it is installed according to the manufacturer's recommendations.

5.3.2 Example of Uncertainty Methodology

An Annubar multiport averaging pitot tube is used to measure the flow of service water. The differential pressure produced by the primary element is measured with a differential pressure transmitter calibrated to an URL of 55 inches of water. The calibrated accuracy of the transmitter is $\pm 0.50\%$ of the URL. The Annubar has a flow coefficient of $137.04 \text{ gpm}/(\text{in. w.g.})^{0.5}$. There is a 90° elbow located 6 feet upstream of the flow element and a "tee" 6.5 feet downstream. During the flow measurement, a data acquisition system was "looped" into the analog output signal of the transmitter, which logged a value every 15 seconds for 10 minutes. A summary of the measurements are provided in Table 5-6.

Table 5-6
Results of Flow Measurements from Annubar

Time (Sec)	Differential Pressure (" w.g.)	Time (Sec)	Differential Pressure (" w.g.)	Time (Sec)	Differential Pressure (" w.g.)
15	19.18	210	19.80	405	19.01
30	19.01	225	18.92	420	18.49
45	18.75	240	19.63	435	19.80
60	19.80	255	18.66	450	18.92
75	18.92	270	18.23	465	19.36
90	19.54	285	19.54	480	19.01
105	18.92	300	18.92	495	18.49
120	19.18	315	19.36	510	19.80
135	19.80	330	19.01	525	18.92
150	19.92	345	18.49	540	19.36
165	19.80	360	19.80	555	19.01
180	18.49	375	18.92	570	18.49
195	19.92	390	19.36	585	19.80
				600	18.49

The square of the average of the square root of the measured differential pressures is 19.17 in. w.g. and the standard deviation of the data sample is 0.227 in. w.g.

5.3.2.1 Definition of Measurement Process

The Annubar multiport averaging pitot tube is a differential pressure producing primary element. The governing equation which relates the measured differential pressure to the flow in the pipe is:

$$q = K\sqrt{h_w} \quad (\text{Eq. 5-15})$$

where,

q	=	volumetric flow
K	=	flow coefficient
h_w	=	measured differential pressure

5.3.2.2 Identification of Elemental Bias Uncertainty Sources

The following elemental error sources have been identified as:

- The accuracy of an uncalibrated Annubar flow element
- The effect of upstream flow disturbances
- The effect of downstream flow disturbances
- The pipe dimensions
- The accuracy of the differential pressure transmitter
- The determination of fluid density

5.3.2.3 Identification of Elemental Precision Uncertainty Sources

The only source of precision error in this measurement system is the scatter of data in the sample population.

5.3.2.4 Evaluation of Elemental Bias Uncertainty Sources

The base uncertainty of the Annubar flow element is a function of the initial calibration, the elapsed time since the last inspection, and the service conditions. Assuming that the system maintenance and water chemistry are adequate to minimize the effects of scaling, deposit accumulation, and erosion of the primary element. Hence, based on the Dieterich Standard *Annubar*[®] *Flow Element Handbook* [9], the base uncertainty for an uncalibrated flow element is:

$$U_{\text{Base}} = \pm 1.0\% \quad (\text{Eq. 5-16})$$

Using the measured flow of 600 GPM, this yields an absolute bias error of ± 6.0 gpm.

The proper conversion from velocity pressure to volumetric flow requires input of the pipe inside diameter (and hence the cross-sectional flow area). Therefore, the uncertainty due to the pipe diameter can have a significant impact on the measured flow.

Typically, the inside diameter of the pipe is not measured; the inside diameter error must be estimated based on the available outside diameter and wall thickness measurements. Hence, the total error of the inside pipe diameter must be calculated by using a root-sum-square combination of the outside diameter and wall thickness error contributions.

The uncertainty in the determination of outside pipe diameter produces an error in determination of the inside diameter. Specifications for steel pipe, ASTM designation A530 states the permissible variations in the outside diameter for nominal pipe sizes of 4 to 8 inches as 0.0625" over to 0.03125" under. In this case, water is flowing through 6 inch schedule 40 carbon steel pipe. Mark's *Standard Handbook for Mechanical Engineers* [38] states that the nominal OD value for this type of pipe is 6.625". Therefore, the maximum pipe outside diameter is 6.6875" and the minimum pipe OD is 6.5938". The difference between the maximum and minimum pipe OD is then 0.0937". The outside diameter bias error expressed about the mean is then

$$B_{d_o} = \pm 0.0469" \quad (\text{Eq. 5-17})$$

Again, referring to Mark's [38], the value of the nominal wall thickness for this type of pipe is given as 0.280". The typical tolerance for the wall thickness, expressed about the mean, is $\pm 12.5\%$. Therefore, the error associated with the wall thickness may be estimated as

$$B_w = \pm 0.035" \quad (\text{Eq. 5-18})$$

Note that the uncertainty due to dimensions can be reduced by taking physical measurements. The differential pressure produced by the flow element is measured by a differential pressure transmitter (secondary element). The error specifications and operating conditions for the differential pressure transmitter are contained in Tables 5-7 and 5-8.

Table 5-7
Differential Pressure Transmitter Error Specifications

Error Source	Listed Specification
Calibration Accuracy	$\pm 0.2\%$ of calibrated span
Temperature Effect	None
Static Pressure Zero Effect	None
Static Pressure Span Effect	None
Mounting Position Effects	None
Stability	0.1% of calibrated span

Table 5-8
Differential Pressure Transmitter Operating Conditions

Parameter	Nominal Value
Transmitter URL	55 in. w.g. (1397 mm w.g.)
Calibration Span	0–55 in w.g. (0–1397 mm w.g.)
Calibration Interval	15 Days
Temperature Variation	$\pm 0^{\circ}\text{F}$ (0°C)
Static Pressure Variation	± 0.0 PSI (0 kPa)

The transmitter error specifications can now be converted into actual error values.

Table 5-9
Differential Pressure Transmitter Error Values

Elemental Error	Error Value
Calibration Accuracy	± 0.275 in. w.g. (6.99 mm w.g.)
Temperature Effect	0 in. w.g. (0 mm w.g.)
Static Pressure Zero Effect	0 in. w.g. (0 mm w.g.)
Static Pressure Span Effect	0 in. w.g. (0 mm w.g.)
Mounting Position Effect	0 in. w.g. (0 mm w.g.)
Stability	± 0.055 in. w.g. (1.4 mm w.g.)

The error values are now combined in a root-sum-square (RSS) fashion to provide a total elemental error for the transmitter.

$$\text{Error} = \sqrt{(0.275)^2 + (0)^2 + (0)^2 + (0)^2 + (0)^2 + (0.55)^2} = \pm 0.615" \text{ w.g.} \quad (\text{Eq. 5-19})$$

5.3.2.5 Evaluation of Elemental Precision Uncertainty Sources

The precision or random uncertainty arises from taking repeated measurements using the same primary and secondary measurement device. The index for the estimation of the random uncertainty is the standard deviation of the sample S_x , which was given in the example as 0.227 in. w.g. (5.77 mm w.g.). Hence, the standard deviation of the sample mean S_x or the scatter of the average of the data sample of population N is calculated as:

$$S_x = \frac{S_x}{\sqrt{N}} = \frac{0.227}{\sqrt{40}} = 0.036" \text{ w.g.} \quad (\text{Eq. 5-20})$$

5.3.2.6 Evaluate Sensitivity Coefficients

The sensitivity coefficients are factors that serve to convert an uncertainty in one parameter to a corresponding uncertainty in the parameter being investigated. In the case of the inside diameter, the equation that relates the outside diameter and wall thickness to the inside diameter is:

$$d_i = d_o - 2w \quad (\text{Eq. 5-21})$$

where,

- d_i = inside diameter of pipe
- d_o = outside diameter of pipe
- w = wall thickness of pipe

The sensitivity coefficients that relate the inside diameter to the outside diameter and wall thickness are calculated by taking the partial derivatives of eq. 5-21.

$$\Theta_{d_o} = \frac{\partial d_i}{\partial d_o} = 1 \quad (\text{Eq. 5-22})$$

and,

$$\Theta_w = \frac{\partial d_i}{\partial w} = -2 \quad (\text{Eq. 5-23})$$

The uncertainty due to errors in the measurement of the inside diameter can now be estimated using the following equation:

$$U_{d_i} = \sqrt{(\Theta_{d_o} * B_{d_o})^2 + (\Theta_w * B_w)^2} = \sqrt{(1 * 0.0469)^2 + (-2 * 0.035)^2} = 0.084" \quad (\text{Eq. 5-24})$$

Now that the uncertainty of the inside diameter has been calculated, the uncertainty of the flow measurement due to uncertainty in the measurement of inside diameter may be calculated. The basic equation relating inside diameter to flow is:

$$q = v_{\text{avg}} * A = \frac{\pi * d_i^2 * v_{\text{avg}}}{4} \quad (\text{Eq. 5-25})$$

where:

- v_{avg} = average water velocity at measurement plane
- A = normal, cross-sectional flow area
- d_i = inside diameter of pipe at measurement plane

The relative sensitivity coefficient, Θ'_{q,d_i} , that relates the uncertainty due to the inside diameter to uncertainty in flow is calculated as:

$$\Theta'_{d_i} = \frac{\partial q}{\partial d_i} * \frac{d_i}{q} = \frac{\partial}{\partial d_i} (1/4 v_{\text{avg}} \pi d_i^2) * \frac{d_i}{(1/4 v_{\text{avg}} \pi d_i^2)} = 2 \quad (\text{Eq. 5-26})$$

This relative sensitivity coefficient is now used to calculate the overall uncertainty, in percent of flow due to inside diameter in accordance with eq. 3.10 of ASME PTC 19.1 [33] as:

$$U_{q,d_i} = \Theta'_{q,d_i} * \frac{B_{d_i}}{d_{i_{\text{no minal}}}} * 100 = 2 * \frac{0.084"}{6.065"} * 100 = 2.77\% \quad (\text{Eq. 5-27})$$

Application of Methodology

This relative uncertainty can now be expressed as an absolute uncertainty by multiplying the relative uncertainty by the measured flow:

$$U_{q,d_i} = 600 * 0.0277 = 16.62 \text{ gpm} \quad (\text{Eq. 5-28})$$

In order to evaluate the absolute uncertainty in the measured flow to the estimated error in measured differential pressure, a sensitivity coefficient must be developed that will relate the measured parameter to the result. The following derivation is the methodology employed based on the basic flow equation:

$$q = K^* \sqrt{h_w} \quad (\text{Eq. 5-29})$$

where,

- q = volumetric flow
- K* = flow constant (137.04 gpm/in. w.g.^{0.5})
- h_w = measured differential pressure head

The governing equation for the calculation of flow, based on the measured differential pressure, is given in eq. 5-32. The equations used in deriving the sensitivity coefficient are provided below:

$$\Theta_{q,h_w} = \frac{\partial q}{\partial h_w} \quad (\text{Eq. 5-30})$$

Differentiating and substituting known values yields

$$\Theta_{q,h_w} = \frac{C}{2\sqrt{h_w}} = \frac{137.04}{2\sqrt{19.13}} = 15.67 \text{ gpm}/" \text{ w.g.} \quad (\text{Eq. 5-31})$$

The differential pressure bias error may now be propagated to the uncertainty in flow using the sensitivity coefficient calculated above and the following equation:

$$B_{q,h_w} = B_{h_w} * \Theta_{q,h_w} \quad (\text{Eq. 5-32})$$

Solving for the uncertainty attributed to the measurement of the differential pressure yields:

$$B_{q,h_w} = 0.615" \text{ w. g.} * 15.67 \text{ gpm/" w. g.} = \pm 9.64 \text{ gpm} \quad (\text{Eq. 5-33})$$

The precision elemental uncertainty can now be propagated to the final result using the same sensitivity coefficient as developed above:

$$S_q = 0.036" \text{ w. g.} * 15.67 \text{ gpm/" w. g.} = 0.56 \text{ gpm} \quad (\text{Eq. 5-34})$$

5.3.2.7 Evaluate Uncertainty of Result

The overall bias or systematic uncertainty of the Annubar can now be calculated as:

$$B_q = \pm \sqrt{(6)^2 + (16.6)^2 + (9.6)^2} = \pm 20.1 \text{ gpm} \quad (\text{Eq. 5-35})$$

Since there were more than 30 measurements made of the differential pressure, the Student's "t" value for 95% coverage is 2.0. Hence, the overall uncertainty in the measurement of flow using the Annubar is found from:

$$U_q = \pm \sqrt{(20.1)^2 + (2.0 * 0.56)^2} = \pm 20.1 \text{ gpm} \quad (\text{Eq. 5-36})$$

This value for the overall uncertainty in the flow measurement is equivalent to $\pm 3.36\%$ of the measured flow.

5.4 Pitot Tube Traverses

5.4.1 Influence Factors

5.4.1.1 Manufacturing Considerations

There are a large variety of pitot tube designs that have been developed for the measurement of water over the years. Types that may be encountered are the basic impact pitot tube, pitot static tube, Simplex pitot tube, Keil pitot tube, Wedge pitot tube, and the “S” pitot tube. Typically, the pitot tube is a pair of tubes enclosed in a casing. One tube transmits the static or reference pressure sensed at the side orifices, and the other tube transmits the impact pressure from the orifice that faces the flow. The sensing ports must be perpendicular to each other in order to provide the proper orientation for pressure sensing. Additionally, the head of the pitot tube must be perpendicular to the supporting stem. ISO Standard 3966-1977, *Measurement of Fluid Flow in Closed Conduits Velocity Area Method Using Pitot Static Tubes*, [27] provides guidance in the design and manufacturing specifications in Section 4.1 and 4.2

5.4.1.2 Installation Considerations

The typical arrangement for pitot insertion taps is two taps, 90° apart located at a given measurement plane. The *Cooling Tower Institute (CTI) Bulletin*, STD-146 [13], in Section II-F specifies the criteria for the installation of taps to minimize any effects from flow stream distortions, turbulent eddies, and vortices near the pipe wall that may result in erroneous flow readings. Further, the *CTI Bulletin* suggests that if possible the taps should be located on a vertically oriented run of pipe to eliminate the potential of having air trapped at the top of the pipe. If a vertical run is not possible, then a tell-tale valve at the top of the pipe should be monitored to ensure that the pipe is completely full.

5.4.1.3 Measurement Loop Considerations

The predominant secondary device used with pitot tube primary elements is the manometer because many field applications preclude the use of electronic differential pressure transmitters. CTI Bulletin STD-146-1995 in Section 7 provides direction for the calibration and use of various types of secondary differential pressure readout devices.

5.4.1.4 Calibration Considerations

All references state categorically that pitot tubes should be calibrated by an independent flow laboratory. Each type of pitot tube has a unique flow coefficient

associated with the design of the head; however, the calibration should be checked in a laboratory periodically to ensure that any minor damage to the pitot head or orifices has not altered the flow coefficient.

5.4.1.5 Instrument Integrity Consideration

ISO 3966-1977 in Section 5.5 provides a checklist of criteria that should be examined both before and after measurements are taken to ensure that no damage to the sensing head has occurred during use. The primary device connections to the secondary device that is used should also be leak-checked and in general accordance with ANSI/ASME MFC-8M-1988, *Fluid Flow in Closed Conduits Connection for Pressure Signal Transmissions Between Primary and Secondary Devices* [37].

5.4.1.6 Spatial Consideration

The pitot tube, by nature of the flow measurement methodology, provides a flow that has been integrated over the cross-sectional flow area. The codes referenced in this guideline suggest that, as a minimum, two diametrical traverses be performed. To further improve the determination of the average flow rate, additional diametrical traverses can be specified.

5.4.1.7 Nonhomogeneous Flow

CTI Bulletin STD-146-1995 in Section 3 suggests that the use of a pitot tube in water with entrained solids is precluded because the probability of orifice pluggage is high. Further, erroneous flows will be calculated if the water has entrained air or gas.

5.4.2 Example of Uncertainty Methodology

A Simplex/Leopold pitot tube, calibrated at a flow laboratory, was used to obtain data to calculate the flow of water in a 12" (30.5 cm) schedule 40S, circular pipe. The coefficient of the pitot tube was reported by the laboratory to be 0.808. A traverse of four radii was conducted with five differential pressure measurements taken at each radius. The length of two diameters was measured using the pitot tube, and the results obtained were: $d_1=11.875"$ (30.163 cm) and $d_2=12.125"$ (30.798 cm). The pitot tube was connected to a differential pressure transmitter that was connected to a data acquisition system programmed to scan every 15 seconds. At least thirty scans were taken at each measurement point. The differential pressure transmitter was calibrated with an URL of 50 in. w.g. and a calibrated accuracy of 0.2% of URL.

Table 5-10 represents the average of all ten measurements at each traverse point.

Table 5-10
Pitot Tube Traverse Data

Traverse Point	Radius 1 Deflection	Radius 1 Std Dev	Radius 2 Deflection	Radius 2 Std Dev
1	17.50	.15	17.25	.20
2	18.75	.25	19.50	.20
3	21.00	.20	22.25	.10
4	21.25	.10	22.75	.15
5	22.50	.15	23.25	.15

	Radius 3 Deflection	Radius 3 Std Dev	Radius 4 Deflection	Radius 4 Std Dev
1	16.75	.15	17.25	.25
2	17.50	.15	17.75	.20
3	20.25	.25	19.50	.15
4	21.25	.25	23.50	.15
5	23.25	.20	24.50	.25

5.4.2.1 Definition of Measurement Process

The flow rate will be calculated using the following equation:

$$q = C * C_p * A_{corr} * \sqrt{\Delta p_{avg}} \tag{Eq. 5-37}$$

where, when compatible units are used

- q = volumetric flow
- C = dimensional coefficient;
- C_p = pitot tube coefficient

$$A_{\text{corr}} = \text{normal, cross-sectional area of pipe at measurement plane, corrected for probe blockage}$$

$$\Delta p_{\text{avg}} = \text{average velocity pressure}$$

5.4.2.2 Identification of Elemental Bias Uncertainty Sources

The systematic error sources identified in this method of flow measurement are:

- Errors in the calibration of the pitot tube that are reflected in the pitot tube coefficient
- Errors in the measurement of the pipe diameter
- The error introduced by the secondary element in reading a differential pressure
- The velocity spatial bias due to the nature of an asymmetric flow profile

5.4.2.3 Identification of Elemental Precision Uncertainty Sources

In this method of obtaining the data, the random error is identified as the random error of the repeated measurements at each independent measurement point.

5.4.2.4 Evaluation of Elemental Bias Uncertainty Sources

A calibration bias of 2% is used for this element, based on a review of calibration laboratory data. This value is typically the largest source of uncertainty in the measurement of flow using a pitot tube. The error value was based on the accuracy of the load cell calibration standards and the velocity dependency of the coefficient.

$$B_{C_p} = 0.02 * 0.808 = \pm 0.01616 \quad (\text{Eq. 5-38})$$

In estimating the error in the measurement of the pipe diameter, consideration is given to how the measurement is made. Typically, the pitot tube is gently extended to the far wall of the pipe in order to prevent disturbing any internal buildups that may be present, and a scribe mark is made on the pitot tube casing. The pitot tube is then withdrawn, noting the deflection indicated by the differential pressure transmitter. Upon reading a zero deflection, which indicates the sensing orifices being just out of the flow stream, a second scribe is made on the pitot tube casing. The distance between the two scribe marks is measured, and the distance from the end of the tube to the orifice (generally on the order of 0.125" or 0.318 cm) is added to the measured value.

Application of Methodology

This is done for each diameter to be traversed. The estimation in measuring the diameter by this manner is $\pm 1/8$ " (0.318 cm).

Hence,

$$B_d = \pm 0.125" \quad (\text{Eq. 5-39})$$

The differential pressure transmitter was calibrated from 0 to 50 in. w.g. (0 to 1270 mm w.g.) and had an accuracy specification of $\pm 0.2\%$ of URL. The transmitter, therefore, will have an absolute error in the conditioning of the differential pressure signal of:

$$B_s = 0.002 * 50 = \pm 0.1" \text{ w.g.} \quad (\text{Eq. 5-40})$$

Since the water in a pipe seldom exhibits an ideal, uniform profile, it is not realistic to anticipate equally distributed readings of concentric velocities around the pipe perimeter. In this treatment, the average velocity pressures and precision indices along each of the four radii will be used to calculate a spatial bias of the velocity pressure.

In doing this it is first necessary to calculate the standard deviation for each radii, where:

$$S_{1,\text{pooled}} = \left[\frac{\sum_{i=1}^5 S_i^2}{5} \right]^{1/2} \quad (\text{Eq. 5-41})$$

and,

$$S_{P_{V_1}} = \frac{S_{1,\text{pooled}}}{\sqrt{5}} \quad (\text{Eq. 5-42})$$

The results for each radii are:

$$S_{pv1} = 0.0794" \text{ w.g.} \quad (2.0168 \text{ mm w.g.}) \quad P_{v1} = 20.2" \text{ w.g.} \quad (513.1 \text{ mm w.g.})$$

$$S_{pv2} = 0.0735" \text{ w.g.} \quad (1.8669 \text{ mm w.g.}) \quad P_{v2} = 21.0" \text{ w.g.} \quad (533.4 \text{ mm w.g.})$$

$$S_{pv3} = 0.0916" \text{ w.g.} \quad (2.3266 \text{ mm w.g.}) \quad P_{v3} = 19.8" \text{ w.g.} \quad (502.9 \text{ mm w.g.})$$

$$S_{pv4} = 0.0916" \text{ w.g.} \quad (2.3266 \text{ mm w.g.}) \quad P_{v4} = 20.5" \text{ w.g.} \quad (520.7 \text{ mm w.g.})$$

From this data, the value of S_{72} may now be evaluated from the following equation:

$$S_{72} = \left[\frac{\sum_{k=1}^L (P_{vi} - P_{v,avg})^2}{L-1} \right]^{1/2} = 0.5058" \text{ w.g.} \quad (\text{Eq. 5-43})$$

The spatial bias, B_{72} , may now be calculated for this data based on 3 degrees of freedom using the following equation, where 3.182 is the Student's "t" value for 95% coverage:

$$B_{72} = \frac{tS}{\sqrt{4}} = \frac{3.182 * 0.5058}{2} = 0.805" \text{ w.g.} \quad (\text{Eq. 5-44})$$

5.4.2.5 Evaluation of Elemental Precision Uncertainty Sources

The precision or random uncertainty element is the scatter of data from the repeated measurements taken of the velocity pressure. Hence, the relationship used for the evaluation of this element is:

$$S_{Pv,pooled} = \left[\frac{\sum_{k=1}^4 S_{Pv,k}^2}{4} \right]^{1/2} = 0.0844" \text{ w.g.} \quad (\text{Eq. 5-45})$$

and,

$$S_{Pv} = \frac{S_{Pv,pooled}}{\sqrt{4 * 5 * 30}} = 0.0034" \text{ w.g.} \quad (\text{Eq. 5-46})$$

5.4.2.6 Evaluate Sensitivity Coefficients

Using the governing equation, the sensitivity coefficients can be calculated for each elemental error source.

The sensitivity coefficient of the flow to the pitot tube coefficient is:

$$\Theta_{q,C_p} = \frac{\partial q}{\partial C_p} = 1039.35 * A_{corr} * \sqrt{\Delta p_{avg}} = 3,612.45 \text{ gpm} \quad (\text{Eq. 5-47})$$

Application of Methodology

where,

A_{corr} = normal, cross-sectional area of pipe at the measurement plane corrected for probe blockage (0.770 ft² or 715.353 cm²)

Δp_{avg} = grand average velocity pressure (20.375 in. w.g. or 517.525 mm w.g.)

The sensitivity coefficient of the flow to the pipe diameter is calculated by:

$$\Theta_{q,d} = \frac{\partial q}{\partial d} = \frac{\left(\frac{d_{\text{avg}}}{2} * \pi\right) - \frac{w}{2}}{144} * 1039.35 * C_p * \sqrt{\Delta p_{\text{avg}}} = 491.02 \text{ gpm / inch (Eq. 5-48)}$$

where,

d_{avg} = average diameter of pipe at measurement plane (12.000" or 30.48 cm)

w = pitot tube width (0.375" 0.953 cm)

C_p = pitot tube coefficient (0.808)

The sensitivity coefficient of the flow to the measured velocity pressure is evaluated as:

$$\Theta_{q,\Delta p} = \frac{\partial q}{\partial \Delta p} = \frac{1 / 2 * 1039.35 * C_p * A_{\text{corr}}}{\sqrt{\Delta p_{\text{avg}}}} = 71.63 \text{ gpm / " w.g. (Eq. 5-49)}$$

5.4.2.7 Evaluate Uncertainty of Result

The combined bias or systematic uncertainty of the flow measurement is expressed as:

$$U_{q,B} = \sqrt{\left(B_{C_p} * \Theta_{q,C_p}\right)^2 + \left(B_d * \Theta_{q,d}\right)^2 + \left(B_{Dp} * \Theta_{q,Dp}\right)^2 + \left(B_{72} * \Theta_{q,Dp}\right)^2} = \pm 102.8 \text{ gpm (Eq. 5-50)}$$

and the precision or random uncertainty component of the flow measurement is calculated to be:

$$U_{q,s} = 0.0034 * 71.63 = \pm 0.24 \text{ gpm} \quad (\text{Eq. 5-51})$$

Therefore, the overall uncertainty in the flow measurement using the pitot tube, considering the Student's "t" value being 2.0 for more than 30 pooled measurements, is:

$$U_q = \sqrt{(102.8)^2 + (2 * 0.24)^2} = \pm 102.8 \text{ gpm} \quad (\text{Eq. 5-52})$$

5.5 Ultrasonic Flow Meters

Over the past five years, refinement of ultrasonic flow meter technology has enabled both flowcell and clamp-on versions to be viable options for fluid flow metering. A feature of the clamp-on ultrasonic flow meter is the ability to be non-intrusively installed and still provide a reasonable level of uncertainty and a high level of repeatability.

5.5.1 Influence Factors

5.5.1.1 Manufacturing Considerations

The ultrasonic transducers are manufactured such that the fluid being measured can be in contact with the fluid (wetted) or mounted on the outside surface of the pipe carrying the fluid (clamp-on). Another option is the use of a manufactured flowcell, which is a spoolpiece with permanently monitored transducers. The entire spoolpiece can be calibrated prior to installation and removed and recalibrated as needed. This will reduce the errors associated with field installation uncertainties such as pipe diameters, pipe material, liners, internal surface roughness, transducer spacing, and orientation.

5.5.1.2 Installation Considerations

If the non-wetted, clamp-on type of transducers are used, the flow calculation must account for the pipe wall material through which the acoustic signal must traverse. This adds an additional uncertainty source to the measurement. In order to minimize this effect, the interface between the transducer and the flow conduit must be sonically coupled.

An ultrasonic flow meter can be set up with a single pair of transducers, which send and receive a single path signal, or with multiple pairs of transducers, which send and receive multiple signals. A typical transit-time single path installation can be set up to traverse the flow in an axial, diametric, or chordal manner. Axial path configurations are typically used in smaller pipe diameters because they are the least sensitive to irregular velocity profiles. Manufacturers' recommendations should be referenced for the required upstream and downstream diameters for given flow disturbances.

5.5.1.3 Calibration Considerations

The calibration of ultrasonic flow systems may be conducted *in situ* or by laboratory methods. *In situ* calibration has the potential to yield the most accurate results due to the system being calibrated in place with all the installation effects such as upstream piping disturbances present. Accurate *in situ* calibrations must be conducted with methods such as dye dilution to attain the required accuracy.

Typically, the calibration procedure generates a correction factor that is applicable to a specific range of flow. An adequate number of calibration points must be utilized in order to characterize the reliability and repeatability of the flow meter. Laboratory calibration is typically performed by constructing a flow section that has identical upstream and downstream piping as the field application. Full flow is then established and measured using a primary standard such as gravimetric or volumetric timed-test runs. Similar to *in situ* calibrations, a correction factor is established for the desired range of flow conditions. When using a laboratory calibration, the uncertainties associated with the field application pipe dimensions, intervening material properties, flow profile variations, transducer spacing, transducer orientation, fluid properties, and surface roughness should all be investigated and included in the overall flow uncertainty

5.5.1.4 Meter Integrity Considerations

Inspection of the measurement site should be performed when possible, in order to minimize the effects of deposits on pipe walls, pipe roughness changes, transducer scale build-up, flow area obstructions, and potential signal disturbances. The inspection frequency will depend on the fluid properties and chemistry, pipe material properties, and the environmental conditions. Most ultrasonic flow metering systems will conduct diagnostic checks to ensure that no major problems exist with the acoustic signal. Diagnostic checks can aid in the evaluation of a potential flow site.

5.5.1.5 Spatial Considerations

Multiple path systems can be configured to traverse diameters or chords. The multiple path configurations decrease the sensitivity to non-uniform velocity profiles. These

systems utilize a weighting factor for each flow path in order to correct for the equivalent area the ultrasonic path traverses. The multiple path configurations require larger pipe diameters in order to measure each signal independently in a practical manner.

Spatial variation along the acoustic path in the intervening materials and fluid introduce uncertainties in the flow rate determination. Spatial dimensional variations can be accounted for by taking multiple measurements of each dimension and assessing the spatial average and uncertainty. Variations in the intervening materials and fluid properties introduce changes in the measured velocity. Most ultrasonic flow meter algorithms are based on homogenous fluid and material properties.

5.5.1.6 Nonhomogeneous Flow Considerations

The effect of entrained air or gas in the flow stream serves to attenuate the acoustic signal and alter the acoustic path, resulting in increased flow measurement uncertainties. Depending on the distribution of the air or gas, the signal may become distorted at low levels of the liquid-gas mixture. Hence, it is not recommended to measure highly aerated streams with transit-time ultrasonics.

Transit-time meters are much less affected by sonically conductive particles than by air or gas, but the flow measurement may still be skewed if the particles distort the ultrasonic signal.

Nonhomogeneous flows are more conducive to measurement with a Doppler type flow meter, but even Doppler meters require that the particles be evenly distributed throughout the flow stream and traveling at the same rate as the fluid.

5.5.2 Example of Uncertainty Methodology

The flow of water was measured to be 1000 gpm (3785.4 lpm) in a 14" (35.6 cm) standard weight A312-69 carbon steel pipe using a transit-time ultrasonic flow meter. The flow meter utilized temporary clamp-on transducers that have a sound speed of 107,480.315 ft/sec. or 32,760 m/sec. Fluid, material property, and dimensional data were determined from reference sources, and the flow meter provided the calculated intermediate values. The following figure illustrates the geometry and nomenclature used in the subsequent uncertainty analysis. The ultrasonic flow system was sent to a flow laboratory and was calibrated to $\pm 1.0\%$ of flow over the range of 500 to 2500 gpm (1892.7 to 9463.5 lpm) on a similar 14" (35.6 cm) A 312-69 carbon steel flow section. The data were taken every minute for an hour and the standard deviation of the population was 58 gpm (219.6 lpm) with a mean measured flow of 1000 gpm (3785.4 lpm).

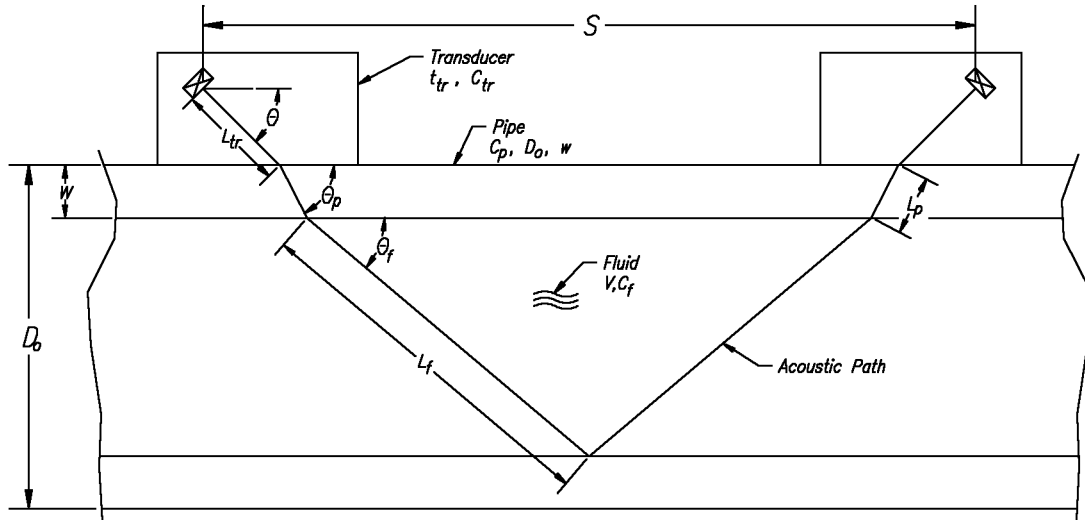


Figure 5-1
Acoustic Path Geometry for Clamp-On Ultrasonic Meter

where,

- Θ = transducer acoustic path relative to horizontal ($^{\circ}$)
- Θ_p = pipe wall acoustic path relative to horizontal ($^{\circ}$)
- Θ_f = fluid acoustic path relative to horizontal ($^{\circ}$)
- S = transducer spacing (in or cm)
- C_f = fluid speed of sound (in/sec or cm/sec)
- C_{tr} = transducer speed of sound (in/sec or cm/sec)
- C_p = pipe wall speed of sound (in/sec or cm/sec)
- L_{tr} = transducer acoustic path length (in or cm)
- L_p = pipe wall acoustic path length (in or cm)
- L_f = fluid acoustic path length (in or cm)
- t_{tr} = transducer transit time (sec)
- D_o = pipe outside diameter (in or cm)

v_f = fluid velocity (in/sec or cm/sec)

w = pipe wall thickness (in or cm)

The following is a summary of the nominal values:

D_o = outside pipe diameter = 14.000" (35.56 cm)

w = wall thickness of pipe = 0.375" (0.95 cm)

S = transducer axial spacing = 14.538" (36.927 cm)

C_{tr} = transducer sound speed = 107,480 in/sec
(272,999 cm/sec)

C_p = sound speed in pipe material = 127,176 in/sec
(323,027 cm/sec)

C_f = sound speed in fluid = 58,464 in/sec
(148,499 cm/sec)

Θ = angle of signal path = 43.4°

α = sound speed ratio factor = 0.39522

t_{tr} = time to transit transducer = 12 μ sec

t_{down} = downstream transit time = 493.34 μ sec

t_{up} = upstream transit time = 493.54 μ sec

ν = kinematic viscosity of fluid = 1.512×10^{-3} in²/sec
(9.755×10^{-3} cm²/sec)

q_{meas} = measured flow rate = 3,850 in³/sec
(63,090 cm³/sec)

5.5.2.1 Define the Measurement Process

The following equations, based on the above drawing, are stated for use in this analysis. The uncorrected flow, correction factor and flow can then be evaluated using the following equations,

$$Q' = \left[\frac{\pi(D_o - 2w)^3}{4\alpha\sqrt{1-\alpha^2}} \right] * \left[\frac{1}{t_{dn}} - \frac{1}{t_{up}} \right] \quad (\text{Eq. 5-53})$$

where,

$$\alpha \equiv \frac{C_f}{C_{tr}} \cos(\Theta) \quad (\text{Eq. 5-54})$$

and,

$$K' = \left(1.119 - 0.011 \log \left(\frac{4Q'}{\pi(D_o - 2w)v} \right) \right)^{-1} \quad (\text{Eq. 5-55})$$

and, finally, the corrected flow,

$$Q_{\text{calc}} = K' * Q' \quad (\text{Eq. 5-56})$$

5.5.2.2 Identification of Elemental Bias Uncertainty Sources

There are seven elemental uncertainty sources identified in this analysis that will impact the measured flow. They are:

- Calibrated accuracy of the ultrasonic flow meter
- Determination of the pipe outside diameter
- Determination of the wall thickness
- Transducer spacing
- Determination of the speed of sound in the pipe
- Determination of the fluid kinematic viscosity
- Uncertainty of the measurement loop
- Upstream and downstream installation requirements

5.5.2.3 Identification of the Elemental Precision Uncertainty Sources

The elemental sources of precision associated with the flow measurement are assumed to be strictly the random error associated with the scatter of the measured flow data.

5.5.2.4 Evaluation of the Elemental Bias Uncertainty Sources

5.5.2.4.1 Calibration Bias Uncertainty

The meter was sent to a qualified laboratory. The flow calibration was conducted on pipes manufactured to similar specifications as those at the field site and at similar flow ranges and conditions as those anticipated in the field measurement. Additionally, the same hand-held flow computer, transducers, and cabling were used in the calibration as were used in the field measurement; therefore, the uncertainties associated with the electronic time measurement and transducer sound speed are included in the calibration uncertainty. The results of the wet flow calibration indicated that the bias uncertainty associated with the flow meter is $\pm 1.0\%$ of flow.

5.5.2.4.2 Pipe Outside Diameter Uncertainty

Although the bias uncertainties are reduced by flow calibration on pipes manufactured to similar specifications and tolerances as those at the measurement site, the uncertainty due to the pipe outside diameter and wall thickness may be significant. However, this contributor to the measurement uncertainty can be minimized by taking physical measurement whenever possible.

The outside pipe diameter was measured at nine distinct points, and the average was input into the flow computer. The specifications for specialized steel pipe, ASTM designation A-312-69, indicates that the permissible variations in the outside diameter for nominal pipe sizes of 8" to 18" (20.3 to 45.7 cm) as 0.093" (0.236 cm) over to 0.031" (0.079 cm) under.

Hence, the maximum pipe outside diameter could be 14.093" (35.796 cm) and the minimum outside pipe diameter could possibly be 13.969" (35.481 cm). The difference between the maximum and the minimum OD is then 0.124" (0.315 cm). The outside diameter uncertainty expressed about the mean is, therefore

$$B_{OD} = \pm 0.062" \quad (\text{Eq. 5-57})$$

Since the outside diameter of the pipe was measured at nine different locations, a spatial bias can be calculated using the outside diameter uncertainty expressed about the mean as:

Application of Methodology

$$S_{72} = \frac{2\sigma}{t} = \frac{0.062''}{2.306} = \pm 0.027'' \quad (\text{Eq. 5-58})$$

and the resulting bias uncertainty is

$$B_{D_o} = \frac{tS_{72}}{\sqrt{M}} = \frac{2.306 * 0.027''}{\sqrt{9}} = \pm 0.021'' \quad (\text{Eq. 5-59})$$

where,

- S_{72} = spatial precision index
- 2σ = outside diameter uncertainty
- t = two-tailed Student's t for 95% confidence with N-1 degrees of freedom
- M = number of measurement locations

It is assumed that the calipers used to measure the outside diameter can accurately measure to ± 5 mils (0.005" or 0.013 cm). Therefore,

$$B_{\text{inst}} = \pm 0.005'' \quad (\text{Eq. 5-60})$$

The resultant bias uncertainty in the outside diameter measurement is then,

$$B_{D_o} = \sqrt{(0.021)^2 + (0.005)^2} = \pm 0.022'' \quad (\text{Eq. 5-61})$$

or expressed in relative terms,

$$B_{D_o} = \frac{0.022}{14.00} * 100 = \pm 0.16\% \quad (\text{Eq. 5-62})$$

5.5.2.4.3 Wall Thickness Uncertainty

The uncertainty in the determination of the wall thickness also produces errors in the evaluation of the inside diameter. Again, the impact of the estimated tolerances can be minimized by taking physical measurements. The wall thickness was measured at 18 discreet points around the circumference of the pipe, and the average was input into

the flow computer for calculating the measured flow. Mark's *Standard Handbook for Mechanical Engineers* [38] indicates that the tolerance of the nominal wall thickness is 12.5%. This yields a tolerance, expressed about the mean as $\pm 6.25\%$. Knowing the nominal wall thickness is 0.375" (0.953 cm) equates to a bias uncertainty in the wall thickness due to manufacturing tolerance of:

$$B_w = \pm 0.023" \quad (\text{Eq. 5-63})$$

The wall thickness was measured at 18 discrete locations; therefore, a spatial bias can be calculated, using the wall thickness uncertainty, as

$$S_{72} = \frac{2\sigma}{t} = \frac{0.023}{2.110} = \pm 0.011" \quad (\text{Eq. 5-64})$$

and the resulting bias uncertainty is,

$$B_w = \frac{tS_{72}}{\sqrt{M}} = \frac{2.110 * 0.011"}{\sqrt{18}} = \pm 0.005" \quad (\text{Eq. 5-65})$$

The ultrasonic thickness measurement device used to measure the wall thickness can accurately measure the thickness to ± 2 mils (0.002" or 0.005 cm). Therefore,

$$B_{\text{inst}} = \pm 0.002" \quad (\text{Eq. 5-66})$$

The resulting composite bias uncertainty in the measurement of the wall thickness is then,

$$B_w = \sqrt{(0.005)^2 + (0.002)^2} = \pm 0.005" \quad (\text{Eq. 5-67})$$

or expressed in relative terms,

$$B_w = \frac{0.005}{0.375} * 100 = \pm 1.3\% \quad (\text{Eq. 5-68})$$

5.5.2.4.4 Transducer Spacing Uncertainty

The uncertainty due to transducer spacing is not included in the calibration uncertainty because the transducers must be re-mounted in the field at the test site. This

Application of Methodology

measurement produces an error in the determination of the acoustic path angle and the acoustic path length, which in turn produces an error in the measured flow rate.

In this example, the transducer spacing will be measured with the scale provided on the transducer mounting bracket. The uncertainty in this measurement is then assumed to be the smallest increment on the scale, which is 0.125" (0.318 cm). Hence, the uncertainty of the spacing is,

$$B_s = \pm 0.125" \quad (\text{Eq. 5-69})$$

or expressed in relative terms,

$$B_s = \frac{0.125}{14.538} * 100 = \pm 0.86\% \quad (\text{Eq. 5-70})$$

5.5.2.4.5 Pipe Sound Speed Uncertainty

The uncertainty due to the pipe sound speed is not included in the calibration due to variations in the pipes used for calibration and the pipes used for the field test. The pipe speed is determined by the pipe material (carbon steel). The ranges given for carbon steel are detailed in the flow meter user's manual. The value farthest from that of the nominal carbon steel value of 127,176 in/sec (10,598 ft/sec) (3230 m/sec) is 124,020 in/sec (10,335 ft/sec) (3150 m/sec) for 1% carbon steel. This uncertainty expressed as a difference about the pipe sound speed mean is,

$$B_{C_p} = \pm 3,156 \text{ ft/sec} \quad (\text{Eq. 5-71})$$

or expressed in relative terms,

$$B_{C_p} = \frac{3,156}{127,176} * 100 = \pm 2.48\% \quad (\text{Eq. 5-72})$$

5.5.2.4.6 Fluid Kinematic Viscosity Uncertainty

The uncertainty due to the fluid kinematic viscosity is dependent on the temperature of the fluid. Using a constant value for this parameter produces an error in the determination of the flow factor, K, which produces an error in the measured flow.

Using a variance of $0.67 \times 10^{-5} \text{ ft}^2/\text{sec}$ ($6.225 \times 10^{-7} \text{ m}^2/\text{sec}$) over a temperature range of 40°F to 180°F (4°C to 82°C) with the nominal value of $1.512 \times 10^{-3} \text{ in}^2/\text{sec}$ ($1.05 \times 10^{-5} \text{ ft}^2/\text{sec}$) ($9.755 \times 10^{-3} \text{ cm}^2/\text{sec}$) yields an uncertainty expressed about the mean of,

$$B_v = \pm 9.65 \times 10^{-4} \text{ in}^2 / \text{sec} \quad (\text{Eq. 5-73})$$

or expressed in relative terms,

$$B_v = \frac{9.65 \times 10^{-4}}{1.512 \times 10^{-3}} * 100 = \pm 63.8\% \quad (\text{Eq. 5-74})$$

5.5.2.4.7 Measurement Loop Uncertainty

The analog output from the flow computer was calibrated by an approved facility and was field verified to within $\pm 0.1\%$ of flow. Therefore,

$$B_{\text{loop}} = \pm 0.1\% \quad (\text{Eq. 5-75})$$

5.5.2.5 Evaluate Sensitivity Coefficients

The sensitivity coefficients are calculated by taking the partial derivatives of the equations relating flow to the parameter of interest. In this case, these coefficients must be determined numerically because there is no closed form solution. The relative sensitivity coefficients will be defined as,

$$\theta_{Q,P}^1 = \frac{\partial Q / Q}{\partial P / P} \cong \frac{\Delta Q / Q}{\Delta P / P} \quad (\text{Eq. 5-76})$$

where,

P = parameter of interest.

The parameter perturbation increment will be defined as 0.0001, or

$$P_f \equiv \frac{\Delta P}{P} = 0.0001 \quad (\text{Eq. 5-77})$$

Application of Methodology

Therefore, the equation for calculating the sensitivity coefficient for a given parameter is,

$$\Theta'_{Q,P} = 10^4 * \frac{\Delta Q}{Q} \tag{Eq. 5-78}$$

Table 5-11 summarizes the sensitivity coefficients calculated for each required parameter.

**Table 5-11
Sensitivity Coefficients**

Parameter	Q (in ³ /sec)	ΔQ (in ³ /sec)	B _p	Θ' _{Q,P} (% flow/% P)	U _p
Cal	na	na	1.0	na	1.0
D _o	3851.007	1.254	0.16	3.26	0.52
w	3851.007	-0.034	1.3	-0.083	-0.11
S	3851.007	-0.215	0.86	-0.558	-0.48
C _p	3851.007	0.099	2.48	0.257	0.64
v	3851.007	-0.002	63.8	-0.0052	-0.33
loop	na	na	0.1	na	0.1

5.5.2.6 Evaluate Bias Uncertainty

The composite instrument bias uncertainty of the flow measurement is evaluated as the RSS of the elemental uncertainties previously determined:

$$U = \sqrt{(1.0)^2 + (0.52)^2 + (-0.11)^2 + (-0.48)^2 + (0.64)^2 + (-0.33)^2 + (0.1)^2} = \pm 1.4\% \tag{Eq. 5-79}$$

5.6 Dye Dilution Methods

Dye (tracer) dilution methods of flow measurement have traditionally been used in open channels with large flows or large volume open loop cooling water systems used to condense steam from turbines. However, this technique has great potential for the use in the measurement of flow in open service water systems because the flow encountered is generally turbulent.

The bulk of information provided in this section comes from two references:

- Alden Research Laboratories Technical Report. *Uncertainty Analysis of Field Turbine Performance Measurements*. 1985.
- Power Generation Technologies Technical Report. *Uncertainty Analysis of Water Flow Rate Measurement by the Dye Dilution Method*. TIN #97-1267. 1997.

5.6.1 Influence Factors

5.6.1.1 Dye Injection Considerations

There are several error sources that must be considered when using the dye dilution method of flow determination. Two resources that detail these considerations are the two technical reports mentioned above. Several error sources pertaining to the injection of the dye tracer are discussed in detail.

5.6.1.2 Sample Extraction Considerations

One of the sampling considerations that must be addressed in the dye dilution method is the mixing length involved. It is imperative that there be sufficient mixing lengths between the injection station and the sample extraction station. Spitzer [8] recommends a minimum of 200 pipe diameters to achieve complete mixing in most cases. However, empirical trials have shown that 100 pipe diameters is generally sufficient.

The method of sample extraction is critical. The preferred method of sample extraction is a continuous stream to the analytical device such that a continuous trend of output from the fluorometer may be acquired for determination of a steady state condition. If it is not possible to obtain a continuous sample stream, grab samples can be taken, but they must be at a sufficient frequency such that attainment of a steady state condition may be determined.

5.6.1.3 Concentration Analysis Considerations

The elemental error sources for the calibration of the fluorometer include the preparation of calibration standards, fluorometer repeatability, and temperature effects on the fluorescing characteristic of the dye.

Typically, the calibration standard solutions are prepared by sequential mass dilution of a stock dye solution. A series of three dilutions are usually required to attain the range necessary to bound the expected concentration of dye in the pipe. The expected concentration can be calculated based on the amount of dye injected and the expected flow rate in the pipe.

5.6.1.4 Interference Considerations

Although there can be many interferences contributing to the error in the measurement of the true concentration ratio of the extracted sample. The major contributors are the salinity and sediment concentration of the water being measured. Empirical tests can provide an estimate of the range of errors associated with the species normally found in the water chemistry. However, since the actual measurement is based on calibration standards made up from the water to be measured, any changes in the concentration of these species between the time the fluorometer is calibrated and the time the measurements are conducted is a concern.

5.6.2 Example of Uncertainty Methodology

A dye dilution system was considered for use in the measurement of flow in a 20" (50.8 cm) service water line. The expected flow was 8400 gpm (31,797 lpm). The water flows from the pump discharge into a complex run of piping that supplies water to a safety-related heat exchanger. The run of piping selected for the proposed dye dilution flow measurement can be isolated from all streams entering and exiting. The overall length of piping from the pump discharge, which was identified as the dye injection point, to immediately upstream of the heat exchanger, which was identified as the sample extraction point, is 375 linear feet (114.3 m). The distance between the proposed injection point and the proposed sampling point is approximately 225 pipe diameters. The plant management, prior to using the dye dilution system requested that a pre-test uncertainty analysis be conducted to assess the uncertainty in using the dye dilution method to measure water flow.

5.6.2.1 Definition of Measurement Process

The mass flow rate at the sampling location is determined by the degree that the concentrated dye at the injection point is diluted by the flow being measured. The

mass flow rate of the injected dye is calculated by timing the injection of a measured mass of concentrated dye. The mass balance of the dye dilution system is expressed by:

$$\dot{m}_{inj}X_{inj} = \dot{m}_sX_s \quad (\text{Eq. 5-80})$$

where,

- \dot{m}_{inj} = mass flow of injected dye
- \dot{m}_s = mass flow of water at the sampling point
- X_{inj} = mass concentration of injected dye
- X_s = mass concentration of dye at the sampling point

Solving for the mass flow rate yields,

$$\dot{m}_s = \dot{m}_{inj} \frac{X_{inj}}{X_s} \quad (\text{Eq. 5-81})$$

The volumetric flow, Q_s , is calculated by,

$$Q = \frac{\dot{m}_s}{\rho_s} = \frac{\dot{m}_{inj}X_{inj}}{\rho_s X_s} \quad (\text{Eq. 5-82})$$

where,

- ρ_s = mass density of the water

The mass concentration at the sampling location (X_s) is determined by interpolation between two mass concentration calibration standards that very closely bracket the mass concentration of the dye at the sampling location. In order to facilitate this, a series of precisely prepared calibration standards must be prepared in increments above and below the target sampling concentration. Estimates of the anticipated test flow are used to adjust the injection rate of the concentrated dye so that the sampled concentration is within the range of the calibration standards. The interpolation equation for determination of the mass concentration at the sampling point is,

$$X_s = X_1 + (X_2 - X_1) * \frac{R_s^* - R_1^*}{R_2^* - R_1^*} \quad (\text{Eq. 5-83})$$

Application of Methodology

or rearranging yields,

$$X_s = \frac{R_2^* - R_s^*}{R_2^* - R_1^*} * X_1 + \frac{R_s^* - R_1^*}{R_2^* - R_1^*} * X_2 \quad (\text{Eq. 5-84})$$

where,

- X_1, X_2 = mass concentration of the two standards whose fluorometer readings bracket that of the sample
- R_1^*, R_2^* = the fluorometer reading of the two selected standards, corrected for background and temperature
- R_s^* = the fluorometer reading of the sample, corrected for background and temperature

The units in which the fluorometer response are expressed are arbitrary. Any consistent set of units may be employed. Correction for temperature is necessary because there is a documented relationship between the fluorometer response and temperature. The effect of temperature on the fluorometer response is governed by the exponential relationship,

$$R_s^* = (R - B)e^{C_1(T - T_{ref})} \quad (\text{Eq. 5-85})$$

where,

- R_s^* = temperature-corrected fluorometer reading of test sample
- R = fluorometer reading of test sample
- B = fluorometer reading of undyed service water
- T = the temperature of the test sample
- T_{ref} = an arbitrarily selected reference temperature
- C_1 = temperature correction coefficient (0.026/°C)

Dividing the mass concentration at the sampling point by the mass concentration of the injected dye yields,

$$\frac{X_s}{X_{inj}} = \left[\frac{R_2^* - R_s^*}{R_s^* - R_1^*} \right] * \frac{X_1}{X_{inj}} + \left[\frac{R_s^* - R_1^*}{R_2^* - R_1^*} \right] * \frac{X_2}{X_{inj}} \quad (\text{Eq. 5-86})$$

where,

$$R_i^* = R_i e^{C_1(T_i - T_{ref})} \quad (\text{Eq. 5-87})$$

The value of the mass dilution ratio, D_s , is calculated from the equation,

$$D_s = \frac{X_{inj}}{X_s} \quad (\text{Eq. 5-88})$$

and the service water flow rate is calculated by,

$$Q = \frac{\dot{m}_{inj}}{\rho_s} * D_s \quad (\text{Eq. 5-89})$$

For this pre-test uncertainty analysis, the following assumptions were made:

- At least 10 grams of dye will be injected for each test.
- The human response time for the stopwatch measurement is estimated to be 0.5 seconds, from previous experience.
- Once set, the injection rate of the dye will remain constant over the duration of the test.
- The change in fluorescence of the Rhodamine WT dye due to changes in temperature are reversible and accurately represented by the referenced equation.
- The temperature coefficient for Rhodamine WT dye is 0.026/°C.
- The change in background fluorescence during the test will be negligible.
- The effect of water chemistry on the fluorescence of the dye will remain constant during the test.
- The pH of the sample water is above 4.0.
- The mixing of the dye at the sampling point is complete.

Application of Methodology

- All test data will have a Gaussian-normal distribution.
- All precision error estimates are calculated using the Student's "t" value corresponding to a 95% confidence level.

5.6.2.2 Identification of Elemental Bias Uncertainty Sources

There are several elemental sources of systematic error sources. This analysis considers the following:

- Total injection rate systematic uncertainty, which is comprised of:
 - Electronic balance uncertainty
 - Stopwatch uncertainty
- Sample concentration uncertainty, which is comprised of:
 - Fluorometer repeatability uncertainty
 - Calibration standard solution uncertainty
 - Dye mixing uncertainty
 - Temperature effect uncertainty
 - Water salinity/sediment effect uncertainty
- Density measurement uncertainty

5.6.2.3 Identification of Elemental Precision Uncertainty Sources

As with the systematic or bias uncertainties, there are many elemental sources of precision or random uncertainties. This analysis considers the following:

- Sample concentration uncertainty
- Calibration standard measurement uncertainty
- Test data precision uncertainty

5.6.2.4 Evaluation of Elemental Bias Uncertainty Sources

In the evaluation of the systematic uncertainty, this section deviates from the generic methodology developed in Section 5.1 in that the sensitivity coefficients are evaluated as needed in the combination of correlated groups of uncertainties. This deviation is due to the complexity of the overall analysis.

5.6.2.4.1 Dye Injection Rate Uncertainty

The expression for the dye injection rate is given by:

$$\dot{m}_{inj} = \frac{m_{inj}}{t} \quad (\text{Eq. 5-90})$$

where,

- m_{inj} = mass of dye injected
- t = time interval of injection

The injection rate total systematic uncertainty is evaluated by the following equation:

$$B_{\dot{m}_{inj}} = \sqrt{\left[\Theta'_{\dot{m}, m_{inj}} * B_{\dot{m}_{inj}} \right]^2 + \left[\Theta'_{\dot{m}, t} * B_t \right]^2} \quad (\text{Eq. 5-91})$$

where,

- $B_{\dot{m}_{inj}}$ = systematic uncertainty of the mass measurement (0.10% of the mass injected when more than 10 grams are injected that is taken from the balance calibration procedure)
- B_t = systematic uncertainty in the stopwatch (0.5 second)

$$\Theta'_{\dot{m}, m_{inj}} = \frac{\partial \dot{m}}{\partial m_{inj}} * \frac{m_{inj}}{\dot{m}} = 1$$

$$\Theta'_{\dot{m}, t} = \frac{\partial \dot{m}}{\partial t} * \frac{t}{\dot{m}} = -1$$

The relative bias uncertainty of the injection rate measurement, based on a 10-minute test is,

$$B_{\min j} = \sqrt{(1*0.1\%)^2 + \left[-1 * \left(\frac{0.5}{600} * 100\% \right) \right]^2} = 0.13\% \quad (\text{Eq. 5-92})$$

5.6.2.4.2 Sample Concentration Bias Uncertainty

The sample concentration bias uncertainty, as described in the Section 5.6.2.2, is comprised of several factors. The first of which is the fluorometer repeatability. Since the water flow rate is evaluated from the ratio of the calibration standards to the dyed water sample, the ability of the fluorometer to determine the absolute concentration of the dye in a solution is not relevant. The error introduced by the fluorometer reading is governed solely by the repeatability of the fluorometer when measuring a solution of fixed concentration. The repeatability is evaluated by making a large solution of dyed water and evaluating the fluorometer response for a series of split samples. The 95% confidence interval for the instrument repeatability is,

$$B_{F,95\%} = \frac{t_{95\%,N-1} * S_{F,R}}{\sqrt{N}} \quad (\text{Eq. 5-93})$$

where, for this analysis,

- N = number of runs with separate split samples (8)
- S_{F,R} = standard deviation of fluorometer response (0.333)
- t_{95%,N-1} = Student's "t" value for N-1 degrees of freedom (2.36 for 7 DOF)

Therefore, the repeatability of the fluorometer is evaluated to be,

$$B_{F,95\%} = \frac{2.36 * 0.033}{\sqrt{8}} = 0.027 \quad (\text{Eq. 5-94})$$

The average value of the fluorometer response during this empirical evaluation was 5.16, so the fluorometer repeatability is 0.53% of the average response. This value will be used as the bias uncertainty of the fluorometer.

The next factor in the assessment of the sample concentration bias uncertainty is the error introduced in the preparation of the calibration standard solutions. Any bias in the preparation of these solutions will show up as a bias in the calibration of the fluorometer.

The calibration solutions are made up by creating a stock solution from the dye concentrate. The subsequent dilutions are made by use of an electronic balance to measure the amount of solution from the previous series which is added to create the next dilution in the series. The equation for calculating the concentration is as follows,

$$D_i = \frac{D_{i-1} * m_i}{M_i} \quad (\text{Eq. 5-95})$$

where,

- D_i = concentration of mixture being made
- D_{i-1} = concentration of dye solution being diluted
- m_i = mass of dye solution added
- M_i = total mass of new solution

For the purposes of calibration, the initial dye solution, D_0 , will be diluted three times in order to achieve the necessary concentrations. Since the electronic balance is the only piece of equipment used for measurement in the dilution process, the uncertainty depends solely on the accuracy of the balance, which was defined earlier in this section.

Because the same balance is used for each mass measurement in the dilution process, there is a correlated uncertainty between each mass measurement made in each series of the dilution process. Further, the uncertainties between each successive series in the dilution are also correlated. The relative bias uncertainty for each dilution in the series can be expressed as:

$$B_{D_i} = \sqrt{\left[\Theta'_{D,m} * B_{m_i} \right]^2 + \left[\Theta'_{D,M} * B_{M_i} \right]^2} \quad (\text{Eq. 5-96})$$

where,

- B_{m_i} = bias error in the mass measurement of the dye solution added (0.1% of the mass added)
- B_{M_i} = bias error in the mass measurement of the resultant dilution (0.1 % of the mass added)

$$\Theta'_{D,m} = \frac{\partial D_i}{\partial m} * \frac{m_i}{D_i} = 1$$

Application of Methodology

$$\Theta_{D_i, M} = \frac{\partial D_i}{\partial M} * \frac{M_i}{D_i} = -1$$

Therefore, the relative bias uncertainty for each dilution will be:

$$B_{D_i} = \sqrt{(1*0.1)^2 + (-1*0.1)^2} = 0.14\% \quad (\text{Eq. 5-97})$$

Since three dilutions are necessary to achieve the desired concentrations, the uncertainty in the final dilution will be:

$$B_D = 3*0.14\% = 0.42\%$$

Another factor in the estimation of the sample concentration bias is the degree of mixing of the injected dye with that of the water being measured. Incomplete mixing can lead to errors of a spatial nature. Since the referenced literature suggests that a sufficient distance for the mixing zone is 200 pipe diameters, the bias estimate for this system will be considered zero by assumption, due to the distance from the injection point to the sampling point being 225 pipe diameters.

A fourth factor in the estimation of the sample concentration bias is that of the temperature effect. The fluorescence of Rhodamine WT dye changes with temperature. Therefore, each data point (fluorometer reading) must be corrected for temperature. The bias of the temperature measurement system has been calculated to be 0.11°F (0.061°C). This will result in a bias uncertainty in the temperature correction for the fluorometer reading. The reference temperature used for the correction is arbitrary; hence, the sources for temperature bias are the temperature measurement itself and the uncertainty in the temperature correction coefficient of the dye. Past investigations into the temperature coefficient of the Rhodamine WT dye demonstrate that the manufacturer supplied constant of 0.026/°C is valid for the range of temperatures expected for the test. Therefore, only the temperature measurement bias will affect the correction. The temperature compensation equation is:

$$R^* = R * e^{0.026(T - T_{ref})} \quad (\text{Eq. 5-98})$$

where,

- R* = temperature-corrected test fluorometer reading
- R = uncorrected test fluorometer reading

T = temperature at the test point, °C

T_{ref} = reference temperature, °C

The bias uncertainty of the temperature correction, $B_{R_{TC}}$, will be,

$$B_{R_{TC}} = \Theta_{R_{TC},T} * B_T \quad (\text{Eq. 5-99})$$

where,

$$\Theta_{R_{TC},T} = \frac{\partial R_{TC}}{\partial T} = 0.026R_{TC} \quad (\text{Eq. 5-100})$$

and, B_T = temperature measurement bias = 0.061°C.

Therefore, the bias uncertainty for the temperature correction due to the temperature measurement bias is,

$$B_{R_{TC}} = (0.026R_{TC})(0.061) = 0.0016R_{TC} \quad (\text{Eq. 5-101})$$

or expressed as a percent of the corrected reading, R_{TC} , the value is,

$$\frac{B_{R_{TC}}}{R_{TC}} * 100 = 0.16\% \quad (\text{Eq. 5-102})$$

A fifth and final factor in the estimation of the sample concentration bias is the fluorometer response to the changes in concentration of salinity or sediment. Although this is a difficult parameter to quantify, a conservative estimate of 0.5% will be used in this analysis, based on past experience.

Finally, using a RSS method, all the aforementioned factors are combined to provide a bias estimate of the sample concentration measurement, as shown in the following expression,

$$B_{\text{sample}} = \sqrt{B_F^2 + B_{\text{mix}}^2 + B_{R_{TC}}^2 + B_S^2} \quad (\text{Eq. 5-103})$$

where,

Application of Methodology

- B_F = fluorometer repeatability (0.53%)
- B_{mix} = mixing bias uncertainty (0.00%)
- $B_{R_{TC}}$ = temperature measurement bias uncertainty (0.16%)
- B_S = salinity/sedimentation bias uncertainty (0.50%)

Therefore, the overall bias uncertainty for the sample concentration measurement is,

$$B_{sample} = \sqrt{(0.53)^2 + (0.00)^2 + (0.16)^2 + (0.5)^2} = 0.75\% \quad (\text{Eq. 5-104})$$

5.6.2.4.3 Density Measurement Uncertainty

The density of the test water will be measured using an electronic balance and a Class A volumetric flask. The bias of the balance is 0.1%, and the bias for a 2000 ml Class A flask is 0.5 ml or 0.25%. Hence, the density measurement bias is expressed by,

$$B_\rho = \sqrt{\left[\Theta'_{\rho,v} * B_v\right]^2 + \left[\Theta'_{\rho,m_s} * B_m\right]^2} \quad (\text{Eq. 5-105})$$

where,

- $\Theta'_{\rho,v}$ = -1
- Θ'_{ρ,m_s} = 1
- B_v = 0.025% (assuming a 2000 ml sample is used)
- B_{ms} = 0.1% of the water sample mass

Therefore, the density measurement bias uncertainty is,

$$B_s = \sqrt{(0.025)^2 + (0.10)^2} = 0.10\% \quad (\text{Eq. 5-106})$$

5.6.2.5 Evaluation of Elemental Precision Uncertainty Sources

5.6.2.5.1 Injection Rate Precision Uncertainty

There is no precision rate uncertainty for this parameter because the injection rate is evaluated as an integrated sample.

5.6.2.5.2 Sample Concentration Precision Uncertainty

The precision uncertainty associated with the sample concentration measurement will be a combination of the precision uncertainties of the following parameters:

- Fluorometer precision
- Mixing quality
- Response changes due to changes in the sediment concentration and salinity during the test run

There is no precision uncertainty for the preparation of the calibration standards because each standard is prepared as a single integrated solution. Additionally, there is also no precision uncertainty in temperature measurement used for the fluorometer temperature correction because the correction is made on a point-by-point basis with single measurements.

5.6.2.5.3 Calibration Sample Measurement Precision Uncertainty

The precision of the calibration standards is primarily a result of the fluorometer precision because the solutions will be premixed, and there will be no changes in salinity or sedimentation. Previous experiences were used as the basis for the following estimate:

- Average temperature corrected reading = 26.9
- Standard deviation of the mean = 0.047
- Population size (N) = 22

The grand average, ($S_{\text{grand avg}}$), is then,

$$S_{\text{grandavg}} = \frac{0.047}{\sqrt{22}} = 0.01 \quad (\text{Eq. 5-107})$$

Application of Methodology

and the Student's "t" value for 95% coverage and 21 degrees of freedom is 2.08.

Hence, the uncertainty due to precision in the calibration standard measurements is,

$$S_{\text{cal}} = 2.08 * 0.01 = 0.0208$$

and the relative precision uncertainty for this parameter is 0.08% of the reading.

5.6.2.5.4 Test Data Precision Uncertainty

The overall precision uncertainty of the test data is represented in the fluorometer measurements. The test data include all of the precision uncertainty associated with the test equipment and test conditions (for example, fluorometer, mixing, salinity/sedimentation). The precision uncertainty due to the equipment manifests itself as a fluctuation in the fluorometer response. It is assumed that significant variations will not be observed, and small fluctuations will appear as an increase in the test scatter and thus be included in the precision uncertainty.

It is desirable to limit the precision uncertainty due to the test data below the threshold value of 1.0%. Based on previous experience with the dye dilution method, a 5% fluctuation in the test data can be expected. This fluctuation will represent the total precision for the test from all sources (for example, background fluctuations, mixing, etc.). Further, the 5% fluctuation can be assumed to represent the 2σ value for the test data. Therefore, the precision uncertainty for this data can be approximately expressed as,

$$2\sigma = tS_x \tag{Eq. 5-108}$$

where,

t = Student's "t" value for the 95% confidence interval

S_x = precision index for the data

Therefore, the parameter precision uncertainty is,

$$tS_{\bar{x}} = \frac{tS_x}{\sqrt{n}} \approx \frac{2\sigma}{\sqrt{n}} \tag{Eq. 5-109}$$

If the 1.0% threshold is required and a 5% fluctuation in the data is expected, the minimum number of data points required can be estimated by,

$$n = \left[\frac{5.0}{1.0} \right]^2 = 25 \quad (\text{Eq. 5-110})$$

At least 25 data points will be required for each test measurement to ensure less than 1.0% precision uncertainty associated with the data scatter.

5.6.2.5.5 Density Measurement Precision Uncertainty

There is no precision in the density measurement because the density is evaluated over one integrated water sample.

5.6.2.6 Evaluate Sensitivity Coefficients

The sensitivity coefficients, which have not already been developed, are evaluated for the effect of each of the measured parameters in the flow rate determination. The basic flow equation is,

$$Q = \frac{\dot{m}_{inj}}{\rho_s} D_s \quad (\text{Eq. 5-111})$$

5.6.2.6.1 Dye Injection Rate Sensitivity Coefficient

The relative sensitivity coefficient for the dye injection rate is,

$$\Theta'_{Q, \dot{m}_{inj}} = \frac{\partial Q}{\partial \dot{m}_{inj}} * \frac{\dot{m}_{inj}}{Q} = \frac{D_s}{\rho_s} * \frac{\dot{m}_{inj}}{\left[\frac{\dot{m}_{inj}}{\rho_s} D_s \right]} = 1 \quad (\text{Eq. 5-112})$$

5.6.2.6.2 Sample Dilution Sensitivity Coefficient

The relative sensitivity coefficient for the sample dilution, D_s , is,

$$\Theta'_{Q, D_s} = \frac{\partial Q}{\partial D_s} * \frac{D_s}{Q} = \frac{\dot{m}_{inj}}{\rho_s} * \frac{D_s}{\left[\frac{\dot{m}_{inj}}{\rho_s} D_s \right]} = 1 \quad (\text{Eq. 5-113})$$

and, the equation relating the sample dilution to the corrected fluorometer readings is,

Application of Methodology

$$D_s = \frac{1}{\left[\frac{R_2^* - R_s^*}{R_2^* - R_1^*} \right] \frac{1}{D_1} + \left[\frac{R_s^* - R_1^*}{R_2^* - R_1^*} \right] \frac{1}{D_2}} \quad (\text{Eq. 5-114})$$

5.6.2.6.3 Corrected Sample Measurement Sensitivity Coefficient

The second expression necessary to relate the fluorometer reading to the measured flow is,

$$\frac{\partial D_s}{\partial R_s^*} = -D_s^2 \left[\frac{\frac{1}{D_2} - \frac{1}{D_1}}{R_2^* - R_1^*} \right] \quad (\text{Eq. 5-115})$$

and the relative sensitivity coefficient is expressed by,

$$\Theta_{D_s, R_s^*}^1 = \frac{\partial D_s}{\partial R_s^*} * \frac{R_s^*}{D_s} \quad (\text{Eq. 5-116})$$

Combining the two expressions, the sensitivity coefficient relating the measured fluorometer response to the calculated flow yields the following relationship,

$$\Theta_{Q, R_s^*}^1 = \Theta_{Q, D_s}^1 * \Theta_{D_s, R_s^*}^1 = -\frac{R_s^*}{D_s} * \left[\frac{D_2 - D_1}{R_2^* - R_1^*} \right] \quad (\text{Eq. 5-117})$$

Using typical values for a test run, a representative sensitivity coefficient is evaluated.

R_1	=	25.5	D_1	=	28.3
R_s	=	26.9	D_s	=	30.1
R_2	=	27.7	D_2	=	31.2

This provides a value for the sensitivity coefficient of 1.18.

5.6.2.6.4 Dilution Ratio Sensitivity Coefficients

The calibration standards impact the uncertainty in the interpolation of the test measured value. The following two sensitivity coefficients are needed to calculate the sample measurement uncertainty,

$$\Theta_{D_s, D_1} = \frac{\partial D_s}{\partial D_1} = \frac{R_2^* - R_s^*}{R_2^* - R_1^*} * \frac{D_s^2}{D_1^2} \quad (\text{Eq. 5-118})$$

and,

$$\Theta'_{D_s, D_2} = \frac{\partial D_s}{\partial D_2} = \frac{R_s^* - R_1^*}{R_2^* - R_1^*} * \frac{D_s^2}{D_2^2} \quad (\text{Eq. 5-119})$$

5.6.2.6.5 Standard Measurement Sensitivity Coefficients

The fluorometer readings impact the uncertainty in the interpolation of the test measured value. The following two sensitivity coefficients are needed to calculate the sample measurement uncertainty,

$$\Theta'_{D_s, R_1^*} = \frac{\partial D_s}{\partial R_1^*} = \frac{R_1^* (R_s^* - R_2^*) \left[\frac{D_s}{D_1} - \frac{D_s}{D_2} \right]}{(R_2^* - R_1^*)^2} \quad (\text{Eq. 5-120})$$

and,

$$\Theta'_{D_s, R_2^*} = \frac{\partial D_s}{\partial R_2^*} = \frac{R_2^* (R_s^* - R_1^*) \left[\frac{D_s}{D_1} - \frac{D_s}{D_2} \right]}{(R_2^* - R_1^*)^2} \quad (\text{Eq. 5-121})$$

5.6.2.7 Evaluate Uncertainty of Result

The relative bias uncertainty for the flow measurement is evaluated from the following expression,

$$B_Q = \sqrt{[\Theta_{Q, D_s} * B_{D_s}]^2 + [\Theta_{Q, m_{inj}} * B_{m_{inj}}]^2 + [\Theta_{Q, \rho_s} * B_{\rho_s}]^2} \quad (\text{Eq. 5-122})$$

Application of Methodology

where,

$$B_{D_s} = \sqrt{\left[\Theta_{D_s,D_1} * B_{D_1}\right]^2 + \left[\Theta_{D_s,D_2} * B_{D_2}\right]^2 + \left[\Theta_{D_s,R_1} * B_{R_1}\right]^2 + \left[\Theta_{D_s,R_2} * B_{R_2}\right]^2 + \left[\Theta_{D_s,R_s} * B_{R_s}\right]^2} \quad (\text{Eq. 5-123})$$

and,

- $B_{m_{inj}}$ = dye injection bias uncertainty (0.13%)
- B_{ρ} = density measurement uncertainty (0.1%)
- B_{di} = calibration solution concentration bias (0.42%)
- B_{ri} = bias in the fluorometer measurements (0.75%)

Table 5-12 summarize the sample measurement , D_s , uncertainty.

Table 5-12
Sample Measurement, D_s , Uncertainty

Parameter	Sensitivity Coefficient	Parameter Bias	Bias Uncertainty
D1	.41	0.42%	0.17%
D2	.59	0.42%	0.25%
R1	-.42	0.75%	-0.32%
R2	.79	0.75%	0.59%
Rs	1.18	0.75%	0.88%
Sample Measurement Bias Uncertainty			1.15%

Therefore, the overall pre-test bias uncertainty is,

$$B_Q = \sqrt{[1*0.13]^2 + [1*1.15]^2 + [1*0.1]^2} = 1.24\% \quad (\text{Eq. 5-124})$$

The overall flow measurement precision uncertainty is calculated in the same manner as was the bias uncertainty. However, because there is no precision uncertainty for the dye injection rate and the density, the only contributor to the precision uncertainty is the sample measurement, as shown in the following equation,

$$S_{D_s} = \sqrt{\left[\Theta_{D_s,D_1} * S_{D_1}\right]^2 + \left[\Theta_{D_s,D_2} * S_{D_2}\right]^2 + \left[\Theta_{D_s,R_1} * S_{R_1}\right]^2 + \left[\Theta_{D_s,R_2} * S_{R_2}\right]^2 + \left[\Theta_{D_s,R_s} * S_{R_s}\right]^2}$$

(Eq. 5-125)

where,

S_{di} = calibration sample reading precision (0.08%)

S_{ri} = precision in the test data (1.0%)

Table 5-13 summarizes the sample measurement , D_s , uncertainty.

Table 5-13
Overall Measurement Precision Uncertainty

Parameter	Sensitivity Coefficient	Parameter Precision	Precision Uncertainty
D1	.41	0.00%	0.00%
D2	.59	0.00%	0.00%
R1	-.42	0.08%	0.03%
R2	.79	0.08%	0.06%
Rs	1.18	1.00%	1.18%
Overall Measurement Precision Uncertainty			1.18%

Therefore, the overall precision uncertainty is 1.18%, and the overall pre-test flow uncertainty is,

$$U = \sqrt{(1.15)^2 + (1.18)^2} = 1.65\%$$

(Eq. 5-126)

5.7 Magnetic Flow Meters

Magnetic flow meters are versatile and accurate when they are properly specified, calibrated, and installed. The main parameter that needs to be quantified prior to considering a magnetic flow meter is the electrical conductivity of the fluid. A fluid that has a minimum conductivity of 5 microsiemens/cm ($\mu\text{S}/\text{cm}$) can generally be considered suitable. There are special circuits that may be specified to accommodate fluids with conductivities as low as 1 $\mu\text{S}/\text{cm}$.

5.7.1 Influence Factors

5.7.1.1 Manufacturing/Specification Considerations

Since the magnetic flow meter has no moving parts, the compatibility of the process stream with the materials of construction, the liner, and the design of the electrodes are the major considerations when specifying a magnetic flow meter. The liner and electrodes are the only parts that have contact with the process fluid, so proper selection is critical or premature failure or degradation of performance will occur. Table 9-2, "Material Selection Guide," in Spitzer [8]; Table 14-7, "Flow Rate Ranges for Selected Liner Materials," in Miller [4]; and Appendix C, "Liner Material Guidelines," in ASME-MFC-16M [22] present various process fluids and the recommended materials for the liner and body of the meter.

Another consideration is the selection of a signal conditioner (secondary element) that will adequately accept the input from the flow meter (primary element) and provide a suitable output signal to either the process control or a data acquisition system. All the references provide information on the selection and design of signal conditioners, but Spitzer [8] provides the most comprehensive treatment.

5.7.1.2 Installation Considerations

Proper installation of the magnetic flow meter is critical to its operation and performance. Orientation, upstream flow disturbances, electrical interferences, and grounding are discussed in detail by all the cited references. MFC-16M [22] and Spitzer [8] provide qualitative assessments and recommendations regarding installation effects and considerations, whereas Miller [4] in Figures 15-24 to 15-34 provides quantitative data for use in assessing the uncertainty due to installation effects such as piping configurations.

5.7.1.3 Measurement Loop Considerations

Spitzer [8] addresses several measurement loop issues pertaining to the signal conditioner (secondary element) and how its selection will impact the performance of the flow meter and affect the engineer's or technician's ability to interact with the system as a whole. The simplest signal conditioners will amplify or convert the signal from the flow meter to a variety of standard outputs. However, more sophisticated models may have a microprocessor that can aid the user in diagnostic checks of the system, configuration, or calibration, or provide digital communication. The selection of a compatible secondary element is as important to this type of flow meter as the primary element. A mismatch of primary and secondary elements will affect the overall performance of the metering system and greatly increase the uncertainty of the flow measurement.

5.7.1.4 Calibration Considerations

A magnetic flow meter is comprised of a primary element and a secondary element. The components of the system may be calibrated separately unless it is specified that they be calibrated as a complete system. The magnetic meter body can be wet calibrated against a primary standard to provide ± 0.25 to 0.50% of flow accuracy; however, if the two are calibrated as a system, then the system has the overall accuracy specified in the calibration. ASME-MFC-16M [22] briefly describes this process. Spitzer [8] provides a very detailed discussion on calibration considerations.

5.7.1.5 Instrument Integrity Considerations

One of the major factors when choosing a magnetic flow meter is the electrode and liner materials. Corrosion of the electrode will serve to offset the flow signal and the subsequent performance of the meter over time. Spitzer [8] provides a detailed discussion of this subject under the topic of “Electrode Coatings.” Both zero shifts and span shifts can occur due to the impedance caused by the coatings. Several meter designs have attempted to minimize this effect by either providing “self-cleaning” electrodes or the ability to remove and clean the electrodes on a regular basis.

5.7.1.6 Spatial Considerations

A magnetic flow meter, by design, measures the average velocity across the diameter of the electrode path. The impact of the flow profile on the subsequent flow measurement is somewhat minimized. Miller [4] provides quantitative information in Figures 15-24 to 15-33 regarding the spatial effects due to a distorted flow profile from upstream piping. The corrections due to spatial effects can be as high as $\pm 0.50\%$ of flow.

5.7.1.7 Nonhomogeneous Flow Considerations

Miller [4] provides empirical data on a flow stream containing entrained air in water. Figure 15-34 depicts the impact on the indicated flow due to various percentages of air in the water. The data suggests that the impact of more than 4% entrained air in water will cause the meter to read low.

5.7.2 Example of Uncertainty Methodology

5.7.2.1 Define the Measurement Process

The equation used by the magnetic meter to calculate the flow rate for water flowing through a circular pipe is,

$$q = C * D * \frac{\pi}{4} * \frac{E}{B} \quad (\text{Eq. 5-127})$$

where, when compatible units are employed,

q	=	volumetric flow
C	=	calibration coefficient
D	=	distance between the electrodes
E	=	flow induced signal voltage
B	=	magnetic flux density

5.7.2.2 Identification of Elemental Bias Uncertainty Sources

There are five elemental sources of bias error identified that will impact the uncertainty of the flow measured by the magnetic meter:

- Calibration error (B_{cal})
- Installation effect error (B_{inst})
- Degradation of the liner material (B_{liner})
- Corrosion/coating of the electrodes (B_{elec})
- Signal conditioning in the secondary element (B_{sec})

The information regarding the initial calibration uncertainty is obtained from either a manufacturer's certificate or an independent flow laboratory. The uncertainty from the installation effects can be obtained from the graphs found in Miller [4]. An estimate for the uncertainty due to liner degradation and electrode effects can be obtained from

Spitzer [8]. The uncertainty due to the signal conditioning can be evaluated from the manufacturer's specification.

Upon evaluation of the aforementioned sources of uncertainty, they should be applied in a similar fashion as previously demonstrated in several examples to obtain the uncertainty in the measured flow.

5.7.2.3 Identification of Elemental Precision Error Sources

The precision errors associated with the measurement of flow with a magnetic flow meter are strictly the random errors associated with the scatter of data.

5.8 Turbine Meters

The measurement of flow by turbine meters is affected by various factors that are addressed in the following discussion. The bulk of this information is extracted from the reference book by Miller, *Flow Measurement Engineering Handbook* [4]. The topics regarding uncertainty in the measurement of flow include integrity of the primary elements, piping configurations, pulsations, and degradation of the elements with respect to time. Calibration considerations due to thermal expansion and changes in fluid viscosity are discussed.

5.8.1 Influence Factors

5.8.1.1 Manufacturing Considerations

The manufacturing considerations addressed by Miller [4] include small and large burrs on the turbine blades and differences in bearing clearances. EG&G Flow Technology's *FT Series Turbine Flowmeter Installation, Operation, and Maintenance Manual* [21] discusses which type of bearings and secondary elements are indicated for a particular type of application, but does not provide any quantitative data regarding the long term impact on the accuracy of the devices.

5.8.1.2 Installation Considerations

Miller [4] in figures 15-38 to 15-42 addresses various types of installation effects including single and double elbows, tube bundles, and orifice plates. These figures do not provide a direct correlation to the effects in terms of flow, but show the impact on the meter K factor. The change in K factor can then be used to calculate a change in flow.

5.8.1.3 Measurement Loop Considerations

There are several secondary devices, generally referred to as "flow computers," that are used to provide a useable output from the meter. Functions of the secondary element include signal conditioning, output linearization, and amplification. The outputs from the secondary element generally include frequency, pulsed dc voltage, and analog signals that are proportional to the flow through the meter.

5.8.1.4 Calibration Considerations

In the EG&G *Flow Technology Manual* [21] and Spitzer's *Flow Measurement* [8], there are discussions of the calibration considerations. The main influence factor discussed is the

impact of multiple viscosity fluids on the calibration constants. Spitzer provides an example of a multiple viscosity calibration and a detailed discussion of how the data should be interpreted and applied to the output of a turbine flow meter. Calibrations should be performed over the entire anticipated service range so that the linearity characteristics can be evaluated.

5.8.1.5 Instrument Integrity Considerations

Miller in Figure 15-44 (a) & (b) provides the changes in K factor over time. This term can be factored into an uncertainty analysis if there is no provision for a calibration. Also, the effects of bearing replacement are addressed in these figures. Bearing replacement is generally the only maintenance necessary over an extended period of time on turbine meters, and the time between replacements can be optimized by proper application with respect to the service fluid.

5.8.1.6 Spatial Considerations

A turbine meter uses the entire flow area to determine the flow of the fluid. There is no spatial consideration that would contribute to the overall uncertainty.

5.8.1.7 Nonhomogeneous Flow Considerations

None of the references surveyed recommend a turbine meter for use where entrained air may be a condition of the service. Miller indicates that with as little as 15% entrained air, there may be an overregistration of as much as 5% in the measured flow.

5.8.2 Example of Uncertainty Methodology

The following example is used to demonstrate a calculation of the uncertainty associated with the measurement of water flow using a turbine meter. Water at 60°F (15.6°C) and 125 psig (862 kPa) was measured using a 4" (10 cm) stainless steel turbine meter. The turbine meter, magnetic pick-off, and signal conditioner were calibrated by the manufacturer prior to installation. The manufacturer provided a calibration certificate that stated that the calibrated K factor is 98 pulses/gallon and that the accuracy is $\pm 0.5\%$ of reading within a 10:1 turndown range of 1250 to 125 gpm (4732 to 473 lpm). The turbine meter's output is sent to a secondary element that amplifies the input signal and has an accuracy of 0.1% of reading. During an inspection after two months of service, it was observed that there were small burrs on the meter blades and that they had a rough finish. There was one 90° elbow 15 pipe diameters upstream of the turbine meter and no disturbances within 200 feet (61 m) downstream. A totalizer was used to count the number of pulses generated by the meter over a 15-second interval. One hundred and twenty 15-second intervals were recorded with the average

number of counts being 7467, which resulted in a frequency of 497.8 Hz. This frequency corresponds to a flow rate of 304.8 gpm (1154 lpm). The standard deviation of the mean frequency was evaluated and found to be 0.97 Hz.

5.8.2.1 Define the Measurement Process

The equation used to calculate the flow rate from turbine meters, in its simplest form is,

$$q = \frac{\lambda * C}{K} \quad \text{(Eq. 5-128)}$$

where,

- q = volumetric flow
- λ = frequency of output signal
- K = meter K-factor
- C = conversion constant

5.8.2.2 Identification of Elemental Bias Uncertainty Sources

The following sources of error will be considered in this analysis:

- Calibration accuracy, B_{cal}
- Condition of the blades, B_{burr} & B_{blade}
- Installation effects, B_{inst}
- Signal conditioning in the secondary element, B_{sec}

The information regarding the installation effects and blade conditions are discussed in Miller [4], while the basis for the initial calibrated accuracy and the signal conditioning errors are taken from the manufacturer's specifications and calibration certificates.

5.8.2.3 Identification of Elemental Precision Uncertainty Sources

The precision errors associated with the flow measured from the turbine meter are strictly the random errors associated with the scatter of data.

5.8.2.4 Evaluation of Elemental Bias Uncertainty Sources

5.8.2.4.1 Calibration Accuracy Uncertainty

Using the manufacturer's accuracy specification of $\pm 0.5\%$ of reading for the turbine meter, the bias in flow is calculated as,

$$B_{\text{cal}} = 304.8 * 0.005 = 1.52 \text{ gpm} \quad (\text{Eq. 5-129})$$

5.8.2.4.2 Blade Condition Uncertainty

There are two components to the blade condition uncertainty, namely, burrs and surface roughness.

The effect of small burrs on turbine meter performance is quantified by Miller [4] in Figure 15-36a. The method used is to calculate a percent change in the base K-factor and apply it to the K-factor for the meter under analysis. At 305 gpm, (1155 lpm) the percent change in the base referenced K-factor to the reference K-factor with small burrs is expressed as,

$$B_{\text{burr}} = \frac{4.46 - 4.385}{4.385} * 100 = 1.7\% \quad (\text{Eq. 5-130})$$

This error, B_{burr} , is expressed in terms of percent of calibrated K-factor (98 pulses/gal) is 1.68 pulses/gal.

The second consideration for the blade condition error is the surface finish of the blades. It was noted that the surface finish appeared to be rough. Using the same relative technique as above, the percent change in K-factor due to surface roughness is evaluated using Figure 15-37a,

$$B_{\text{blade}} = \frac{4.38 - 4.345}{4.38} * 100 = 0.81\% \quad (\text{Eq. 5-131})$$

This translates into $B_{\text{blade}} = 0.8$ pulses/gal. Sensitivity coefficients are developed in Section 5.8.2.6 that will allow propagation of these bias values into the flow.

Application of Methodology

5.8.2.4.3 Installation Effect Uncertainty

The quantitative impact of a 90° elbow located 15 pipe diameters upstream can be found in Figure 15-40a. Based on information found in this figure, the K-factor change is 0.25%, hence, $B_{inst} = 0.25$ pulses/gal. Again, a sensitivity coefficient is developed in Section 5.8.2.6 that will allow propagation of this bias into the flow.

5.8.2.4.4 Signal Conditioning Uncertainty

The manufacturer’s specification indicated that the error associated with the signal conditioning would be ±0.1% of the measured frequency. Therefore, the error would be,

$$B_{sig} = 497.8 * 0.001 = \pm 0.5 \text{ Hz} \quad (\text{Eq. 5-132})$$

A sensitivity coefficient is developed in Section 5.8.2.6 that will propagate this bias value into the flow.

5.8.2.5 Evaluation of Elemental Precision Uncertainty Sources

The precision or random uncertainty arises from the acquisition of repeated measurements using the same primary and secondary measurement devices. The index for the estimation of the random uncertainty is the standard deviation of the sample, which was given in the example to be 0.97 Hz. The standard deviation of the sample mean, or the scatter from the average of the data population, is expressed by,

$$S_{\bar{x}} = \frac{S_x}{\sqrt{N}} = \frac{0.97}{\sqrt{120}} = 0.09 \text{ Hz} \quad (\text{Eq. 5-133})$$

A sensitivity coefficient is developed in the following section that will allow propagation of this value into a final result of flow.

5.8.2.6 Evaluate Sensitivity Coefficients

There are two sensitivity coefficients that need to be expressed such that the bias and precision values not yet expressed in terms of the flow can be propagated.

5.8.2.6.1 Sensitivity Coefficient for the K-Factor

The expression for the flow determination is,

$$q = \frac{\lambda * C}{K} \quad (\text{Eq. 5-134})$$

The sensitivity coefficient can be expressed as,

$$\Theta_{q,K} = \frac{\partial q}{\partial K} = -\frac{\lambda * C}{K^2} \quad (\text{Eq. 5-135})$$

Substituting known values into this expression yields,

$$\Theta_{q,K} = -\frac{60 * 497.8}{98^2} = 3.11 \text{ gpm} / \text{pulse} / \text{gal} \quad (\text{Eq. 5-136})$$

5.8.2.6.2 Sensitivity Coefficient for the Frequency

In order to derive an expression for this sensitivity coefficient, eq. 5-134 is differentiated with respect to the frequency

$$\Theta_{q,\lambda} = \frac{\partial q}{\partial \lambda} = \frac{C}{K} \quad (\text{Eq. 5-137})$$

Substituting known values into this expression yields,

$$\Theta_{q,\lambda} = \frac{60}{98} = 0.61 \text{ gpm} / \text{Hz} \quad (\text{Eq. 5-138})$$

5.8.2.7 Evaluate Uncertainty of Result

In order to evaluate the overall uncertainty of the flow, it is necessary to propagate those bias values not yet expressed as flow.

The result of the burrs on the blade was to increase the K-factor by the amount estimated, $B_{\text{burr}} = 1.68$ pulses/gal. Combining this value with the sensitivity coefficient yields an uncertainty due to the burrs of,

$$B_{\text{burr}} = B_{\text{burr},K} * \Theta_{q,K} = 1.68 * -3.11 = -5.22 \text{ gpm} \quad (\text{Eq. 5-139})$$

Application of Methodology

The result of the roughness of the blade was also to increase the K-factor by the amount estimated, $B_{blade} = 0.8$ pulses/gal. Combining this value with the sensitivity coefficient yields an uncertainty component of,

$$B_{blade} = B_{blade,K} * \Theta_{q,K} = 0.8 * -3.11 = -2.5 \text{ gpm} \quad (\text{Eq. 5-140})$$

The secondary element signal conditioner uncertainty must also be propagated from the value estimated, $B_{sig} = \pm 0.5$ Hz, to an uncertainty in the flow,

$$B_{sig} = B_{sig,\lambda} * \Theta_{q,\lambda} = \pm 0.5 * 0.61 = 0.31 \text{ gpm} \quad (\text{Eq. 5-141})$$

Finally, the precision uncertainty estimate must be propagated into the flow,

$$S_{\bar{X}} = S_{\bar{X},\lambda} * \Theta_{q,\lambda} = 0.09 * 0.61 = 0.06 \text{ gpm} \quad (\text{Eq. 5-142})$$

In this example, the bias that was estimated is of a nonsymmetric nature. In accordance with ASME PTC 19.1 [29], a separate RSS should be used to obtain the upper and lower bias limits, such that,

$$B^+ = \sqrt{(B_{cal})^2 + (B_{inst})^2 + (B_{sec})^2} = \sqrt{(1.52)^2 + (0.78)^2 + (0.31)^2} = 1.7 \text{ gpm} \quad (\text{Eq. 5-143})$$

and,

$$B^- = \sqrt{(B_{cal})^2 + (B_{burr})^2 + (B_{blade})^2 + (B_{sec})^2} \quad (\text{Eq. 5-144})$$

$$B^- = \sqrt{(1.52)^2 + (-5.22)^2 + (-2.5)^2 + (0.31)^2} = 5.99 \text{ gpm} \quad (\text{Eq. 5-145})$$

The overall uncertainty of the result can now be expressed for a nonsymmetrical interval as,

$$U_q^+ = \sqrt{(B^+)^2 + (t_{95,v} * S_{\bar{X}})^2} = \sqrt{(1.7)^2 + (2 * 0.06)^2} = 1.7 \text{ gpm} \quad (\text{Eq. 5-146})$$

and

$$U_q^- = \sqrt{(B^-)^2 + (t_{95,v} * S_{\bar{X}})^2} = \sqrt{(5.99)^2 + (2 * 0.06)^2} = 5.99 \text{ gpm} \quad (\text{Eq. 5-147})$$

5.9 Vortex Meters

The vortex meter is similar in nature to the turbine meter in that the primary output is in the form of a frequency. The output frequency, which is generated by the vortices formed behind the bluff body, varies linearly with the velocity of the fluid being measured over a specific Reynolds number range. The governing equation for the vortex meter is similar to the turbine meter in that the characteristic parameter is represented by a K-factor that relates the fluid flow to the frequency output. The K-factor is a function of several components inherent to the vortex meter, such as the bluff body width and Strouhal number. The major difference between the vortex meter and the turbine meter is that the vortex meter has no moving parts, which lends to lower maintenance costs over time.

All of the references selected for vortex meters discuss some of the influence variable topics associated with the measurement of flow, but Spitzer, *Industrial Flow Measurement* [7], has a more detailed discussion of the influence variables. Miller [4] provides Figures 15-53 to 15-64 that contain quantitative values of the impact of several influence variables that impact the performance of the vortex meter.

5.9.1 Influence Factors

5.9.1.1 Manufacturing/Specification

A vortex meter, like a magnetic meter, has no moving parts, so the major consideration in the selection of a vortex meter is the compatibility of the materials of construction with the process fluid that is being measured. The primary element must be considered since this will impact the overall performance based on the value of the Reynolds number. Spitzer provides several examples demonstrating meter sizing and how it affects the performance of the meter.

5.9.1.2 Installation Considerations

Spitzer [7] and ASME-MFC-6M [32] have qualitative discussions of the installation effects specific to the vortex meter, including piping configuration, meter orientation, vibration, and electrical installation precautions. They address the impact of the Reynolds number and flow profile effects upon the flowmeter. Conversely, Miller's [4] focus is to quantify many of these installation effects on the performance of the vortex meter.

5.9.1.3 Measurement Loop Considerations

The vortex sensing element of the primary element can be one of several types of devices primarily dependent on the manufacturer. Some types are listed in Spitzer [7] and include oscillating disc, pressure, temperature, torque, and ultrasonic. Spitzer provides a description and some of the key maintenance advantages and/or shortcomings inherent to each. The type of primary sensing element must be compatible with the signal conditioning (secondary element) in order to optimize the performance of the meter. Spitzer recommends that the manufacturer be consulted as to the options available.

5.9.1.4 Calibration Considerations

Spitzer [7] and ASME-MFC-6M [32] address the calibration considerations for the vortex flow meter. The methods described are similar to all linear flow meters. Both references recommend a wet calibration with a primary standard and that the primary and secondary flow meter elements be calibrated together. The references discuss thermal expansion effects, low Reynolds number calibrations, and K-factor evaluation by dimensional measurements.

5.9.1.5 Instrument Integrity Considerations

Since the vortex meter has no moving parts, the instrument integrity is very good over time. The major concerns for this type of meter are the wear of the bluff body and secondary element drift. Spitzer [7] states, “The effect of normal shedder wear on the vortex shedding flowmeter performance is usually not a problem.” The secondary elements, which are prone to drift over time, should be placed on a regular calibration schedule.

5.9.1.6 Spatial Considerations

The vortex shedding bluff body comprises a large percentage of the available cross-sectional flow area to generate the vortices. There is a relatively small spatial variation that would contribute to the overall flow uncertainty.

5.9.2 Application of Methodology

5.9.2.1 Define the Measurement Process

The equation used to calculate the flow for a vortex meter is:

$$q = A * \frac{\lambda * d}{St} \quad (\text{Eq. 5-148})$$

where,

q	=	volumetric flow
A	=	normal, cross-sectional flow area
λ	=	frequency of vortex formation
d	=	width of the bluff body
St	=	Strouhal number

5.9.2.2 Identification of Elemental Bias Uncertainty Sources

Listed below are the sources of error identified that will impact the uncertainty of the measured flow from a vortex meter:

- The calibrated accuracy, B_{cal} , which includes the factors of linearity, base temperature, Strouhal number, and Reynolds number
- Installation effects, B_{inst} , which accounts for the uncertainty of the existing piping configuration, flow straighteners, and pulsations
- Signal conditioning in the secondary element loop

The information regarding the initial calibration uncertainty and the signal conditioning uncertainty can be found in manufacturer's specifications or calibration efforts from a qualified flow laboratory. Information regarding the installation effects can be found in the quantitative information in the figures provided by Miller [4]. The evaluation of these sources is carried out in a similar manner to the methods developed for the turbine meter to achieve an overall uncertainty in the flow measured by a vortex shedding flow meter.

5.9.2.3 Identification of Elemental Precision Uncertainty Sources

The precision errors associated with the measurement of flow from a vortex shedding flow meter are limited to the random errors associated with the scatter of data.

5.10 Coriolis Meters

The Coriolis mass flow meter operates on the principle that the flow of a fluid through a vibrating tube will produce a Coriolis force. The meters have a very high accuracy but are cost intensive. Their insensitivity to installation effects allows them to be used in areas that may not facilitate any other type of meter.

5.10.1 Influence Factors

5.10.1.1 Manufacturing/Specification Considerations

The construction of Coriolis flow meters varies widely, but the basis of their design is similar. The primary measurement system should be made of corrosion-resistant metal tubing; for water applications, this is typically 316L stainless steel. The end of the flow tube is rigidly attached to a flow splitter. The flow splitter forms a transition between the process piping and the primary measuring tubes, which are vibrated at a specific frequency. The junction between the process connection and the vibrating element is an area of high cyclic stress. Spitzer [8] provides several examples of designs for the vibrating flow tube assemblies, such as cantilevered, projected loop, straight tube, and oscillating U-tube.

5.10.1.2 Installation Considerations

The consensus of the references is that the Coriolis mass flow meter is extremely insensitive to upstream and downstream flow disturbances. Miller [4] points out that they are sensitive to orientation and external vibratory influences. The meter, when possible, should be installed vertically to self-purge any gas or vapor in the system. Spitzer [8] indicates that most manufacturers state that there are no specific upstream or downstream straight piping requirements, but he also points out that one manufacturer requires 30 diameters of straight pipe both upstream and downstream. A downstream shutoff valve is recommended to provide the ability to obtain a zero flow condition for making zero adjustments at rated pressure. Spitzer describes several considerations for supporting the meter and the nearby piping to ensure that the weight of the nearby piping and valving is not concentrated into the flow element. Additionally, inadequate support for the meter and piping can affect the accuracy of the meter if the frequency of the vibration in the piping is within 20% of the operational frequency of the meter.

These types of meters have high permanent pressure losses associated with their design and may lead to cavitation.

5.10.1.3 Measurement Loop Considerations

The rangeability of the Coriolis meter is very good with a typical turndown of 25:1 with no appreciable loss of accuracy. Spitzer [8] indicates that turndowns of 100:1 are achievable with good accuracy. There is a “zero shift” effect that is due to small offsets between the sensor and the electronics. This can add uncertainty to the lower end of the dynamic flow range. Miller [4] provides Table 15-5 that presents the impact of the zero on the calibration curve for a Coriolis mass flowmeter. The design of the electronics that detect the Coriolis force is critical because the Δt signal, which is the basis of the mass flow measurement, needs to be resolved to the nanosecond. Sources of electrical interference must be identified and isolated to maintain the signal integrity. Spitzer [8] recommends that a calibration of the electronics be regularly conducted on at least a semi-annual basis.

5.10.1.4 Calibration Considerations

Coriolis mass flow meters are designed to be unaffected by fluid parameters and calibration of the meter on one type of fluid is directly transferable to another type of fluid. Miller [4] provides Tables 15-6 and 15-7 that show the effect of pressure and temperature on the zero of the flowmeter. ASME-MFC-11M-1989 (Reaffirmed 1994) [23] indicated that the flow meter manufacturer should supply the meter calibration in suitable units and the expected accuracy under the stated reference conditions. Further, MFC-11M-1989 indicates the acceptable standard methods for calibration. Spitzer [8] provides recommendations on various calibration scenarios that vary depending on the desired accuracy.

5.10.1.5 Instrument Integrity Considerations

The meter should be inspected for leaks around the welded joint that attaches the primary measuring tubes to the process flow splitter because this is an area of high stress.

5.10.1.6 Spatial Considerations

There is no impact of spatial bias on the mass flow meter.

5.10.1.7 Nonhomogeneous Flow Considerations

The Coriolis flow meter can accurately measure multicomponent flows such as slurries. Miller [4] provides Tables 15-2 and 15-3 that present the effects of entrained voids and bubbles in the measured flow stream.

5.11 Variable Area Flow Meters

Variable area flow meters, also called rotameters, are an economical means of measuring flow if the desired accuracy is not greater than $\pm 2.0\%$ and the maximum flow is not greater than 200 gpm. One of the main advantages of this type of flow meter is that it has a local readout that is directly related to the flow passing through the meter. These flow meters operate with a constant differential pressure produced by exposing the flow to a variation in the area by using a float or piston that slides vertically in a tapered tube. In ASME *Fluid Meters, Their Theory and Application* [3], there is a detailed discussion that develops engineering equations regarding the method of flow measurement in a variable area flow meter.

5.11.1 Influence Factors

5.11.1.1 Manufacturing/Specification Considerations

Manufacturing considerations for variable area flow meters include process fluid pressure, temperature, flow, and chemical composition. The process fluid will dictate the materials for the flow meter tube and float to provide safe and accurate operation. There are three basic types of tube materials that consist of plastic, glass, and metal. A high-pressure application would require a metal tube design due to the lack of strength inherent in plastic and glass. A metal tube design would also require a means of coupling the internal float to an external readout device because the float cannot be observed, as in the case of plastic or glass tubes. As mentioned in all of the references, there are special designs for the floats to compensate for different fluid properties.

5.11.1.2 Installation Considerations

Variable area flow meters must be installed in a vertical orientation with the flow inlet at the bottom for the meter to function properly. Unlike other flowmeters, a variable area flow meter does not require minimum upstream and downstream straight lengths of piping or flow conditioners in order to achieve the stated accuracy. A bypass flow section should be installed so that maintenance can be performed on the flow meter without an interruption in the process stream.

5.11.1.3 Measurement Loop Considerations

Since the vast majority of variable area flowmeters only have local indication of flow, there are no measurement loop considerations.

5.11.1.4 Calibration Considerations

A variable area flow meter usually has accuracy specifications in terms of a percent of full scale, which should be considered when choosing a particular type of meter. Choosing a meter with a range that is too large could cause inaccurate readings at low to intermediate flow conditions. A variable area flow meter may either be used with standard manufacturer's specifications, or it may be calibrated against an appropriate primary or secondary standard. A noncalibrated flow meter will generally have accuracies of 2 to 5% of full scale, whereas a calibrated version may be accurate to 0.5% of full scale. In ASME *Fluid Meters, Their Theory and Application* [3] and Miller [4], there are discussions pertaining to correction equations if the fluid being measured does not have the same properties as the flow meter was designed or calibrated to measure.

5.11.1.5 Instrument Integrity Considerations

A variable area flow meter does not require any routine maintenance because there are no parts to wear out, but it should be cleaned from time to time due to dirt that can build up in the tube or on the float. If the tube or float needs to be replaced, it can generally be replaced without affecting the accuracy of the meter.

5.11.1.6 Spatial Considerations

The variable area flow meter, like an orifice, integrates the velocity across the entire cross-sectional flow area; hence, there is no spatial bias consideration that would contribute to the overall uncertainty.

5.11.2 Example of Uncertainty Methodology

5.11.2.1 Define the Measurement Process

The equation used to calculate the flow from a variable area flowmeter is:

$$q = C_d * A \sqrt{\frac{2g_c \rho W_f (\rho_f - \rho)}{\rho_f}} \quad (\text{Eq. 5-149})$$

where, when compatible units are used,

$$\begin{aligned} q &= \text{volumetric flow} \\ C_d &= \text{discharge coefficient} \end{aligned}$$

Application of Methodology

A	=	normal, cross-sectional area of flow
g_c	=	gravitational constant
ρ	=	density of fluid
W_f	=	weight of float
ρ_f	=	density of float material

5.11.2.2 Identification of Elemental Bias Uncertainty Sources

There are two sources of error described below that will impact the uncertainty of the flow measurement using a variable area flow meter:

- Calibration accuracy (B_{cal})
- Fluid properties (B_{prop})

The information regarding the initial calibration accuracy can be found from manufacturer specifications. The information pertaining to corrections for fluid properties can be found in ASME *Fluid Meters* [3] and Tables 14-11 and 14-12 from Miller [4]. The evaluation of these sources of error can be applied in a similar fashion as that for an orifice meter to achieve an overall uncertainty in the measurement of flow using a variable area flow meter.

5.11.2.3 Identification of Elemental Precision Uncertainty Sources

The precision errors associated with the measurement of flow from a variable area flow meter are strictly the random errors associated with the scatter of data.

5.12 References

1. American National Standards Institute/American Society of Mechanical Engineers. MFC-3M-1989 (Reaffirmed 1995). *Measurement of Fluid Flow in Pipe Using Orifice, Nozzle, and Venturi*. ASME, 1990.
2. International Organization on Standardization. ISO 5167-1980. *Measurement of Fluid Flow by Means of Orifice Plates, Nozzles, and Venturi Tubes Inserted in Circular Cross-Section Conduits Running Full*. ISO, 1981.
3. American Society of Mechanical Engineers. *Part II of ASME Fluid Meters, Their Theory and Application*, Sixth Edition. ASME, 1971.

4. R. Miller. *Flow Measurement Engineering Handbook*, Third Edition. McGraw Hill, 1996.
5. American Society of Mechanical Engineers. *PTC Report - 1985, Guidance for Evaluation of Measurement Uncertainty in Performance Tests of Steam Turbines*. ASME, 1986.
6. American National Standards Institute/American Society of Mechanical Engineers. MFC-2M-1983 (Reaffirmed 1988). *Measurement Uncertainty for Fluid Flow in Closed Conduits*. ASME, 1984.
7. D. Spitzer. *Industrial Flow Measurement*. ISA, 1990.
8. D. Spitzer. *Flow Measurement*. ISA, 1991.
9. Dieterich Standard Corporation. *Annubar Handbook*. Dieterich Standard Corporation, 1993.
10. American National Standards Institute/American Society of Mechanical Engineers. MFC-5M-1985 (Reaffirmed 1994). *Measurement of Liquid Flow in Closed Conduits Using Transit-Time Ultrasonic Flow Meters*. ASME, 1986.
11. L. Lynnworth. *Ultrasonic Measurements for Process Control, Theory, Techniques, Applications*. Academic Press, 1989.
12. *Instrumentation Handbook for Integrated Power Plant Water Management*. EPRI, Palo Alto, CA: 1988. Report CS-5873.
13. Cooling Tower Institute. "Standard for Water Flow Measurement," *CTI Bulletin*, STD-146 (95), 1995.
14. M. S. Beck and A. Plaskowski. *Cross-Correlation Flow Meters*. Adam Hilger, Bristol, England, 1987.
15. Y. Gurevich, A.M. Lopez, R. Flemons, D. Z. Zobin, "Theory and Application of Non-invasive Ultrasonic Cross-Correlation Flowmeter," presented at the 9th International Conference on Flow Measurement, Lund, Sweden (June 1998).
16. W. H. Morgan, *et al*, "Validation of the Use of Dye Dilution Method for Flow Measurement in Large Open and Closed Channel Flows," presented at the NBS Flow Measurement Symposium, Gaithersburg, MD (1977).
17. J. B. Nystrom and G. E. Hecker, "Uncertainty Analysis of Field Turbine Performance Measurements," *Proceedings of an International Conference on Hydropower*, American Society of Civil Engineers, 1985.

Application of Methodology

18. K. W. Hennon and G. R. McNutt. *Pre-Test Uncertainty Analysis for Dye Dilution Flow Measurement*. Power Generation Technologies Technical Paper. TIN 97-1267.
19. American National Standards Institute/Instrument Society America. RP31.1-1977. *Specification, Installation, and Calibration of Turbine Flowmeters*. ISA, 1977.
20. K. Hennon and D. Wheeler, "Uncertainty Analysis of Cooling Tower Performance," Power Generation Technologies Technical Report presented at the Cooling Tower Institute Winter Meeting, 1996.
21. EG&G Flow Technology. *FT Series Turbine Flowmeter Installation, Operation, and Maintenance Manual*. TM-86675, Rev. H-1996.
22. American National Standards Institute/American Society of Mechanical Engineers. MFC-16M-1995. *Measurement of Fluid Flow in Closed Conduits by Means of Electromagnetic Flowmeters*. ASME, 1995.
23. American National Standards Institute/American Society of Mechanical Engineers. MFC-11M-1989 (Reaffirmed 1994). *Measurement of Fluid Flow by Means of Coriolis Mass Flowmeters*. ASME, 1995.
24. Instrument Society of America. 11ISA-RP16.5-1961. *Installation, Operation, and Maintenance Instructions for Glass Tube Variable Area Meters (Rotameters)*. ISA, 1961.
25. American National Standards Institute/American Society of Mechanical Engineers. PTC 6 -1976 (Reaffirmed 1982). *Steam Turbines*. ASME, 1982.
26. J. A. Rabensteine and C. E. Arnsdorf. *Flow Determination by Acoustic Transit Time*. Power Generation Technologies Calculation, 1997.
27. International Organization on Standardization. ISO Standard 3977-1977. *Measurement of Fluid Flow in Closed Conduits - Velocity Method Using Pitot Static Tubes*. ISO, 1997.
28. International Organization on Standardization. ISO Technical Report 12765:1997 (E). *Measurement of Fluid Flow in Closed Conduits - Method Using Transit Time Ultrasonic Flowmeters*. ISO, 1997.
29. Advanced Measurement and Analysis Group, Inc. *CROSSFLOW[®] User Guide for Ultrasonic Flow Measurement*. 1998.
30. International Organization Standardization. ISO-9104:1991. *Measurement of Fluid Flow in Closed Conduits - Methods of Evaluating the Performance of Electromagnetic Flowmeters for Liquids*. ISO, 1991.

31. Southwest Research Institute Report. *Baseline and Installation Effects Tests of the V-Cone Meter*. SRI, 1984.
32. American National Standards Institute/American Society of Mechanical Engineers. MFC-6M-1987. *Measurement of Fluid Flow in Pipes Using Vortex Flow Meters*. ASME, 1987.
33. American National Standards Institute/American Society of Mechanical Engineers. PTC 19.1. *Measurement Uncertainty*. ASME, 1985.
34. American National Standards Institute/American Society of Mechanical Engineers. MFC-10M-1994. *Methods for Establishing Installation Effects on Flowmeters*. ASME, 1994.
35. American National Standards Institute/American Society of Mechanical Engineers. MFC-9M-1988. *Measurement of Liquid Flow in Closed Conduits by Weighing Method*. ASME, 1989.

6

APPENDIX A: NOMENCLATURE

6.1 Statistical Nomenclature

β' = true bias error, i.e., the fixed systematic, or constant component of the total error.

δ_k = total error, that is, the difference between the observed measurement and the true value.

ϵ_k = the random component of total error k , sometimes called repeatability error or sampling error.

μ = the true, unknown average.

ν = degrees of freedom.

σ = the true standard deviation of repeated values of the measurement; also, the standard deviation of the error. This variation is due to random error.

σ^2 = the variance, that is, the square of the standard deviation.

B = the estimate of the upper limit of the bias error β' .

B_{ij} = an estimate of the upper limit of an elemental bias error. The i subscript is the number of error sources within the process. If i is more than a single digit, a comma is used between i and j . The j subscript indicates the process, that is:

$$B = \sqrt{\sum_i \sum_j B_{i,j}^2} \quad (\text{Eq. 6-1})$$

N = the number of samples or the sample size.

S = an estimate of the standard deviation obtained by taking the square root of S^2 . It is the precision index.

Appendix A: Nomenclature

S_{ij} = the estimate of the precision index from one elemental source. The subscripts are the same as defined under B_{ij} above.

$$S = \sqrt{\sum_i \sum_j S_{i,j}^2} \quad (\text{Eq. 6-2})$$

S^2 = an unbiased estimate of the variance σ^2 .

t_{95} = “Student's t” statistical parameter at the 95% confidence level. The degree of freedom of the sample estimate of the standard deviation is needed to obtain the t value.

U = an estimate of the error band, centered about the measurement within which the true value should include the true value with high probability.

X_i = an individual measurement.

\bar{X} = sample average of measurement, where,

$$\bar{X} = \frac{\sum_{i=1}^N X_i}{N}$$

6.2 Engineering Nomenclature

β = ratio of diameters (d/D) (dimensionless)

Δp = differential pressure (PSI or ft of fluid, kPa)

ρ = mass density (lbm/ft³)

A = area of an orifice, flow nozzle, or Venturi throat (ft² or m²)

C_d = coefficient of discharge (dimensionless)

d = diameter of orifice, flow nozzle throat, or Venturi throat (ft or m)

D = diameter of pipe or conduit (ft or m)

g = acceleration due to local gravity (ft/sec² or m/sec²)

g_c = proportionality constant in the force-mass-acceleration equation (lbm*ft/lbf*s²);

h	=	effective differential pressure (ft of fluid)
h_w	=	effective differential pressure (in. of water at 68°F)
q_m	=	mass rate of flow (lbm/sec)
q_v	=	volumetric rate of flow (ft ³ /sec or m ³ /sec)
p	=	absolute pressure (PSIA)
R_D	=	Reynolds number based on D (dimensionless)
R_d	=	Reynolds number based on d (dimensionless)
St	=	Strouhal number (dimensionless)
T	=	absolute temperature (°R)
V	=	fluid velocity (ft/sec or m/sec)
v	=	specific volume (ft ³ /lbm)

7

APPENDIX B: GLOSSARY

This appendix is provided as a reference for the definitions of terms used in this guideline.

7.1 General Terms

7.1.1 *Cavitation*

The violent collapse of vapor bubbles formed after flashing when the line pressure rises above the vapor pressure of the liquid.

7.1.2 *Flashing*

The formation of vapor bubbles in a liquid when the line pressure falls to or below the vapor pressure of the liquid.

7.1.3 *Flow Conditioner*

A general term used to describe any one of a variety of devices intended to reduce swirl and/or regulate the velocity profile.

7.1.4 *Flow Rate*

The quantity of fluid flowing through a cross-section of pipe per unit time.

7.1.5 *Gauge Pressure*

The difference between the local absolute pressure of the fluid and the atmospheric pressure at the place of measurement.

7.1.6 *Hydraulic Diameter*

The ratio of four times the cross-sectional area of the flow to the wetted perimeter.

7.1.7 Laminar Flow

Flow under conditions where forces due to viscosity are more significant than forces due to inertia.

7.1.8 Pipe

A tube, usually circular in cross-section, used for conveying a fluid.

7.1.9 Reynolds Number (Re)

A dimensionless parameter expressing the ratio between inertial and viscous forces.

7.1.10 Stagnation Pressure

Also known as total pressure; the pressure corresponding to that obtained when bringing the fluid to a standstill without an increase in the entropy.

7.1.11 Static Pressure

The pressure of a fluid that is independent of the kinetic energy of the fluid.

7.1.12 Steady Flow

Flow in which the flow rate in a measuring section is constant within the measurement uncertainty and over the time period of interest.

7.1.13 Strouhal Number (St)

The Strouhal number, in this guideline, is a dimensionless parameter that is relevant to the characterization of flow meters having a cyclic output, such as a turbine meter or vortex shedding device.

7.1.14 Transition Flow

Flow between a laminar and turbulent flow. Generally, $2000 < Re < 10,000$.

7.1.15 Turbulent Flow

Flow under conditions where the forces due to inertia are more significant than forces due to viscosity.

7.1.16 Velocity Distribution

7.1.16.1 Flow Profile

Graphic representation of the velocity distribution.

7.1.16.2 Fully Developed Velocity Distribution

A velocity distribution, in a straight length of pipe, that has zero radial and azimuthal fluid velocity components and an axisymmetrical axial velocity profile that is independent of axial position along the pipe.

7.2 Flow Meter Terms

7.2.1 Area Meter

A device in which a variation of the cross-section of the fluid stream under constant head is used as an indication of the rate of flow.

7.2.2 Diameter Ratio (β)

The diameter of the orifice (or throat) of the primary device divided by the inside diameter of the pipe upstream of the primary device.

7.2.3 Differential Pressure Device

A device inserted in a pipe to create a pressure difference whose measurement, together with a knowledge of the fluid conditions and the geometry of the device and the pipe, enables the flow rate to be calculated.

7.2.4 Discharge Coefficient (C)

Dimensionless coefficient given by the formula

$$C = \frac{\text{actual rate of flow}}{\text{theoretical rate of flow}}$$

7.2.5 Flow Meter

A device for measuring the quantity or rate of flow of a moving fluid in a pipe. It may consist of a primary or secondary device.

7.2.5.1 Primary Device

A device generating a signal or signals responding to the flow from which the flow rate may be inferred.

7.2.5.2 Secondary Device

A device that receives a signal from the primary device and displays, records, and/or transmits it as a measure of the flow rate.

7.2.6 Measuring Point

Any point where the local velocity of the flow is measured.

7.2.7 Nozzle

A convergent device having a curved profile with no discontinuities leading to a cylindrical throat.

7.2.8 Orifice (or Throat)

Opening of minimum cross-sectional area in a primary device.

7.2.9 Orifice Plate

A plate having a specified orifice.

7.2.10 Pitot-Static Tube

A pitot tube provided with static pressure tap holes drilled at specific positions on the circumference of the cylinder that is oriented parallel to the direction of flow.

7.2.11 Pressure Loss

The irrecoverable pressure loss caused by the presence of a primary device in the pipe.

7.2.12 Pressure Taps

Holes in the wall of the pipe or throat to allow measurement of the pressure.

7.2.12.1 Corner Taps

Wall pressure taps drilled on either side of an orifice plate or nozzle, with the spacing between the pressure taps and the respective faces of the plate or nozzle equal to half the diameter of the taps themselves so that the holes break through the pipe wall flush with the faces of the plate or nozzle.

7.2.12.2 Flange Taps

Wall pressure taps drilled on either side of an orifice plate with their axes being 1 in. (2.54 cm) from the upstream or downstream faces of the plate, respectively.

7.2.12.3 Wall Taps

Annular or circular hole drilled in the wall of the pipe in such a way that its edge is flush with the internal surface of the pipe.

7.2.13 Rangeability

The ratio of the maximum flow rate to the minimum flow rate of a meter. Accuracy tolerance limits and operating conditions must be specified.

7.2.14 Tracer Methods

Methods of measuring the flow rate that involve the injection and detection of a tracer in the flow.

7.2.14.1 Concentration

The mass of tracer per unit volume or mass of fluid.

7.2.14.2 Constant Rate Injection Method

The method of measuring the flow rate in which a tracer solution of known concentration is injected at a constant and known flow rate at one cross-section of a pipe. This injection must be sustained for a period long enough to establish a steady concentration with respect to time at a second cross-section downstream from the first

Appendix B: Glossary

and distant enough to produce adequate mixing. The flow rate is determined by comparing the concentration of the tracer in the second cross-section with that of the injected solution.

7.2.14.3 Dilution Methods

Methods in which the flow rate is deduced from the determination of the ratio of the dilution of the tracer injected to that of the tracer at the sampling cross-section.

7.2.14.4 Dilution Rate (or Ratio)

The ratio of the concentration of tracer in the injected solution to that in the sampling cross-section.

7.2.14.5 Mixing Length

The minimum distance downstream of the injection cross-section beyond which the injected solution is sufficiently distributed over a cross-section to enable the flow rate to be measured to the required accuracy.

7.2.15 Turbine Meter

A turbine meter is a velocity device in which the primary device is an axial flow type turbine whose rotating member is driven by the fluid and essentially all the fluid passes through the rotating member.

7.2.16 Ultrasonic Flow Meter

A device that uses the travel time of acoustic pulses transmitted between upstream and downstream transducers to derive an average velocity from which the flow rate may be deduced.

7.2.16.1 Acoustic Path

The path that the acoustic signals follow as they propagate through the measurement section between the transducer elements.

7.2.16.2 Clamp-On Meter

A flow meter in which the transducers are fixed on the outside of the pipe in which the flow rate is to be measured.

7.2.16.3 Cross-Correlation Meter

A flow meter that operates on the principle that two known signals, a known distance apart, are modulated by eddies in the fluid flow. These signals are compared by a correlator, the time taken for an eddy to travel between the two receivers is identified, and the flow rate is calculated.

7.2.16.4 Transit Time

The time required for an acoustic signal to traverse an acoustic path.

7.2.17 Velocity Meter

A device in which the primary device consists of a way to measure the average velocity within a known cross-section.

7.2.17.1 Calibration Factor of the Primary Device

The number that enables the flow signal to be related to the flow rate under defined reference conditions for a given value of the reference signal.

7.2.17.2 Electrode Signal

The total potential difference between the electrodes, consisting of the flow signal and signals not related to flow such as in-phase, quadrature, and common mode.

7.2.17.3 Electromagnetic Flow Meter

A flow meter that creates a magnetic field perpendicular to the flow, enabling the flow rate to be deduced from the induced electromotive force produced by the motion of a conducting fluid in the magnetic field.

7.2.17.4 Magnetic Field

The magnetic flux generated by the electromagnet in the primary device and which passes through the meter tube and flowing fluid.

7.2.17.5 Meter Electrodes

The two contacts by means of which the induced voltage is collected.

Appendix B: Glossary

7.2.17.6 Output Signal

The output from the secondary device, which is proportional to flow rate and in the form of a standardized transmission signal.

7.2.17.7 Primary Device

This device contains a meter tube, a pair of diametrically opposed electrodes, and an electromagnet. The primary device develops the electrode signal, which contains a signal proportional to the flow rate.

7.2.17.8 Secondary Device

The device that contains the circuitry that extracts the flow signal from the electrode signal and converts it to a standardized output signal directly proportional to the flow rate.

7.2.18 Velocity of Approach Factor

Coefficient given by the formula

$$E = \sqrt{(1 - \beta^4)}$$

where,

- β = diameter ratio (d/D)
- D = pipe inside diameter
- d = diameter of the primary device

7.2.19 Vent Holes

Holes drilled through the pipe wall to facilitate the removal from the metered liquid undesirable vapor or fluids with densities lighter than that of the metered liquid.

7.2.20 Venturi Tube

A device consisting of a cylindrical entrance section, a converging section, a cylindrical throat section, and a diverging section.

7.2.21 Volumetric Method

A method of measurement in which the flow is directed into or out of a calibrated volumetric tank during a certain period of time.

7.2.22 Vortex Meter

A flow meter that produces a vortex sheet downstream of an obstacle to enable the flow rate to be determined.

7.2.22.1 Linearity

Linearity refers to the constancy of the K factor over a specified range, defined by either the pipe Reynolds number or the flow rate. This linear range is usually specified by a band defined by maximum and minimum K factors, within which the K factor is assumed K_{mean} . The upper and lower limits of this range can be specified by the manufacturer as either a maximum and minimum Reynolds number range or a flow rate range.

7.2.22.2 Vortex-Shedding Meter

A flow meter that comprises a bluff body from which a succession of vortices are shed alternately on each side of the bluff body. For a given range of flow, the frequency at which the vortices are shed is directly proportional to the flow and can be counted using a wide range of detectors.

7.2.23 Weighing Method

A method of measurement, suitable only for liquids, in which the flow is directed either intermittently or continuously into a container on the scale of a weighing machine.

7.2.24 Working Pressure (Flowing Pressure)

The static pressure of the fluid immediately upstream or downstream of the primary device.

7.2.25 Working Temperature (Flowing Temperature)

The temperature of the fluid immediately upstream or downstream of the primary device.

8

APPENDIX C: WEIGH TANK CALIBRATION OF ULTRASONIC AND PITOT TUBE FLOW METERS IN SIMULATED COOLING WATER PIPING

Prepared by:
A. Jay Leavitt
Larry J. Sexton
Florida Power Corporation
James B. Nystrom
Alden Research Laboratory
June, 1998

Introduction

This case study describes the design considerations and calibration methods of an ultrasonic and an insert averaging pitot tube flow meter using test piping simulating the field installation to improve measurement uncertainty in a plant cooling water system. At Florida Power Corporation's Crystal River Unit 3, operations and maintenance personnel desired to improve process flow monitoring instrumentation used for the Raw Water System which has untreated sea water as process fluid. As a regulatory commitment for In-Service Inspection and In-Service Test (ISI/IST) per ASME Section XI of the Boiling and Pressure Vessel Code, flow instrumentation is required to operation with $\pm 2.0\%$ (total loop accuracy). In addition to quantifying process flow, this instrumentation is used to correlate flow and pump kW loading to determine pump efficiency and potential pump degradation (e.g., impeller wear).

Existing instrumentation (a pitot tube installed when the plant was built) had proven unreliable with no assurance that flow could be measured with any better than $\pm 10\%$ accuracy. Plant engineering moved to identify, procure, and install an instrumentation system which could be released to operations within eight weeks to support plant restart commitments. Several technologies were considered, with focus not only on an aggressive project schedule, but also in accordance with ASME code and seismic design requirements. Although several technologies presented high accuracy solutions, a

number of factors led the team to adopt a non-intrusive ultrasonic flow meter and an averaging insert pitot tube flow meter as a backup.

After particular attention was given to modeling the system flow geometry and performing closely controlled and monitored flow calibrations, the final installed instrumentation performed well within operational requirements.

Raw Water System Design Constraints

The Raw Water System (RW) provides cooling water directly from the Gulf of Mexico to the Service water heat exchangers. The process fluid is untreated, and receives only coarse straining as it passes through traveling screens. Along with normally anticipated suspended matter, fluid turbidity intermittently increases due to fuel barge operations in a canal proximate to the intake structure. Additionally, Raw Water Pump NPSH is affected by tidal conditions in the Gulf, such that process flow conditions and the measurement thereof could be affected by the cycling of the tides. Previous instrument anomalies had been attributed to this tidal effect, along with the potential adverse effect of increased turbidity in the process stream.

The RW processing piping is 24" O.D. carbon steel which is run overhead in the Service Water Room. In order to prevent corrosion, the inside surface of the RW system piping had been coated with a urethane liner. The available measurement location was downstream from the RW Pump discharge header which included a limiting orifice plate at the header tee, out of plane 90° bends, and a rolled pair of 45° bends downstream. Available straight pipe run length after a tee and several bends was slightly less than nine (9) diameters. Conventional flow orifice, Venturi, or other in-line components did not present viable solutions, since this instrumentation requires at least five to ten diameters upstream, and two to five diameters downstream. Also, flow straighteners were ruled out due to the suspended solids and the potential for fouling, separation, and associated safety issues.

The solution was required to eliminate the potential problems arising from untreated sea water passing through a lined pipe, with less than nine diameters of straight run length. Additionally, ASME Section XI requirements were to be met for any pressure boundary components, welded sections, or fittings; structural integrity was to be maintained with seismic analysis and qualification demonstrating the ability of the instrumentation to satisfy applicable seismic requirements. Further, instrument accuracy of $\pm 2.0\%$ had to be demonstrable, either through test or analysis. These constraint led the team to consider a wide variety of alternative solutions.

Alternative Solutions

Considering the various design constraints which could affect the performance of the Raw Water System flow measurement instrumentation, the initial limiter was overall

accuracy. With the knowledge that device accuracy is degraded if straight pipe run lengths are compromised, consideration was given to instrumentation which would be impervious to the flow geometry. The following four technologies were considered: Magnetic, V-Cone, Ultrasonic, and insert averaging pitot tube.

Magnetic flow sensors were an attractive solution requiring minimal straight run lengths, and having good accuracy. Although the installation would require the removal and replacement of sections of pipe, there is no in-line flow obstruction so that there would be no fouling due to the suspended solids or corrosive nature of the untreated sea water. Ultimately, long lead time and unfamiliarity with the technology resulted in its exclusion.

The V-Cone provides an advantage over other differential devices because the Vee section is an inherent flow straightener such that the manufacture recommends no minimal straight run length requirements. However, the properties of the process fluid are likely to cause corrosion of the Vee section, and possibly promote barnacle build-up. Thus, the V-Cone was not further considered.

Ultrasonics (UT) are offered in two technologies: (1) Doppler ultrasonics, and (2) transit time ultrasonics. The Doppler method measures frequency shift resulting from the source signal reflecting off particles or bubbles in the entrained fluid, where the frequency shift is proportional to flow; while transit time ultrasonics, which measure the difference in travel time of a pulse signal (proportional to flow) between a transmitter and receiver. Doppler methodology was deemed to be less reliable in the seawater application and transit time methodology was adopted. The advantages of the UT were equipment was available in the required time frame, no intrusion into the flow was required, and accuracy requirements could be met. Although ultrasonic flow instrumentation has been used successfully in custodial transfer (e.g., gas line) applications, results have not been widely established in the power industry. Therefore, as a fallback position, in conjunction with the use of UT technology, an averaging pitot tube with smart transmitter was specified for test to both provide a diverse means of validation of data and an alternate method for field measurement should the UT system not satisfy the performance needs.

Raw Water (RW) Instrumentation Design Approach and Specifications

With the decision to use UT instrumentation, the problems dealing with lined 24" O.D. process piping and irregular flow geometrics required resolution. An uncertainty better than $\pm 2\%$ over the entire instrument loop had to be assured in order to satisfy ASME Section XI ISI/IST requirements. With less than ideal flow conditions (insufficient straight pipe runs), and with the need to remove a section of lined process piping, the flow sensing instrumentation itself presented only a portion of the scope of the modification. Thus, a project team was assembled consisting of representatives from the test laboratory, meter manufacturer, piping fabricators, and Florida Power

Appendix C: Weigh Tank Calibration of Ultrasonic and Pitot Tube Flow Meters In Simulated Cooling Water Piping

Corporation (FPC) to provide close coordination of the fabrication, testing, and installation of the new RW instrumentation to satisfy both the short time constraints and the strict requirements for ASME ISI/IST testing. By modeling the field configuration in a controlled test process, both the ultrasonic and pitot tube instrument accuracy could be quantified.

Due to the corrosive nature of the process fluid (i.e., untreated seawater), the existing urethane lined pipe spool was to be replaced with a 24" O.D. segment of Monel 400, a nickel chromium non-carbon steel pipe to be resistant to corrosion while providing ultrasonic permeability. The ultrasonic published data gave instrument (sensor) accuracy of $\pm 2\%$ for the single path transit time UT System with proper upstream piping. However, the application (and associated instrument uncertainty calculations) must consider additional uncertainties due to installation effects, total loop length (including receiver), Measurement and Test Equipment (M&TE), and process errors. The team was concerned that the combined effect of these errors would be an overall accuracy greater than $\pm 2\%$, which is unacceptable for ASME Section XI ISI/IST.

The manufacturer suggested the use of a two-path system, employing two pairs of UT sensors, with the electronic receiver/indicator programmed to output average value. By doubling the number of data points, and with averaging, the published accuracy for the two-path system is $\pm 1.5\%$. Although this improved performance, combined (Square-Root-Sum-of-the-Squares) with the other loop errors would satisfy the $\pm 2.0\%$ criteria, there would be little margin. The intent of testing was to further minimize errors due to flow patterns by reproducing field piping geometry. The manufacturer expressed confidence that a two-path system calibrated in a modeled flow condition would perform better than $\pm 1.5\%$.

To further reduce potential errors in reproducing laboratory calibration results in the field, a wetted UT System was employed. This required the removal of the existing 24" O.D. pipe spool and its replacement with an integrated spool/ultrasonic assembly. By permanently affixing the UT sensors in welded adapters with specified installation points, the test results obtained from the test laboratory would be reproduced in the plant (eliminating uncertainties of sensor placement and pipe wall thickness and diameter variations).

With the instrument approach determined and the fabrication of the 24" O.D. spool from Monel 400 (as reviewed and approved by FPC engineering as a suitable material for untreated sea water), the remaining issues related to test setup and procedure. It was critical to emulate the field process conditions in the calibration process to assure applicable test results. The team did not solely depend on the use of existing plant piping drawings due to the concern for close fit-up of the Monel 400 spool, which was fabricated based on field walkdown and drawings.

Weigh Tank Flow Calibration

The test laboratory providing calibration services used a primary flow measurement standard, the gravimetric method, in which a weigh tank measures diverted water (95,000 lbs or about 11,000 gallons) over a measured time interval. Line temperature measurement allows calculation of density and volumetric flow. Overall flow measurement uncertainty was estimated at better than 0.15% at the 95% confidence level for all flows.

Field piping from the flow limiting orifice at the pump discharge to the elbows downstream of the meter spool were simulated in the test. All test fittings, spool pieces, and instruments were installed as shown in Figure 8-1 at the test laboratory in late September 1997. With a design flow rate of between 8,000 and 14,000 gpm, the test range was set to be between 4,000 and 18,000 gpm, providing additional data to assure instrument accuracy and bounded the field flow conditions, so that any anomalies at either extreme would be identifiable as upper or lower limit trend data (none occurred).

Test runs were conducted from maximum to minimum in 1,000 gpm increments by a downstream flow throttle valve. As flow was diverted into or out of the weigh tank for measurement, the trigger signal interfaced with the ultrasonic meter to integrate the UT meter output and average the pitot tube differential pressure signal for the time of diversion. The UT meter provided flows for Path 1, Path 2, and average (all in gpm). Fifteen tests were performed with 1.000 k-factor correction (e.g., no calibration adjustment) for both channels. The initial UT average flow from the two path measurements are compared to the gravimetric flow in Figure 8-2 which show the actual flow divided by the UT meter output as a function of flow. A linear regression with its 95% confidence limits shows essentially no dependence on flow with an average deviation of about 1.9%. The average difference between the measured flow and each UT path resulted in k-factor corrections of 1.059 and 0.980, showing the individual channels had considerably greater deviation than the average due to the skewed velocity distribution caused by the upstream fittings. After the k-factor corrections were programmed into the meter, fifteen test runs were taken over the test flow range to verify performance as shown in Figure 8-3, again with the linear regression and 95% confidence level. The best fit curve passes through 1.00 at 10,000 gpm with an average deviation of 1.0011 indicating excellent agreement with measured flow and essentially no dependence on flow, proving the k-factor determination was accurate and reproducible.

Simultaneous data were recorded for the Pitot tube with the UT testing. Test results for the pitot tube are shown in Figure 8-4 as a discharge coefficient versus flow with a second order curve fit including the 95% confidence interval of the curve fit shown as dotted lines. The manufacturer's predicted coefficient was 0.636 for this size and style meter, while the measured coefficient averaged 0.6713 and varied 0.667 at the higher

flows to about 0.685 at the lowest flow tested. Repeatability was good as indicated by the small uncertainty band indicated by the dotted lines and in use measurement uncertainty could be reduced by using a coefficient variable with flow in calculations.

Conclusions

The manufacturer's predicted accuracy for a two-path system ultrasonic (i.e., $\pm 1.5\%$ flow), was not met in the rigorous conditions resulting from the upstream fittings. Uncalibrated results showed a 2% deviation from the weigh tank flows using the average of both paths. Single path measurements deviations were substantially greater than 2.0%. After determination of the calibration factors for each path, test results indicated deviations substantially reduced with the average deviation less than 0.5%.

While the averaging pitot tube demonstrated predictable performance with relatively low scatter after calibration, the discharge coefficient in the disturbed velocity profile caused by the upstream piping resulted in a deviation of about 5% from the predicted value for a fully developed symmetrical velocity profile.

The unwieldy nature of a 24" (insertion length) pitot tube has deemed it suitable for use in a back-up role, while the UT Sensors are used for continuous, real-time flow monitoring.

Final test data was incorporated in an FPC uncertainty calculation, corrected for density of fresh water versus seawater, and considering M&TE and process errors. As concluded therein, the overall two-path ultrasonic system accuracy was $\pm 1.75\%$ (well within the $\pm 2.0\%$ requirement for ASME Section XI ISI/IST testing). The Raw Water System was returned to service with a new Monel 400 spool piece with integrated UT instrumentation by early October, 1997 (eight week turnaround).

Appendix C: Weigh Tank Calibration of Ultrasonic and Pitot Tube Flow Meters In Simulated Cooling Water Piping

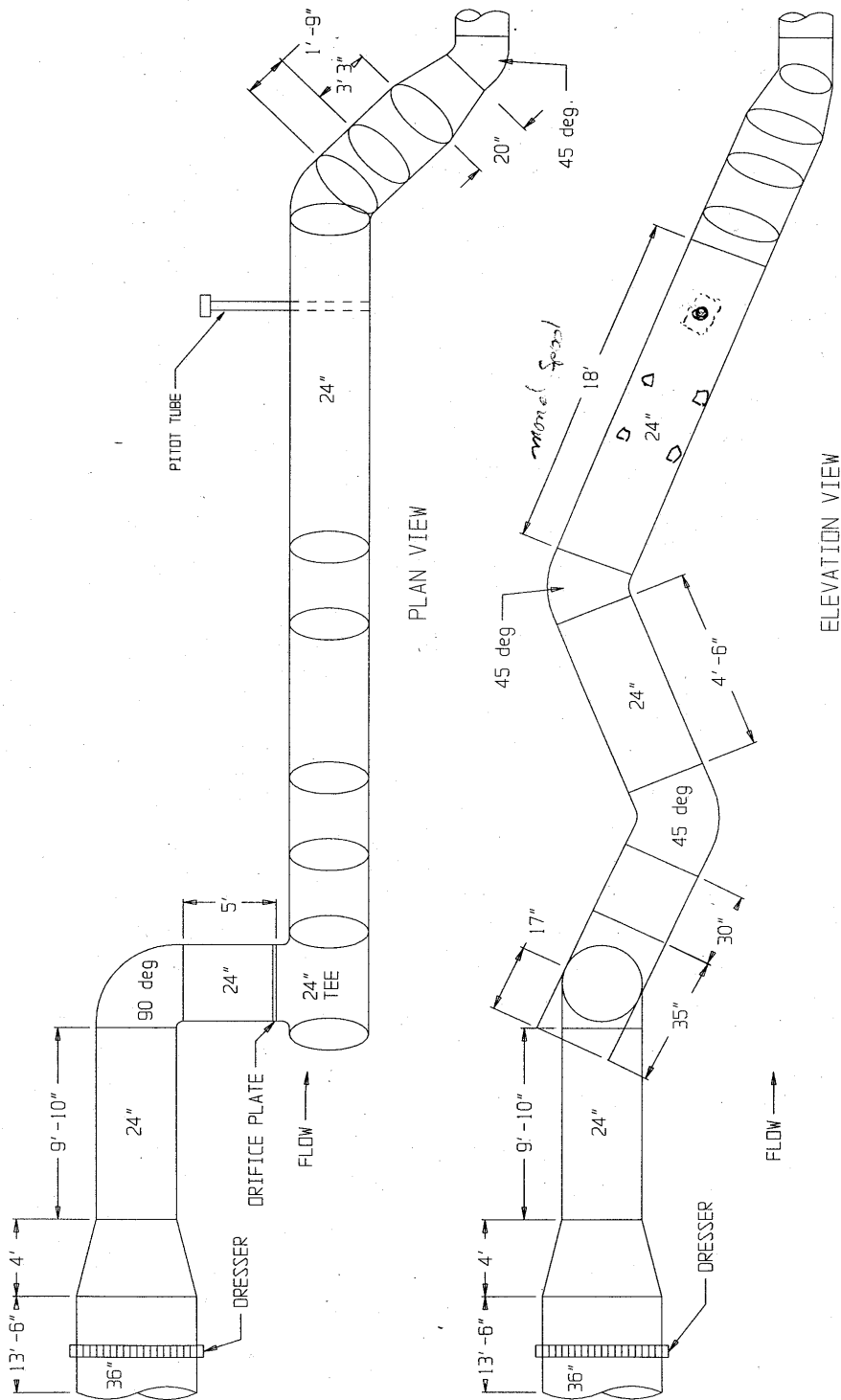


Figure 8-1
Test Fittings, Spool Pieces, and Instruments

Appendix C: Weigh Tank Calibration of Ultrasonic and Pitot Tube Flow Meters In Simulated Cooling Water Piping

Weigh Tank Calibration of Ultrasonic and Pitot Tube Flow Meters In Simulated Cooling Water Piping

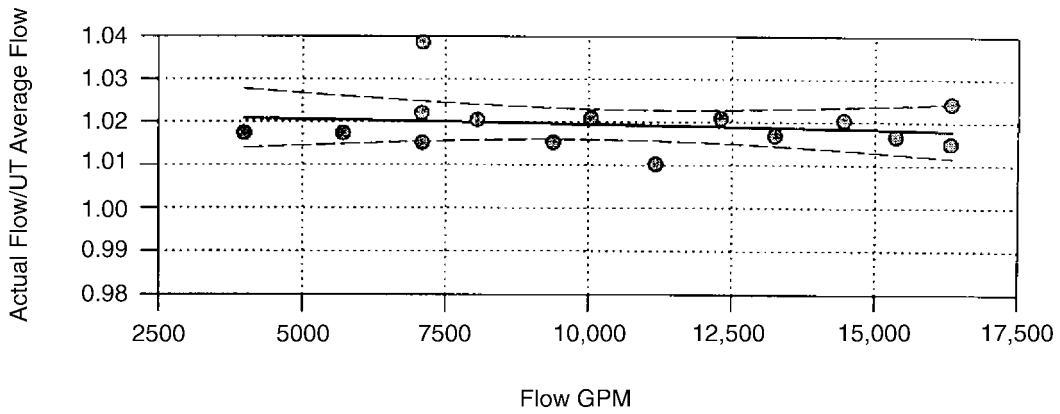


Figure 8-2
Ultrasonic Flow Meter Performance with K-Factors = 1000

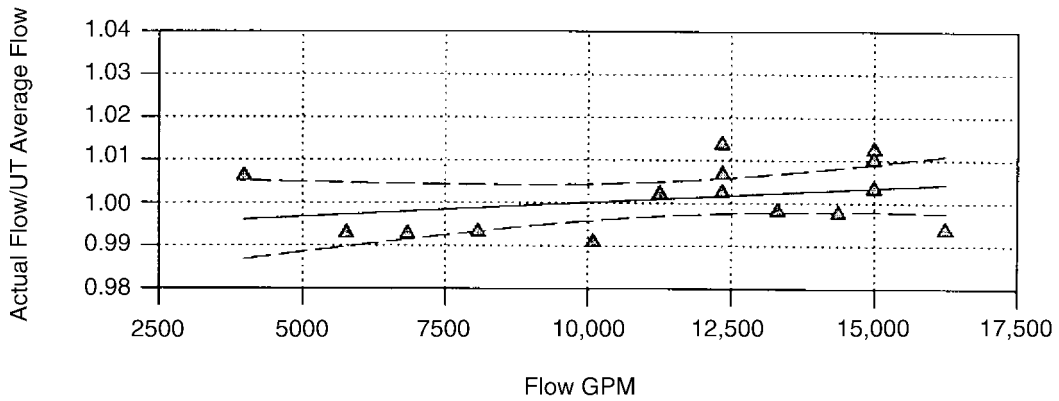


Figure 8-3
Ultrasonic Flow Meter K-Factors Adjusted

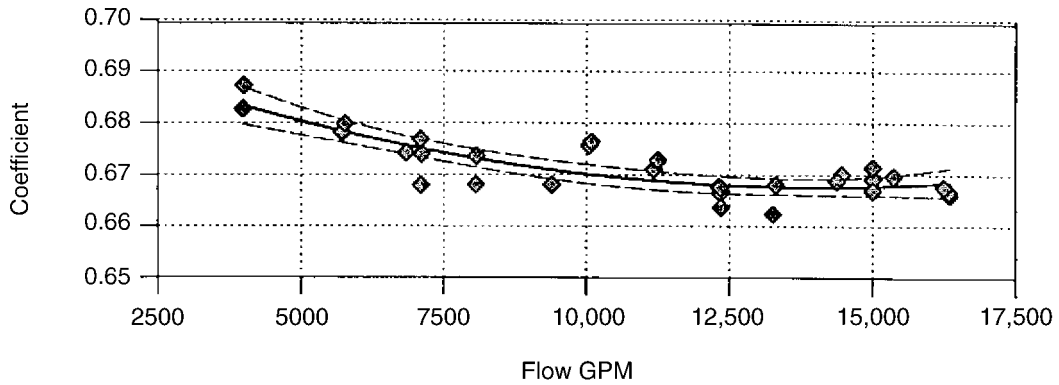


Figure 8-4
Pitot Tube Performance

9

APPENDIX D: CALIBRATION OF A 16" V-CONE SPOOL PIECE

CME 94-034, Rev. 0
NAPS RSHX SW V-CONE FLOW TEST
DC 94-006-3
REG. GUIDE 1.97 - V-CONE & FLOW TRANSMITTER INSTALLATION
NORTH ANNA POWER STATION - UNITS 1 & 2

Source Document:

1. DC 94-006-3 REG. GUIDE 1.97 - V-CONE & FLOW TRANSMITTER INSTALLATION

References

The purpose of this Engineering Transmittal is to document the calibration of a 16 in. V-Cone spool piece by the attached flow report from Alden Research Laboratory, Inc.. This flow test determined the flow coefficient of four configurations of the North Anna Power Station SW RSHX discharge lines. The flow configurations tested were the worst case condition of a close downstream tee with and without cross flow; the second worst case of a close downstream 90° elbow and an ideal case of a straight pipe where no flow disturbances were found for several pipe diameters upstream and downstream. The following results were achieved from this test:

Appendix D: Calibration of a 16" V-Cone Spool Piece

**Table 9-1
Results from Flow Test**

FLOW CASE	FLOW COEFFICIENT	STANDARD DEVIATION	FLOW RANGE (GPM)
Downstream Tee with cross-flow	0.8042	0.0071	1694.5 - 6065
Downstream Tee without cross-flow	0.8067	0.0017	2024.1 - 5844.9
Downstream 90° Elbow	0.8046	0.0030	1943 - 6697
Straight Pipe	0.8019	0.0023	1936 - 5992

The results reported are traceable to National Institute of Standards and Technology (NIST) with a flow measurement uncertainty of $\pm 0.25\%$.

In addition this flow test found the unrecoverable head loss ranged from 35.4 - 41.4% of the flow differential with flows ranging from 2977 - 5992 GPM.

Prepared by: D. S. Nichols

Reviewed by: J. D. Waddill

Approved by: R. L. Rasnic

Attachments

1. Alden Research Laboratory Report, Calibration of a 16" V-Cone spool piece, P. O. #BNT 466762, ARL NO. 114-94/C250, June 1994.

CALIBRATION OF
A 16" V-CONE SPOOL PIECE
VIRGINIA ELECTRIC AND POWER COMPANY
PURCHASE ORDER NUMBER BNT 466762
JUNE 1994 - ARL NO. 114-94/C250

CERTIFIED BY

James B. Nystrom

ALDEN RESEARCH LABORATORY, INC.
30 Shrewsbury Street
Holden, Massachusetts 01520

INTRODUCTION

A 16" V-Cone Spool Piece was calibrated at the Alden Research Laboratory, Inc. (ARL) for Virginia Electric and Power Company under their Purchase Order Number BNT 466762, using ARL's standard test procedures, QA-AGF-7-86, Revision 3. Flow element performance is presented as a discharge coefficient, C , versus pipe Reynolds number, in both tabular and graphical format. Tests were conducted in a straight line and with an upstream butterfly valve for downstream piping with an elbow and with a tee having cross flow.

FLOW ELEMENT INSTALLATION

The V-cone meter was installed in Test Lines 1 and 2 in Building 1, shown in plan view on Figure 9-1. Two centrifugal pumps (300 horsepower), which are used in parallel, provide a maximum head of about 130 ft. and a maximum flow of 44 ft³/s. Water was provided from a heated 180,000 gallon sump under the test floor.

Tests were conducted in a straight line with more than 30 feet of schedule 30 16" upstream pipe and the detailed piping arrangement is shown in Figure 9-2. VEPCO supplied a butterfly valve, which was installed in the wide open position about two diameters upstream of the V-cone spool piece and a 90 degree long radius elbow was installed 2.75 pipe diameters downstream for the second test series, as shown in Figure 9-3. The last test series replaced the elbow with a 24" tee having a cross flow and the detailed piping arrangement is shown in Figure 9-4. The cross flow was measured with a previously calibrated venturi meter. Flow through the V-Cone meter was the difference in the total flow measured by the gravimetric method and the cross flow. Careful attention was given to align the flow element with the test line piping, and to assure no gaskets between flanged sections protruded into the flow. Vents were provided at critical locations of the test line to purge the system of air.

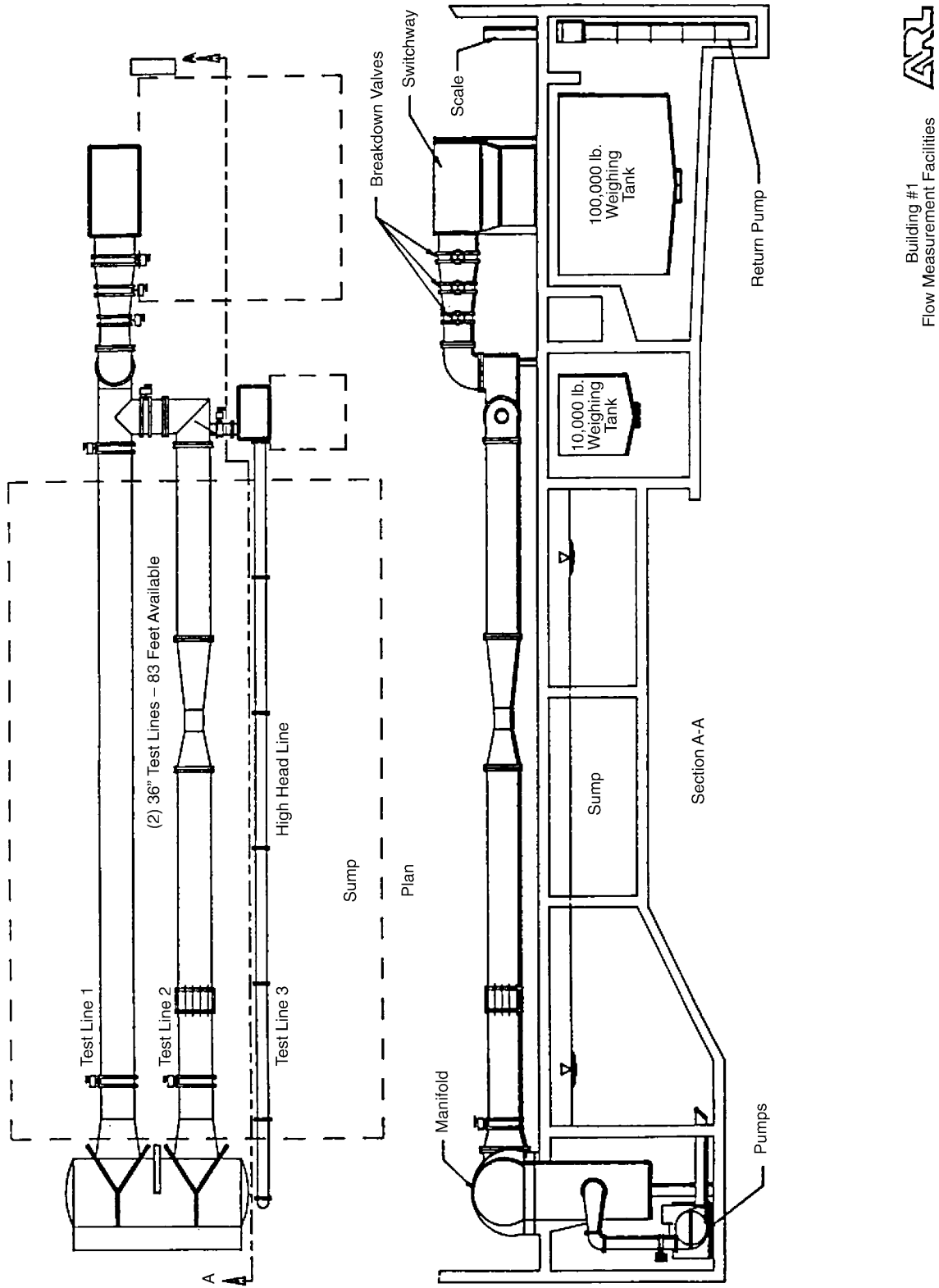


Figure 9-1
V-Cone Meter Installation



Building #1
Flow Measurement Facilities

Appendix D: Calibration of a 16" V-Cone Spool Piece

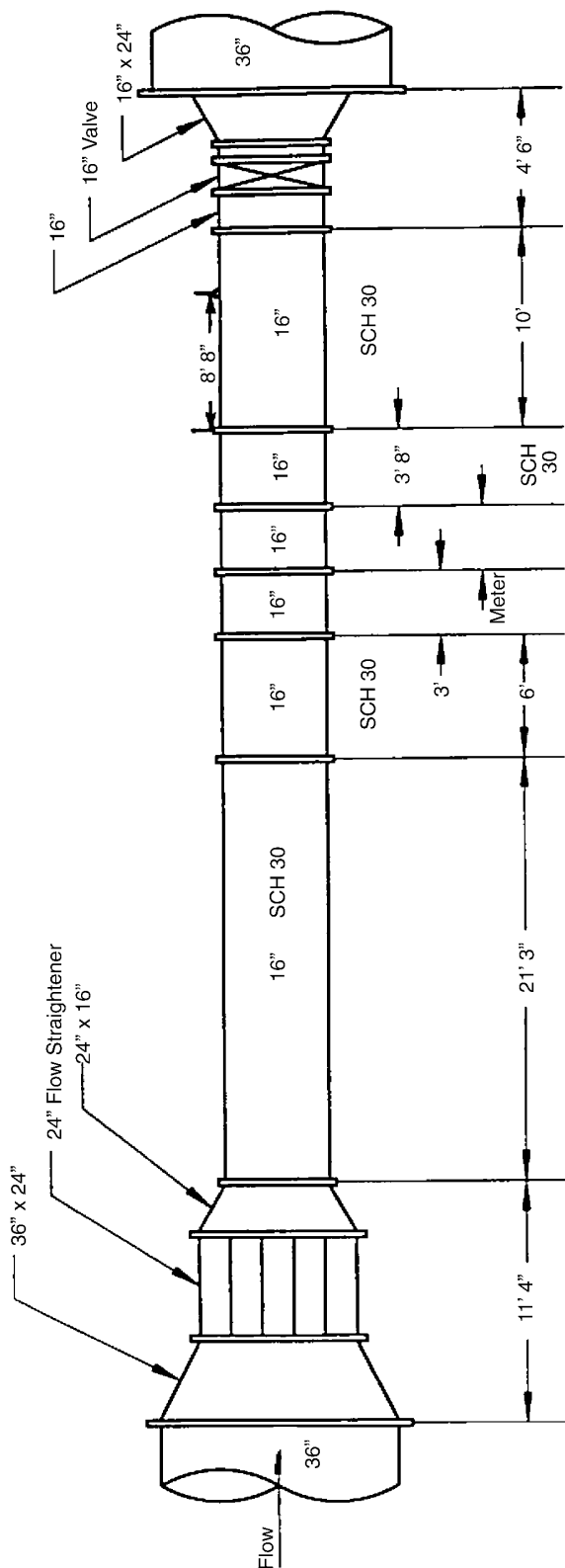
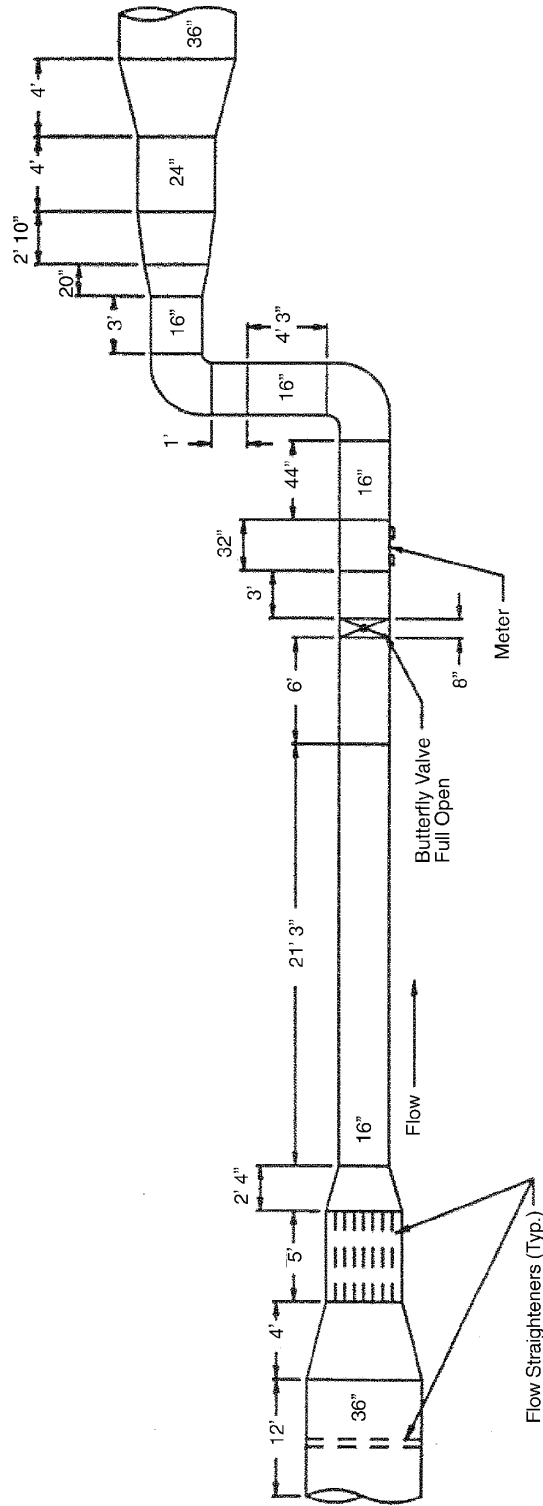


Figure 9-2
Straight Line Piping

Virginia Electric and Power Company
Purchase Order Number: BNT 466762
16" V-Cone Spool Piece
June 1994

Plan View, Building 1, Line 2





Virginia Electric and Power Company
 Purchase Order Number: BNT 466762
 16" V-Cone Spool Piece
 June 1994

Plan View, Building 1, Lines 1 & 2

Figure 9-3
 Downstream Elbow

TEST PROCEDURE

The test technician verified proper installation of the flow element in the test line prior to introducing water into the system to equalize test line piping and primary element temperature to water temperature. After attaining thermal equilibrium the test line downstream control valve was then closed and vent valves in the test line were opened to remove air from the system. With the line flow shut off, the flow meter output was checked for zero flow indication.

Prior to the test run, the control valve was set to produce the desired flow, while the flow was directed to waste. Sufficient time was allowed to stabilize both the flow and the instrument readings, after which the weigh tank discharge valve was closed and the weigh tank scale indicator and the electric timer were both zeroed. To begin the test run, flow was diverted into the weigh tank, which automatically started the timer.

After the test run began, multiple readings of the meter output were recorded while the weigh tank was filling. Data recording was stopped when the weigh tank filled to a preselected weight (usually about 95,000 lb.). After each test run, the meter readings were averaged and recorded.

To complete the test run, when the preselected weight of water was collected, flow was diverted away from the weigh tank, and the timer stopped automatically. The weight of water in the tank, elapsed time, line water temperature, and average meter output were recorded on a data sheet. The control valve was then adjusted to produce the next flow, and the procedure repeated. During the time allowed to stabilize the new flow, the previous run data were entered into a data reduction computer to determine the discharge coefficient and the Reynolds number, and the results plotted so that the results of each test run were evaluated before the next run began.

For the test series with cross flow through the tee, the differential head produced by the venturi meter was read simultaneously with the V-Cone output using a second calibrated differential pressure transmitter. Since both lines were supplied from a common header, the cross flow was controlled by an upstream valve in conjunction with the downstream valve controlling total flow.

FLOW MEASUREMENT METHOD

Flow was measured by the gravimetric method using a tank mounted on Toledo scales having a capacity of 100,000 pounds with a resolution 5 lb. Water passing through the flow element was diverted into the tank with a hydraulically operated knife edge passing through a rectangular jet produced by a diverted head box. A Hewlett-Packard "5301A" 10 MHz Frequency Counter with a resolution 0.001 sec was started upon flow diversion into the tank by an optical switch, which is positioned at the center of the jet. The timer was stopped upon flow diversion back to waste and the elapsed diversion time was recorded. A thermistor thermometer measured water temperature to allow calculation of water density. Volumetric flow was calculated by Equation (9-1).

$$q_a = \frac{W}{T\rho_w B_c} \quad (\text{Eq. 9-1})$$

Where	q_a	=	volumetric flow, ft ³ /sec
	W	=	net accumulated weight, lb _m
	T	=	diversion time, sec
	ρ_w	=	density of water run temperature, lb _m /ft ³
	B_c	=	buoyancy correction, dimensionless
		=	$1 - \rho_a / \rho_w$
	ρ_a	=	density of ambient moist air, lb _m /ft ³

The buoyancy correction includes air density calculated by perfect gas laws with the standard barometric pressure, a relative humidity of 75%, and measured air temperature. The weigh tank is periodically calibrated to full scale by the step method using 10,00 lb_m of cast iron weights, whose calibration is traceable to NIST. Flow calculations are computerized to assure consistency. Weigh tank calibration data and water density as a function of temperature, are stored on disk file. Data were recorded manually and on disk file for later review and reporting. As an option, flow may be expressed in different units, as required, by the application of standard conversions.

DISCHARGE COEFFICIENT CALCULATIONS

Discharge coefficient, C , is defined by Equation (9-2) and plotted versus pipe or throat Reynolds number. The discharge coefficient relates the theoretical flow to the actual flow.

$$C = \frac{q_a}{q_{th}} = \frac{q_a}{F_a K_M \sqrt{\Delta h}} \quad (\text{Eq. 9-2})$$

where:

- C = discharge coefficient, dimensionless
- q_{th} = theoretical flow, ft^3/sec
- Δh = differential head, feet of water at run temperature
- F_a = thermal expansion factor, dimensionless
- K_M = proportionally constant, $\text{ft}^{5/2}/\text{sec}$

The theoretical proportionality constant, K_M , between flow and square root of differential head is a function of the meter throat area, the ratio of equivalent throat diameter to pipe diameter, and the local gravitational constant, as defined by Equation (9-3). Since the meter had an annular throat, an equivalent throat diameter was calculated, which resulted in the same area as the annular passage.

$$K_m = \text{meter constant} = \frac{a_t \sqrt{2g}}{\sqrt{1-\beta^4}} \quad (\text{Eq. 9-3})$$

where:

- a_t = equivalent throat area, ft^2
- g = local acceleration of gravity, 32.163 ft/s^2
- β = ratio of equivalent throat diameter to pipe diameter, dimensionless

Appendix D: Calibration of a 16" V-Cone Spool Piece

The effect of fluid properties, viscosity and density, on the discharge coefficient is determined by Reynolds number, the ratio of inertial to viscous forces. To evaluate flow meter performance, the discharge coefficient is plotted versus Reynolds number. Pipe Reynolds number, R_D , was used, and is defined by Equation (9-4).

$$R_D = \frac{Dq_a}{a_p V} \quad (\text{Eq. 9-4})$$

where:

- R_D = pipe Reynolds number, dimensionless
- $D(d)$ = pipe diameter, ft
- a_p = pipe cross-sectional area, ft²
- V = kinematic viscosity of water at run temperature in ft²/s

FLOW METER SIGNAL RECORDING

The secondary element, which converts the flow meter signal into engineering units, was one of two Rosemont 3051C Smart Differential Pressure Transmitters having ranges of 250" H₂O and 25" H₂O. The transmitters were calibrated with dead weight testers having an accuracy of 0.02% of reading. The transmitter signal was recorded by a PC based data acquisition system having a 16 bit A to D board. Transmitter calibrations were conducted with the PC system such that an end to end calibration was achieved. Transmitter output was read simultaneously with the diversion of flow into the weigh tank at a rate of 34 Hz for each test run (flow) and averaged to obtain a precise differential head. The average transmitter reading was converted to feet of flowing water using a linear regression analysis of the calibration data and line water temperatures to calculate appropriate specific weight. Calibrations were conducted before and after testing and the calibration results showed essentially no transmitter calibration drift.

TEST RESULTS

The results are shown both in tabular form and plotted versus Reynolds number and flow in gpm. The measured values of weight, time, and line temperature, which are used to calculate the listed flow, are shown in the tables. The average transmitters reading used to calculate the differential head in feet of water at line temperature is also shown in the tables. Flow element performance is given as discharge coefficient versus pipe Reynolds number and flow in gpm. The discharge coefficient was averaged over the tested Reynolds number range and the standard deviation is listed. In the straight line calibration, the 16" V-Cone Spool Piece had an average discharge coefficient of 0.8019 with a standard deviation of 0.0023 over a pipe Reynolds number range of 500,000 to 1,900,000.

The gross head loss across the meter was measured and the net head loss due to the meter was calculated by subtracting the loss due to the pipe length between the head loss piezometer taps to determine the unrecoverable head loss due to the meter. Head loss was expressed in feet and percent of differential, which is plotted versus flow in gpm.

Eighteen tests were conducted with the downstream elbow for a range of flows from 1,943 gpm to 6,697 gpm. For tests with the downstream tee flow, eighteen tests were conducted with cross flows of between 3,058 gpm and 6,474 gpm. At low flows through the V-Cone Spool, the accuracy of the calculated discharge coefficient was decreased since the V-Cone flow is the difference of two relatively large flows, one of which has an uncertainty near 0.25% (the venturi meter). An additional eleven tests were conducted with zero cross flow. The average coefficient without cross flow was 0.8067 with a standard deviation of 0.0017.

Analysis indicates that the flow measurement uncertainty is within 0.25% of the true value for each test run. Calibrations of the test instrumentation (temperature, time, weight, and length measurements) are traceable to the National Institute of Standards and Technology (formerly the National Bureau of Standards).

VIRGINIA ELECTRIC AND POWER CO.
 Purchase Order Number: BNT 466762
 16" V-CONE SPOOL PIECE
 Straight Line

CALIBRATION
 Date: June 8, 1994
 PIPE DIAMETER = 15.2500
 EQUIVALENT THROAT DIAMETER = 11.5075

Run #	Line Temp Deg F	Air Temp Deg F	Net Weight lb.	Run Duration secs.	Output (see note)	Flow GPM	H Line FT H ₂ O	Pipe Rey. # x 10 ⁶	Coef.
1	92	77	95608	137.376	5.007~	5036.	3.945	1.3911	0.8015
2	92	75	95498	137.826	4.974~	5014.	3.901	1.3772	0.8023
3	92	75	95468	137.998	4.968~	5006.	3.893	1.3735	0.8019
4	91	74	95317	157.750	4.265~	4372.	2.970	1.1956	0.8019
5	91	74	95387	152.299	4.424~	4532.	3.179	1.2393	0.8033
6	91	74	95442	152.439	4.426~	4530.	3.181	1.2375	0.8028
7	91	74	95362	169.820	3.945~	4063.	2.550	1.1099	0.8042
8	91	74	95337	170.096	3.948~	4055.	2.553	1.1066	0.8022
9	91	74	95297	170.240	3.941~	4050.	2.545	1.1052	0.8025
10	91	74	95156	336.473	4.497~	2046.	0.656	0.5583	0.7986
11	91	75	95106	336.289	4.496~	2046.	0.655	0.5584	0.7989
12	91	75	95166	231.282	7.255~	2977.	1.381	0.8115	0.8008
13	91	75	95197	231.322	7.242~	2977.	1.378	0.8107	0.8018
14	91	75	95116	231.060	3.046~	2978.	1.369	0.8109	0.8045
15	91	76	95186	231.242	3.048~	2978.	1.373	0.8100	0.8034
16	91	76	95663	115.496	6.282~	5992.	5.617	1.6299	
17	90	76	95638	115.464	6.280~	5992.	5.614	1.6245	0.7992
18	90	76	95126	354.840	2.443~	1939.	0.579	0.5258	0.7994
19	90	76	95176	355.642	2.442~	1936.	0.577	0.5255	0.8055
20	90	76	95166	355.588	4.243~	1936.	0.589	0.5255	0.8056
									0.7974

For Pipe Rey. #s above 0.10 x 10⁶ Avg Coef = 0.8019 With Standard Deviation = 0.0023

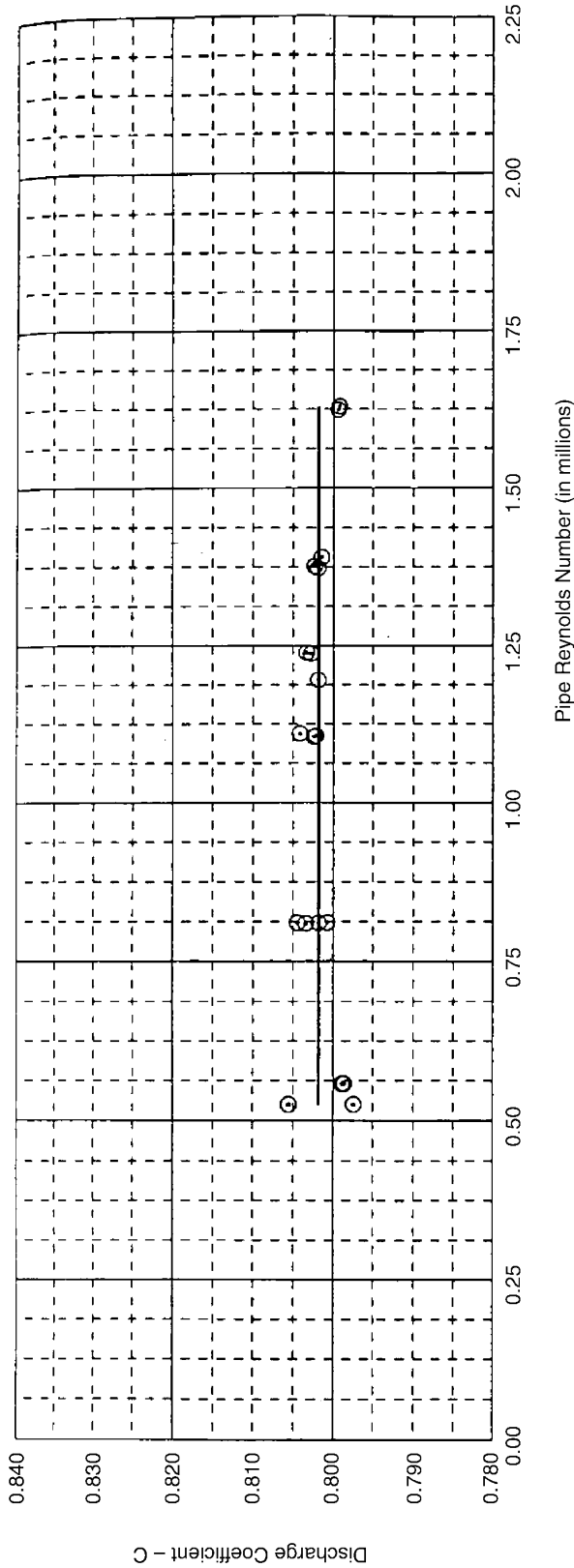
~ dp transmitter volts

The data reported on herein was obtained by measuring equipment the calibration of which is traceable to NIST, following the installation and test procedures referenced in this report, resulting in a flow measurement uncertainty of ±0.25% or less

Calibrated by: S.V.K. Certified by: _____ signature

Witnessed by a company representative.

ARL



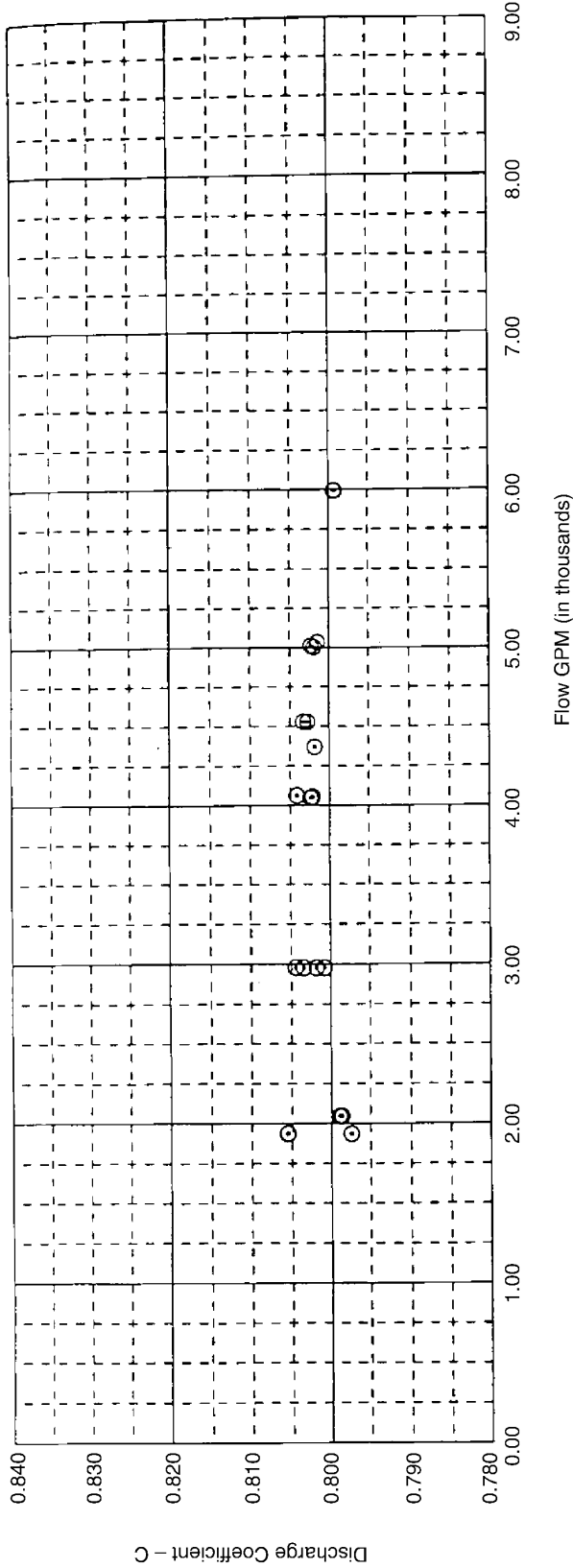
Virginia Electric and Power Company
 Purchase Order Number: BNT 466762
 16" V-Cone Spool Piece
 June 8, 1994
 Straight Line



Certified By: *J. E. D. S. P. S.*

$q_a = C F_a K_M \sqrt{\Delta h}$	
q_a = Actual Flow (ft ³ /sec)	
C = Discharge Coefficient (Dimensionless)	
Δh = Pressure Differential (Feet of Water at Run Temperature)	
K_M = Meter Constant = $\frac{a\sqrt{2g}}{\sqrt{1-\beta^4}}$	7.0466
F_a = Average Thermal Expansion Factor	1.0004
a = Throat Area (ft ²)	0.7223
g = Local Acceleration of Gravity (ft/sec ²)	32.1625
β = Ratio of Throat to Pipe Diameter (Dimensionless)	0.7546
Pipe Diameter (Inches)	15.2500
Throat Diameter (Inches)	11.5075
For Pipe Reynolds Number > 0.10 x 10 ⁶ avg coefficient	0.8019
Dimensions By: VIRGINIA ELECTRIC AND POWER CO.	

Appendix D: Calibration of a 16" V-Cone Spool Piece



Virginia Electric and Power Company
 Purchase Order Number: BNT 466762
 16" V-Cone Spool Piece
 June 8, 1994
 Straight Line



Certified By: *J. B. DePina*

$q_a = C F_a K_M \sqrt{\Delta h}$	
q_a = Actual Flow (ft ³ /sec)	
C = Discharge Coefficient (Dimensionless)	
Δh = Pressure Differential (Feet of Water at Run Temperature)	
K_M = Meter Constant = $\frac{a\sqrt{2g}}{\sqrt{1-\beta^4}}$	7.0466
F_a = Average Thermal Expansion Factor	1.0004
a = Throat Area (ft ²)	0.7223
g = Local Acceleration of Gravity (ft/sec ²)	32.1625
β = Ratio of Throat to Pipe Diameter (Dimensionless)	0.7546
Pipe Diameter (Inches)	15.2500
Throat Diameter (Inches)	11.5075
Error - No runs with reynolds# above 1.000000e+05 were found= Dimensions By: VIRGINIA ELECTRIC AND POWER CO.	

VIRGINIA ELECTRIC AND POWER CO.
 Purchase Order Number: BNT 466762
 16" V-CONE SPOOL PIECE
 Head Loss

CALIBRATION
 Date: June 8, 1994
 PIPE DIAMETER = 15.2500
 EQUIVALENT THROAT DIAMETER = 11.5075

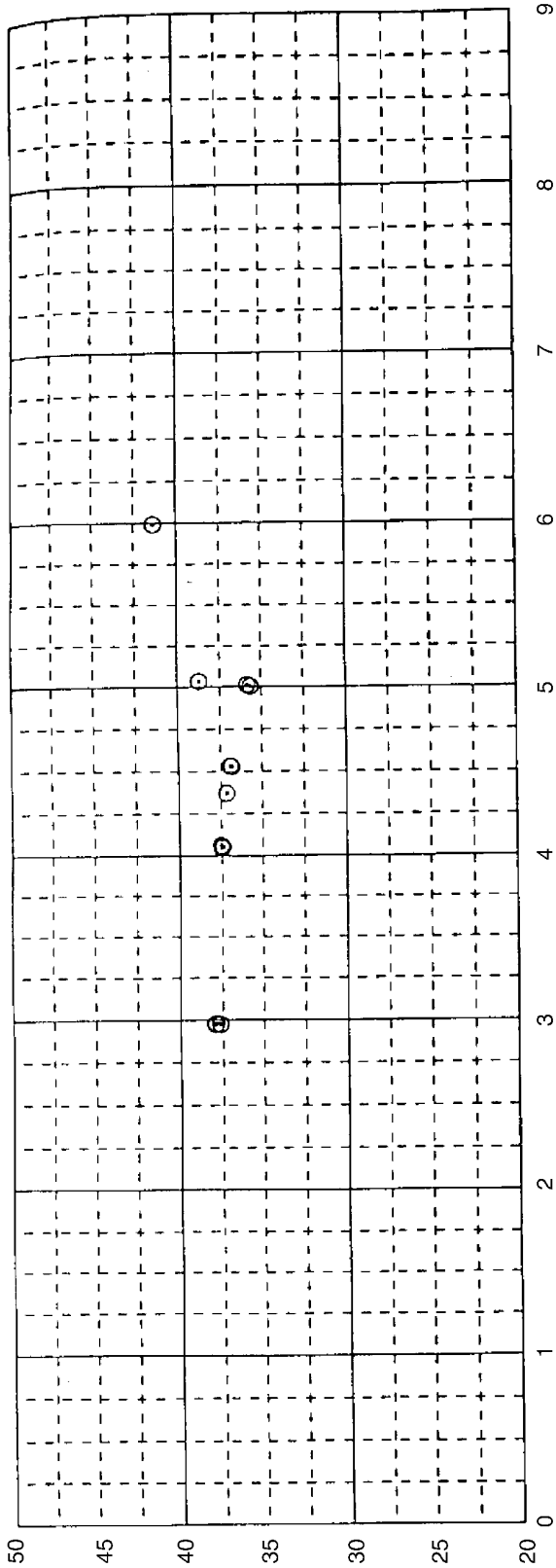
Run #	Net Weight lb.	Run Duration secs.	Line Temp Deg F	Flow GPM	H Line FT H ₂ O	H-Loss Reading	H-Loss Feet Gross	Pipe Loss Feet	H-Loss Feet Net	Loss Percent of Differential
1	95608	137.376	92	5036.	3.945	8.7622	1.7735	0.2457	1.5278	38.7
2	95498	137.826	92	5014.	3.901	8.2608	1.6422	0.2437	1.3986	35.8
3	95468	137.998	92	5006.	3.893	8.2170	1.6307	0.2429	1.3878	35.6
4	95317	157.750	91	4372.	2.970	6.9282	1.2932	0.1893	1.1039	37.2
5	95387	152.299	91	4532.	3.179	7.2479	1.3769	0.2023	1.1747	36.9
6	95442	152.439	91	4530.	3.181	7.2349	1.3735	0.2021	1.1714	36.8
7	95362	169.820	91	4063.	2.550	6.2781	1.1230	0.1654	0.9575	37.5
8	95337	170.096	91	4055.	2.553	6.2684	1.1204	0.1649	0.9556	37.4
9	95297	170.240	91	4050.	2.545	6.2636	1.1192	0.1645	0.9547	37.5
12	95166	231.282	91	2977.	1.381	4.3311	0.6131	0.0933	0.5198	37.6
13	95197	231.322	91	2977.	1.378	4.3283	0.6124	0.0933	0.5190	37.7
14	95116	231.060	91	2978.	1.369	4.3297	0.6127	0.0934	0.5194	37.9
15	95186	231.242	91	2978.	1.373	4.3363	0.6145	0.0334	0.5211	38.0
16	95663	115.496	91	5992.	5.617	4.0161	2.6595	0.3384	2.3211	41.3
17	95638	115.464	90	5992.	5.614	4.0168	2.6602	0.3383	2.3218	41.4

The data reported on herein was obtained by measuring equipment the calibration of which is traceable to NIST, following the installation and test procedure referenced in this report, resulting in a flow measurement uncertainty of ±0.25% or less.

Calibrated by S.V.K.

Certified by: _____signature

Appendix D: Calibration of a 16" V-Cone Spool Piece



81-6

H-Loss Percent of Differential

Flow GPM (in thousands)

Virginia Electric and Power Company
Purchase Order Number: BNT 466762
16" V-Cone Spool Piece
June 8, 1994

Head Loss

Certified By: *[Signature]*



VIRGINIA ELECTRIC AND POWER CO.
 Purchase Order Number: BNT 466762
 16" V-CONE SPOOL PIECE
 Downstream Elbow

CALIBRATION
 Date: June 8, 1994
 PIPE DIAMETER = 15.2500
 EQUIVALENT THROAT DIAMETER = 11.5075

Run #	Line Temp Deg F	Net Weight lb.	Run Duration secs.	Output (see note)	Flow GPM	H Line FT H ₂ O	Pipe Rey. # x 10 ⁶	Coef.
1	92	95749	103.464	7.303~	6697.	6.959	1.8539	0.8024
2	92	95608	114.347	6.342~	6051.	5.697	1.6769	0.8013
3	92	95478	114.257	6.330~	6048.	5.681	1.6778	0.8020
4	92	95412	138.664	4.929~	4980.	3.843	1.3816	0.8029
5	93	95352	138.606	4.931~	4979.	3.846	1.3828	0.8024
6	93	95448	138.852	4.927~	4975.	3.840	1.3833	0.8024
7	93	95262	153.680	4.371~	4486.	3.110	1.2488	0.8041
8	93	95367	154.004	4.374~	4482.	3.114	1.2490	0.8028
9	93	95427	154.170	4.370~	4480.	3.109	1.2498	0.8031
10	93	95327	171.202	3.917~	4030.	2.514	1.1256	0.8033
11	93	95307	171.153	3.905~	4030.	2.498	1.1257	0.8060
12	93	95317	171.210	3.918~	4029.	2.515	1.1254	0.8031
13	93	95156	354.337	2.438~	1943.	0.572	0.5447	0.8124
14	93	94966	353.708	2.439~	1943.	0.573	0.5446	0.8111
15	93	95076	354.078	4.209~	1943.	0.580	0.5447	0.8065
16	94	95096	354.178	4.216~	1943.	0.582	0.5453	0.8051
17	94	95106	229.191	7.276~	3003.	1.387	0.8427	0.8061
18	94	95217	229.464	7.287~	3003.	1.390	0.8446	0.8053

For Pipe Rey. #s above 0.50 x 10⁶ Avg Coef = 0.8046 With Standard Deviation = 0.0030

The data reported on herein was obtained by measuring equipment the calibration of which is traceable to NIST, following the installation and test procedures referenced in this report, resulting in a flow measurement uncertainty of ±0.25% or less.

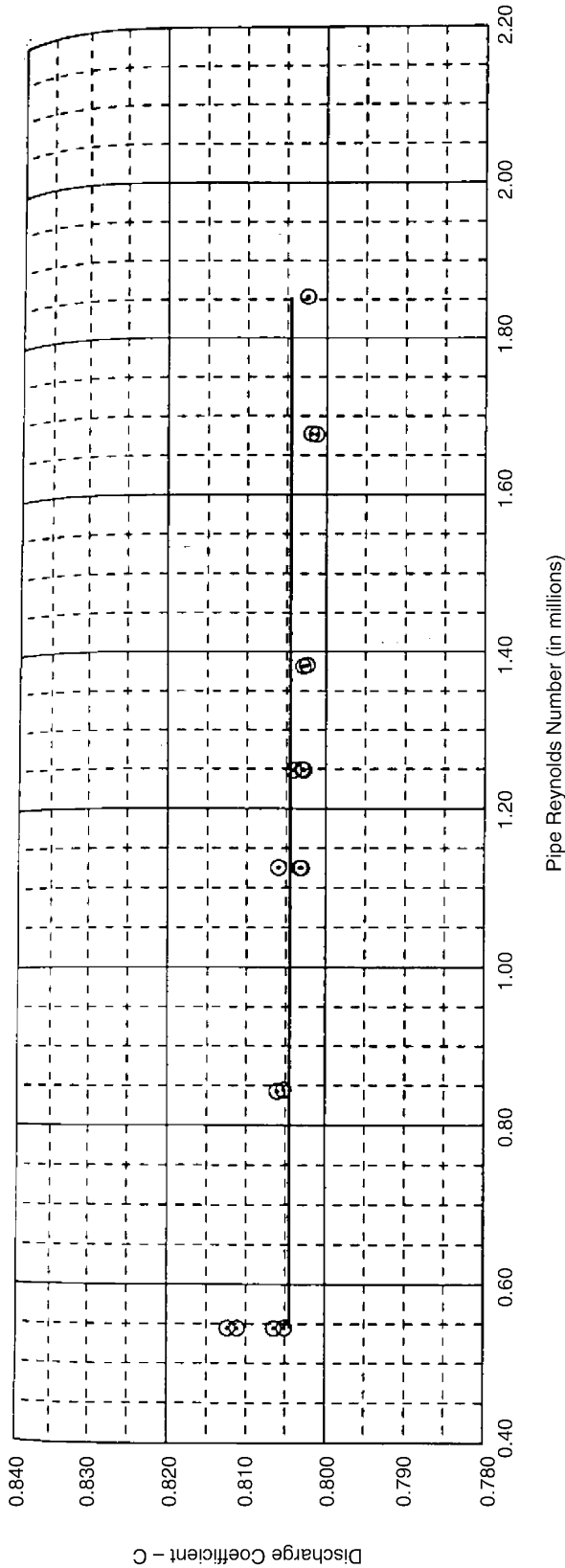
~ dp transmitter volts

Calibrated by S.V.K.

Certified by: _____signature

ARL

Appendix D: Calibration of a 16" V-Cone Spool Piece



Virginia Electric and Power Company
 Purchase Order Number: BNT 466762
 16" V-Cone Spool Piece
 June 8, 1994

Downstream Elbow



Certified By: *J. B. D. P. L.*

$q_a = C F_a K_M \sqrt{\Delta h}$	
q_a = Actual Flow (ft ³ /sec)	= 7.0466
C = Discharge Coefficient (Dimensionless)	= 1.0004
Δh = Pressure Differential (Feet of Water at Run Temperature)	= 0.7223
K_M = Meter Constant = $\frac{a\sqrt{2g}}{\sqrt{1 - \beta^4}}$	= 32.1625
F_a = Average Thermal Expansion Factor	= 0.7546
a = Throat Area (ft ²)	= 15.2500
g = Local Acceleration of Gravity (ft/sec ²)	= 11.5075
β = Ratio of Throat to Pipe Diameter (Dimensionless)	= 0.8046
Pipe Diameter (Inches)	
Throat Diameter (Inches)	

For Pipe Reynolds Number > 0.50 x 10⁶ avg coefficient
 Dimensions By: VIRGINIA ELECTRIC AND POWRE CO.

EPRI Licensed Material

VIRGINIA ELECTRIC AND POWER CO.
 Purchase Order Number: BNT 466762
 16" V-CONE SPOOL PIECE
 Downstream Tee with Cross Flow

CALIBRATION
 Date: June 7, 1994
 PIPE DIAMETER = 15.2500
 EQUIVALENT THROAT DIAMETER = 11.5075

Run #	Line Temp Deg F	Net Weight lb.	Run Duration secs.	Output (See Note)	Total Flow GPM	Bypass Flow GPM	V-Cone Flow GPM	V-Cone Head FT H ₂ O	Pipe Reynolds # x 10 ⁶	V-Cone Coefficient
1	89	95949	95.024	2.994~	7303.8	4361.2	2942.6	1.318	0.803	0.8101
2	90	95578	122.555	2.673~	5641.5	3271.6	2369.9	0.895	0.647	0.7915
3	90	95949	81.190	3.405~	8549.5	5063.9	3485.6	1.857	0.951	0.8083
4	90	95909	81.173	3.426~	8547.8	5055.7	3492.1	1.884	0.953	0.8040
5	90	96471	63.859	4.316~	10929.3	6474.3	4455.0	3.053	1.216	0.8058
6	90	96441	63.874	4.305~	10923.7	6470.0	4453.7	3.038	1.215	0.8075
7	91	96090	80.480	3.496~	8638.5	5055.7	3582.8	1.977	0.978	0.8054
8	91	95954	80.366	3.482~	8638.7	5065.8	3572.9	1.959	0.975	0.8069
9	91	96241	71.322	4.835~	9763.5	4848.4	4915.1	3.735	1.341	0.8038
10	91	96190	71.334	4.821~	9756.9	4840.7	4916.2	3.717	1.341	0.8060
11	91	96502	63.494	6.289~	10997.5	4932.5	6065.0	5.645	1.655	0.8068
12	91	96371	63.430	6.281~	10993.9	4944.7	6049.2	5.634	1.651	0.8055
13	92	95909	74.886	4.141~	9267.8	4986.6	4281.2	2.824	1.168	0.8052
14	92	95965	74.899	4.155~	9271.7	4965.2	4306.5	2.842	1.175	0.8074
15	92	95422	133.828	2.523	5160.0	3079.3	2080.7	0.699	0.568	0.7866
16	92	95528	133.920	2.529~	5162.3	3058.2	2104.1	0.707	0.574	0.7912
17	92	95678	101.435	2.321~	6826.5	5132.0	1694.5	0.434	0.462	0.8129
18	92	95678	101.395	2.325~	6829.4	5131.1	1698.3	0.439	0.463	0.8106
19	93	95638	118.436	6.001~	5844.9	0.0	5844.9	5.268	1.595	0.8049
20	93	95558	118.481	5.984~	5837.9	0.0	5837.9	5.246	1.593	0.8055

~dp transmitter volts

ARL

EPRI Licensed Material

VIRGINIA ELECTRIC AND POWER CO.
 Purchase Order Number: BNT 466762
 16" V-CONE SPOOL PIECE
 Downstream Tee with Cross Flow

CALIBRATION
 Date: June 7, 1994
 PIPE DIAMETER = 15.2500
 EQUIVALENT THROAT DIAMETER = 11.5075

Run #	Line Temp Deg F	Net Weight lb.	Run Duration secs.	Output (See Note)	Total Flow GPM	Bypass Flow GPM	V-Cone Flow GPM	V-Cone Head FT H ₂ O	Pipe Reynolds # x 10 ⁶	V-Cone Coefficient
21	93	95357	140.528	4.813~	4911.6	0.0	4911.6	3.707	1.340	0.8062
22	93	95468	140.680	4.823~	4912.2	0.0	4912.2	3.721	1.340	0.8048
23	93	95347	154.470	4.331	4468.1	0.0	4468.1	3.075	1.219	0.8053
24	93	95437	154.608	4.324~	4468.4	0.0	4468.4	3.065	1.219	0.8067
25	94	95176	230.640	3.033	2987.3	0.0	2987.3	1.369	0.815	0.8070
26	94	95197	230.811	3.022~	2985.8	0.0	2985.8	1.355	0.815	0.8106
27	94	95126	230.911	3.032~	2982.3	0.0	2982.3	1.367	0.814	0.8060
28	94	95056	336.391	2.478~	2045.8	0.0	2045.8	0.640	0.558	0.8081
29	94	95066	336.547	2.478~	2045.1	0.0	2045.1	0.640	0.558	0.8081

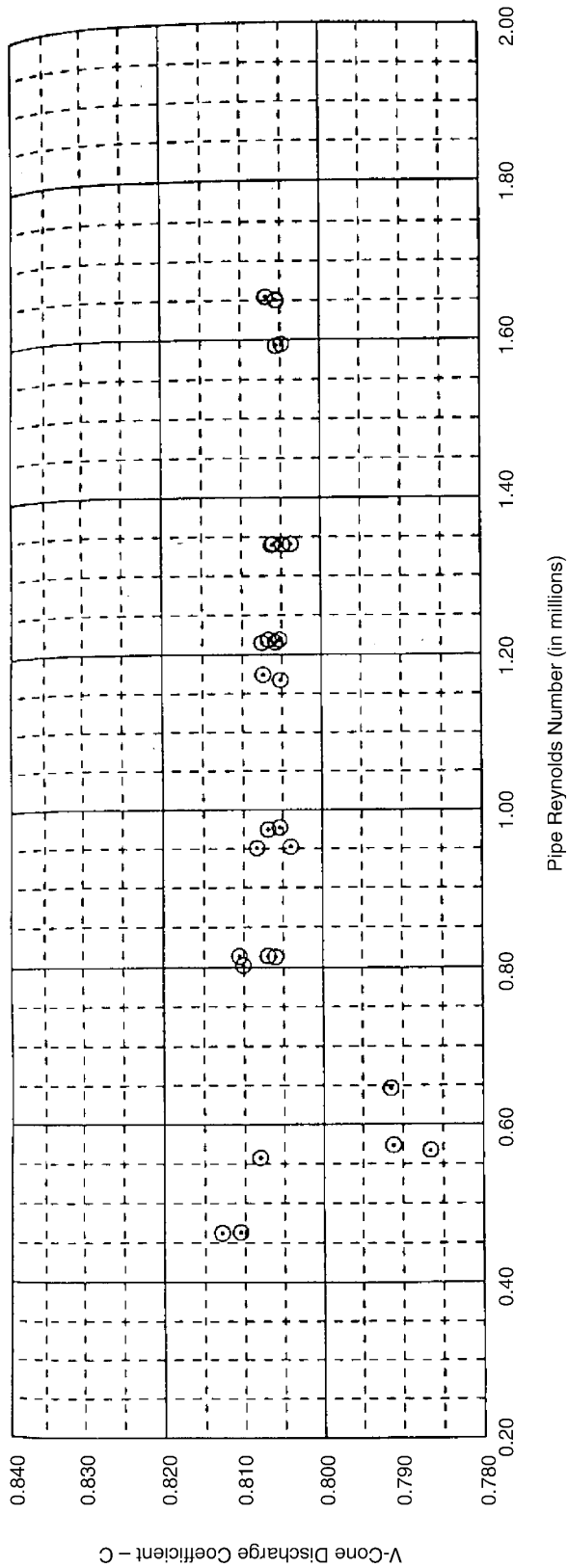
~ dp transmitter volts

The data reported on herein was obtained by measuring equipment the calibration of which is traceable to NIST, following the installation and test procedures referenced in this report, resulting in a flow measurement uncertainty of $\pm 0.25\%$ or less.

Calibrated by S.V.K.

Certified by: _____signature

ARL



$q_a = C F_a K_M \sqrt{\Delta h}$	
q_a = Actual Flow (ft ³ /sec)	
C = Discharge Coefficient (Dimensionless)	
Δh = Pressure Differential (Feet of Water at Run Temperature)	
K_M Meter Constant = $\frac{a\sqrt{2g}}{\sqrt{1-\beta^4}}$	7.0466
F_a = Average Thermal Expansion Factor	1.0004
a = Throat Area (ft ²)	0.7223
g = Local Acceleration of Gravity (ft/sec ²)	32.1625
β = Ratio of Throat to Pipe Diameter (Dimensionless)	0.7546
Pipe Diameter (Inches)	15.2500
Throat Diameter (Inches)	11.5075
Dimensions By:	

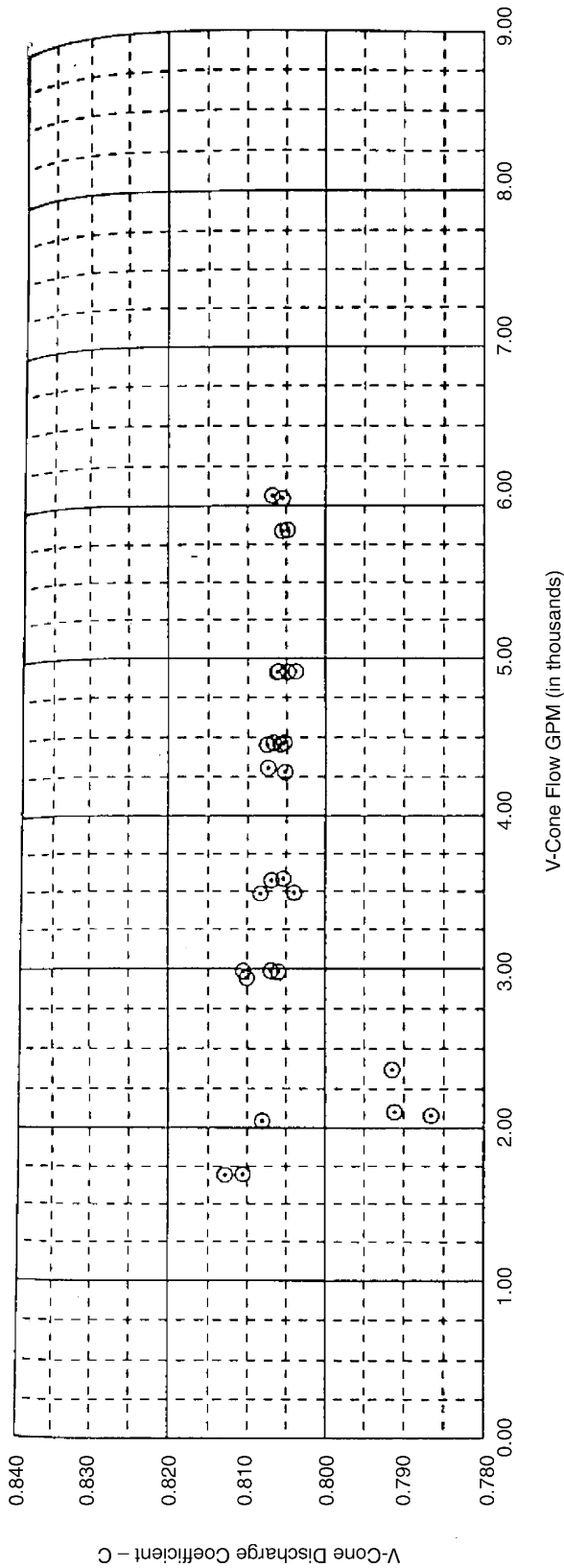
Virginia Electric and Power Company
 Purchase Order Number: BNT 466762
 16" V-Cone Spool Piece
 June 7, 1994

Downstream Tee with Cross Flow

Certified By: *J. B. Decker*



Appendix D: Calibration of a 16" V-Cone Spool Piece



Virginia Electric and Power Company
 Purchase Order Number: BNT 466762
 16" V-Cone Spool Piece
 June 7, 1994

Downstream Tee with Cross Flow

Certified By: *J. B. [Signature]*



$q_a = C F_a K_M \sqrt{\Delta h}$	
q_a = Actual Flow (ft ³ /sec)	
C = Discharge Coefficient (Dimensionless)	
Δh = Pressure Differential (Feet of Water at Run Temperature)	
K_M = Meter Constant = $\frac{a\sqrt{2g}}{\sqrt{1-\beta^4}}$	7.0466
F_a = Average Thermal Expansion Factor	1.0004
a = Throat Area (ft ²)	0.7223
g = Local Acceleration of Gravity (ft/sec ²)	32.1625
β = Ratio of Throat to Pipe Diameter (Dimensionless)	0.7546
Pipe Diameter (Inches)	15.2500
Throat Diameter (Inches)	11.5075
Dimensions By:	

UNCERTAINTY ANALYSIS
VIRGINIA ELECTRIC AND POWER COMPANY 16" V-CONE

An analysis of the test result uncertainty was conducted by evaluating each elementary error source for the measurement of flow, differential head, and meter constants. The precision uncertainties were estimated from the test data and systematic uncertainties were estimated from experience.

Since an essentially full weigh tank (about 95,000 lb.) was used in all flow measurements, the uncertainties for mass determination are essentially constant. Time measurement uncertainties are relatively low and, for a conservative estimate, the minimum time was used to determine the percent uncertainties. Differential pressure measurement uncertainty is a function of the pressure level, which is dependent on Reynolds number (flow). The precision index of the average differential pressure was determined as the standard deviation of the measured differential pressure divided by the square root of the number of readings minus one. Since data was recorded at 34 Hz for the entire mass collection period, the number of points was greater than 4600. The precision index of the average was calculated as a percent of reading for each test and is plotted versus flow. The maximum precision index, 0.12%, will be used in the analysis of overall uncertainty to achieve a conservative estimate applicable to all tests.

Tables 9-2 through 9-6 list the elementary error sources for each measured component and combine the sources by the root sum square (RSS) method to obtain the overall discharge uncertainty in Table 9-7 of about 0.16% at the 95% confidence level.

VEPCO 16" V-CONE

**Table 9-2
Mass Uncertainty**

	<u>Systematic</u>	<u>Random</u>
Calibration	56.97	NA
Buoyancy	13	NA
Reading	NA	5
Hysteresis	NA	30
Ageing	30	NA
Leakage	2	NA
<hr/>		
RSS Uncertainty (lb)	65.71	30.41
RSS Uncertainty at (%) 95126	0.0691	0.0320

**Table 9-3
Time Uncertainty**

	<u>Systematic</u>	<u>Random</u>
Time Standard	0.0005	NA
Resolution	NA	0.001
Trigger	0.0054	0.002
<hr/>		
RSS Uncertainty (sec)	0.0058	0.0022
RSS Uncertainty at (%) 137.376	0.0043	0.0016

**Table 9-4
Density Uncertainty Percent at 100F**

	<u>Systematic</u>	<u>Random</u>
Temperature	0.02	0.01
Impurities	0.0106	NA
<hr/>		
RSS Uncertainty (%)	0.0226	0.0100

VEPCO 16" V-CONE

**Table 9-5
Overall Flow Uncertainty (%)**

	<u>Systematic</u>	<u>Random</u>
Mass	0.0691	0.0320
Time	0.0043	0.0016
Diverter	0.0250	NA
Density	0.0226	0.0100
<hr/>		
RSS Uncertainty (%)	0.00770	0.0335

**Table 9-6
Differential Pressure Uncertainty Uncertainties in % of Reading**

	<u>Systematic</u>	<u>Random</u>
Calibration	0.040	NA
Span and Zero	0.015	NA
Fluctuations	NA	0.120
Temperature Correction	0.0356	0.018
Thermal Gradients	0.019	NA
<hr/>		
RSS Uncertainty (%)	0.059	0.121
Discharge Coefficient	0.059	0.121
Sensitivity = 0.5		
Student T - 2		

**Table 9-7
Discharge Coefficient Uncertainty**

	<u>Systematic</u>	<u>Random</u>
Flow	0.077	0.034
Differential Head	0.059	0.121
Thermal Expansion	0.010	NA
Local Gravity	0.0008	NA
Meter Dimensions	0.037	NA
<hr/>		
RSS Uncertainty (%)	0.1042	0.1259
<hr/>		
Total Uncertainty URSS (%)	0.163	
95% Confidence Level		

Appendix D: Calibration of a 16" V-Cone Spool Piece

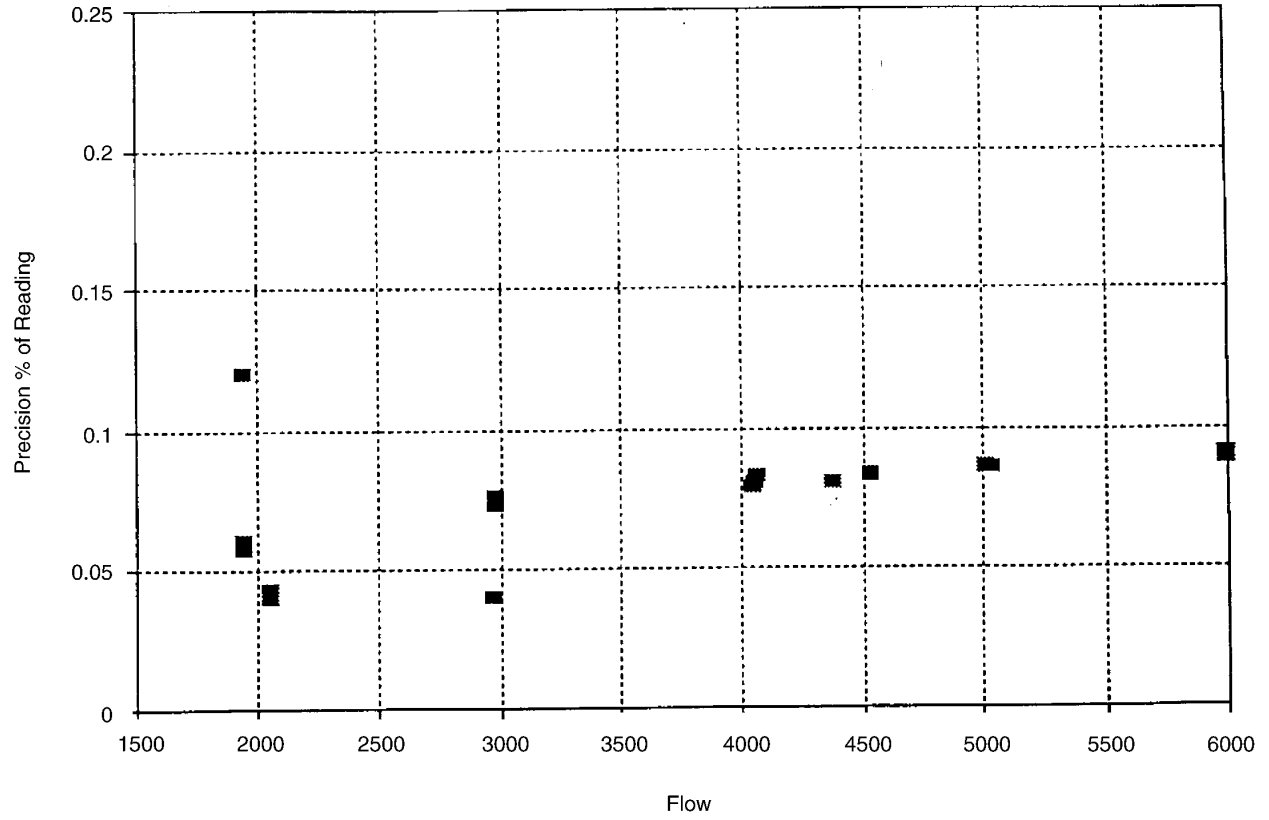


Figure 9-5
Precision Index of Mean Head

Thermal Expansion Factor

The dimensions of a primary flow element are affected by the operating temperature, requiring a Thermal Expansion Factor (F_a) to be included in the calculations. The calculation requires the temperature at which the meter dimensions were measured be known. If this information is not available, an ambient temperature of 70°F is assumed. The Thermal Expansion Factor is calculated according to the American Society of Mechanical Engineers Standard ASME MFC-3M-1985, Equation 17 (pg 10).

$$F_a = 1 + \frac{2}{(1 - \beta^4)} (\alpha_{pE} - \beta^4 \alpha_p) (t - t_{meas}) \quad (\text{Eq. 9-5})$$

Where:

- β = ratio of throat diameter to pipe diameter, dimensionless
- α_{pE} = thermal expansion factor of primary element, F
- α_p = thermal expansion factor of pipe, F
- t = temperature of flowing fluid, F
- t_{meas} = temperature of measurements, F

Thermal expansion factors, α , excerpted from MFC-3M-1985, are listed in Table 9-8 below for six typically used materials at three temperatures. Linear interpolation is used to determine the coefficients at the line temperature.

Table 9-8
Thermal Expansion Factors x 10⁶

Material	-50F	70F	200F
Carbon Steel (low chrome)	5.80	6.07	6.38
Intermediate Steel (5 to 9 Cr-Mo)	5.45	5.73	6.04
Austenitic stainless steels	8.90	9.11	9.34
Straight chromium stainless steel	5.00	5.24	5.50
Monel (67Ni-30Cu)	7.15	7.48	7.84
Bronze	9.15	9.57	10.03

Appendix D: Calibration of a 16" V-Cone Spool Piece

Table 9-9
Density of Water and Mercury

Temperature Fahrenheit	Water Density lb _m /ft ³	Mercury Density lb _m /ft ³	Temperature Fahrenheit	Water Density lb _m /ft ³	Mercury Density lb _m /ft ³
32	62.4179	848.717	73	62.2774	846.409
33	62.4201	848.632	74	62.2692	846.324
34	62.4220	848.546	75	62.2608	846.239
35	62.4235	848.461	76	62.2522	846.153
36	62.4246	848.375	77	62.2434	846.068
37	62.4255	848.290	78	62.2344	845.982
38	62.4260	848.205	79	62.2252	845.897
39	62.4262	848.119	80	62.2159	845.811
40	62.4261	848.034	81	62.2063	845.726
41	62.4257	847.948	82	62.1966	845.640
42	62.4250	847.863	83	62.1868	845.555
43	62.4240	847.777	84	62.1767	845.469
44	62.4227	847.692	85	62.1665	845.384
45	62.4211	847.606	86	62.1561	845.298
46	62.4193	847.521	87	62.1456	845.213
47	62.4171	847.435	88	62.1348	845.127
48	62.4147	847.350	89	62.1239	845.042
49	62.4121	847.264	90	62.1129	844.956
50	62.4092	847.179	91	62.1017	844.871
51	62.4060	847.093	92	62.0903	844.785
52	62.4025	847.008	93	62.0788	844.700
53	62.3988	846.922	94	62.0671	844.614
54	62.3949	846.837	95	62.0552	844.529
55	62.3907	846.751	96	62.0432	844.443
56	62.3863	846.666	97	62.0311	844.358
57	62.3816	846.580	98	62.0188	844.273
58	62.3768	846.495	99	62.0063	844.187
59	62.3716	846.409	100	61.9937	844.102
60	62.3663	846.324	101	61.9810	844.016
61	62.3607	846.239	102	61.9681	843.931
62	62.3549	846.153	103	61.9551	843.845
63	62.3489	846.068	104	61.9419	843.760
64	62.3427	845.982	105	61.9286	843.674
65	62.3363	845.897	106	61.9151	843.589
66	62.3296	845.811	107	61.9015	843.503
67	62.3228	845.726	108	61.8878	843.418
68	62.3157	845.640	109	61.8739	843.332
69	62.3084	845.555	110	61.8599	843.247
70	62.3010	845.469	111	61.8458	843.161
71	62.2933	845.384	112	61.8315	843.076

ARL INSTRUMENT TRACEABILITY TO NIST
VIRGINIA ELECTRIC AND POWER COMPANY
PURCHASE ORDER NUMBER 466762

Calibration Dates: June 7 & 8, 1994

I. Weigh Tank Calibrations

a) Weight Transfer Standards

1. GURLEY Stainless Steel Weights (Set of 6)

Massachusetts Test No. 9091-F039

NIST Test No. 42587

Calibration Date: 1/11/91

Due Date: 1/11/96

2. GURLEY Stainless Steel 20 lb.

Massachusetts Test No. 9091-F038

NIST Test No. 42587

Calibration Date: 1/8/91

Due Date: 1/8/96

3. ARL Cast Iron Transfer Weight (50 lb)

Massachusetts Test No. 9091-F037

NIST Test No. 42587

Calibration Date: 1/7/91

Due Date: 1/7/96

4. ARL Cast Iron Transfer Weights (10,000lb)

ARL Calibration with Transfer Standards

Calibration Date: 9/8/93

Due Date: 9/8/95

b) ARL Weigh Tanks

1. TOLEDO 100,000 lb. ARL SN 0756 Building 1 Lines 1 & 2

Calibration Date: 4/20/94

Due Date: 10/20/94

2. TOLEDO 10,000 lb. ARL SN 0757 Building 1 Line 3

Calibration Date: 4/26/94

Due Date: 10/26/94

3. FAIRBANKS 50,000 lb. ARL SN 101 2 Building 2 Lines 1 & 2

Calibration Date: 3/4/94

Due Date: 9/4/94

4. THURMAN 10,000 lb. ARL SN 1018 Building 2 Line 4

Calibration Date: 3/2/94

Due Date: 9/2/94

ARL INSTRUMENT TRACEABILITY TO NIST
VIRGINIA ELECTRIC AND POWER COMPANY
PURCHASE ORDER NUMBER 466762

Calibration Dates: June 7 & 8, 1994

II. Timer Calibrations

a. Timer Transfer Standard

Crystal Oscillator ARL SN 0129

Calibrated Weekly versus NIST STATION WWV

Calibration Date: 6/6/94

Due Date: 6/13/94

b. Timers

1. Hewlett-Packard Counter ARL SN 0105 Building 1 Lines 1 & 2

2. DIGITEC Counter SN 8150 Building 1 Line 3

3. Hewlett-Packard Counters ARL SN 1013 & 0032 Building 2

Frequency Checked Daily

III. Thermometer Calibrations

a. Temperature Transfer Standard

1. THERMOMETRICS S-10 Thermistor SN 189

NIST Test No. 229549, 222047, 229192

Calibration Date: 10/2/92

Due Date: 10/2/95

b. ARL Line Temperature Thermometers

1. OMEGA DP41-RTD Thermometer ARL S/N 0469, 0470 & 0471

Calibration Date: 4/18/94

Due Date: 10/18/94

2. OMEGA Thermometer ARL SN 0119 Building 2 Line 1

Calibration Date: 4/18/94

Due Date: 10/18/94

3. OMEGA Thermometer ARL SN 0159 Building 2 Line 4

Calibration Date: 4/18/94

Due Date: 10/18/94

10

APPENDIX E: CROSS-CORRELATION ULTRASONIC FLOWMETER EVALUATION TESTS

Case Study

1.0 Introduction

This case study describes a series of blind tests performed to evaluate the performance of CROSSFLOW, a cross-correlation ultrasonic flow meter. The tests were performed at the EVEREST Flow Laboratory, Chatou, France between September 9-11, 1998. This facility is operated by Electricite de France(EdF) to calibrate or evaluate the accuracy of any flow meter.

These tests were performed specifically at the EVEREST Flow Laboratory because Electricite de France was looking for a flow meter that can be used to calibrate in-situ existing pressure differential flow meters at their power plants. The current practice is to periodically remove the installed pressure differential flow meters and send them for calibration. Obviously, an in-situ calibration, if it can be done, will be cheaper.

To perform an in-situ calibration, EdF requires the calibrating flow meter to satisfy the following criteria:

- it must be non-intrusive so that the existing configuration is not disturbed
- it must be accurate to within less than 1% at different flow rates (different Reynolds Number)
- it should be easy to install
- it must have acceptable reproducibility error, since it may be used at different plants.

2.0 Test Facility

The test facility at the Everest Flow Laboratory is divided in three functional sections:

1. Operation section which comprised of the pump, the heat exchanger, the pressurizer, the feed tanks, and the flow, pressure and temperature controllers
2. Reference section where very accurate calibrated reference flow meters are installed.
3. Test section where the meter under test is installed

The Everest loop has a digital control system (SNCC). All measurements are taken by SNCC and transmitted to the data acquisition system PATERN. The operating conditions of the facility are as follows:

**Table 10-1
Operating Conditions**

Parameter	Range of Operation	Stability
Flow	5 cu. M/h to 1100 cu. M/h	±1%
Temperature	20 deg C to 60 deg C	±1 deg C
Pressure	3 to 5 bars	=/-0.1 bar

The reference section is divided into two flow measurement systems in series. The first has three magnetic flow meters and one Coriolis flow meter. The other section has a venturi and a reducer.

These different flow meters measure flow using different principles. This combination of flow meters eliminates common mode source of errors since each one has a different sensitivity to different source of external perturbations that can affect the flow measurement

3.0 Cross-Correlation Flow Meter – Meter Under Test

The flow meter under test is a cross-correlation flow meter manufactured by AMAG (Advanced Measurement & Analysis Group, Inc.). A block diagram of its components are given in Figure 10-1 below.

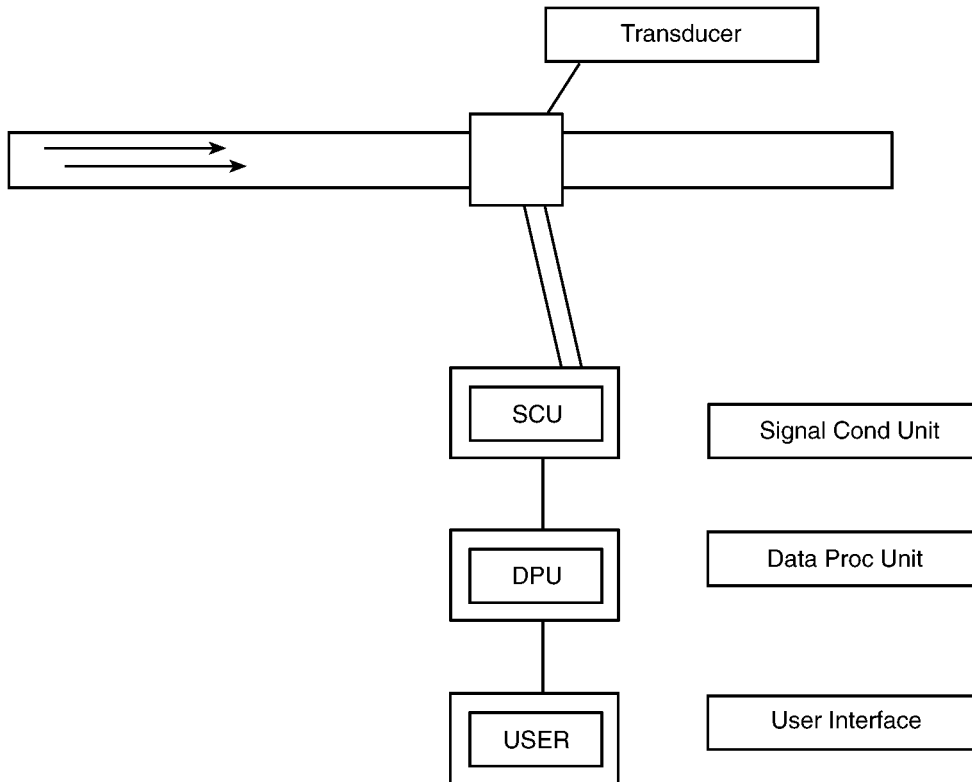


Figure 10-1
Cross-Correlation Flow Meter Block Diagram

4.0 Test Configurations

There were two test configurations: (a) a straight pipe configuration, where the meter under test was installed far enough away from the nearest elbow so that the flow profile was fully developed (b) a pipe configuration simulating the Bugey Nuclear Power Plant feed water configuration.

5.0 Reference Tests - Straight Pipe Configuration

For this configuration, the objective of the tests was two-fold:

1. to evaluate the accuracy of the meter under test with different flow rates (Reynolds number from $3.7 * 10^5$ to $1.4 * 10^6$). Four flow rates were used. For each flow rate, the flow was measured with the cross-correlation meter for at least 0.5 hour. The average flow rate was compared with the Loop instrumentation.
2. to determine the reproducibility of the measured flows when the transducer is installed and de-installed. For this test, the flow rate was maintained steady at all times. The reproducibility tests consisted of removing the probes from the transducer frames and then re-installing them and removing probes and bracket and re-installing them. The frames were also rotated and re-installed.

This reference pipe configuration used a carbon steel pipe with an internal diameter of 35.6 cm. Downstream of a 90 degree elbow, a flow straightener was installed. The meter under test was installed more than 40 diameters downstream of the flow straightener thus ensuring a fully developed flow profile.

The flow loop used several reference meters. The accuracy of the loop instrumentation is $\pm 0.30\%$.

5.1 Results – Meter Performance with Different Flow Rates

The results of the test are given in Table 10-2 below.

Table 10-2
Performance with Different Flow Rates¹ EdF – Everest Flow Laboratory, Chatou France
September 9-10, 1998

Test #	Date	Start	End	CROSSFLOW (MUT) ²	CHATOU	DIFF(%)
1	9-Sep	16:26	16:54	1082.73	1084.54	0.17%
2	9-Sep	16:58	17:29	901.19	902.7	0.17%
3	9-Sep	17:35	18:06	701.21	699.73	-0.21%
4	10-Sep	8:25	9:22	589.43	590.53	0.19%

Average Difference = +0.08%

Standard Deviation = ±0.19%

Note that the agreement between the CROSSFLOW – cross-correlation flow meter under test and the Everest Loop instrumentation is less than ±0.2%. The Everest Loop instrumentation has an accuracy of ±0.3%.

¹ Flow Rates in m³/h

² MUT – Meter Under Test

5.2 Results – Reproducibility Tests

The purpose of this test is to determine the reproducibility of the measurement results when the transducer components (probes, frame) are removed and re-installed at approximately the same location under a specified flow condition.

Table 10-3
Reproducibility Tests – Flow Rate³ Constant EdF – Everest Flow Laboratory, Chatou
France – September 10, 1998

Test #	Comments	Start	End	CROSSFLOW (MUT) ⁴	CHATOU (REF) ⁵	DIFF(%)
1	Probes removed and re-installed.	10:16	10:38	1076.82	1079.46	0.24%
2	Probes removed. Frame loosened & reinstalled.	10:43	11:15	1077.75	1079.49	0.10%
3	Probes removed. Frame loosened, displaced, reinstalled.	11:18	11:45	1078.61	1079.59	0.09%
4	Probes removed. Frame loosened, rotated, reinstalled.	11:48	12:09	1076.73	1079.59	0.26%
5	Probes removed. Frame loosened, removed, re-installed.	12:23	12:34	1078.57	1079.56	0.09%
6	Probes removed. Frame loosened, move sideways, reinstalled.	14:06	14:27	1080.57	1079.70	-0.08%
7	Probes removed, Frame loosened rotated and moved sideways, reinstalled.	14:38	15:00	1078.99	1079.58	0.05%
8	Rec & trans probes interchanged. Frame loosened & reinstalled.	15:06	15:26	1080.78	1079.59	-0.11%
9	Probes removed. Frame loosened, rotated, displaced, reinstalled.	15:35	15:53	1080.86	1079.58	-0.12%

Average Difference = 0.07%
Std Deviation = ±0.15%

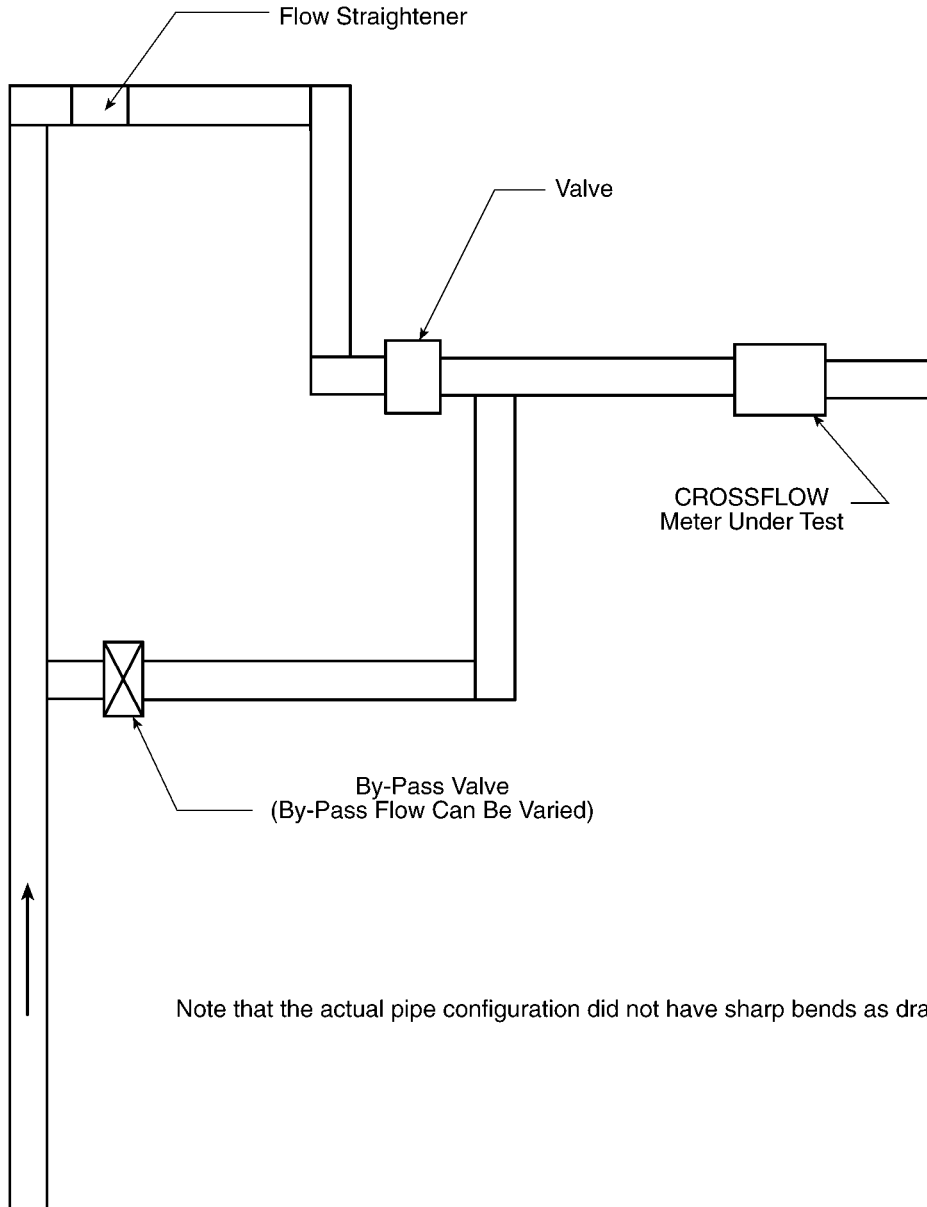
³ Flow Rates in m³/h

⁴ MUT – Meter Under Test

⁵ REF – Reference Meters (Everest Loop)

6.0 Bugey Pipe Configuration

The Bugey pipe configuration is a more complicated piping arrangement than the reference test configuration above. An oversimplified schematic diagram of the piping configuration is given below.



Note that the actual pipe configuration did not have sharp bends as drawn here.

Figure 10-2
Piping Configuration Diagram

The purpose of this test was to derive an empirical calibration factor that can be used in the actual plant. Extrapolation to the actual operating conditions (higher Reynolds number) was done using a theoretical curve for the cross-correlation meter that predicts the effect of higher temperature and pressure.

The tests included setting the flow rate to maximum and then varying the by-pass flow rate. Then the maximum by-pass flow (20%), the orientation of the transducer was changed to determine the effect on the calibration factor.

6.1 Results – Calibration Factor for the Bugey Configuration

The results showed that relative to the reference pipe configuration (straight pipe), the calibration factor for the Bugey configuration is increased by approximately 2%. The results also showed that there was no significant dependence on the transducer orientation.

6.2 Results – Measurement at the Bugey Nuclear Power Plant

Actual measurement was performed at the Bugey Nuclear Power Plant using the calibration factor obtained from the Everest Laboratory but extrapolated to high Reynolds Number using a theoretical formula.

The plant instrumentation is a pressure differential device. The results of the measurement showed that the plant flow and the cross-correlation flow agreed to within less than 0.5%.

7.0 CONCLUSION

This case study demonstrated that for a fully developed flow, the cross-correlation flow meter accuracy is less than 0.5%.

The case study also demonstrated that for complicated pipe geometries, a scale model of the actual pipe configuration can be built to derive the appropriate calibration factor. Extrapolation to high Reynolds Number – actual operating conditions was demonstrated by actual measurement at the Bugey Nuclear Power Plant.

11

APPENDIX F: ULTRASONIC FLOWMETER SITE SETUP

SITE SELECTION

Select the best site available using the manufacturer's guidelines on upstream and downstream pipe diameters. These should be considered as minimums since many pipe configurations (particularly multiple elbows out of plane) require much longer upstream runs without flow disturbances. If these minimums cannot be met, choose the best available site and perform multiple rotation checks. Horizontal pipes are preferred but vertical pipes with flow going in the up direction (to ensure that the pipe is full) can be used.

SITE PREPARATION

Make a template for each site. Measure and mark the flowmeter path locations for each flow profile rotation position on the template. This ensures that the beams for each path (for the number of flow profile rotations being planned) are evenly spaced and that the transducers are 180 degrees apart (if using the direct or two pass flowmeter set up methods).

Set up the flowmeter at the first position on the pipe using the template and the following guidelines:

1. Dual beams should be used on pipes with diameters of 10 inches and larger.
2. A minimum of three positions (rotations) for flow profile are recommended but more can be performed (i.e. on less than ideal locations or when using a single beam set up on pipes large enough to perform flow profile rotations).
3. Positions should be evenly spaced unless physical plant configuration prevents this. As an example of a dual beam setup, position one would have beam #1 at 22.5° and beam #2 at 295.5° . Position two would have beam #1 at 45° and beam #2 at 315° . Position three would have beam #1 at 67.5° and beam #2 at 337.5° .

Appendix F: Ultrasonic Flowmeter Site Setup

Note: All positions are from an upstream facing downstream perspective with 0 degrees being the top of the pipe on horizontal pipes and the north side for vertical pipes.

4. Use a level to ensure that the tracks are level.
5. Using a grease pencil or permanent marker, outline the track and transducer locations on the pipe. This saves time when performing the rotation checks and ensures that the flowmeter is returned to the same location each time it is set up (by aligning the tracks with the outlined marks).
6. Remove all paint and/or rust from the transducer locations. This ensures the accuracy of the ultrasonic thickness readings and improves signal strength.
7. Repeat the above steps for the other flow rotation positions.
8. Remove the tracks from the pipe and take pipe OD readings using an outside micrometer or PI tape. Take five readings along the area of the beam paths, average them and use the result as input for the flowmeter.
9. Take ultrasonic thickness measurements. Take three readings along the contact point of each transducer and average the six readings for each beam (three for the upstream transducer and three for the downstream transducer). This number is supplied to the flowmeter for that beam.

If applicable a liner thickness is measured, if possible, or the nominal value must be used.

10. Continue with flowmeter set up at position one.

FLOW PROFILE ROTATION CHECK

Starting with position one, follow the steps below to determine the best position for the flowmeter and to calculate spatial bias. To ensure that the flowmeter setup is the same each time, note the serial number of the upstream and downstream transducers. At each location the diagnostics should be checked to ensure a usable signal. If using a Controlotron Model 990, an oscilloscope should be used to verify the "x" count (the count from the beginning of the signal to the beginning of the signal window). To save time while performing the rotation check, the flowmeter can be set up at each position and the setup can be verified and saved in the flowmeter's memory. All site setup parameters and diagnostic information should be recorded for each position.

Note: System flow must remain stable for the duration of the rotation checks. If there is a possibility that flow could change an additional flowmeter should be set up

on the pipe that flow changes can be detected. (This flowmeter need not be highly accurate since only changes need to be detected).

1. Ensure that system flow is appropriately equal to the flow that the meter will be used to measure.
2. Measure and record thirty-one or more 15 second averages of the flow.
3. Rotate the flowmeter to position two and repeat step #2. Repeat this step for position three and, if necessary, for the remaining rotation check positions.
4. Average the thirty-one 15 second averages for each position. Calculate the grand average flow for the entire rotation check and set up the flowmeter in the position that has the smallest flow deviation from the grand average flow.

COMPLETING THE FLOWMETER SETUP

After setting up the flowmeter in the final position, check all diagnostics (and "x" count if applicable) to verify proper flowmeter operation. Perform the following:

1. Zero the flowmeter if applicable.
2. Enter the calibration coefficient.
3. Take thirty-one or more 5 or 6 minute flow averages to calculate a precision index. System flow should be stable during this data collection.
4. Save the site into the flowmeter's memory.
5. Calculate the site uncertainty taking into account calibration bias, dimensional bias (including liner thickness if applicable), spatial bias, and precision index.
6. After completion of flowmeter set up, record all of the "As Left" site setup and diagnostic information.
7. Combine all data collected into a flowmeter flowsite setup report. This report should include the following information:

Flowsite location description and/or drawings indicating pipe configuration.

Pipe dimensional readings. Include the serial number and calibration date for the instruments used to obtain measurements.

Appendix F: Ultrasonic Flowmeter Site Setup

Transducer pair wet flow calibration report(s) for the proper pipe size and flow range.

If applicable, the flow profile rotation data. Include the site setup parameters, diagnostic readings, all flow readings and the average for each position of the rotation check.

All "As Left" data including rotation position used, site setup parameters, precision index data, and zeroing method used (if applicable).

12

APPENDIX G: FLOW METER INSTALLATION EFFECTS

Flow meter installation effects (FMIE) are the effects on flow meter performance that can result from the fact that "ideal" meter performance can be very different from their "non-ideal" conditions. As the number of non-ideal installations is essentially infinite, it is pertinent to study and assess only the prevalent installations that occur in normal practice. The National Institute of Standards and Technology, Fluid Flow group, Process Measurements Division, Chemical Science and Technology Laboratory, located in Gaithersburg, MD 20899, (NIST) has studied, using Laser Doppler Velocimetry (LDV), a number of installations and the FMIE produced on only certain kinds of meters. The following 2 papers present some of these results. Both of these papers were written by G. E. Mattingly and T.T. Yeh and are copied here with their permission.

Pipeflow Downstream Of A Reducer And Its Effects On Flowmeters

Abstract

The pipeflow profile and its influence on orifice coefficients downstream of a reducer have been studied experimentally in a 5.25 cm (2.07 in.) diameter water flow facility. The mean and turbulence velocities, obtained by laser Doppler velocimetry (LDV) are presented. From the measured velocity profiles, the profile characteristics of the pipeflow are described qualitatively and quantitatively. Several profile indexes are introduced to characterize the profile features (peaknesses and flow displacements). These indexes are then correlated with flowmeter performance in these flows. It is shown that these profile indexes correlate well with changes in discharge coefficient for the orifice meters and thus could be used to develop criteria for improving the performance of orifice meters or other types of meter in non-ideal installation conditions.

Keywords: orifice meters; pipeflow profile; laser Doppler velocimetry

Introduction

This paper presents results obtained in an industry-government consortium-sponsored research program on flowmeter installation effects being conducted at NIST-Gaithersburg, MD. The program is a cooperative research effort on generic technical issues to produce flow metering improvements needed by industry when meters are

installed in non-ideal conditions. Ideal meter installation conditions are those where long straight lengths of constant diameter precede the meter locations. Actual installations seldom conform to these conditions. The non-ideal condition is any of the infinitude of conditions where the upstream piping conditions produce pipeflow distributions that differ from those associated with fully developed flow. These non-ideal pipeflows can significantly affect the flowmeter performance.

Improvements for meter performance are sought from many starting points. Normally, meters are retrofitted into fluid systems that were not designed for them and are thus installed and operated in non-ideal installation conditions. Flow metering improvements are also desired for existing meter systems-either by upgrading the inlet flow conditions or by replacing the metering device itself so that accuracy levels are increased. Flow conditioning devices of one geometry or another are frequently recommend for improving flowmeter performance when installation conditions are not ideal, however, it has been shown that certain flow conditioner installations can produce serious deviations from the ideal installation performance of specific meters. To establish accurate flowmeter performance in the flows produced by different pipe configurations, we would have to understand the basic flow fields involved and how these interact with the specific meter geometry.

The objective of the NIST research program is (a) to produce a basic understanding of the flow phenomena that are produced in non-ideal pipe flows and to quantify these phenomena relative to reference fluid dynamic conditions; and (b) to correlate meter-factor shifts for flowmeters installed downstream from these pipeline elements with quantified flow features so as to be able to improve meter performance in non-ideal installations. The program is based upon measurements of pipeflows using laser Doppler velocimetry (LDV) and meter calibrations using transfer standards. This approach has been utilized in several different types of flowmeter installations downstream of several different pipe configurations.¹⁻⁵ These results have also been incorporated into the new standards on methods for establishing flowmeter installation effects.⁶

The pipeflow produced by conventional concentric reducers is the focus of the present experimental study. The piping configuration is sketched in Figure 12-1 with the coordinate system selected. The results given are the velocity profile measurements and the performance characteristics of a range of orifice meter geometries downstream of the reducer.

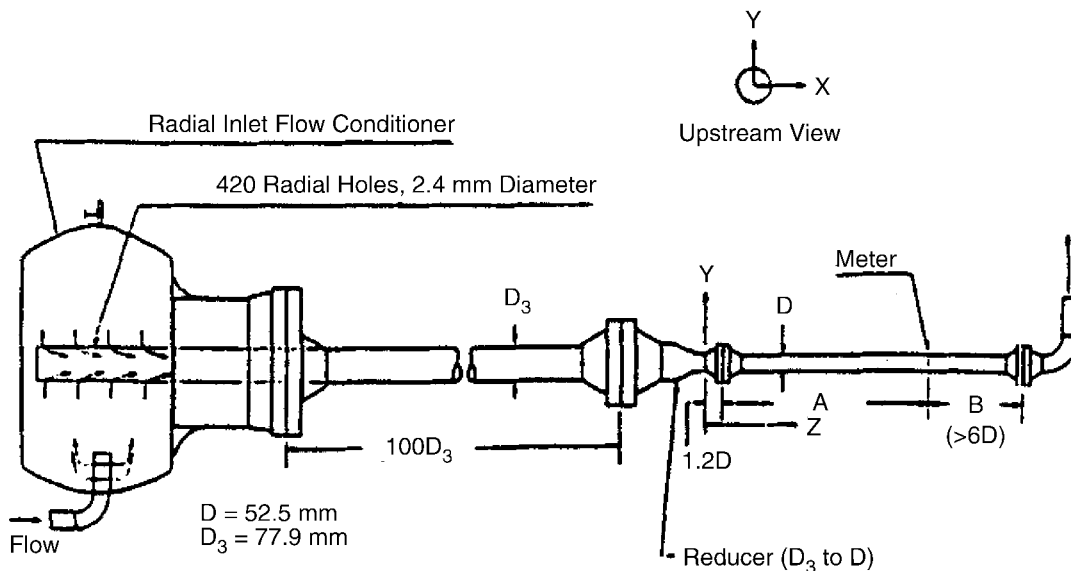


Figure 12-1
Sketch of the reducer piping configurations and the coordinate system

Experiment

Experiments were conducted in the NIST laser Doppler velocimetry equipped Fluid Metering Research Facility. The flow facility has 5.25 cm (2.07 in) diameter, smooth, stainless steel piping, and the fluid is water. The source of flow is an NIST fluid metering calibration facility which uses an accurate weigh-time system to determine the bulk flow rate. However, during the tests the bulk flow rate is determined by using transfer standards. A magnetic flowmeter calibrated by the accurate weigh-time system is used to determine the test flow rate. This facility has a centrifugal pump to provide flow up to a diametral Reynolds number, $Re + W_b D / \nu$, exceeding 10^5 , where W_b is the bulk flow velocity, D is the inner pipe diameter and ν is the fluid kinematic viscosity. Water temperature is controlled using a heat exchanger to maintain a set temperature of 21°C. The relative roughness of this pipe has been measured with a profilometer to indicate a value of 0.006% based on interior pipe diameter. The pertinent parameters considered important in the current experiments are Reynolds numbers and pipe relative roughness; it is assumed that the fluid compressibility and gravitational effects are negligible.

The LDV system is described elsewhere.⁷ Briefly, it consists of a stationary, 2 W argon ion laser with dual beam optics mounted on a computer-controlled, six axes traversing system. Pertinent signal processing equipment produces appropriate computations. This system allows continuous movement of the measuring volume along each of the three perpendicular coordinate axes with a resolution of 5 μm . A thin-walled round glass pipe is used in the test section, which contains a water-filled enclosure having fat, thick (1.9 cm) optical glass sides, so that the laser beams are minimally deflected by the

curvature of the round glass pipe. The LDV system is equipped with Bragg-cell frequency shifter and so is capable of measuring low mean velocities with flow reversals. In this work, the dual-beam signal processors have been used.

The pipeflows reported here are produced in smooth, stainless steel piping. The joints are arranged through weld-neck type flanges where special attention has been paid to smooth concentric alignments for all welded joints. All flange joints are concentricity aligned via pins; these joints are sealed using O-rings to minimize gaps. Where steel pipe joins the glass tube test section, care was taken to produce a concentric joint with no abrupt changes in the inner pipe diameter.

Figure 12-1 is a sketch of the piping configurations and the coordinate system. The reducer used is of the standard belled (not conical) shaped type, and weld-neck flanges are welded onto both ends of the reducer configuration. This unit reduces the diameter from 7.79 cm (3.07in) to 5.25 cm (2.07 in). The coordinate origin is chosen as the center of the pipe in the exit plane of the reducer. The Z-coordinate is streamwise, with downstream being positive; x is the horizontal diameter and y is the vertical coordinate with upwards being positive. The reducer installation was arranged so that over 100 pipe diameters (100D) of straight, constant diameter (7.79cm) piping preceded the reducer. A special radial inlet flow conditioner was installed at the upstream end of this length of piping so that no axial vorticity was produced by this entrance condition. Although the pipeflow produced by this inlet LDV measurements downstream from the single elbow showed that the effects of the elbow were negligible after about 30 pipe diameters for Reynolds number 100 000 and relative roughness 0.006%. Since, in this was 66 000 (corresponding to 100 000 in the 5.25 cm pipe), the pipeflow profile after 100 diameters of this piping and the same pipe roughness conditions was assumed to be fully developed.

The reference condition of the facility can be arranged downstream of an approximately 200 constant diameter (5.25 cm) straight pipe. The measurements made include profiles of both streamwise and vertical components of the mean and turbulence velocities. In this arrangement, it is found that the pipe flow is fully developed, and its mean streamwise velocity is described very closely by the modified logarithmic profile of the Bogue and Metzner profile.⁸ The velocity measurements of the vertical component V and axial component W were made at varying axial distances, z downstream from the exit plane of the reducer. In all of the results that follow, non-dimensionalized quantities will be used. Lengths and velocities are normalized using the inside pipe diameter D and bulk-average velocity W_b , respectively. Meter performances are given via orifice discharge coefficients C_d for three beta ratios (0.363, 0.50 and 0.75).

Results and discussion

Pipe flow measurements

Results presented and discussed here are for a single flow rate at a dimetral Reynolds number Re of 10^5 . The time-averaged velocity components, W/W_b and V/W_b , respectively, in the streamwise and vertical directions along the horizontal diameter (X/D) at four different axial locations (Z/D) are shown in Figure 12-2. The data are presented by the symbols. The solid curve on Figure 12-2(a), the W component, is fully developed equilibrated pipeflow distribution put forth by Bogue and Metzner.⁸ This streamwise velocity profile is the modified logarithmic distribution which would occur after the flow passes through very long lengths of straight, smooth, constant diameter piping.

The effects of the reducer produce, near the exit of the reducer ($Z/D=2.7$), very uniform velocity profiles compared with the fully developed distributions for these conditions as indicated in Figure 12-2(a). With downstream distance, the mean velocity profile approaches the fully developed pipeflow. At $Z/D=11.2$, the streamwise velocity profile continues to show that the center core of this flow is slower and the flow in the wall region is higher than the corresponding fully developed velocities. The diameter of the slow core region is about one third of the pipe diameter. However, at the $20D$ location, the profile shows that the center core of this pipeflow crosses over and produces velocities in excess of the fully developed distribution in the center portion of the pipeflow.

The effects of the reducer produce, near the exit of the reducer ($Z/D=2.7$), very uniform velocity profiles compared with the fully developed distributions for these conditions as indicated in Figure 12-2(a). With downstream distance, the mean velocity profile approaches the fully developed pipeflow. At $Z/D=11.2$, the streamwise velocity profile continues to show that the center core of this flow is slower and the flow in the wall region is higher than the corresponding fully developed velocities. The diameter of the slow core region is about one third of the pipe diameter. However, at the $20D$ location, the profile shows that the center core of this pipeflow crosses over and produces velocities in excess of the fully developed distribution in the center portion of the pipeflow.

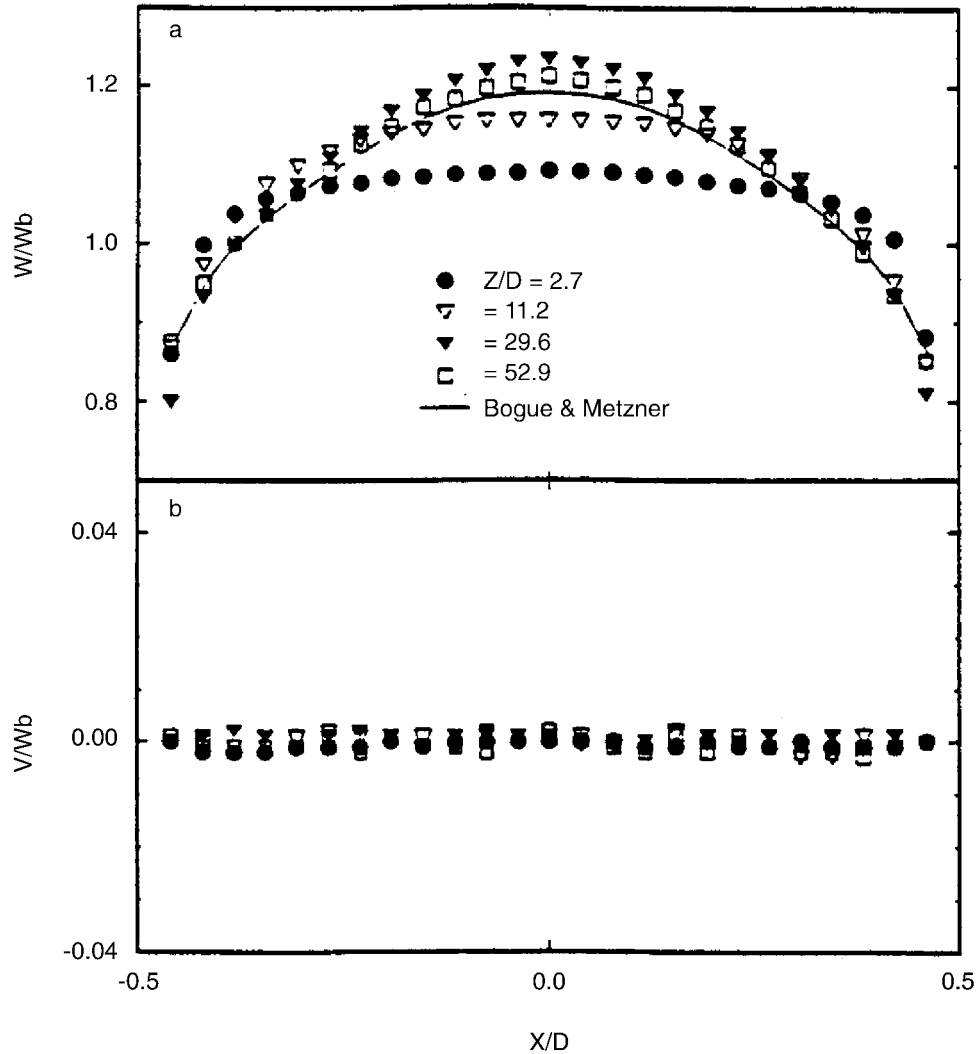


Figure 12-2
Mean velocity profiles of the streamwise and vertical components downstream of a reducer vs. the horizontal diameter positions for $Re=100,000$. The solid line is the ideal pipe flow of Bogue and Metzner.⁸

The crossover position where the profile closely approximates the fully developed pipeflow distribution is about $20D$ downstream of the exit of the reducer. The diameter of this fast flow core is about one-half of a pipe diameter; the maximum velocity measured in these results is about 5% greater than the centerline value for the fully developed distribution. This fast core flow continues to grow as indicated at $Z/D=29.6$ and then decreases to that of the fully developed flow profile as the distance increases.

Figure 12-2 (b) shows the vertical mean velocity profiles V/W_b versus horizontal radial position at different downstream positions from the reducer for $Re=100\,000$. These results show that the reducer does not appear to produce transverse velocity or swirl

flow. For an ideal fully developed pipeflow these velocities should be zero everywhere.

The root mean square (r.m.s) turbulent velocity profiles of the axial (w/W_b) and vertical (v/W_b) components downstream of the reducer at four axial locations (Z/D) are presented in Figure 12-3. Figures 12-3(a) and (b) are the profiles along the horizontal radial position from the pipe centerline, while in Figure 12-3(c) the radial position is along the vertical y-axis. For comparison, the results measured by Laufer at $Re=41\ 000^9$ are also shown in the figure via the solid profile. These results indicate that the turbulent intensity near the exit of the reducer in the center core of the pipe is lower than the result given by Laufer. Near the pipe walls, the intensity exceeds the levels measured by Laufer.

The lower turbulent intensity in the center core of the pipe is due to the fact that the turbulence found in the fully developed flow upstream of the reducer in the 7.79 cm pipe is convected through the reducer without significant change and is normalized with the higher bulk average velocity in the smaller 5.25 cm diameter pipe. At $Z/D=29.6$, the streamwise turbulent velocity is very close to the Laufer even at $Z/D=52.9$, especially near the center core. The velocity profiles shown are presented along the horizontal diameter, since the data indicated that these pipeflows are essentially axisymmetric at all stations measured.

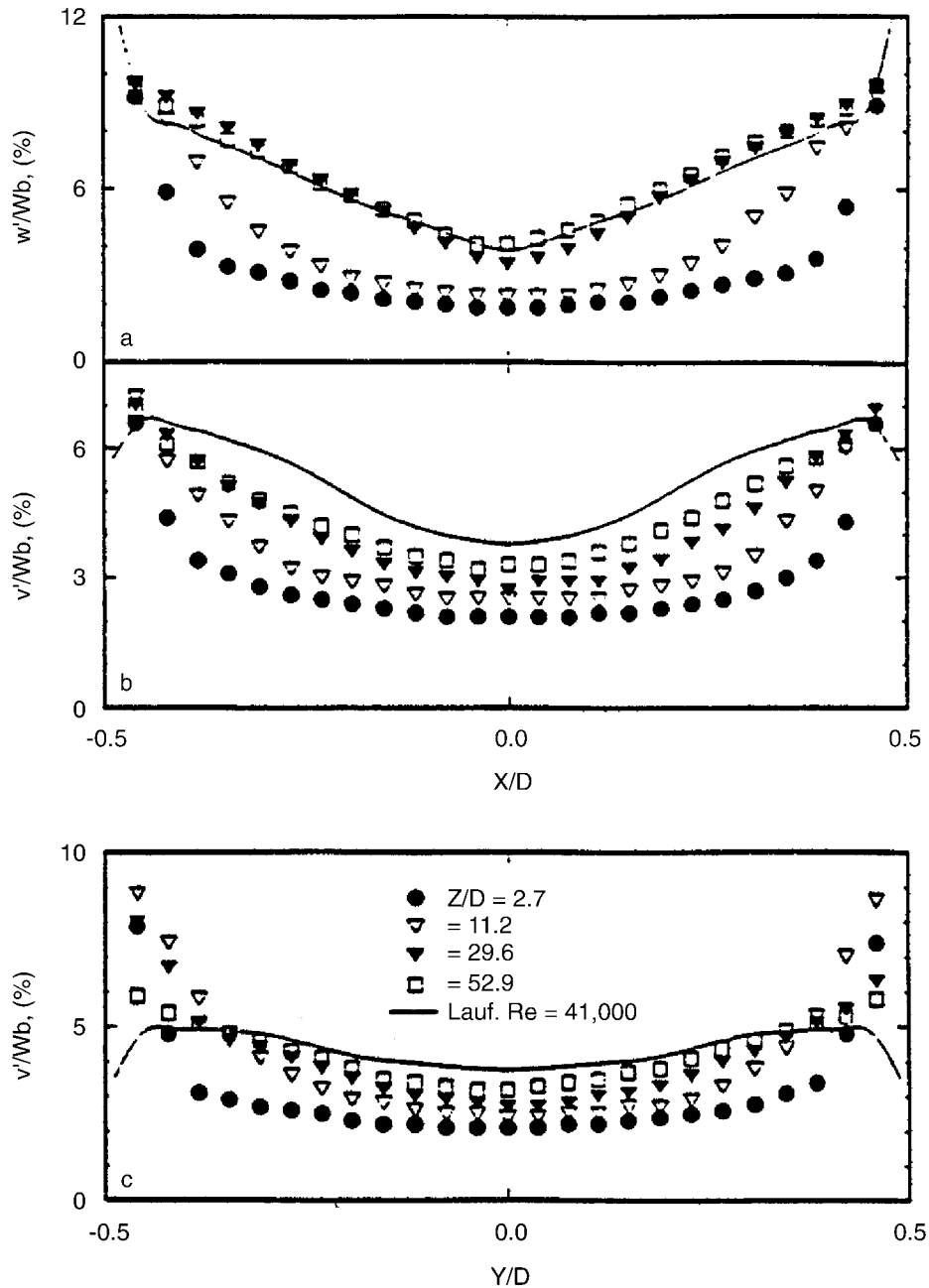


Figure 12-3
 Root mean square turbulent velocity profiles of the streamwise and vertical components downstream of a reducer for $Re=100,000$. (a) w'/W_b vs. X/D , (b) v'/W_b vs. X/D and (c) v'/W_b vs. Y/D . Solid lines refer to Lafer's data⁹ at $Re=41,000$

Orifice meter downstream of the reducer

Figure 12-4 presents results for orifice meters downstream of the reducer shown in Figure 12-1. The ordinate in each of these figures is the percentage shift in discharge coefficient (C_d) relative to that obtained for the reference condition at each flowrate.

Figure 12-4(a) shows the C_d change versus pipe Reynolds number Re for $\beta=0.75$ and four different installation positions. The symbols plotted are the data and the curves are the third-order least square fits to the data. At each flow rate, five data points are obtained. The results for $\beta=0.363$ and 0.50 are similar and are not shown here. These results show that for all β ratios the discharge coefficient is shifted negatively when the orifice meter is installed near the reducer. As the distance between the orifice meter and the reducer increases, the negative C_d shift decreases. This decrease continues until a 'zero-shift' installation location occurs.

For installations beyond this location the shift overshoots the zero shift condition, becomes positive, reaches a maximum and then returns to zero about 50-60 diameters downstream from the reducer. Figure 12-4(b) presents the results in a different format. In this figure the results obtained for the different meter geometries tested downstream of this reducer are presented. Again, the ordinate is the percentage change in discharge coefficient relative to the reference value at each flow rate. In this case, the abscissa is the downstream distance from the reducer. Only three test conditions are shown. In each case the data are for the highest Reynolds number tested for each β ratio.

Appendix G: Flow Meter Installation Effects

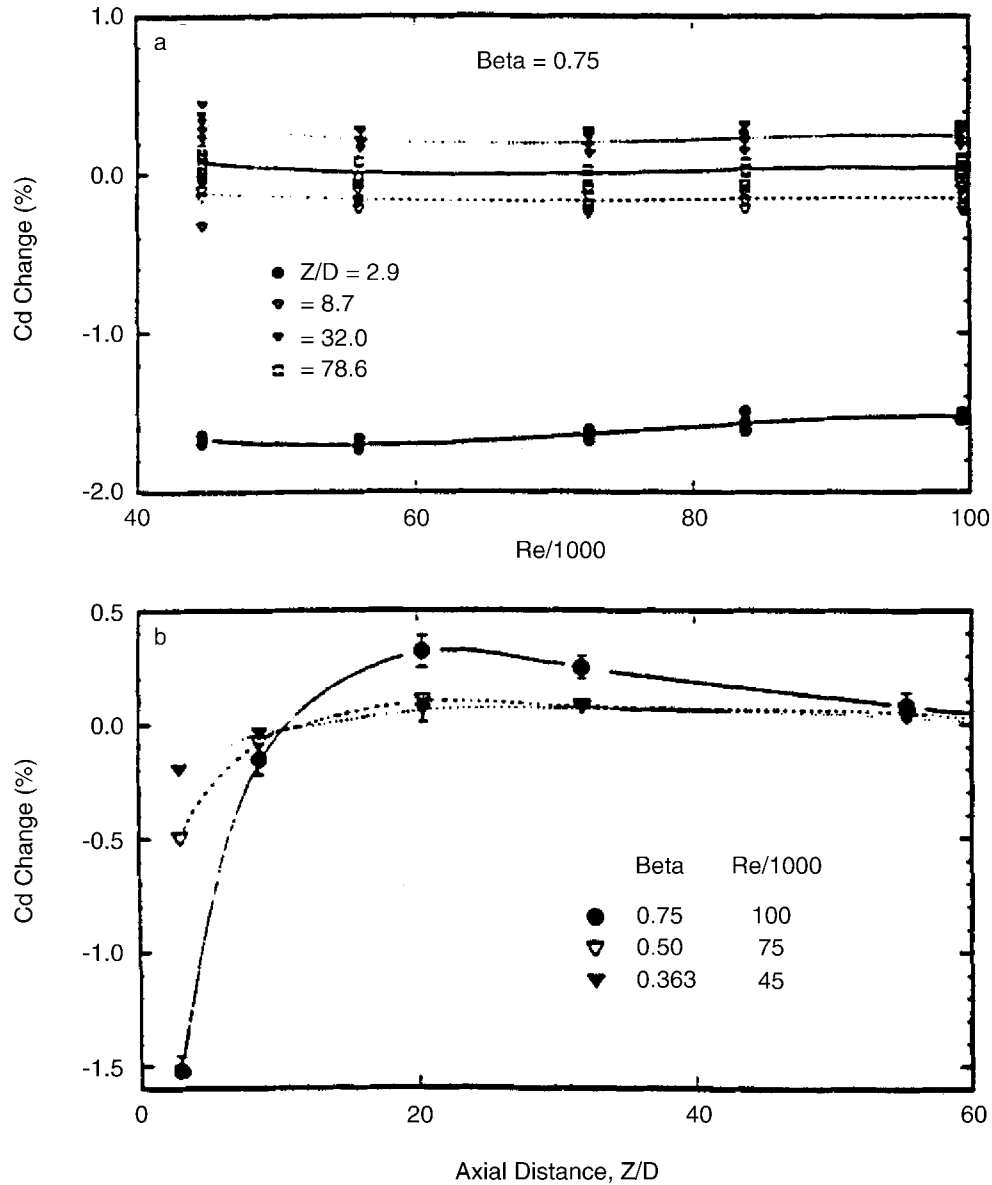


Figure 12-4
 Percentage change in discharge coefficient (a) for a $\beta=0.75$ orifice meter vs. Re and (b) for three values of β as functions of the distance downstream of a reducer for Re=100 000. (a) and (b) are for peakness and (c) is for displacement.

The data are shown by the symbols and each data point is an average of five determinations, as are those shown in Figure 12-4(a). The curves are cubic spline fits to the averaged data. The error bars denote one standard deviation of the repeated readings about the mean value.

These results show clearly the dependence of the orifice characteristics for the three meters at the same meter locations. The shifted discharge coefficients are considered

sizable, especially for larger β ratio meters. The amount of negative shift ranges from about -0.2% for the small β of 0.363 to -1.6% for the largest β of 0.75. For installations near the reducer, at $Z/D=2.9$, where all of the discharge coefficients are shifted negatively with respect to the reference values, the $\beta=0.75$ meter has a deviation that is about eight times that for the $\beta=0.363$ meter.

When the orifice meter is installed further from the reducer, these negative shifts diminish and become zero at around a downstream position of 11-13D from the reducer. However, with increased downstream distance, orifice discharge coefficients are shifted positively relative to reference values. These positive shifts appear, from these results, to be maxima at the installation position 20D downstream from the reducer. These maxima also appear to be dependent upon the β ratio, with the smallest shift of about +0.1% occurring for $\beta=0.363$ at the 30D location and the largest of about +0.3% for $\beta=0.75$ at the 20D location. For practical purposes, there is no overshoot situation for the cases of $\beta=0.50$ and 0.363 ratio, and beyond $Z/D = 10$ the shift can be considered essentially zero since these positive overshoots are less than 0.1%.

As for the largest β ratio of 0.75, when the installation is made further than 20D downstream of the reducer, the results show that the positive shifts in discharge coefficient decrease, so that deviations from reference condition values are essentially less than 0.1% beyond the 55D location.

Profile peakness and flow displacement

The results previously presented include both the velocity profiles and the meter performance downstream of the reducer. The next effort is to seek the relationship between the two and to find some criteria for improving the meter performance prediction in these non-ideal conditions.

Different piping configurations produce different velocity profiles. These different velocity profiles could significantly affect flowmeter performance. Based on the measured velocities, various flow field parameters can be defined and quantified. Some parameters may be more important than others in affecting meter performance. Previous research results have shown that swirling flows produced by several different pipe configurations can have very strong effects on the meter performance of selected meters.^{1,5}

One quantity believed to be important in the performance of orifice meters is the character of the peakness or the flatness of the velocity profile. Because the velocity field produced by the reducer is a swirl-free, skew-free, axisymmetric flow, as shown earlier, this flow field is a good candidate for studying the effects of profile peakness on orifice meter performance. To quantify the peakness of the velocity profiles produced by the reducer, a range of peakness parameters are introduced. These include:

Appendix G: Flow Meter Installation Effects

$$P_1 = \frac{W_c}{W_b} - 1 \quad (1)$$

$$P_2 = \frac{W_c^2}{W_b^2} - 1 \quad (2)$$

$$P_3 = 1 - \frac{W_b}{W_c} \quad (3)$$

$$P_4 = \frac{W_c}{W_w} \quad (4)$$

$$P_5 = \frac{\int (W_c - W) dr}{W_b D} \quad (5)$$

$$P_6 = \frac{\int (W_c^2 - W^2) dr}{W_b^2 D} \quad (6)$$

$$P_7 = \frac{\int W(W_c - W) dr}{W_b^2 D} \quad (7)$$

where W_c and W_w are the velocities at the pipe centerline and at a point near the wall ($r=0.475D$) respectively. All the parameters have a similar meaning for characterizing the distribution of the velocity field. A larger peakness index will mean high flow velocities, i.e. a more peaked profile near the center core. Both P_1 and P_2 show the overshoot of the centerline velocity from the average bulk velocity, except that P_1 is normalized by the average bulk velocity while P_3 is normalized by the centerline velocity/ P_2 is the overshoot of the centerline dynamic pressure over the dynamic pressure based on the averaged velocity. P_4 is the ratio between the centerline velocity and the velocity near the pipe wall (at 2.5% diameter from the wall). The parameters P_1 , P_2 and P_3 are determined only by the centerline velocity, P_4 is determined by two local velocities (the centerline and near-wall velocities), and P_5 , P_6 , and P_7 are determined from the integration of velocities over the pipe diameter. These integrated quantities are similar to the displacement thickness and momentum thickness parameters commonly used in studying boundary layer flows.¹⁰

Other investigators have introduced some of these parameters in their studies. Klein^{11,12} called P_3 the block factor in studying the turbulent developing pipe flow and the effects of inlet conditions on conical diffuser performance. In studying the effect of flow profiles on orifice meter performance Ghazi¹³ has introduced the parameters F_1 and F_2 which are closely related to the peakness parameters P_1 and P_4 respectively: $F_1=1-P_3$ and $F_2=1/P_4$.

Besides these peakness parameters, other parameters that quantify how the flow is displaced from the center of the pipe can also be used. A more peaked flow at the pipe center will mean that the flow is more concentrated here and less displaced from the pipe centerline. A displacement parameter is thus introduced to quantify the average flow displacement from the pipe centerline for a selected quantity, as follows:

Here four flow displacement parameters are considered. D_{10} is for the velocity W , D_{11} is for the first radial moment of axial velocity, Wr , D_{20} is for the dynamic pressure W^2 , and D_{21} is for the first radial moment of the dynamic pressure, W^2r .

These profile peaknesses and flow displacements as functions of the axial distance downstream from the reducer for $Re=100\ 000$ are shown in Figure 12-5. To compare these with the values for the fully developed profile these parameters are normalized by those of the straight pipe case, denoted with a subscript, s . Thus, if a profile is flatter than the ideal profile, the value of the peakness will be less than one. In this case, the flow field is displaced further from the center line and the value of this displacement should be larger than 1.

Figures 12-5(a) and (b) show the peakness indexes, $P_i/P_{i,s}$ as functions of Z/D while Figure 12-5(c) is for the displacement indexes, $D_{mm}/D_{mm,s}$ as functions of Z/D . As shown in Figure 12-5, at small values of Z/D the peaknesses are less than one.

With downstream distance, the values increase to and through 1 to reach respective maximal values and then decrease monotonically to the ideal case of 1. The sequence is opposite for the flow displacement parameters. As shown in Figure 12-5(c), the displacement indexes are greater than one for small values of the distance Z/D . With downstream distance, they decrease and pass the value of 1 to reach respective minima, and then approach monotonically the ideal value of 1.

Appendix G: Flow Meter Installation Effects

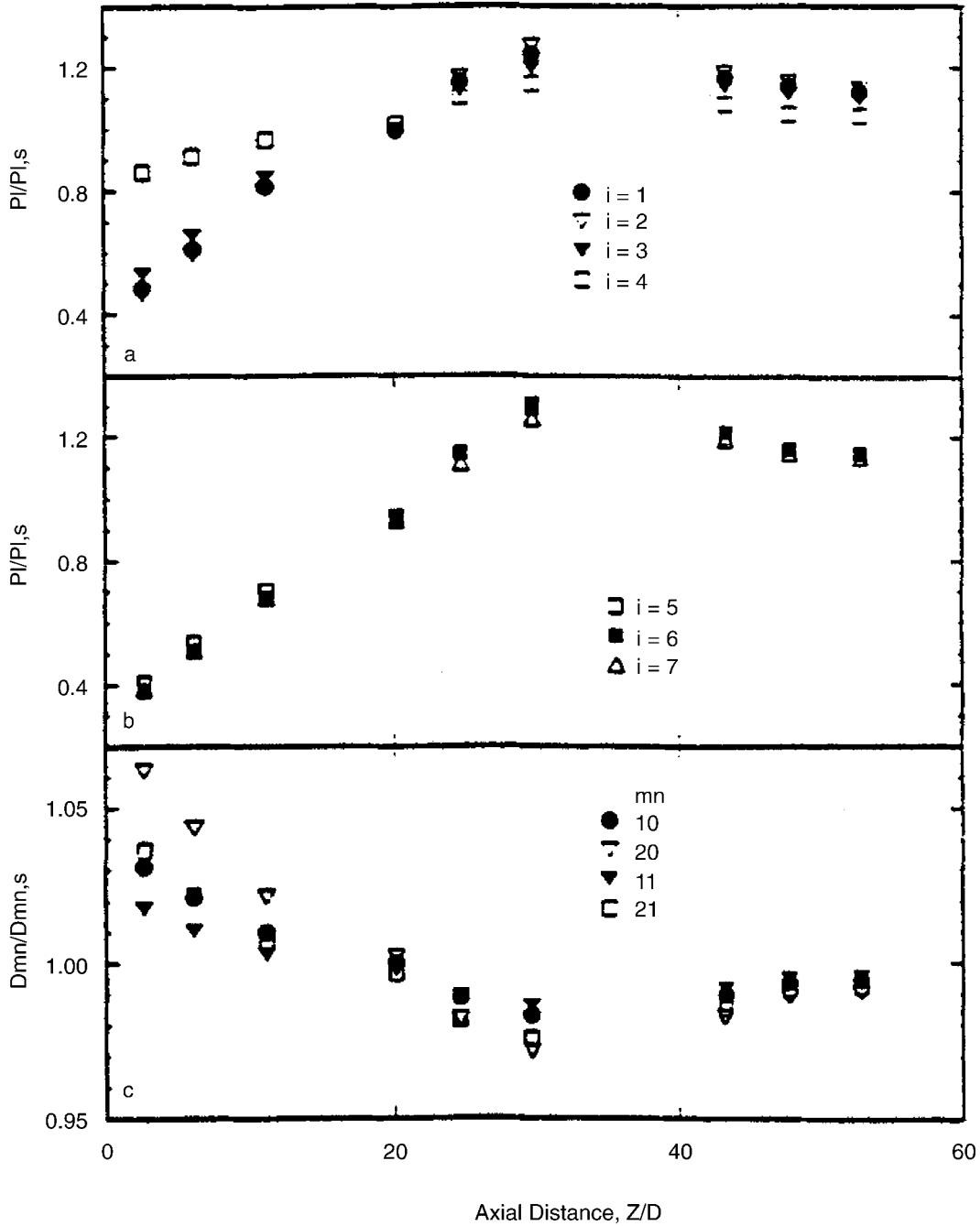


Figure 12-5
 Profile indexes downstream of a reducer for $Re=100\ 000$. (A) and (b) are for peakness and (c) is for displacement.

Now that we have the distribution data for both orifice meter performance and the flow profile indexes we can analyze the correlations between them. From Figure 12-4(b) and Figure 12-5 the relationship can be obtained.

Figures 12-6 and 12-7 show the relationships between C_d changes and the parameter indexes. Figure 12-6(a) shows the C_d change as a function of the peakness index $P_2/P_{2,s}$. The dotted line is a second order regression curve fit. These data indicate there is a strong relationship between the peakness index P_2 and the C_d coefficient change. The relationship indicates that the C_d value in the non-ideal installation could be corrected somehow according to the empirical peakness- C_d curve.

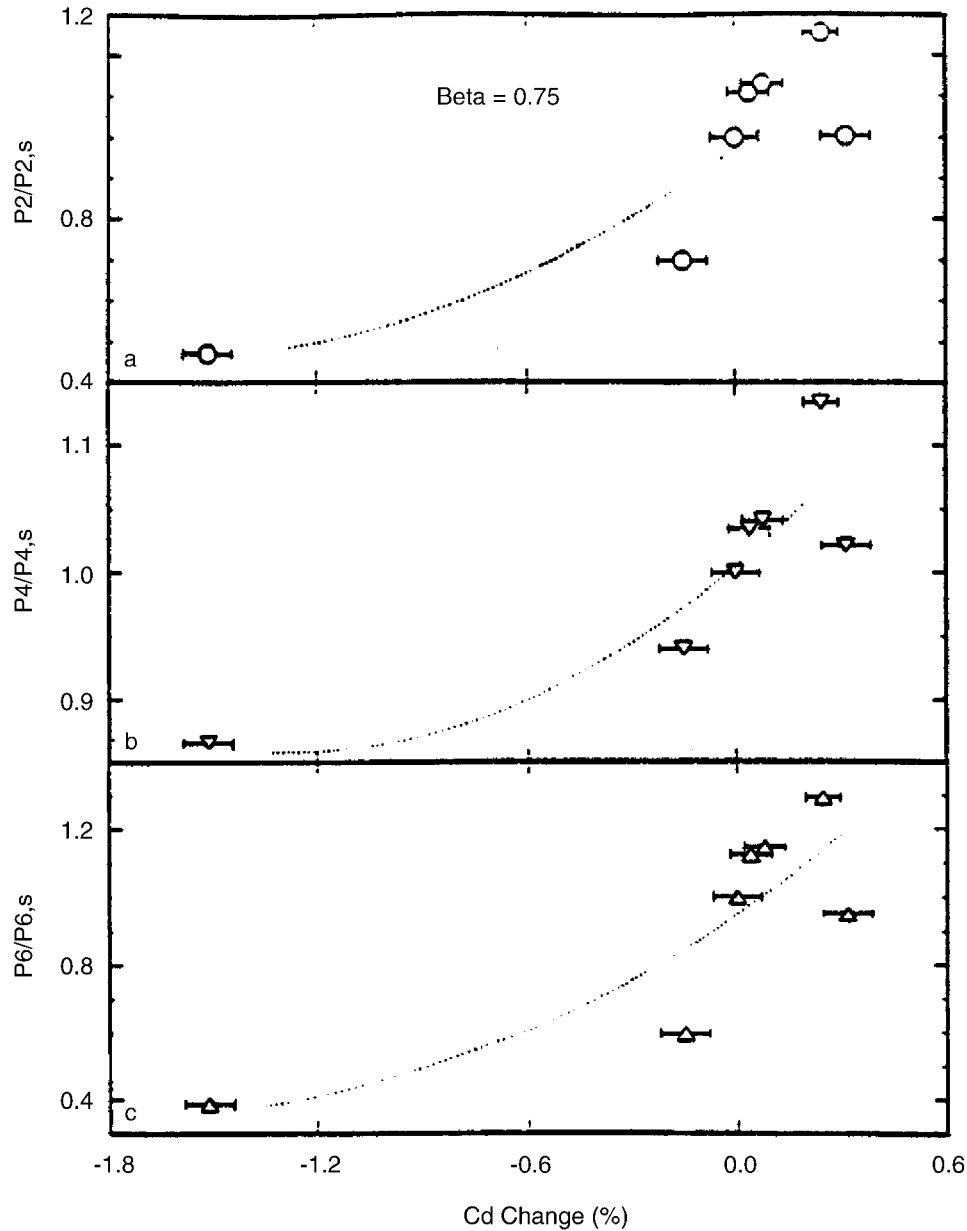


Figure 12-6
 Relationship between the C_d change and profile peakness index for $\beta=0.75$: (a) P_2 ,
 (b) P_4 and (c) P_6

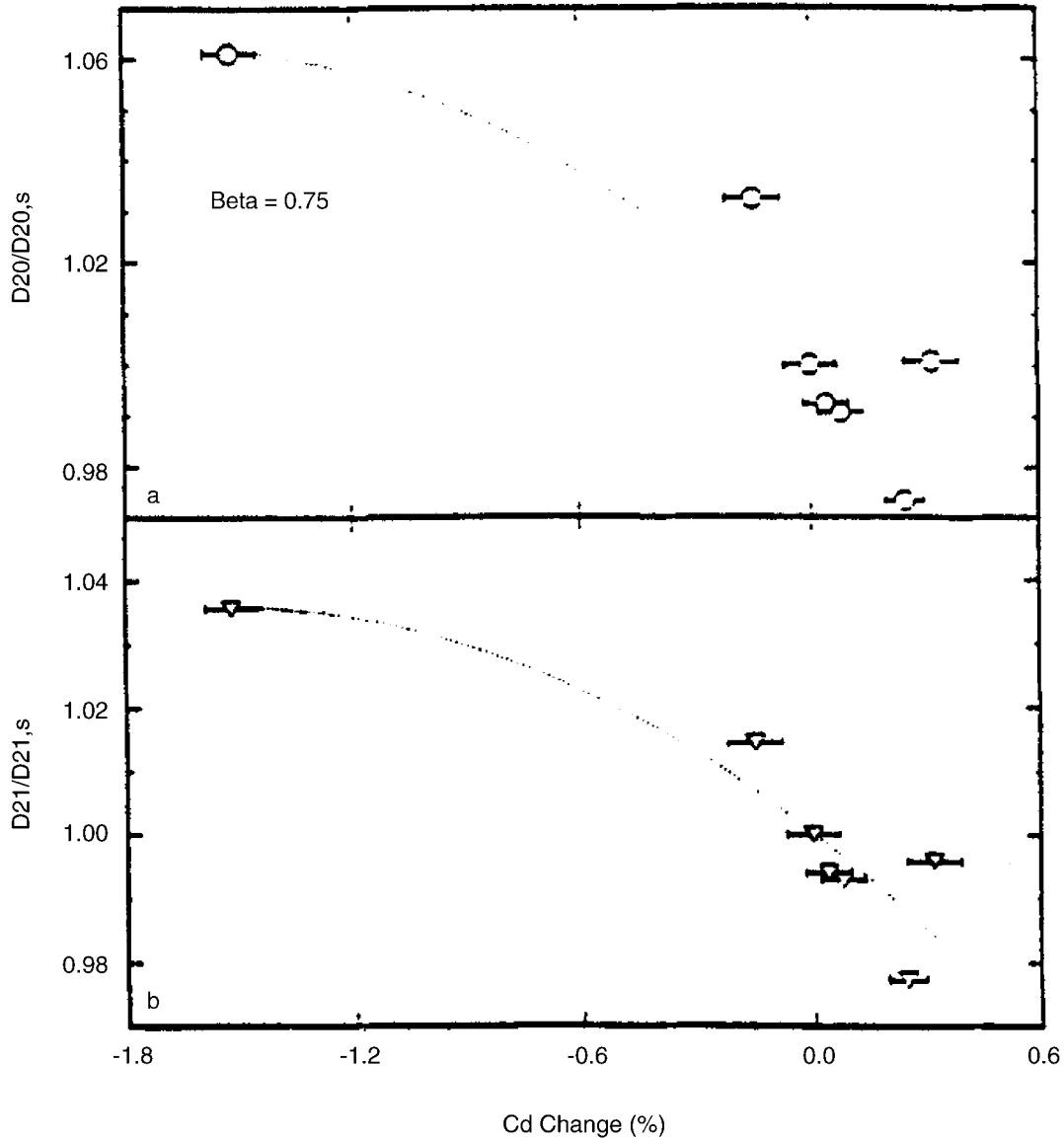


Figure 12-7
Relationship between the Cd change and flow displacement index for $\beta=0.75$:
(a) D_{20} and (b) D_{21}

Similar relationships for the peakness indexes $P_4/P_{4,s}$ and $P_6/P_{6,s}$ are presented in Figures 12-6(b) and (c), respectively. All these data show a quantitatively consistent relationship that a larger peakness produces a larger C_d coefficient. The prediction curves for the displacement indexes $D_{20}/D_{20,s}$ and $D_{21}/D_{21,s}$ are given in Figures 12-7(a) and (b), respectively. The data again shows a strong relationship between the flow displacement indexes and the C_d change. Here, as expected, a larger displacement produces a smaller C_d coefficient.

These data show that all the parameter indexes have a strong relationship with the meter performance. As expected, a profile having a smaller peakness or having larger displacement will result in a lower value of C_d or a negative C_d shift. This is due to the increased pressure drop across the orifice plate required to move the additional fluid near the wall through the hole in the orifice plate. As the profile peakness increases or the flow displacement decreases, the discharge coefficient C_d increases. All these curves indicate that the discharge coefficient C_d for the axisymmetric non-ideal installation conditions could be corrected through the empirical correlation curves. For these curves the P_4 and D_{21} parameters seem to have good prospects for making this compensation.

Summary and conclusions

Experimental measurements have been made using laser Doppler velocimetry and meter calibrations using gravimetric standards in the pipe flows produced by a reducer. This arrangement is known to be the cause of metering inaccuracies for meters installed in the downstream piping near these reducers. With a limited set of measurements of fluid velocity, the profile characteristics of the mean velocity downstream of a reducer is described both qualitatively and quantitatively. The flow is found to have profile characteristics that can strongly affect the performance of orifice flowmeters.

The velocity profile measurements made downstream from this reducer for the selected fluid indicate that the reducer initially produces a velocity profile that is flatter than the fully developed distribution that is pertinent to the Reynolds number and relative roughness conditions. With increasing downstream distance the pipeflow evolves from the flatter profile to a more peaked profile and then converges it to the fully developed pipeflow profile. The dissipation of the reducer effects does not occur with a monotonic progression of the mean axial velocity profile to that for the ideal distribution. Instead, the profile overshoots the ideal distribution to produce a core of fast flow in the center of the pipeflow. Further downstream of the reducer the profile returns to the fully developed pipeflow.

Meters such as orifice plates, which can be sensitive to such profile anomalies, can be expected to show such effects. Three β ratio orifice meters were tested. Results show that there is a pronounced β ratio dependence in the orifice characteristics. Low β ratios (0.36) are hardly affected except where they are installed close to the reducer; large ratios (0.75) show significant deviations from ideal discharge coefficient values, and they show strong dependence upon profile overshoot.

It is now well known that the different velocity profiles produced by different pipe configurations can significantly affect flowmeter performance. These include swirl, skew and turbulence. The effects of the profile peakness on orifice meter performance are the focus of the present experimental study. Several profile indexes are introduced

to characterize the profile peaknesses and flow displacements. These indexes are then correlated with orifice meter performance. It is shown that these profile indexes have strong relationships with the changes in the discharge coefficient of the different orifice meters and thus could be used to develop criteria for improving the meter performance in axisymmetric non-ideal installation conditions.

Acknowledgments

The authors acknowledge the partial support of the industry-government consortium formed at NIST to investigate pipeflow fluid mechanics and corresponding meter performance under non-ideal installations. Special acknowledgment is made for the support provided by the Gas Research Institute, Chicago IL.

References

1. Mattingly, G.E. and Yeh, T. T. *NIST's industry-government consortium research program on flowmeter installation effects: Report of results for the research period July-December 1987, NISTIR-88-3898, November 1988*
2. Mattingly, G. E. And Yeh, T. T. *NIST's industry-government consortium research program on flowmeter installation effects: Report of results for the research period January-July 1988, NISTIR-89-4080, April 1989*
3. Mattingly, G. E. And Yeh, T. T. *NIST's industry-government consortium research program on flowmeter installation effects: Report of results for the research period November 1988-May 1989, NISTIR 4310, April 1990*
4. Mattingly, G. E. And Yeh, T. T. *Effects of non-ideal pipeflows and tube bundles on orifice and turbine meters, Flow Meas. Instrum. (1991) 2 1-19*
5. Mattingly, G.E. and Yeh, T. T. *Flowmeter installation effects, Proc. National Conference of Standards Laboratories Annual Conference, Washington DC, August 14-18, 1988, NCSL, Boulder CO.*
6. ASME, *MFC-10M Method for establishing installation effects on flowmeter, AM. Soc. Mech. Eng. November 1988, New York, NY 10017.*
7. Yeh, T. T., Robertson, B. And Mattar, W.M. *LDV measurements near a vortex shredding strut mounted in a pipe, J. Fluids Eng. ASME, 105 (1983) 185-196*
8. Bogue, D. C. And Metzner, A.B. *Velocity profiles in turbulent pipe flow, I &EC Fundamentals, 2 (2) (1963) 143-149*
9. Laufer, J. *The structure of turbulence in fully developed pipe flow, NBS Rept 1974, September 1952*

10. Schlichting, H. *'Boundary Layer Theory'*, 4th ed., McGraw-Hill, New York (1960)
11. Klein, A. *Review: Effects of inlet conditions on conical-diffuser performance, J. Fluids Eng.* 103 (1981) 243-249
12. Klein, A. *Review: Effects of inlet conditions on conical-diffuser performance, J. Fluids Eng.* 103 (1981) 250
13. Ghazi, H.S. *A pressure index for predicting the effect of flow profiles on orifice meter performance, J. Basic Eng. March (1966) 93-100*

The second paper from Dr. Mattingly follows:

**Effects Of Pipe Elbows And Tube Bundles
On Selected Types Of Flowmeters**

Abstract

This paper presents experimental results for the decay of pipe elbow-produced swirl in pipeflows and its effects on flowmeter measurement accuracy. Experiments include the decay of swirl produced by single and double elbow configurations for pipe diameter Reynolds numbers of 10^4 to 10^5 using water in a 50 mm diameter facility at NIST in Gaithersburg, MD. Results show that different types of swirl are produced by the different piping configurations. The swirl decay is found to be dependent on the type of swirl and the pipe Reynolds number. At high Reynolds number very long lengths of straight, constant diameter pipe are required to dissipate the single eddy tube swirl that is produced by the two elbows out-of-plane configuration. Without flow conditioning, it is concluded that the specifications of upstream pipe lengths in the current flow metering standards may not be sufficient to achieve the desired flow metering accuracy.

Experimental results are also presented for the effects produced by tube bundle-type flow conditioners. These results show shifts in orifice meter discharge coefficients that are both positive and negative depending upon pertinent conditions. A range of orifice geometries, Reynolds numbers and meter locations are studied and explanations are put forth to explain these shifts. Results are also presented for a specific type of turbine meter. These show meter factor shifts that are also both positive or negative depending upon the type of swirl pattern entering this meter. An example is given in which the insertion of a tube bundle flow conditioner between a single elbow and the turbine meter produces a larger disturbance to the meter factor than would occur without the conditioner.

Keywords: swirl, measurement accuracy, pipe elbows, tube bundles

The effects of swirl on orifice meter performance were initially observed in the US in the early 1900s^{1,2}. Consequently, early testing programs, sponsored by the American Gas Association (AGA), were devised to describe and quantify these effects, see Appendix No. 3 in reference 1. These early US programs were followed by others that were supported by the gas industry and other sources such as the American Society of Mechanical Engineers (ASME), the National Institute of Standards and Technology (NIST) and the American Petroleum Institute (AP).

A better understanding of the effects of pipeflow swirl on practical flow measurements and related fluid mechanics phenomena can be obtained through experimental fluid

metering research programs that use the currently available flow research tools². The results produced herein are considered to be the type of data that will be needed to improve current flow measurement standards and associated metering practice.

The upstream pipe length requirements in two international orifice metering standards - ISO-5167 and ANSI/API-2530- are quite different^{1,3}. ISO-5167 specifies that the upstream pipe length for a beta ratio = 0.75 (orifice hole to pipe diameter ratio) meter installed downstream of double elbows out-of-plane should be equal to or greater than 70 diameters (D); ANSI/API-2530 specifies $35D$ for the same conditions. The ISO standard also specifies that swirl angles should be less than $\pm 2^\circ$ everywhere in the pipe cross-sectional area at the location where the meter is to be installed; the ANSI/API makes no such stipulation. In both of these standards, no dependence is given for the effects of the type of swirl, the Reynolds number, the pipe roughness etc.

This paper presents experimental data on : (1) the decay of two different types of swirl generated by conventional pipe elbow configurations, (2) the dependence of these swirls on Reynolds number and (3) the resulting swirl effects on the performance of specific types of flowmeter. The elbows used in this study have centerline curvature of $1.5D$. Results indicate that both of the standards mentioned above need to have the sections on installation specifications improved.

The effects of flow conditioning devices, especially the tube bundle type, are included in orifice meter standards. Here, they are described as effective elements for reducing the lengths of upstream piping needed to reduce or eliminate shifts in discharge coefficient produced by swirl caused by piping effects. The experimental results presented here show that tube bundle type flow conditioners can have the opposite effect on both orifice and turbine meter performance.

Experimental procedure

Experiments in a NIST water flow facility have been used to characterize swirl decay in a 50 mm diameter pipe at Reynolds numbers of 10^4 and 10^5 . Two different types of swirl were generated using two pipe arrangements: (1) a single long radius elbow and (2) two long-radius elbows in an out-of-plane configuration. These configurations and the coordinate systems used are shown in Figure 12-8, where the flowrate is Q . Velocity profiles were measured with a laser Doppler velocimeter (LDV)⁴. These results have been produced in piping with surface roughness of $3\mu\text{m}$ (relative roughness of $6 \times 10^{-3}\%$ based on D) as measured with a calibrated profilometer⁵⁻⁸. For each of these piping configurations, the entering pipeflow was that from the same, very long ($80D$) pipe which was preceded by several flow conditioners. When the flow from this unit of pipe work was measured using LDV, it was found that the mean velocity profile conformed to the power law distribution with the appropriate exponent⁵⁻⁸.

Results

All of the pipeflow profile results shown below are for a diametral Reynolds number of 10^5 .

Single elbow

Velocity profile measurements for the standard long-radius elbow are shown in Figure 12-9(a). These results pertain to different downstream distances for the elbow for a pipe Reynolds number of 10^5 . Only two velocity components were measured: the streamwise component labeled W in the Z direction, and the vertical component V in the Y direction, refer to Figure 12-8(a).

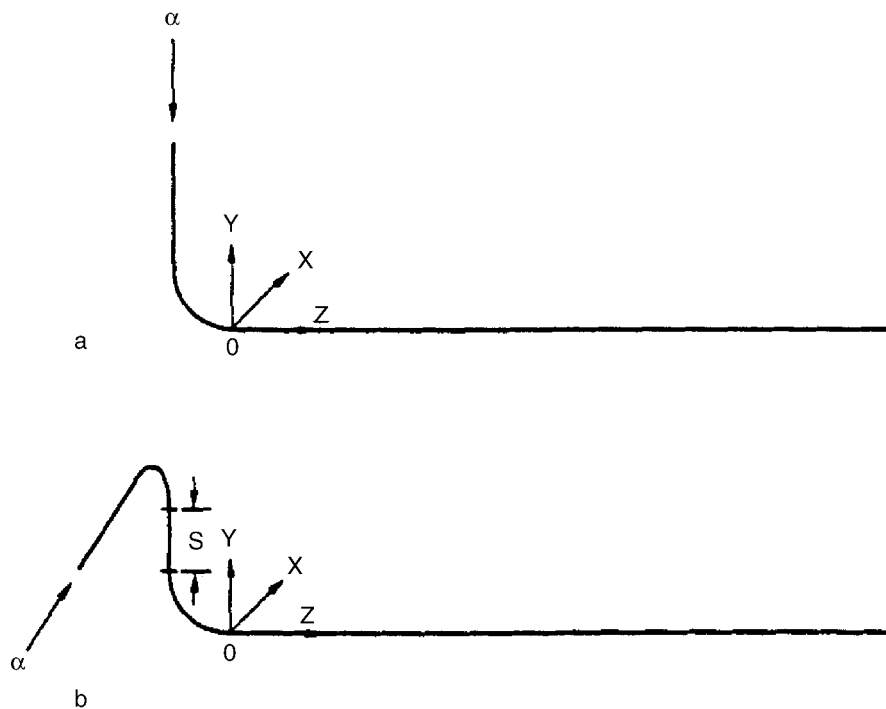


Figure 12-8
(a) Single elbow configuration; (b) double elbow out-of-plane configuration with spacing, s

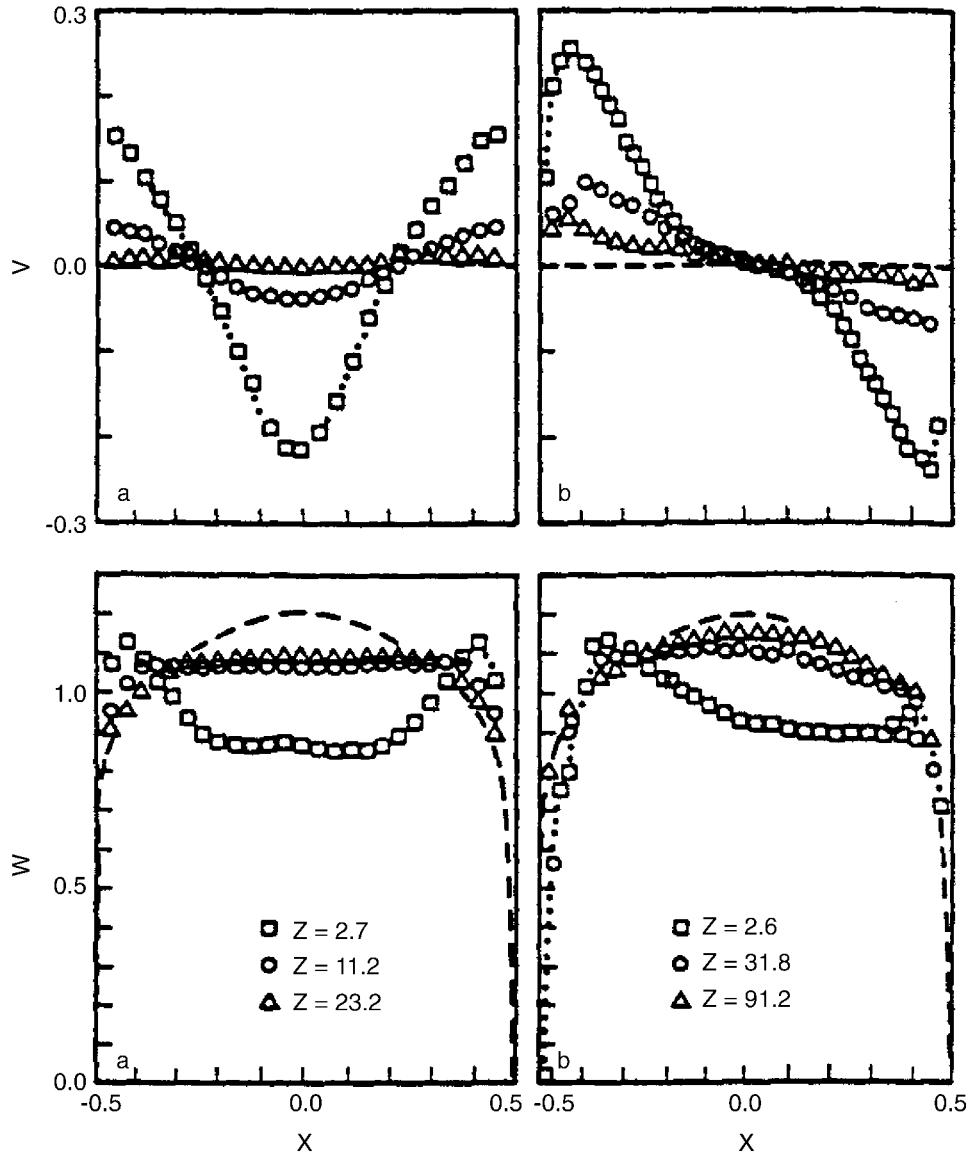


Figure 12-9
 Vertical, V , and streamwise, W , velocity profiles along the horizontal diameter for: (a) the single elbow configuration, and (b) the closely coupled double elbows out-of-plane configuration. Downstream distances are in diameters. Ideal profiles are shown by dashed lines.

Velocities and lengths are normalized using, respectively, the cross-sectional average of the axial velocity and the inner pipe diameter. The profiles for the ideal flows are denoted by the dashed lines. For an ideal flow, the vertical velocity is zero everywhere and the streamwise velocity profile is the pertinent power law distribution. The exponent for these conditions is taken to be 7. The centerline slope discontinuity associated with the power law distribution has been smoothed. The profile between $X = \pm 0.1$ is smoothed using a parabola based on the values at $X = \pm 0.1$ and ± 0.15 . The data

Appendix G: Flow Meter Installation Effects

indicates that the standard long radius produces a dual-eddy (defined here as type II) swirl pattern that has two counter-rotating vortices on either side of the center plane of the elbow^{7,8}. These vortices produce a strong transverse flow directed toward the outside of the elbow. The center core of this flow is found to have axial velocities that are much slower than the corresponding ideal flow.

A time-averaged swirl angle can be defined as the arc tangent of the mean vertical velocity component divided by the mean streamwise component, and results are shown in Figure 12-10(a). The results close to the elbow show that the transverse flow produced by the counter-rotating vortices give swirl angles of -14° near the center of the pipe while the flows near either pipe wall give angles of $+8^\circ$.

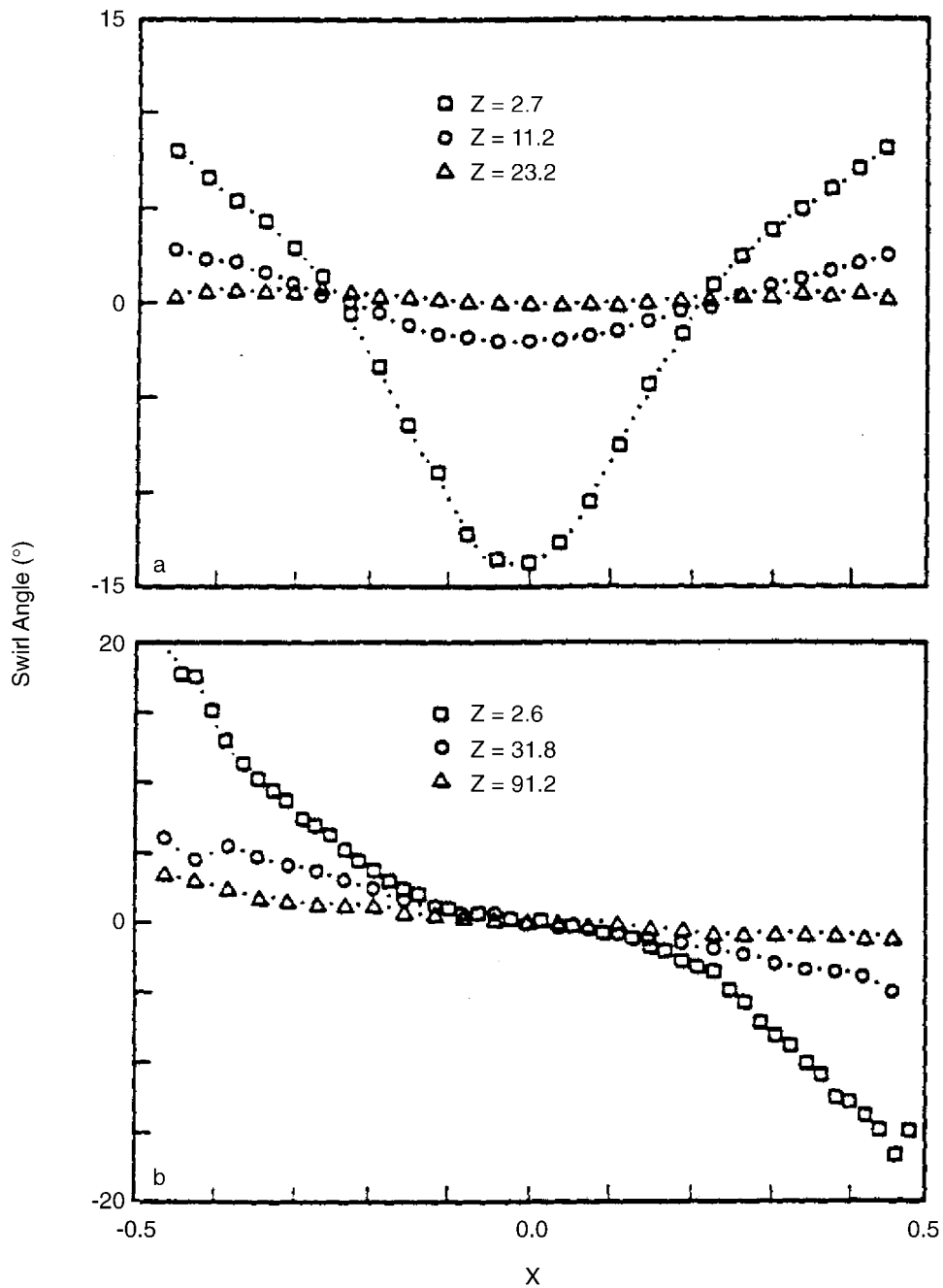


Figure 12-10
Swirl angle distributions produced by: (a) the single elbow configuration , and (b) the closely coupled double elbows out-of-plane configuration. Downstream distances are in diameters.

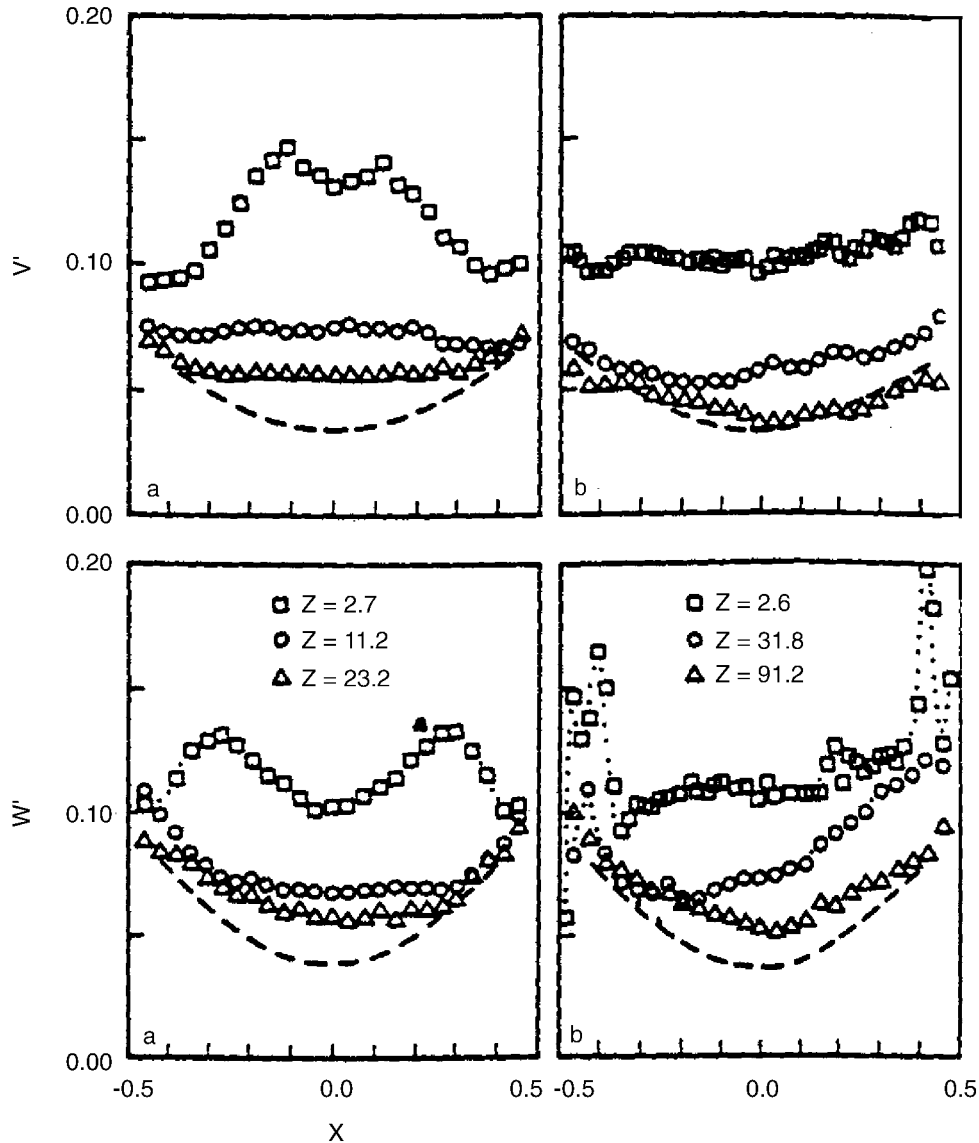


Figure 12-11

Cross-stream profiles of the root mean square values of the vertical, V' , and streamwise, W' , turbulent velocity components; (a) the single elbow, and (b) the closely coupled double elbows out-of-plane configuration. Downstream distances are in diameters. The dashed lines refer to Laufer's data.

The corresponding turbulent velocity distributions are presented in Figure 12-11(a). The dashed lines in these figures are the distributions measured by Laufer⁹ in straight pipe in an airflow at Reynolds number 4×10^5 . The turbulence measured in the present experiments is greater than that found by Laufer. However, Laufer's experimental arrangement had different inlet conditions, which are interpreted here as the explanation for the increased levels of turbulence found in the present experiments. These results show that the distributions of mean and turbulent velocities decay in different ways according to the type of swirl and the pertinent Reynolds number.

Double elbows out-of-plane

For this configuration where the two elbows are closely coupled, ($s = 0$ in Figure 12-8(b), i.e. no straight pipe separates them) intense, single-eddy (defined here as type I) swirl is created. Velocity profiles are shown in Figure 12-9(b) for Reynolds number 10^5 . Details can be found in references 5 and 6.

Swirl angle distributions are presented in Figure 12-10(b) for a pipe Reynolds number of 10^5 . These distributions show that in the downstream piping near these elbows: (1) swirl angles are about $\pm 20^\circ$ near the pipe walls and (2) in a core region about the center of the pipe, the swirl angle is essentially zero, indicating that little or no swirl is present. This suggests that a flow conditioning element placed near the pipe wall could be very effective to reduce this swirl. This type of swirl is found to decay very slowly with down-stream distance as compared to the single elbow swirl patterns described above.

The corresponding turbulent velocity distributions are presented in Figure 12-11(b). As noted above these distributions are different for those for the single elbow and from those measured by Laufer.

Decay of swirl

The decay of both types of swirl is shown in Figure 12-12 by the maximum swirl angles. These maximum swirl angle distributions are defined as half of the difference between the maximum and minimum swirl angles shown in Figure 12-10. In 20 diameters, the type II swirl has dissipated more than 90% (as quantified via the maximum value of the swirl angle) for a Reynolds number of 10^5 . Single-eddy type swirl (type I) that is produced by two close-coupled elbows decays much more slowly. The swirl produced by spaced double elbows is much more complicated^{6,7}. It is a composite of type I and type II swirl depending on the length of the spacer, s . For a long spacer, the swirl should approach that of a single elbow case. The data for $s = 2.4 D$ and $5.3 D$ show that the type I swirl flow pattern still dominates the swirl interactions, although the initial swirl is much smaller than that for close-coupled elbows. The decay of this swirl is also slow compared to that for type II swirl. The Reynolds number dependence of type I swirl shows that the decay rate decreases markedly as the Reynolds number increases⁷. Very long lengths of pipe are required to dissipate this single-eddy type swirl⁸.

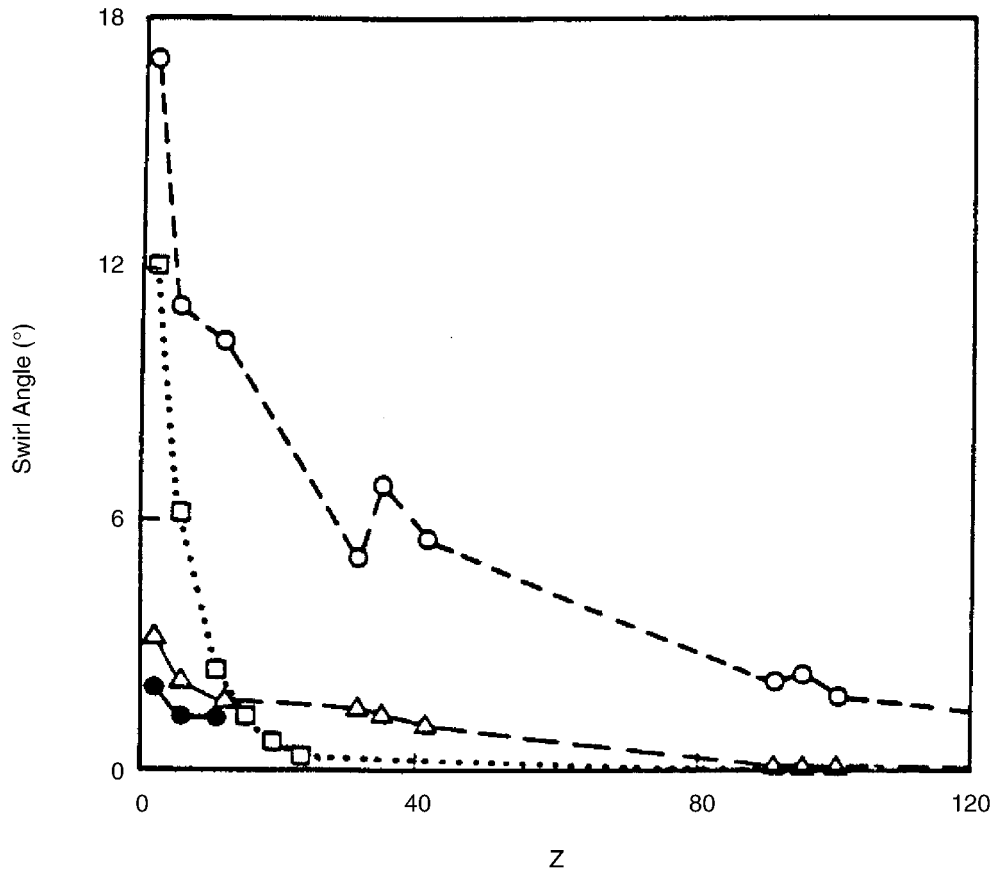


Figure 12-12
Streamwise distributions of the mean swirl angles for the single elbow configuration (□) and for the double elbows out-of-plane configurations (o- closely coupled, Δ - spaced at 2.4 diameters, and • - spaced at 5.3 diameters)

Other researchers¹⁰⁻¹⁴ have described the decay of swirl as an exponential decay function of the following form:

$$S/S_0 = e^{-\alpha Z}$$

where S is some selected measure of the swirl (angular momentum, angular momentum flux, mean swirl angle, etc.), S_0 is the value of S where $Z=0$, α is the swirl decay parameter, and Z is the number of diameters of straight, constant diameter piping downstream of the initial position where $S = S_0$. This function can be used for predicting the percentage of initial swirl as a function of the dimensionless axial distance Z .

The decay parameter, α , depends on the type of swirl, the selected measure of the swirl, and the pipe diametral Reynolds number, Re_D . To estimate squares fit of the experimental data was made for each swirl quantity, S , for each Reynolds number. This fit was produced using an iteration technique until the change in the squared

error was less than 0.1%. If S is taken to be the maximum swirl angle, then at a Reynolds number of 10^5 , α will be 0.026 and 0.186 for the single-eddy and double-eddy type swirls, respectively; at a Reynolds number of 10^4 , α will be 0.029 and 0.201 for single-eddy and double-eddy type swirls, respectively. These equations show that swirl decays more slowly at higher Reynolds numbers. Therefore, the double-eddy swirl decays much faster than the single-eddy swirl at the same Reynolds number. Using these values we obtain the following Reynolds number dependencies. For the maximum swirl angle, we have :

for a single-eddy (type I) swirl

$$\alpha = 0.045 Re_D^{-0.047}$$

For a double-eddy (type II) swirl

$$\alpha = 0.275 Re_D^{-0.034}$$

These experimental results can also be used to evaluate the installation specifications in current flow measurement standards^{1,3}. For the case of a single elbow producing (type II) swirl angles of up to 19° , to reduce that swirl to less than 2° at a pipe Reynolds number of 10^5 , about $12D$ would be required. The ISO-5167 specification of $36D$ for a 0.75 beta orifice meter for this situation would be very conservative, whereas the ANSI/API-2530 specification of 13.5 seems to be barely sufficient. For the case of a double elbow producing a single-eddy (type I) swirl of 20° , to reduce the swirl to less than 2° at a pipe Reynolds number of 10^5 , about 89 diameters would be necessary. Neither ISO nor ANSI specifications would provide sufficient upstream length to reduce this swirl to the acceptable levels quoted. When Reynolds numbers are very high, i.e. 10^6 or 10^7 , which can frequently occur in metering practice, the current specifications would appear to grossly under predict the necessary upstream lengths for orifice meters installed downstream of this double elbow configuration.

While the decay analysis presented above is applied to the maximum value of the swirl angle found along the horizontal diameter, other swirl parameters can be generated as based upon angular momentum parameters and analyzed to describe swirl decay phenomena. Several of these have been found to be very effective for accurately predicting the performance of different types of flowmeters when installation conditions are not ideal⁵⁻⁸. Because of differences in the mean and turbulent velocity distributions, the performance of some flowmeters installed in these pipeflows can be expected to be different from the performance expected in ideal pipeflow.

Pipe elbow effects on orifice meters

Orifice flowmeters of different geometries were calibrated in installations affected by the types of swirl described above. These were tested in a NIST 50 mm diameter

water flow facility⁵⁻⁸. The orifice taps were the flange-type and oriented in the $X-Z$ plane and on the positive X -axis side, see Figures 12-8(a) and (b). The meter calibration results are considered in terms of shifts relative to the averaged discharge coefficient from ideal installation conditions. Ideal installation conditions would be where $200D$ of straight, constant diameter piping is installed upstream of the meter; about $25D$ of piping is installed downstream. The results were taken over the range of Reynolds numbers tested, these are, in terms of orifice hole to pipe diameter ration (β): (1) $\beta = 0.363$, $15\,000 \leq Re_D \leq 45\,000$, (2) $\beta = 0.50$, $30\,000 \leq Re_D \leq 75\,000$, (3) $\beta = 0.75$, $45\,000 \leq Re_D \leq 100\,000$. It should be emphasized that, in the orifice effects described below, the discharge coefficients plotted for each position are mean values that are determined over the ranges of Reynolds numbers specified above. As such, the values plotted have ranges associated with them and, therefore, definitive specifications can only be made within these tolerances. The Reynolds number ranges for the following results depend upon the beta ration of the meter and specific values are given above. In this way, the results that follow should be taken in the appropriate context, that is, for the pertinent parameters of Reynolds number, beta ratio, relative pipe roughness etc.

Pipeflow effects on orifice geometries can be complex to interpret. It is apparent that velocity and swirl distributions together with turbulent profiles interact with fluid and flow conditions and the meter geometry to produce the observed discharge coefficients. The interpretations that follow focus on the flow phenomena that influence the pressure distributions in the regions of the pressure taps.

Figure 12-13(a) presents the effects of single elbow (type II) swirl on these meters: C_d is the orifice discharge coefficient. These results show that the single elbow flow reduces the discharge coefficients for these conditions. Relative to the ideal situation, these reductions range between -0.1% and -5.0%, when these meters are installed between 20 and $2.5D$, respectively, from the elbow. The reduction of the discharge coefficient is largest for the installation nearest the elbow and the magnitude of the reduction increases with beta ratio.

Figure 12-13(b) presents the effects of the double elbows out-of-plane (type 1) swirl on these meters; c_d is the orifice discharge coefficient. These results show that the double elbows out-of-plane flow can either increase or decrease discharge coefficients depending upon conditions. Increased discharge coefficients are speculated to be the result of type I swirl effects that reduce the orifice differential pressure. Decreased discharge coefficients can be explained by the flatness of the axial velocity distribution as compared to the ideal profile. This flatness would tend to increase the pressure at the upstream tap thereby increasing the pressure difference and thus reducing the discharge coefficient.

Increased discharge coefficients can be explained by swirl effects propagating through the orifice and elevating the pressure at the downstream tap via conservation of angular momentum principles. The relative significance of these effects is different for

different beta ratios. It is shown elsewhere that these elbow flows influence orifice meters differently for different Reynolds number conditions^{5-8, 13}. The erratic results found in Figure 12-13(b) for the largest beta ratio are interpreted to be the result of the complicated nature of this pipeflow very near the exit from this elbow configuration, see Figure 12-9(b).

Based on these orifice test results, it appears that the 2° limit on swirl angle is not a sufficient criterion to guarantee that orifice meter performance will be within ±0.5% of the ideal installation value. Specifically, for the 0.75 beta orifice meter the 2° swirl angle criterion indicates the meter should be installed 12D downstream of the single elbow configuration, but the shift in discharge coefficient at this location is found from Figure 12-13(a) to be -2%. Conversely, for the 0.363 beta orifice meter, the 2° swirl angle criterion is quite conservative since the discharge coefficient shift is only -0.25% at this location. If a ±0.5% tolerance on the discharge coefficient is allowed for the 0.363 beta meter downstream of the single elbow, this can be achieved with $Z = 8$ (where the swirl angle is 4°).

Furthermore, for the closely coupled double elbow configuration, the 2° swirl angle criterion produces discharge coefficient shifts less than ±0.5% for all beta ratios. For an installation criterion based upon ±0.5% in the discharge coefficient, our results show that : (1) a 0.75 beta orifice meter requires $Z = 50$ (where the swirl angle is greater than 4°), and (2) a 0.363 beta meter requires only $Z +20$ (where the swirl angle is 8°).

Appendix G: Flow Meter Installation Effects

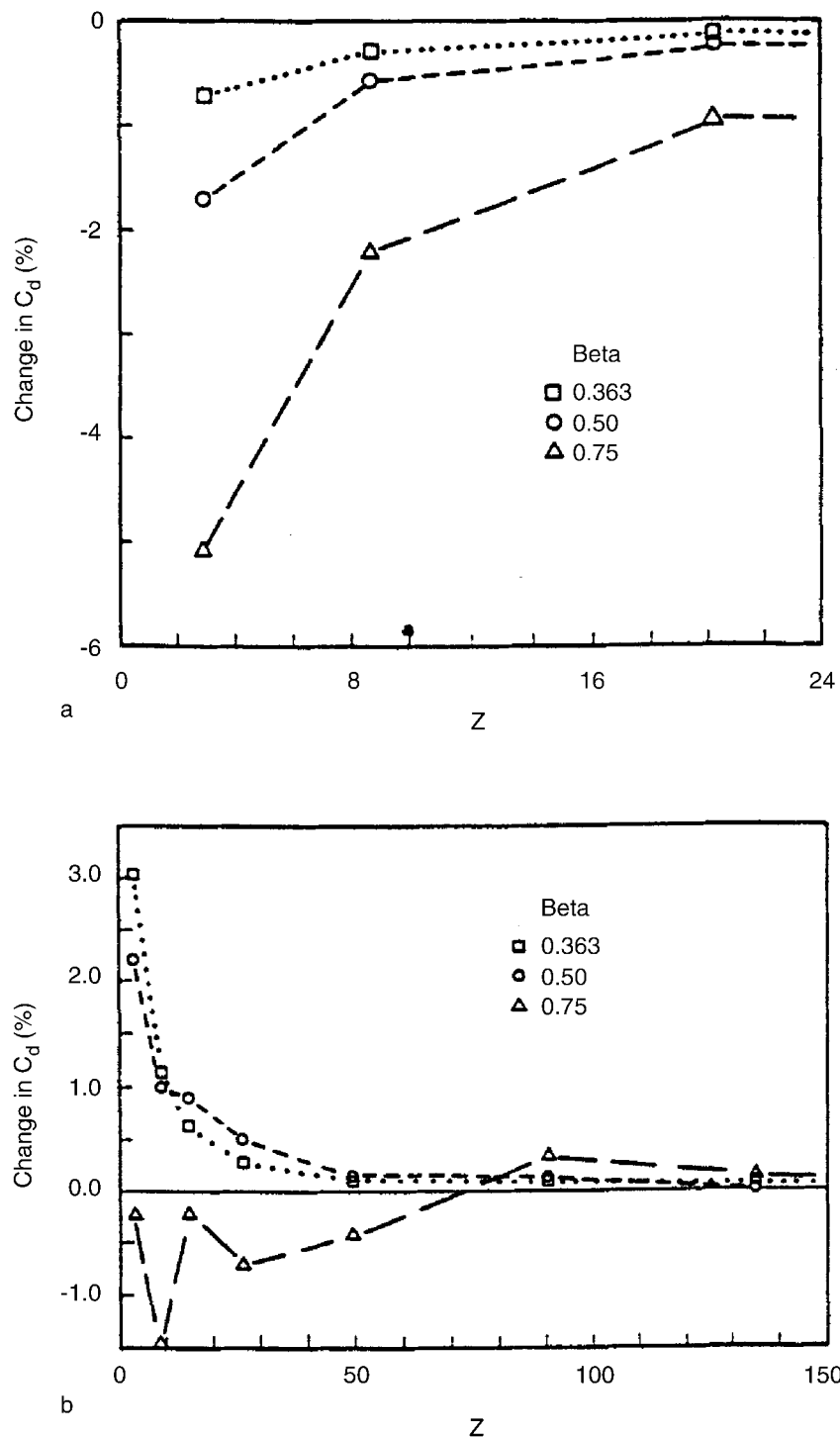


Figure 12-13
Calibration results for orifice-type meters installed in non-ideal conditions
downstream of: (a) a single elbow; (b) a closely coupled double elbows out-of-
plane configuration

Pipe elbow effects on turbine-type flowmeters

A specific type of turbine flowmeter was tested downstream of the single and closely coupled double elbows out-of-plane configurations. Results are shown in Figure 12-14, where the ordinate is the mean value of the change in the Strouhal number relative to that in the ideal installation conditions over the flowrate range, $45\,000 \leq Re \leq 100\,000$. The Strouhal number is a dimensionless meter factor. This meter is designed so that the propeller rotates counter-clockwise looking downstream. Consequently, for installation positions near the double elbows out-of-plane configuration a positive shift occurs in meter factor. Therefore, in the flow field shown via Figures 12-9(b) and 12-10(b), the meter factor results in Figure 12-14 show shifts up to almost +2% depending upon meter position downstream from the exit plane of the double elbows out-of-plane configuration.

Downstream from the single elbow the meter factor shifts downward to a lower limit of about -0.5%. This downward shift is interpreted to be due to a spatial averaging effect of the turbine propeller over the type II swirl and the altered distribution of axial velocity. It is also noted in Figure 12-14 that for downstream installation locations of 20-30 D, the meter factor shift is very small for the single elbow case, while for the double elbow situation the positive shift in meter factor is about 1%.

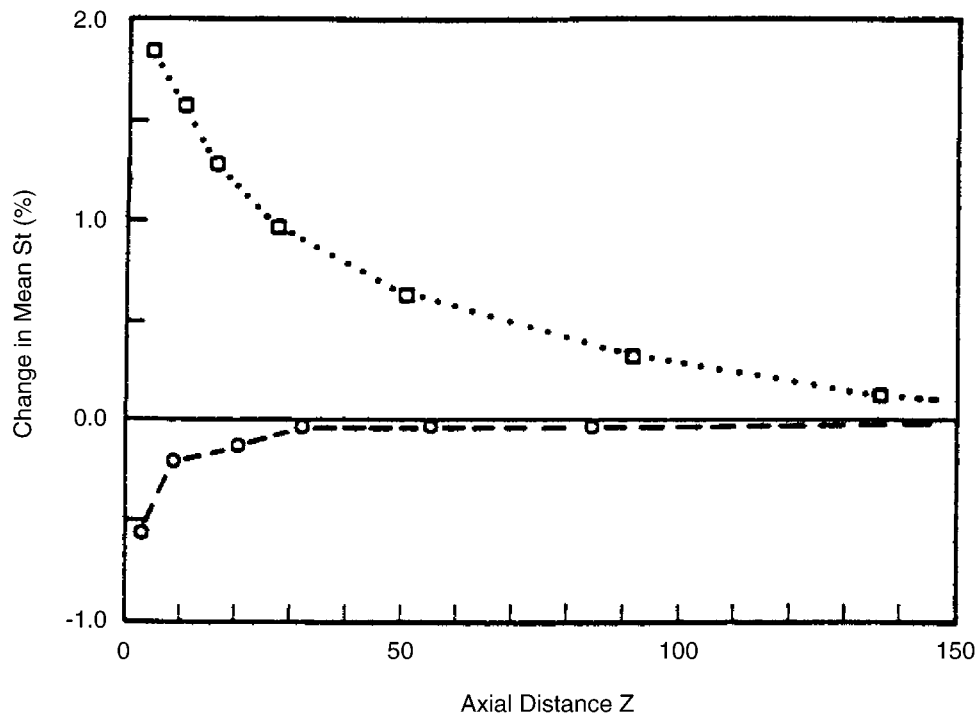


Figure 12-14
Calibration results for a turbine-type meter installed in non-ideal conditions downstream of single (o) and double elbows out-of-plane (□) configurations

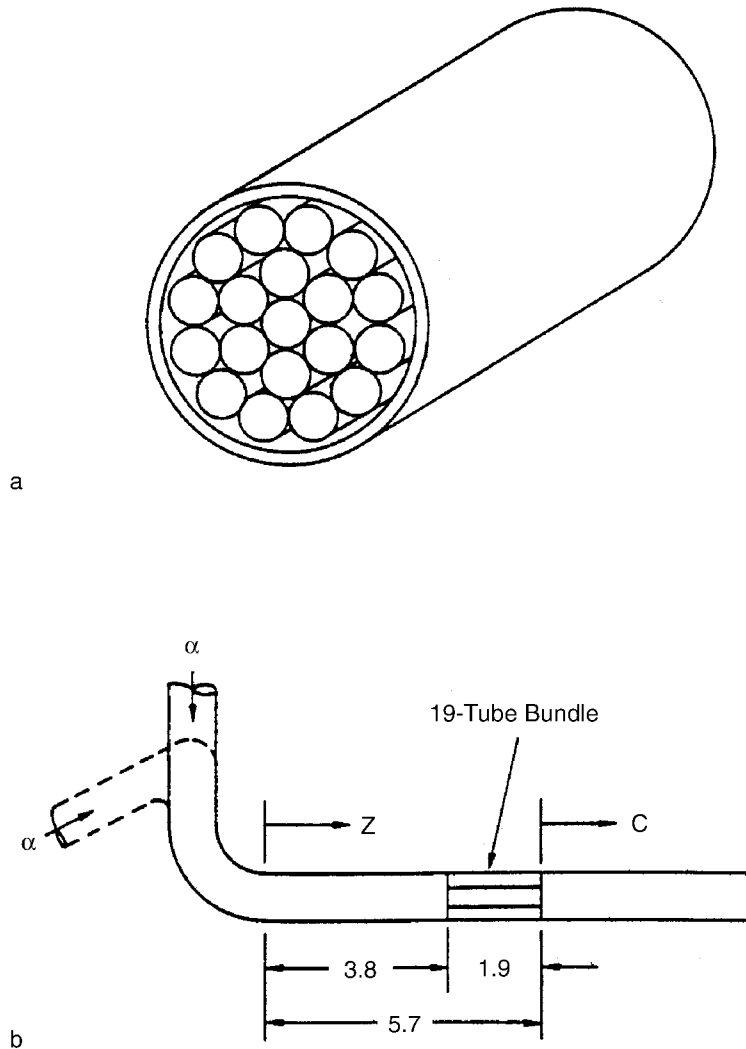


Figure 12-15
Flow conditioning arrangements: (a) tube bundle geometry; and (b) insulation
relative to elbow configurations

Although the discharge coefficient shifts described in the previous section and the metro factor shifts given above can be large and positive or negative, it is feasible to predict flowmeter performance in such non-ideal installation conditions⁵⁻⁸.

Alternatively, the installation of flow conditioners downstream of pipe-work disturbances can be done to try to improve the pipeflow so that flowmeter performance is satisfactory.

Flow conditioners are designed using several strategies. Early designs attempted to remove swirl while adding only small increases to frictional pressure loss to that of the piping system. Other designs were intended to generate intense turbulent mixing which was to efficiently produce the ideal pipeflow distribution that would occur via very long lengths of straight, constant diameter piping. Still other designs attempted to

produce the same pipeflow distribution regardless of the upstream piping configuration: these invariably had considerable pressure losses associated with them. Of all the types of flow conditioners, the tube bundle type is probably the most prevalently used and, for this reason, it was selected for testing in the current phase of this program.

Tube bundle effects

For the test described below, the tube bundle-type flow conditioner shown in Figure 12-15(a) was installed as shown in Figure 12-15(b). This tube bundle geometry was selected for the 50 mm diameter pipe to produce a geometrically scaled version of the shape that is conventionally used in US orifice metering practice. The small tubes are 9.5 mm in diameter, with wall thickness of 0.4 mm. For the Reynolds number ranges covered by the present tests, the results obtained should be identical to the many practical installations-in gases and liquids- where pertinent, non-dimensional parameters are duplicated.

Profile measurements are presented in Figure 12-16 for the vertical and streamwise components of the mean velocity both upstream and downstream of the tube bundle. Again, the dashed line shows the ideal distributions for these conditions. The profiles shown in Figures 12-16(a) and (b) that are measured at $Z = 2.6$ or 2.7 are distributions upstream of the tube bundle. In Figures 12-16(b), the profile labeled with an asterisk refers to a distribution measured with the tube bundle removed, that is, the same profile as shown in Figures 12-9(b). Since these distributions shown in Figures 12-9(a) and 12-16(a) were found to be the same, the profile between the tube bundle and the double elbow configuration was not remeasured but the asterisk is inserted to denote the fact that these profiles are those shown in Figures 12-9(a). The profiles in Figure 12-16 that are measured downstream of the tube bundle clearly show both the swirl reduction and the jetting effects from the individual tubes.

Appendix G: Flow Meter Installation Effects

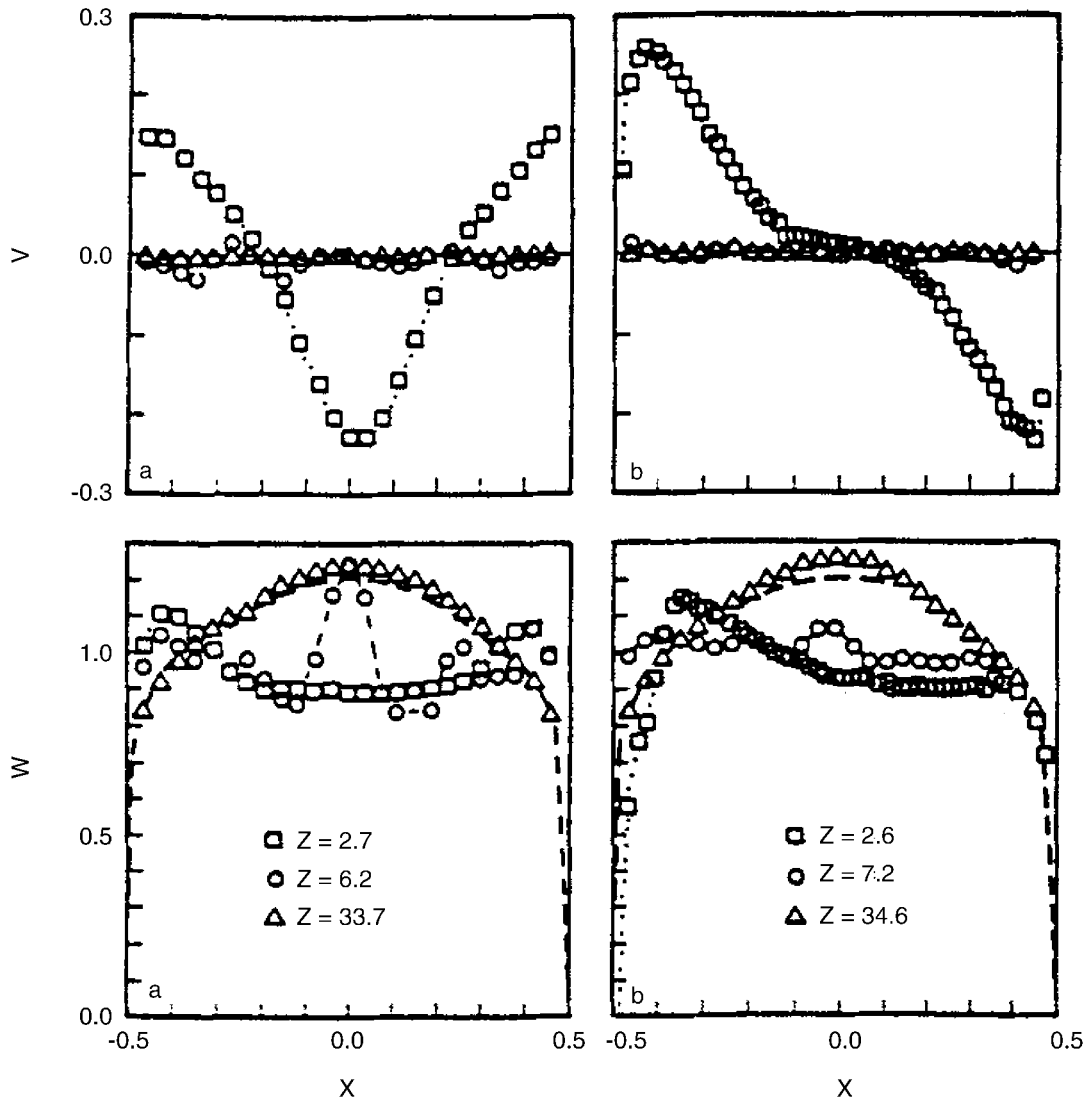


Figure 12-16
 Vertical, V, and streamwise, W, velocity profiles upstream and downstream of the tube bundle installed downstream of : (a) the single elbow and (b) the double elbows out-of-plane configuration. Downstream distances are in diameters. Ideal profiles are shown by dashed lines.

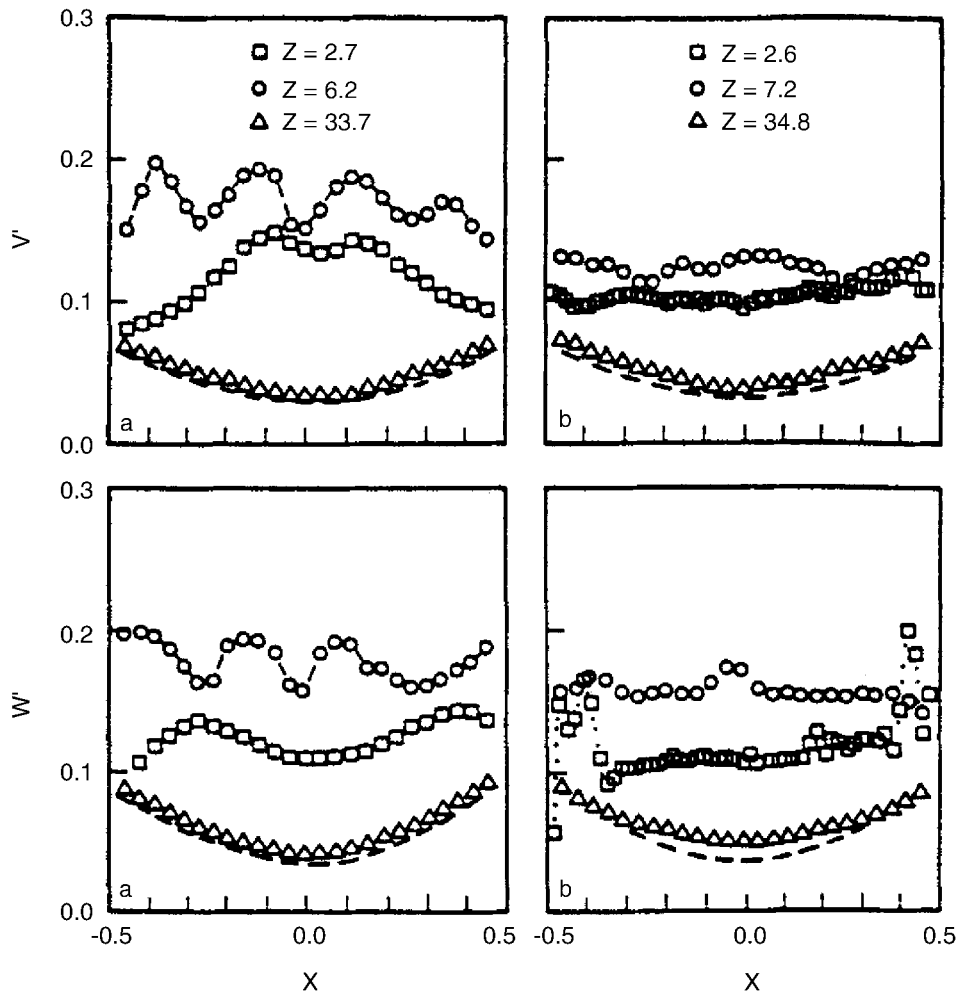


Figure 12-17
 Cross-stream profiles of the root mean square values of the vertical, V' , and streamwise, W' , turbulent velocity components upstream and downstream of the tube bundle installed downstream of: (a) the single elbow and (b) the double elbows. Downstream distances are in diameters. The dashed lines refer to Laufer's data.

The vertical velocity distributions downstream of both elbow configurations and the tube bundle are essentially zero for all of the stations measured—thus showing how these conditioners successfully remove swirl. The streamwise velocity distributions just downstream of the tube bundle show, for the single elbow case, peaked values which align with the five tubes arranged essentially along the diameter of this tube geometry, see Figure 12-16(a). This effect is less conspicuous in the results for the double elbow configuration where the data is taken further downstream than that for the single elbow. At the most downstream station measured, the streamwise velocity distributions for both configurations are found to have flow in the central core of the pipe with velocities exceeding those for the ideal profiles. It appears that, for both of these piping configurations, the tube bundle produces flow effects that “overdevelop”

the pipeflow. Figures 12-17(a) and (b) present results for the vertical and streamwise components of the turbulent velocity both upstream and downstream of the tube bundle for the single elbow and the double elbow configurations, respectively. The asterisk is noted in Figure 12-17(b) where it has the same meaning as described above for the Figure 12-16(b). The results in Figure 12-17(a) show clearly, in the profile just downstream of the tube bundles, the effects of the peaked turbulence levels in the regions between the jetting effects noted in Figure 12-16(a). These effects are interpreted to be the results of the mixing processes which occur between the adjacent jetting flows from the individual tubes. These effects are less apparent in Figure 12-17(b) for the double elbow case where results are presented at a location further downstream. Figures 12-17(a) and (b) show that the profiles just downstream of the tube bundle have higher averaged levels of turbulence as compared to the cases without the tube bundle, see Figure 12-11. These enhanced turbulence distributions produced by the tube bundle may be influential in overdeveloping the pipeflows so that the streamwise profiles have the high speed core flows some 30D downstream from the exit plane of the elbow.

Tube bundle effects on orifice meters

For conditions duplicating those described above for the three orifice geometries, the calibrations were repeated downstream of the tube bundle. Figure 12-18(a) presents the effects on these meters of the single elbow followed by the tube bundle installed as shown in Figure 12-15(b). The abscissa, C , is the orifice location downstream from the tube bundle expressed in D , see Figure 12-15(b). The ordinate is the percentage change in the mean value of the discharge coefficient relative to that for the ideal installation as plotted in Figures 12-13(a) and (b). It is apparent that when these orifice meters are installed within $10D$ downstream from the tube bundle, the discharge coefficients are lowered in comparison with the values for the ideal installation. These reductions are dependent upon beta ratio. These results show that the discharge coefficient is markedly reduced when the meter is installed within 11 to $13D$ from the exit plane of the tube bundle.

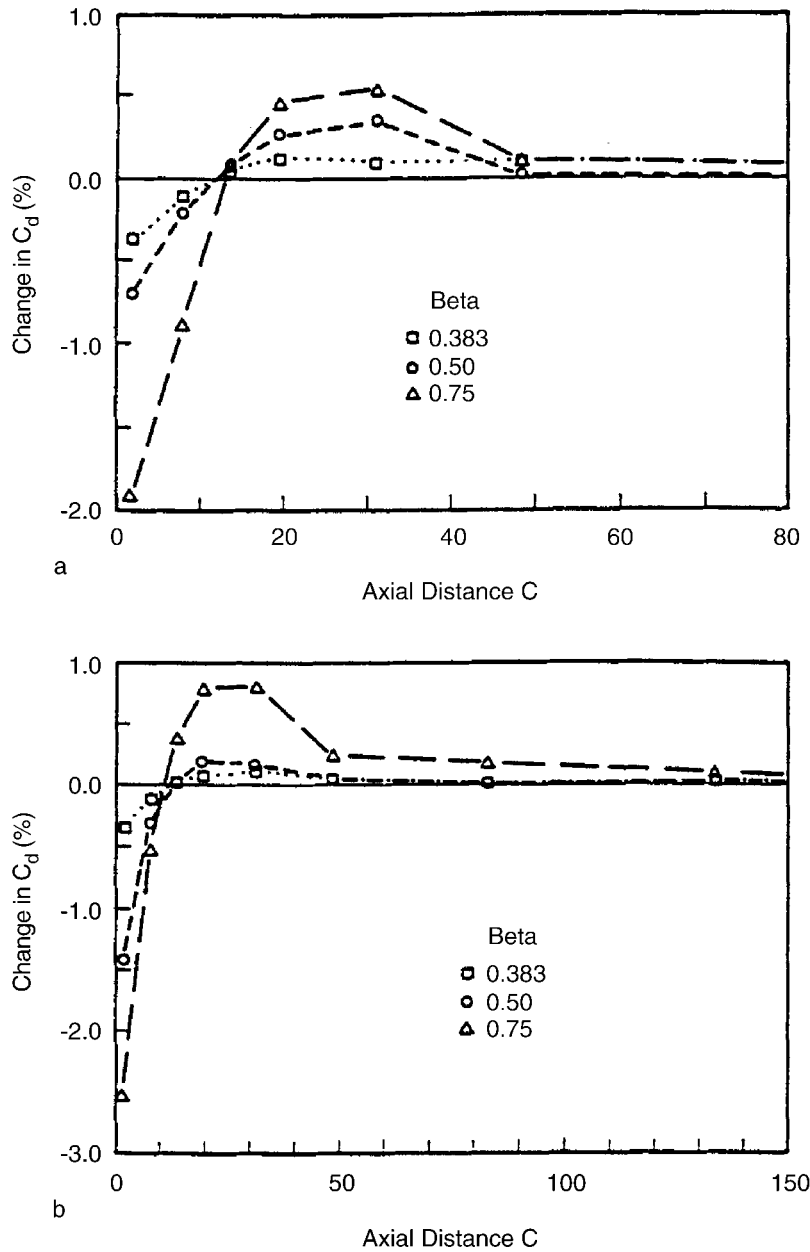


Figure 12-18
 Calibration results for orifice-type meters installed downstream of: (a) a single elbow and a tube bundle flow conditioner, and (b) a closely coupled double elbows out-of-plane configuration and a tube bundle flow conditioner

From the streamwise velocity profiles measured in these pipe intervals, it is found that these profiles are relatively uniform and are undoubtedly influential in producing these reduced changes in discharge coefficients. This profile uniformity is concluded to elevate the pressure levels in the flow near the upstream pressure tap location over that level which would prevail for the ideal orifice installation. This effect increases the

pressure difference across the meter thereby lowering the discharge coefficient. The magnitude of those effects increases with the beta ratio as shown in Figure 12-18(a).

The orifice discharge coefficient distribution for installation positions further downstream than the 11 to 13 D location show positive shifts relative to those for ideal conditions. Such results can be interpreted as being due to the overdeveloped distributions measured for the streamwise component of the time-averaged profiles shown in Figure 12-16(a). For these profiles the pressure levels in the region near the upstream taps are lowered because the flow velocity near the pipe wall is lower than that for the ideal conditions, thereby reducing the differential pressure across the meter and thus increasing the discharge coefficients. These positive shifts in orifice discharge coefficients persist for these conditions, to about the 50 D location. It is expected that, for different Reynolds number or roughness conditions, the levels of coefficient shifts as well as the orifice location intervals will vary.

Figure 12-18(b) presents orifice discharge coefficient results for installations downstream of the double elbows out-of-plane and the tube bundle. Again, orifice effects similar to those observed for the single elbow and tube bundle are found. For orifice installation positions closer than about 12 to 15 D to the exit plane of the tube bundle, discharge coefficient shifts are negative. The explanation given is the same as that given above for the negative shift found for the single elbow. For corresponding locations and beta ratios, the negative shifts found for the double elbows out of place and tube bundle configuration are larger in magnitude than those for the single elbow and tube bundle. When these orifice meters are located further downstream than the 12 to 15 D position, the discharge coefficient shifts are equal to or greater than those for the single elbow and tube bundle arrangement. For the largest beta ratio, the positive shifts in orifice discharge coefficient persist with orifice installation position, C , and can be detected until or beyond the 100 D location.

It is concluded that the effects of tube bundle flow conditioners significantly alter pipeflows. Although some quantitative differences are observed in coefficient shifts these alterations are shown to produce the same generic quantitative patterns on the performance of orifice meters installed downstream. Therefore, it appears that tube bundle effects on orifice meters appear to be the main source of the disturbed orifice performance and upstream piping configurations appear to be less significant.

Tube bundle effects on a turbine-type meter

For conditions duplicating those described above, the calibrations were repeated for the turbine-type flowmeter downstream of the tube bundle. Figure 12-19 presents these effects versus the axial distance, C , defined as before. These results show that this flow conditioner reduces the Strouhal number shift for installations downstream of the double elbows out-of-plane to less than about +0.2%. These results can be interpreted as due to the fluid interactions with the meter geometry-its design and bearing

characteristics and the pertinent fluid and flow parameters. While the vertical velocity distribution presented in Figure 12-16(b) shows that the tube bundle has essentially removed the swirl from the pipeflow, both the mean axial velocity distribution and the turbulence profiles shown in Figure 12-17(b) are not the equilibrated profiles. In spite of this, this meter shows performance characteristics close to 'ideal' when this tube bundle is used and the meter is installed $10D$ or more downstream from it.

The Strouhal number results downstream of the single elbow and tube bundle indicate reduced shifts for $C \leq 15$. However, for meter reinstallation's closer than $10D$ from the tube bundle, this meter exhibits shifts which equal or exceed those for corresponding distances from the elbow without the tube bundle. For example, if this meter should be installed $10D$ from the single elbow, Figure 12-14 shows that a mean meter factor shift of about -0.2% can be expected. If a tube bundle is installed between the elbow and meter as shown in Figure 12-15, then since $Z = C + 5.7$, this situation corresponds to about $C = 4$. Figure 12-19 shows that for $C = 4$, the mean meter factor shift is about -0.75% . Therefore, it appears that it is important to understand how specific meters respond to specific, non-ideal, meter installation effects before tube bundle flow conditioners are indiscriminately used.

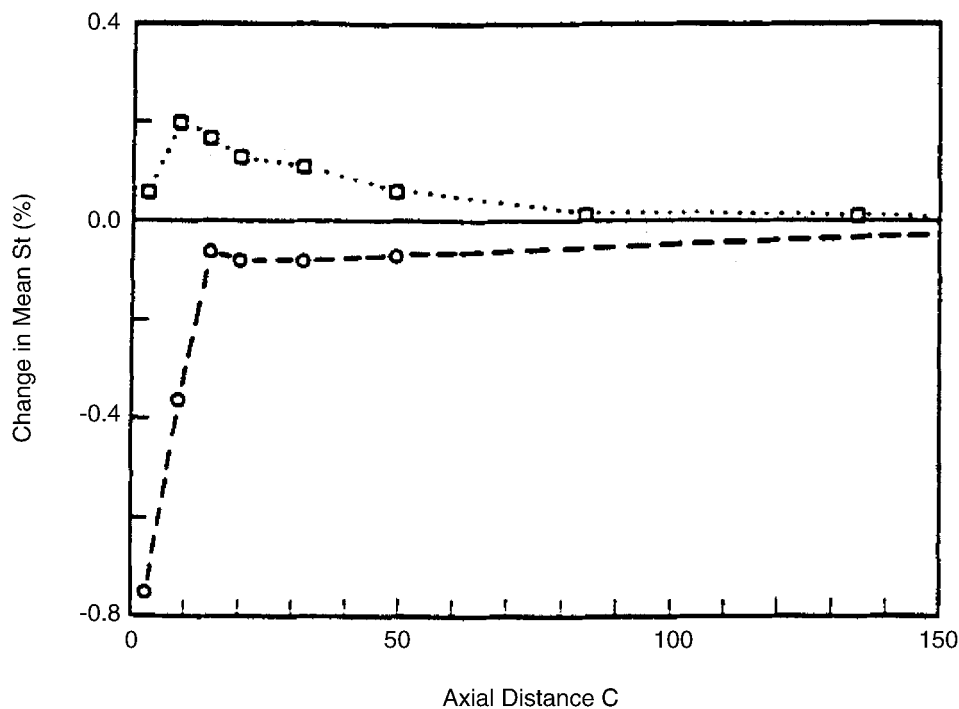


Figure 12-19
Calibration results for a turbine-type meter installed downstream of single (O) and double elbows out-of-plane (□) configurations and tube bundle flow conditioner

Discussion

To improve the performance of the types of meters described above, a number of conventional strategies can be used. Firstly, a prevalent strategy has been to perform a calibration using the identical conditions of fluid, piping, meter, flowrate range etc. However, this is not always feasible or convenient.

Secondly, the use of flow conditioning elements installed in the piping between the elbow configuration and the meter can possibly produce improved metering performance. These flow conditioning elements vary widely in their geometrical arrangements; their conditioning capabilities can be dependent on the type of pipeflow and their geometry; they can cause significant pressure losses in the pipeflow¹⁵. In view of the present results, flow conditioner and flowmeter combinations should be tested together. The present results also indicate that the widely used tube bundle which does remove swirl can also produce some significant negative or positive shifts in meter performance depending upon conditions.

Thirdly, it has recently been demonstrated that satisfactory metering performance can be successfully predicted and achieved without resorting to flow conditioners if sufficient data is available on the non-ideal pipeflow and data is obtained for how to respective meter is shifted with respect to the non-ideal pipeflow^{5,7}. By correlating the pipeflow data with the meter shifts, it has been demonstrated that it is feasible to adjust the ideal meter performance so that accurate flow measurements can be obtained in the non-ideal meter installations.^{8,16}

Although not investigated here, the role of pipe roughness on swirl decay has been studied elsewhere. Mottram and Rawat¹⁷ have shown that increased pipe roughness can reduce the lengths of piping required to dissipate pipeflow swirl.

Conclusions

Different pipe configurations produce different types of swirl patterns. The decay of swirl is dependent on the Reynolds number and the type of swirl. Installation specifications in the current flow measurement standards are concluded to be insufficient. This is especially true if strong, single-eddy (type 1) swirl is present. In this case, extremely long lengths of pipe are required to naturally dissipate this type of swirl at high Reynolds numbers. Meter installations where measurement accuracy is important should be re-evaluated to ensure that disturbed pipeflow phenomena do not detrimentally affect the particular meter in the specific location.

It is concluded that the 2° swirl angle criteria for orifice installations should be re-evaluated. All significant factors that can influence orifice performance should be incorporated into such specifications.

The effects of single and double eddy type of swirl are found to significantly change the performance of orifice and turbine type flowmeters. These shifts in performance vary both in direction and in magnitude depending on the type and strength of swirl, Reynolds number and the specific type and design on the flowmeter. The effects of tube bundle-type flow conditioners are found to effectively reduce swirl. However, it is also found that tube bundle effects radically alter orifice meter performance. These effects cause negative shifts in orifice discharge coefficients relative to ideal values for all three of the beta ratios tested when these meters are installed near the tube bundle. When the meter is installed further downstream from the tube bundle, the shift is reduced to zero but then becomes positive when positions further downstream are tested. These positive shifts are interpreted to be due to the overdeveloped, streamwise velocity profiles observed for both piping configurations in these locations. When very distant meter locations are tested, the positive shift reduces asymptotically to zero.

To the suggestion that orifice installations be specified according to the position downstream of the tube bundle where this shift changes sign, our conclusion would be that this solution may not give satisfactory results for all conditions due to a number of reasons. Firstly, the sensitivity of orifice discharge coefficient to downstream orifice position is significant for specific conditions such as larger beta ratios. Therefore, if small deviations in actual installation locations were to occur, the discharge coefficient could be changed significantly. Additionally, this orifice location where the discharge coefficient changes sign could be dependent upon a number of other factors such as Reynolds number range, relative pipe roughness etc. Consequently, it is concluded that a satisfactory specification for an orifice meter downstream of this type of tube bundle could be quite complicated-especially when the practical ranges of Reynolds number and relative roughness can vary so widely.

The conclusions for the turbine meter test results indicate that while tube bundle flow conditioners can remove swirl from pipeflows, this should not imply that ideal meter performance can be expected. On the contrary, the single elbow results show that for a specific meter installation some $10D$ from the single elbow configuration, a mean meter factor shift of some -0.2% occurred. The remedial insertion of a conventional tube bundle caused this shift to increase to about -0.8% . Therefore, the important conclusion here is that meter performance should be based upon pertinent test results or a fundamental understanding of the flow effects not only produced by flow conditioning elements but also affecting flowmeters, or both.

Acknowledgments

This research is supported by an industry-government consortium formed by NIST to conduct critical research on generic fluid measurement topics. The members of this consortium as of June 1990 are : Ketema-McCrometer, Chevron Oil, Controlotron, Dow Chemical, E. I. DuPont de Nemours, Ford Motor Co, Gas Research Institute, Gas Unie, ITT Barton, Kimmon Mfg. Ltd., Equimeter and Rosemount. Special acknowledgment is

given to Dr. K. M. Kothari of the Gas Research Institute for his technical input and support for this program. The technical efforts put forth by Mr. B. L. Shomaker in producing the experimental piping configuration and assisting with other technical matters are gratefully acknowledged. Last, but certainly not least, the competent secretarial capabilities of Mrs. G. M. Kline are gratefully acknowledged for her patient preparations of numerous drafts of this paper.

References

1. *Orifice metering of natural gas and other related hydro-carbon fluids. AGA Report No. 3, Second Edition (1985) American Gas Association, Arlington, Virginia. This document is alternatively named ANSI/API-2530*
2. *Mattingly, G.E., Spencer, E. A. And Klein, M. Workshop on fundamental research issues in orifice metering, Gas Research Inst. (GRI) Rept. 84/0190, (Sept. 1984)*
3. *Measurement of fluid flow by means of orifice plates, nozzles and venturi tubes inserted in circular cross-section conduits running full. International Organization for Standardization, ISO 5167-1980(E), First Edition*
4. *Yeh, T. T., Robertson, B. And Mattar, W. D. LDV measurement near a vortex shredding strut mounted in a pipe. ASME J. Fluid Engng. 105 (June 1983) 185-196*
5. *Mattingly, G. E. And Yeh, T. T. Flowmeter installation effects. Proc. Annual NCSL Symp., Washington, DC (August 1988)*
6. *Mattingly, G. E. And Yeh, T. T. NBS industry-government consortium research program on flowmeter installation effects: Summary report with emphasis on research period July-December 1987. NISTIR 88-3898 (November 1988)*
7. *Mattingly, G. E. And Yeh, T. T. NBS industry-government consortium research program on flowmeter installation effects: Summary report with emphasis on reset period January-July 1988. NISTIR 89-4080 (April 1989)*
8. *Yeh, T. T. And Mattingly, G. E. Prediction of flowmeter installation effects. Presented at the American Institute of Chemical Engineers 1989 Spring National Meeting, Houston, Texas, April 2-6, 1989, Paper 51e*
9. *Lauger, J. The structure of turbulence in fully developed pipe flow. NBS Rept. 1974 (Sept. 1952)*
10. *Fejer, A., Lavan, Z. And Wolf, Jr, L. Study of swirling fluid flow. ARL68-0713, Aerospace Reset Laboratories, USAF, Wright-Patterson Air Force Base, Ohio (October 1968)*

11. Kreith, F. And Sonju, O.K. *The decay of a turbulent swirl in a pipe. J. Fluid Mech.* 22(2) (1965) 257-271
12. Miler, R. W. *Flow measurement engineering handbook.* McGraw-Hill, New York, NY (1983)
13. Norman, R., et al. *Swirl decay in pipeflow. Proc 1989 International Gas Research Conf., Tokyo*
14. Musolf, A. O. *An experimental investigation of the decay of turbulent swirl flow in a pipe. MS Thesis, University of Colorado, Department of Civil Engineering (1963)*
15. Miller, R. W. *Flow measurement engineering handbook,* McGraw-Hill, New York (1985)
16. ASME MRC-10M-1988, *Method for establishing installation effects on flowmeters.* Amer. Soc. Mech. Engrs (ASME), New York, NY
17. Mottram, R. C. And Rawat, M.S. *Attenuation effects of pipe roughness on swirl and the implications for flowmeter installation. Int. Symp. Fluid Flow Meas. Amer. Gas Assoc., Arlington, VA (1986)*

13

APPENDIX H: USE OF TIMED ACCUMULATION METHODOLOGY TO DETERMINE FLOW TO SAFETY- RELATED COMPONENTS

Case Study

Accurate flow determination is a cornerstone of many Generic Letter 89-13 programs, as it shows that adequate coolant is available to the component that requires cooling, and by doing so, assures that the safety design basis requirements can be met.

Traditionally, such flows have been monitored by a number of methods. These methods include the use of permanently installed instruments and temporary ultrasonic flow meters. In situations where no permanent flow meter is installed, and the use of temporary meters such as ultrasonics is inappropriate due to the difficulty in obtaining a reading, or where such readings are subject to internal or regulatory challenge, the use of timed accumulation is a reasonable alternative.

The purpose of a timed accumulation test is to measure the as-found conditions within the piping system, and then divert flow under controlled conditions to an external measurement device. One such methodology is explored here.

In this case, a GE BWR was experiencing problems obtaining repeatable flow measurements using ultrasonic flow meters on the Low Pressure Core Spray Motor Cooler. This was attributed to the time in service on the carbon steel line, and the extensive corrosion present within the line.

A review of the design requirements for the system showed that the motor required a minimum of 2.0 gallons per minute in worst case accident conditions. The associated penalty factors were calculated to account for the differences between expected worst case accident conditions and normal operating conditions, and amounted to 0.7 gallons per minute. This in turn was added to the required value to provide a minimum flow limit of 2.7 gallons per minute to the motor cooler.

At this point, options were evaluated to obtain an accurate flow measurement. These included the use of a rotometer and timed accumulation. The least intrusive method that would provide the most reliable result was determined to be the timed accumulation, as the rotometer was difficult to read in the lower flow range that was expected.

The accumulation test was designed to demonstrate that the entire flow path that supported the motor cooler was acceptable. This was accomplished by first taking pressure measurements of the outlet piping, which provided a backpressure resistance reading using high-accuracy gauges. With this reading in hand, the outlet valve was closed to the cooler, and the drain valve was throttled to simulate the backpressure on the line by setting the pressure at the drain valve to the same value as the as found in-service pressure. (See Figure 13-1)

Proper simulation of the backpressure is critical in this methodology, as it represents the flow resistance in the outlet piping. Tolerances were set up as part of the test process to assure that the backpressure was simulated in a conservative fashion.

Following initial setup, a calibrated stopwatch was used to time water accumulation into a bucket. The water from the bucket was then poured into a precision volumetric measurement device in order to allow quantification of the flow value.

In order to account for the uncertainty of this process, the Utility assigned a 5% value based on engineering judgment. This was intended to cover any errors made in the use of the stopwatch, as well as human reaction delay time in shifting the hose from the drain to the bucket, and back out again.

In order to assure repeatability, three tests are conducted in series. The lowest flow value of the series, which in this case would be most limiting for the component in question, is then taken as the “as-found” flow value. (See Figure 13-2)

Another method that would be of equal value for flow verification would be to use a mass-based evaluation of flow. In this example, flow is diverted to a container on a high precision scale, and the mass of a timed amount of water is weighed and converted to gallons using the same methodology described above for the bucket test.

In all tests conducted, a before and after calibration of the instruments used is vital to assure the integrity of the test. This includes the precision pressure gauge, and if a weigh test is chosen, the scale and temperature measurement devices.

The results of this testing methodology have been repeatable, and have offered results that have been reasonably close to that of previously performed ultrasonic flow tests. The approach also reduced technician time and cost, as the pipe condition made ultrasonic setup a time consuming process.

LPCS MOTOR COOLER TIMED FLOW ACCUMULATION TEST

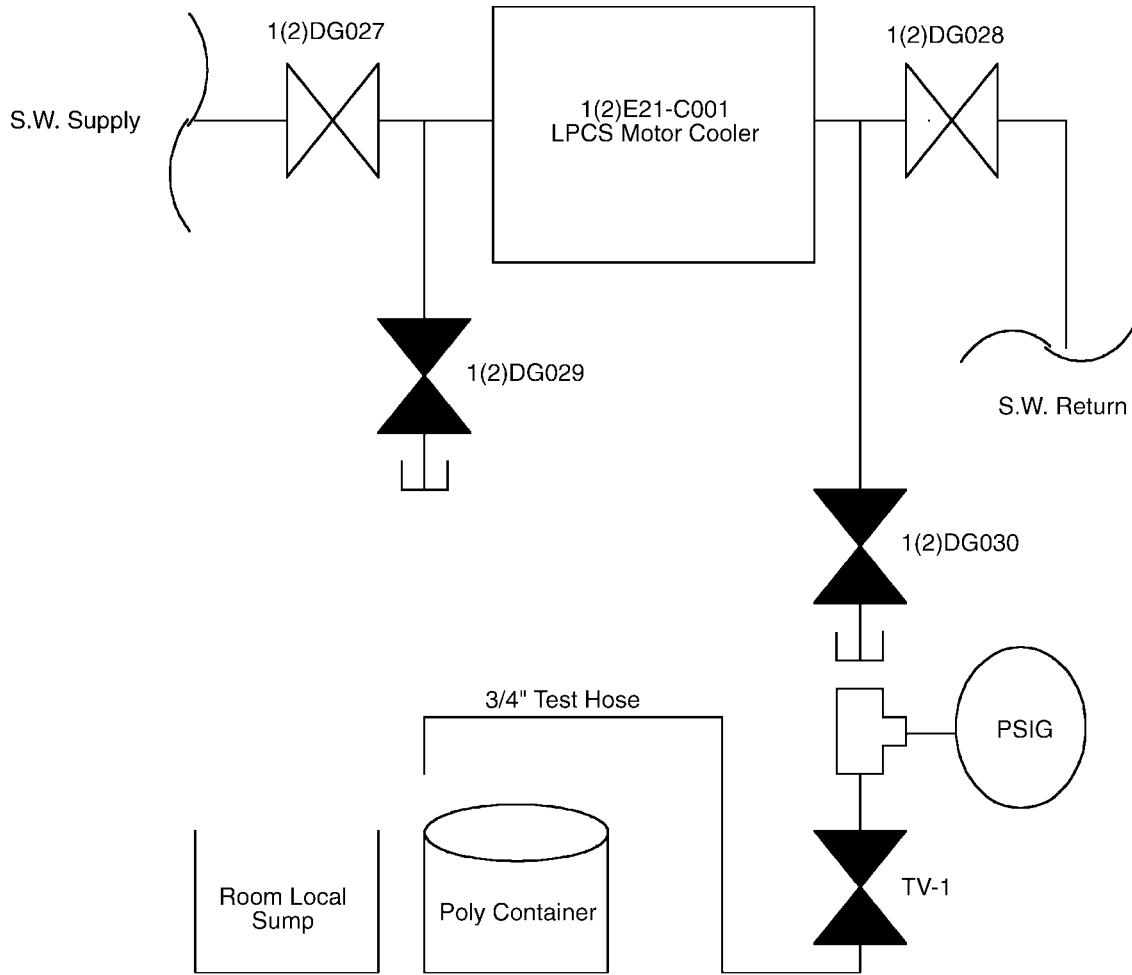


Figure 13-1
Setup Diagram

FIGURE 13-2 – Procedure Step Example

A.1 PERFORM the following three times to determine LPCS Pump Service Water flowrate:

- While monitoring test gauge, THROTTLE OPEN test line valve TV-1 until Test pressure gauge indicates the same pressure obtained in step monitoring test gauge, THROTTLE OPEN test line valve TV-1 until Test pressure gauge indicates the same pressure obtained in step C.6 (+1.0, -0.0 psig)
- SIMULTANEOUSLY:
 - o Transfer test hose to empty poly container.
 - o START stopwatch
- When poly container reference mark is reached, STOP stopwatch and route test hose to local sump.
- CLOSE test line valve TV-1.
- RECORD data in next step and calculate flowrate.

A.2 CALCULATE LPCS motor cooler flowrate as follows LPCS motor cooler flowrate as follows:

$$\frac{\text{_____ gallons}}{\text{Poly container reference mark volume}} \div \frac{\text{_____ seconds}}{\text{Stopwatch time}} \times \frac{60 \text{ seconds}}{1 \text{ minute}} = \text{_____ gpm}$$

$$\frac{\text{_____ gallons}}{\text{Poly container reference mark volume}} \div \frac{\text{_____ seconds}}{\text{Stopwatch time}} \times \frac{60 \text{ seconds}}{1 \text{ minute}} = \text{_____ gpm}$$

$$\frac{\text{_____ gallons}}{\text{Poly container reference mark volume}} \div \frac{\text{_____ seconds}}{\text{Stopwatch time}} \times \frac{60 \text{ seconds}}{1 \text{ minute}} = \text{_____ gpm}$$

Independent Verification of calculations performed by:

A.3 RECORD lowest calculated LPCS motor cooler Service Water side flow rate in Attachment A.